Casimir Force in Non-Planar Geometric Configurations

Sung Nae Cho

Dissertation submitted to the Faculty of the
Virginia Polytechnic Institute and State University
in partial fulfillment of the requirements for the degree of

Doctor of Philosophy
in
Physics

Tetsuro Mizutani, Chair
John R. Ficenec
Harry W. Gibson
A. L. Ritter
Uwe C. Tauber

April 26, 2004
Blacksburg, Virginia

Keywords: Casimir Effect, Casimir Force, Dynamical Casimir Force, Quantum Electrodynamics (QED), Vacuum Energy

Casimir Force in Non-Planar Geometric Configurations

Sung Nae Cho

(ABSTRACT)

The Casimir force for charge-neutral, perfect conductors of non-planar geometric configurations have been investigated. The configurations were: (1) the plate-hemisphere, (2) the hemisphere-hemisphere and (3) the spherical shell. The resulting Casimir forces for these physical arrangements have been found to be attractive. The repulsive Casimir force found by Boyer for a spherical shell is a special case requiring stringent material property of the sphere, as well as the specific boundary conditions for the wave modes inside and outside of the sphere. The necessary criteria in detecting Boyer's repulsive Casimir force for a sphere are discussed at the end of this thesis.

Acknowledgments

I would like to thank Professor M. Di Ventra for suggesting this thesis topic. The continuing support and encouragement from Professor J. Ficenec and Mrs. C. Thomas are gracefully acknowledged. Thanks are due to Professor T. Mizutani for fruitful discussions which have affected certain aspects of this investigation. Finally, I express my gratitude for the financial support of the Department of Physics of Virginia Polytechnic Institute and State University.

Contents

List of Figures

1. Introduction

The introduction is divided into three parts: (1) *physics*, (2) *applications*, and (3) *developments*. A brief outline of the physics behind the Casimir effect is discussed in item (1). In the item (2), major impact of Casimir effect on technology and science is outlined. Finally, the introduction of this thesis is concluded with a brief review of the past developments, followed by a brief outline of the organization of this thesis and its contributions to the physics.

1.1. Physics

When two electrically neutral, conducting plates are placed parallel to each other, our understanding from classical electrodynamics tell us that nothing should happen for these plates. The plates are assumed to be that made of perfect conductors for simplicity. In 1948, H. B. G. Casimir and D. Polder faced a similar problem in studying forces between polarizable neutral molecules in colloidal solutions. Colloidal solutions are viscous materials, such as paint, that contain micron-sized particles in a liquid matrix. It had been thought that forces between such polarizable, neutral molecules were governed by the van der Waals interaction. The van der Waals interaction is also referred to as the Lennard-Jones interaction. It is a long range electrostatic interaction that acts to attract two nearby polarizable molecules. Casimir and Polder found to their surprise that there existed an attractive force which could not be ascribed to the van der Waals theory. Their experimental result could not be correctly explained unless the retardation effect was included in the van der Waals' theory. This retarded van der Waals interaction or Lienard-Wiechert dipole-dipole interaction [1] is now known as the Casimir-Polder interaction [2]. Casimir, following this first work, elaborated on the Casimir-Polder interaction in predicting the existence of an attractive force between two electrically neutral, parallel plates of perfect conductors separated by a small gap [3]. This alternative derivation of the Casimir force is in terms of the difference between the zero-point energy in vacuum and the zero-point energy in the presence of boundaries. This force has been confirmed by experiments and the phenomenon is what is now known as the "Casimir Effect." The force responsible for the attraction of two uncharged conducting plates is accordingly termed the "Casimir Force." It was shown later that the Casimir force could be both attractive or repulsive depending on the geometry and the material property of the conductors [4, 5, 6].

The Casimir effect is regarded as macroscopic manifestation of the retarded van der Waals interaction between uncharged polarizable atoms. Microscopically, the Casimir effect is due to interactions between induced multipole moments, where the dipole term is the most dominant contributor if it is non-vanishing. Therefore, the dipole interaction is exclusively referred to, unless otherwise explicitly stated, throughout the thesis. The induced dipole moments can be qualitatively explained by quantum fluctuations in matter which leads to the energy imbalance $\triangle E$ due to charge-separation between virtual positive and negative charge contents that lasts for a time interval $\triangle t$ consistent with the Heisenberg uncertainty principle $\triangle E \triangle t \geq h/4\pi$, where h is the Planck constant. The fluctuations in the induced dipoles then result in fluctuating zero-point electromagnetic fields in the space around conductors. It is the presence of these fluctuating vacuum fields that lead to the phenomenon of the Casimir effect. However, the dipole strength is left as a free parameter in the calculations because it cannot be readily calculated. Its value must be determined from experiments.

Once this idea is accepted, one can then move forward to calculate the effective, temperature averaged, energy due to the dipole-dipole interactions with the time retardation effect folded in. The energy between the dielectric (or conducting) media is obtained from the allowed modes of electromagnetic waves determined by the Maxwell equations together with the boundary conditions. The Casimir force is then obtained by taking the negative gradient of the energy in space. This approach, as opposed to full atomistic treatment of the dielectrics (or conductors), is justified as long as the most significant field wavelengths determining the interaction are large when compared with the spacing of the lattice points in the media. The effect of all the multiple dipole scattering by atoms in the dielectric (or conducting) media simply enforces the macroscopic reflection laws of electromagnetic waves. For instance, in the case of the two parallel plates, the most significant wavelengths are those of the order of the plate gap distance. When this wavelength is large compared with the interatomic distances, the macroscopic electromagnetic theory can be used

with impunity. But, to handle the effective dipole-dipole interaction Hamiltonian, the classical electromagnetic fields have to be quantized. Then the geometric configuration can introduce significant complications, which is the subject matter this study is going to address.

Finally, it is to be noticed that the Casimir force on two uncharged, perfectly conducting parallel plates originally calculated by H. B. G. Casimir was done under the assumption of absolute zero temperature. In such condition, the occupational number n_s for photon is zero; and hence, there are no photons involved in Casimir's calculation for his parallel plates. However, the occupation number convention for photons refers to those photons with electromagnetic energy in quantum of $E_{photon} = \hbar\omega$, where $\hbar$ is the Planck constant divided by 2π and ω, the angular frequency. The zero-point quantum of energy, $E_{vac} = \hbar\omega/2$, involved in Casimir effect at absolute zero temperature is also of electromagnetic origin in nature; however, we do not classify such quantum of energy as a photon. Therefore, this quantum of electromagnetic energy, $E_{vac} = \hbar\omega/2$, will be simply denoted "zero-point energy" throughout this thesis. By convention, the lowest energy state, the vacuum, is also referred to as a zero-point.

1.2. Applications

In order to appreciate the importance of the Casimir effect from industry's point of view, we first examine the theoretical value for the attractive force between two uncharged conducting parallel plates separated by a gap of distance d : $F_C = -240^{-1}\pi^2 d^{-4}\hbar c$, where c is the speed of light in vacuum and d is the plate gap distance. To get a sense of the magnitude of this force, two mirrors of an area of $\sim 1\,cm^2$ separated by a distance of $\sim 1\,\mu m$ would experience an attractive Casimir force of roughly $\sim 10^{-7}\,N$, which is about the weight of a water droplet of half a millimeter in diameter. Naturally, the scale of size plays a crucial role in the Casimir effect. At a gap separation in the ranges of $\sim 10\,nm$, which is roughly about a hundred times the typical size of an atom, the equivalent Casimir force would be in the range of 1 atmospheric pressure. The Casimir force have been verified by Steven Lamoreaux [7] in 1996 to within an experimental uncertainty of 5%. An independent verification of this force have been done recently by U. Mohideen and Anushree Roy [8] in 1998 to within an experimental uncertainty of 1%.

The importance of Casimir effect is most significant for the miniaturization of modern electronics. The technology already in use that is affected by the Casimir effect is that of the microelectromechanical systems (MEMS). These are devices fabricated on the scale of microns and sub-micron sizes. The order of the magnitude of Casimir force at such a small length scale can be enormous. It can cause mechanical malfunctions if the Casimir force is not properly taken into account in the design, e.g., mechanical parts of a structure could stick together, etc [9]. The Casimir force may someday be put to good use in other fields where nonlinearity is important. Such potential applications requiring nonlinear phenomena have been demonstrated [10]. The technology of MEMS hold many promising applications in science and engineering. With the MEMS soon to be replaced by the next generation of its kind, the nanoelectromechanical systems or NEMS, understanding the phenomenon of the Casimir effect become even more crucial.

Aside from the technology and engineering applications, the Casimir effect plays a crucial role in accurate force measurements at nanometer and micrometer scales [11]. As an example, if one wants to measure the gravitational force at a distance of atomic scale, not only the subtraction of the dominant Coulomb force has to be done, but also the Casimir force, assuming that there is no effect due to strong and weak interactions.

Most recently, a new Casimir-like quantum phenomenon have been predicted by Feigel [12]. The contribution of vacuum fluctuations to the motion of dielectric liquids in crossed electric and magnetic fields could generate velocities of $\sim 50\,nm/s$. Unlike the ordinary Casimir effect where its contribution is solely due to low frequency vacuum modes, the new Casimir-like phenomenon predicted recently by Feigel is due to the contribution of high frequency vacuum modes. If this phenomenon is verified, it could be used in the future as an investigating tool for vacuum fluctuations. Other possible applications of this new effect lie in fields of microfluidics or precise positioning of micro-objects such as cold atoms or molecules.

Everything that was said above dealt with only one aspect of the Casimir effect, the attractive Casimir force. In spite of many technical challenges in precision Casimir force measurements [7, 8], the attractive Casimir force is fairly well established. This aspect of the theory is not however what drives most of the researches in the field. The Casimir effect also predicts a repulsive force and many researchers in the field today are focusing on this phenomenon yet to be confirmed experimentally. Theoretical calculations suggest that for certain geometric configurations, two neutral conductors would exhibit repulsive behavior rather than being attractive. The classic result that started it all is that of Boyer's work on the Casimir force calculation for an uncharged spherical conducting shell [4]. For a spherical conductor, the net electromagnetic radiation pressure, which constitute the Casimir force, has a positive sign, thus

being repulsive. This conclusion seems to violate fundamental principle of physics for the fields outside of the sphere take on continuum in allowed modes, where as the fields inside the sphere can only assume discrete wave modes. However, no one has been able to experimentally confirm this repulsive Casimir force.

The phenomenon of Casimir effect is too broad, both in theory and in engineering applications, to be completely summarized here. I hope this informal brief survey of the phenomenon could motivate people interested in this remarkable area of quantum physics.

1.3. Developments

Casimir's result of attractive force between two uncharged, parallel conducting plates is thought to be a remarkable application of QED. This attractive force have been confirmed experimentally to a great precision as mentioned earlier [7, 8]. However, it must be emphasized that even these experiments are not done exactly in the same context as Casimir's original configuration due to technical difficulties associated with Casimir's idealized perfectly flat surfaces.

Casimir's attractive force result between two parallel plates has been unanimously thought to be obvious. Its origin can also be attributed to the differences in vacuum-field energies between those inside and outside of the resonator. However, in 1968, T. H. Boyer, then at Harvard working on his thesis on Casimir effect for an uncharged spherical shell, had come to a conclusion that the Casimir force was repulsive for his configuration, which was contrary to popular belief. His result is the well known repulsive Casimir force prediction for an uncharged spherical shell of a perfect conductor [4].

The surprising result of Boyer's work has motivated many physicists, both in theory and experiment, to search for its evidence. On the theoretical side, people have tried different configurations, such as cylinders, cube, etc., and found many more configurations that can give a repulsive Casimir force [5, 13, 14]. Completely different methodologies were developed in striving to correctly explain the Casimir effect. For example, the "Source Theory" was employed by Schwinger for the explanation of the Casimir effect [14, 15, 16, 17]. In spite of the success in finding many boundary geometries that gave rise to the repulsive Casimir force, the experimental evidence of a repulsive Casimir effect is yet to be found. The lack of experimental evidence of a repulsive Casimir force has triggered further examination of Boyer's work.

The physics and the techniques employed in the Casimir force calculations are well established. The Casimir force calculations involve summing up of the allowed modes of waves in the given resonator. This turned out to be one of the difficulties in Casimir force calculations. For the Casimir's original parallel plate configuration, the calculation was particularly simple due to the fact that zeroes of the sinusoidal modes are provided by a simple functional relationship, $kd = n\pi$, where k is the wave number, d is the plate gap distance and n is a positive integer. This technique can be easily extended to other boundary geometries such as sphere, cylinder, cone or a cube, etc. For a sphere, the functional relation that determines the allowed wave modes in the resonator is $kr_o = \alpha_{s,l}$, where r_o is the radius of the sphere; and $\alpha_{s,l}$, the zeroes of the spherical Bessel functions j_s. In the notation $\alpha_{s,l}$ denotes lth zero of the spherical Bessel function j_s. The same convention is applied to all other Bessel function solutions. The allowed wave modes of a cylindrical resonator is determined by a simple functional relation $ka_o = \beta_{s,l}$, where a_o is the cylinder radius and $\beta_{s,l}$ are now the zeroes of cylindrical Bessel functions J_s.

One of the major difficulties in the Casimir force calculation for nontrivial boundaries such as those considered in this thesis is in defining the functional relation that determines the allowed modes in the given resonator. For example, for the hemisphere-hemisphere boundary configuration, the radiation originating from one hemisphere would enter the other and run through a complex series of reflections before escaping the hemispherical cavity. The allowed vacuum-field modes in the resonator is then governed by a functional relation $k\left\|\vec{R'}_2 - \vec{R'}_1\right\| = n\pi$, where $\left\|\vec{R'}_2 - \vec{R'}_1\right\|$ is the distance between two successive reflection points $\vec{R'}_1$ and $\vec{R'}_2$ of the resonator, as is illustrated in Figure 3.1. As will be shown in the subsequent sections, the actual functional form for $\left\|\vec{R'}_2 - \vec{R'}_1\right\|$ is not simple even though the physics behind $\left\|\vec{R'}_2 - \vec{R'}_1\right\|$ is particularly simple: the application of the law of reflections. The task of obtaining the functional relation $k\left\|\vec{R'}_2 - \vec{R'}_1\right\| = n\pi$ for the hemisphere-hemisphere, the plate-hemisphere, and the sphere configuration formed by bringing in two hemispheres together is to the best of my knowledge my original development. It constitutes the major part of this thesis.

This thesis is not about questioning the theoretical origin of the Casimir effect. Instead, its emphasis is on applying the Casimir effect as already known to determine the sign of Casimir force for the realistic experiments. In spite of a

number of successes in the theoretical study of repulsive Casimir force, most of the configurations are unrealistic. In order to experimentally verify Boyer's repulsive force for a charge-neutral spherical shell made of perfect conductor, one should consider the case where the sphere is formed by bringing in two hemispheres together. When the two hemispheres are closed, it mimics that of Boyer's sphere. It is, however, shown later in this thesis that a configuration change from hemisphere-hemisphere to a sphere induces non-spherically symmetric energy flow that is not present in Boyer's sphere. Because Boyer's sphere gives a repulsive Casimir force, once those two closed hemispheres are released, they must repulse if Boyer's prediction were correct. Although the two hemisphere configuration have been studied for decades, no one has yet carried out its analytical calculation successfully. The analytical solutions on two hemispheres, existing so far, was done by considering the two hemispheres that were separated by an infinitesimal distance. In this thesis, the consideration of two hemispheres is not limited to such infinitesimal separations.

The three physical arrangements being studied in this thesis are: (1) the plate-hemisphere, (2) the hemisphere-hemisphere and (3) the sphere formed by brining in two hemispheres together. Although there are many other boundary configurations that give repulsive Casimir force, the configurations under consideration were chosen mainly because of the following reasons: (1) to be able to confirm experimentally the Boyer's repulsive Casimir force result for a spherical shell, (2) the experimental work involving configurations similar to that of the plate-hemisphere configuration is underway [10]; and (3) to the best of my knowledge, no detailed analytical study on these three configurations exists to date.

My motivation to mathematically model the plate-hemisphere system came from the experiment done by a group at the Bell Laboratory [10] in which they bring in an atomic-force-probe to a flopping plate to observe the Casimir force which can affect the motion of the plate. In my derivations for equations of motion, the configuration is that of the "plate displaced on upper side of a bowl (hemisphere)." The Bell Laboratory apparatus can be easily mimicked by simply displacing the plate to the under side of the bowl, which I have not done. The motivation behind the hemisphere-hemisphere system actually arose from an article by Kenneth and Nussinov [18]. In their paper, they speculate on how the edges of the hemispheres may produce effects such that two arbitrarily close hemispheres cannot mimic Boyer's sphere. This led to their heuristic conclusion which stated that Boyer's sphere can never be the same as the two arbitrarily close hemispheres.

To the best of my knowledge, two of the geometrical configurations investigated in this thesis work have not yet been investigated by others. They are the plate-hemisphere and the hemisphere-hemisphere configurations. This does not mean that these boundary configurations were not known to the researchers in the field, e.g., [18]. For the case of the hemisphere-hemisphere configuration, people realized that it could be the best way to test for the existence of a repulsive Casimir force for a sphere as predicted by Boyer. The sphere configuration investigated in this thesis, which is formed by bringing two hemispheres together, contains non-spherically symmetric energy flows that are not present in Boyer's sphere. In that regards, the treatment of the sphere geometry here is different from that of Boyer.

The basic layout of the thesis is as follows: (1) *Introduction*, (2) *Theory*, (3) *Calculations*, and (4) *Results*. The formal introduction of the theory is addressed in chapters (1) and (2). The original developments resulting from this thesis are contained in chapters (3) and (4). The brief outline of each chapter is the following: In chapter (1), a brief introduction to the physics is addressed; and the application importance and major developments in this field are discussed. In chapter (2), the formal aspect of the theory is addressed, which includes the detailed outline of the Casimir-Polder interaction and brief descriptions of various techniques that are currently used in Casimir force calculations. In chapter (3), the actual Casimir force calculations pertaining to the boundary geometries considered in this thesis are derived. The important functional relation for $\left\|\vec{R'}_2 - \vec{R'}_1\right\|$ is developed here. The dynamical aspect of the Casimir effect is also introduced here. Due to the technical nature of the derivations, many of the results presented are referred to the detailed derivations contained in the appendices. In chapter (4), the results are summarized. Lastly, the appendices have been added in order to accommodate the tedious and lengthy derivations to keep the text from losing focus due to mathematical details. To the best of my knowledge, everything in the appendices represent original developments, with a few indicated exceptions.

The goal in this thesis is not to embark so much on the theory side of the Casimir effect. Instead, its emphasis is on bringing forth the suggestions that might be useful in detecting the repulsive Casimir effect originally initiated by Boyer on an uncharged spherical shell. In concluding this brief outline of the motivation behind this thesis work, I must add that if by any chance someone already did these work that I have claimed to represent my original developments, I was not aware of their work at the time of this thesis was being prepared. And, should that turn out to be the case, I would like to express my apology for not referencing their work in this thesis.

2. Casimir Effect

The Casimir effect is divided into two major categories: (1) the electromagnetic Casimir effect and (2) the fermionic Casimir effect. As the titles suggest, the electromagnetic Casimir effect is due to the fluctuations in a massless Maxwell bosonic fields, whereas the fermionic Casimir effect is due to the fluctuations in a massless Dirac fermionic fields. The primary distinction between the two types of Casimir effect is in the boundary conditions. The boundary conditions appropriate to the Dirac equations are the so called "bag-model" boundary conditions, whereas the electromagnetic Casimir effect follows the boundary conditions of the Maxwell equations. The details of the fermionic force can be found in references [14, 17].

In this thesis, only the electromagnetic Casimir effect is considered. As it is inherently an electromagnetic phenomenon, we begin with a brief introduction to the Maxwell equations, followed by the quantization of electromagnetic fields.

2.1. Quantization of Free Maxwell Field

There are four Maxwell equations:

$$\vec{\nabla} \bullet \vec{E}\left(\vec{R},t\right) = 4\pi\rho\left(\vec{R},t\right), \qquad \vec{\nabla} \times \vec{E}\left(\vec{R},t\right) = -\frac{1}{c}\frac{\partial \vec{B}\left(\vec{R},t\right)}{\partial t}, \tag{2.1}$$

$$\vec{\nabla} \bullet \vec{B}\left(\vec{R},t\right) = 0, \qquad \vec{\nabla} \times \vec{B}\left(\vec{R},t\right) = \frac{4\pi}{c}\vec{J}\left(\vec{R},t\right) + \frac{1}{c}\frac{\partial \vec{E}\left(\vec{R},t\right)}{\partial t}, \tag{2.2}$$

where the Gaussian system of units have been adopted. The electric and the magnetic field are defined respectively by $\vec{E} = -\vec{\nabla}\Phi - c^{-1}\partial_t\vec{A}$ and $\vec{B} = \vec{\nabla} \times \vec{A}$, where Φ is the scalar potential and $\vec{A}$ is the vector potential. Equations (2.1) and (2.2) are combined to give

$$\sum_{l=1}^{3}\Bigg\{4\pi\partial_l\rho + \frac{4\pi}{c^2}\partial_t J_l - \sum_{m=1}^{3}\partial_m^2\left[\partial_l\Phi + \frac{1}{c}\partial_t A_l + \epsilon_{ljk}\partial_j A_k\right] + \frac{4\pi}{c}\epsilon_{lmn}\partial_m J_n + \frac{1}{c^2}\partial_t^2\left[\partial_l\Phi + \frac{1}{c}\partial_t A_l\right] + \frac{1}{c^2}\epsilon_{ljk}\partial_j\partial_t^2 A_k\Bigg\}\hat{e}_l = 0,$$

where the Einstein summation convention is assumed for repeated indices. Because the components along basis direction $\hat{e}_l$ are independent of each other, the above vector algebraic relation becomes three equations:

$$4\pi\partial_l\rho + \frac{4\pi}{c^2}\partial_t J_l - \sum_{m=1}^{3}\partial_m^2\left[\partial_l\Phi + \frac{1}{c}\partial_t A_l + \epsilon_{ljk}\partial_j A_k\right] + \frac{4\pi}{c}\epsilon_{lmn}\partial_m J_n + \frac{1}{c^2}\partial_t^2\left[\partial_l\Phi + \frac{1}{c}\partial_t A_l\right] + \frac{1}{c^2}\epsilon_{ljk}\partial_j\partial_t^2 A_k = 0, \tag{2.3}$$

where $l = 1, 2, 3$.

To understand the full implications of electrodynamics, one has to solve the above set of coupled differential equations. Unfortunately, they are in general too complicated to solve exactly. The need to choose an appropriate gauge to approximately solve the above equations is not only an option, it is a must. Also, for what is concerned with the vacuum-fields, that is, the radiation from matter when it is in its lowest energy state, information about the charge density ρ and the current density $\vec{J}$ must be first prescribed. Unfortunately, to describe properly the charge and current

densities of matter is a major difficulty in its own. Therefore, the charge density ρ and the current density $\vec{J}$ are set to be zero for the sake of simplicity and the Coulomb gauge, $\vec{\nabla} \bullet \vec{A} = 0$, is adopted. Under these conditions, equation (2.3) is simplified to $\partial_l^2 A_l - c^{-2}\partial_t^2 A_l = 0$, where $l = 1, 2, 3$. The steady state monochromatic solution is of the form

$$\begin{aligned}\vec{A}\left(\vec{R},t\right) &= \alpha\left(t\right)\vec{A}_0\left(\vec{R}\right) + \alpha^*\left(t\right)\vec{A}_0^*\left(\vec{R}\right) \\ &= \alpha\left(0\right)\exp\left(-i\omega t\right)\vec{A}_0\left(\vec{R}\right) + \alpha^*\left(0\right)\exp\left(i\omega t\right)\vec{A}_0^*\left(\vec{R}\right),\end{aligned}$$

where $\vec{A}_0\left(\vec{R}\right)$ is the solution to the Helmholtz equation $\nabla^2\vec{A}_0\left(\vec{R}\right) + c^{-2}\omega^2\vec{A}_0\left(\vec{R}\right) = 0$ and $\alpha\left(t\right)$ is the solution of the temporal differential relation satisfying $\ddot{\alpha}\left(t\right) + \omega^2\alpha\left(t\right) = 0$. With the solution $\vec{A}\left(\vec{R},t\right)$, the electric and the magnetic fields are found to be

$$\vec{E}\left(\vec{R},t\right) = -c^{-1}\left[\dot{\alpha}\left(t\right)\vec{A}_0\left(\vec{R}\right) + \dot{\alpha}^*\left(t\right)\vec{A}_0^*\left(\vec{R}\right)\right]$$

and

$$\vec{B}\left(\vec{R},t\right) = \alpha\left(t\right)\vec{\nabla}\times\vec{A}_0\left(\vec{R}\right) + \alpha^*\left(t\right)\vec{\nabla}\times\vec{A}_0^*\left(\vec{R}\right).$$

The electromagnetic field Hamiltonian becomes:

$$\mathcal{H}_F = \frac{1}{8\pi}\int_R\left[\vec{E}^* \bullet \vec{E} + \vec{B}^* \bullet \vec{B}\right]d^3R = \frac{k^2}{2\pi}\left\|\alpha\left(t\right)\right\|^2, \tag{2.4}$$

where k is a wave number and $\vec{A}_0\left(\vec{R}\right)$ have been normalized such that $\int_R A_{0,l}\left(R\right)d^3R = 1$ with $A_{0,l}\left(R\right)$ representing the lth component of $\vec{A}_0\left(\vec{R}\right)$.

We can transform $\mathcal{H}_F$ into the "normal coordinate representation" through the introduction of "creation" and "annihilation" operators, $a^\dagger$ and a. The resulting field Hamiltonian $\mathcal{H}_F$ of equation (2.4) is identical in form to that of the canonically transformed simple harmonic oscillator, $\mathcal{H}_{SH} \propto p^2 + q^2 \rightarrow K_{SH} \propto a^\dagger a$. For the free electromagnetic field Hamiltonian, the canonical transformation is to follow the sequence $K_{SH} \propto \left\|\alpha\left(t\right)\right\|^2 \rightarrow \mathcal{H}_{SH} \propto E^2 + B^2$ under a properly chosen generating function. The result is that with the following physical quantities,

$$q\left(t\right) = \frac{i}{c\sqrt{4\pi}}\left[\alpha\left(t\right) - \alpha^*\left(t\right)\right], \qquad p\left(t\right) = \frac{k}{\sqrt{4\pi}}\left[\alpha\left(t\right) + \alpha^*\left(t\right)\right],$$

the free field Hamiltonian of equation (2.4) becomes

$$\mathcal{H}_F = \frac{1}{2}\left[p^2\left(t\right) + \omega^2 q^2\left(t\right)\right], \tag{2.5}$$

which is identical to the Hamiltonian of the simple harmonic oscillator. Then, through a direct comparison and observation with the usual simple harmonic oscillator Hamiltonian in quantum mechanics, the following replacements are made

$$\alpha\left(t\right) \rightarrow \sqrt{\frac{2\pi\hbar c^2}{\omega}}a\left(t\right), \qquad \alpha^*\left(t\right) \rightarrow \sqrt{\frac{2\pi\hbar c^2}{\omega}}a^\dagger\left(t\right),$$

and, the quantized relations for $\vec{A}\left(\vec{R},t\right)$, $\vec{E}\left(\vec{R},t\right)$ and $\vec{B}\left(\vec{R},t\right)$ are found,

$$\vec{A}\left(\vec{R},t\right) = \sqrt{\frac{2\pi\hbar c^2}{\omega}}\left[a\left(t\right)\vec{A}_0\left(\vec{R}\right) + a^\dagger\left(t\right)\vec{A}_0^*\left(\vec{R}\right)\right],$$

$$\vec{E}\left(\vec{R},t\right) = i\sqrt{2\pi\hbar\omega}\left[a\left(t\right)\vec{A}_0\left(\vec{R}\right) - a^\dagger\left(t\right)\vec{A}_0^*\left(\vec{R}\right)\right],$$

$$\vec{B}\left(\vec{R},t\right)=\sqrt{\frac{2\pi\hbar c^{2}}{\omega}}\left[a\left(t\right)\vec{\nabla}\times\vec{A}_{0}\left(\vec{R}\right)+a^{\dagger}\left(t\right)\vec{\nabla}\times\vec{A}_{0}^{*}\left(\vec{R}\right)\right],$$

where it is understood that $\vec{A}\left(\vec{R},t\right)$, $\vec{E}\left(\vec{R},t\right)$ and $\vec{B}\left(\vec{R},t\right)$ are now quantum mechanical operators.

The associated field Hamiltonian operator for the photon becomes

$$\hat{\mathcal{H}}_{F}=\hbar\omega\left[a^{\dagger}\left(t\right)a\left(t\right)+\frac{1}{2}\right], \tag{2.6}$$

where the hat $(\wedge)$ over $\mathcal{H}_F$ now denotes an operator. The quantum mechanical expression for the free electromagnetic field energy per mode of angular frequency ω', summed over all occupation numbers becomes

$$\mathcal{H}_{F}\equiv\sum_{n_{s}=0}^{\infty}\left\langle n_{s}\left|\hat{\mathcal{H}}_{F}\right|n_{s}\right\rangle=\sum_{n_{s}=0}^{\infty}\left[n_{s}+\frac{1}{2}\right]\hbar\omega',$$

where $\omega'\equiv\omega'\left(n\right)$ and n_s is the occupation number corresponding to the quantum state $\left|n_s\right\rangle$. Summation over all angular frequency modes n and polarizations $\Theta_{\omega'}$ gives

$$\mathcal{H}_{F}=\sum_{n_{s}=0}^{\infty}\left\{\left[n_{s}+\frac{1}{2}\right]\hbar\Theta_{\omega'}\sum_{n=0}^{\infty}\omega'\left(n\right)\right\}\equiv\sum_{n_{s}=0}^{\infty}\mathcal{H}'_{n_{s}},$$

where $\mathcal{H}'_{n_s}$ is defined by

$$\mathcal{H}'_{n_{s}}=\left[n_{s}+\frac{1}{2}\right]\hbar\Theta_{\omega'}\sum_{n=0}^{\infty}\omega'\left(n\right),\qquad\left\{\begin{array}{c}n_{s}=0,1,2,3,\cdots,\\ \omega'\left(n\right)\equiv\left\|\vec{\omega'}\left(n\right)\right\|>0.\end{array}\right. \tag{2.7}$$

Here $\omega'\left(n\right)\equiv\left\|\vec{\omega'}\left(n\right)\right\|$ is the magnitude of nth angular frequency of the electromagnetic field, $\vec{\omega'}\left(n\right)=\sum_{i=1}^{3}\omega'_{i}\left(n_{i}\right)\hat{e}_{i}$, and $\Theta_{\omega'}$ is the number of independent polarizations of the field. The energy equation (2.7) is valid for the case where the angular frequency vector $\vec{\omega'}_{n}$ happens to be parallel to one of the coordinate axes. For the general case where $\vec{\omega'}_{n}$ is not necessarily parallel to any one of coordinate axes, the angular frequency is given by $\omega'\left(n\right)=\left\{\sum_{i=1}^{3}\left[\omega'_{i}\left(n_{i}\right)\right]^{2}\right\}^{1/2}$. The stationary energy is therefore

$$\mathcal{H}'_{n_{s},b}\equiv\mathcal{H}'_{n_{s}}=\left[n_{s}+\frac{1}{2}\right]\hbar c\Theta_{k'}\sum_{n_{1}=0}^{\infty}\sum_{n_{2}=0}^{\infty}\sum_{n_{3}=0}^{\infty}\left\{\sum_{i=1}^{3}\left[k'_{i}\left(n_{i},L_{i}\right)\right]^{2}\right\}^{1/2}, \tag{2.8}$$

where the substitution $\omega'_{i}\left(n_{i}\right)=ck'_{i}\left(n_{i},L_{i}\right)$ have been made. Here L_i is the quantization length, $\Theta_{\omega'}$ has been been changed to $\Theta_{k'}$, and the subscript b of $\mathcal{H}'_{n_s,b}$ denotes bounded space.

When the dimensions of boundaries are such that the difference, $\triangle k'_{i}\left(n_{i},L_{i}\right)=k'_{i}\left(n_{i}+1,L_{i}\right)-k'_{i}\left(n_{i},L_{i}\right)$, is infinitesimally small, we can replace the summation in equation (2.8) by integration,

$$\sum_{n_{1}=0}^{\infty}\sum_{n_{2}=0}^{\infty}\sum_{n_{3}=0}^{\infty}\rightarrow\int_{n_{1}=0}^{\infty}\int_{n_{2}=0}^{\infty}\int_{n_{3}=0}^{\infty}dn_{1}dn_{2}dn_{3}\rightarrow\left[f_{1}\left(L_{1}\right)f_{2}\left(L_{2}\right)f_{3}\left(L_{3}\right)\right]^{-1}\int_{0}^{\infty}\int_{0}^{\infty}\int_{0}^{\infty}dk'_{1}dk'_{2}dk'_{3},$$

where in the last step the functional definition for $k'_{i}\equiv k'_{i}\left(n_{i},L_{i}\right)=n_{i}f_{i}\left(L_{i}\right)$ have been used to replace dn_i by $dk'_{i}/f_{i}\left(L_{i}\right)$. In free space, the electromagnetic field energy for quantum state $\left|n_s\right\rangle$ is given by

$$\mathcal{H}'_{n_{s},u}\equiv\mathcal{H}'_{n_{s}}=\frac{\left[n_{s}+\frac{1}{2}\right]\hbar c\Theta_{k'}}{f_{1}\left(L_{1}\right)f_{2}\left(L_{2}\right)f_{3}\left(L_{3}\right)}\int_{0}^{\infty}\int_{0}^{\infty}\int_{0}^{\infty}\left\{\sum_{i=1}^{3}\left[k'_{i}\left(n_{i},L_{i}\right)\right]^{2}\right\}^{1/2}dk'_{1}dk'_{2}dk'_{3}, \tag{2.9}$$

where the subscript u of $\mathcal{H}'_{n_s,u}$ denotes free or unbounded space, and the functional $f_i\left(L_i\right)$ in the denominator is equal to $\zeta_{zero}n_{i}^{-1}L_{i}^{-1}$ for a given L_i. Here ζ_{zero} is the zeroes of the function representing the transversal component of the

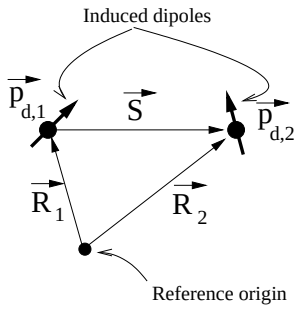

Figure 2.1.: Two interacting molecules through induced dipole interactions.

electric field.

2.2. Casimir-Polder Interaction

The phenomenon referred to as Casimir effect has its root in van der Waals interaction between neutral particles that are polarizable. The Casimir force may be regarded as a macroscopic manifestations of the retarded van der Waals force. The energy associated with an electric dipole moment $\vec{p}_d$ in a given electric field $\vec{E}$ is $\mathcal{H}_d = -\vec{p}_d \bullet \vec{E}$. When the involved dipole moment $\vec{p}_d$ is that of the induced rather than that of the permanent one, the induced dipole interaction energy is reduced by a factor of two, $\mathcal{H}_d = -\vec{p}_d \bullet \vec{E}/2$. The factor of one half is due to the fact that $\mathcal{H}_d$ now represents the energy of a polarizable particle in an external field, rather than a permanent dipole. The role of an external field here is played by the vacuum-field. Since the polarizability is linearly proportional to the external field, the average value leads to a factor of one half in the induced dipole interaction energy. Here the medium of the dielectric is assumed to be linear. Throughout this thesis, the dipole moments induced by vacuum polarization are considered as a free parameters.

The interaction energy between two induced dipoles shown in Figure 2.1 are given by

$$\mathcal{H}_{int} = \frac{1}{2}\left\|\vec{R}_2 - \vec{R}_1\right\|^{-5}\left\{\left[\vec{p}_{d,1} \bullet \vec{p}_{d,2}\right]\left\|\vec{R}_2 - \vec{R}_1\right\|^2 - 3\left[\vec{p}_{d,1} \bullet \left(\vec{R}_2 - \vec{R}_1\right)\right]\left[\vec{p}_{d,2} \bullet \left(\vec{R}_2 - \vec{R}_1\right)\right]\right\},$$

where $\vec{R}_i$ is the position of ith dipole. For an isolated system, the first order perturbation energy $\left\langle \mathcal{H}_{int}^{(1)} \right\rangle$ vanishes due to the fact that dipoles are randomly oriented, i.e., $\langle \vec{p}_{d,i} \rangle = 0$. The first non-vanishing perturbation energy is that of the second order, $U_{eff,static} = \left\langle \mathcal{H}_{int}^{(2)} \right\rangle = \sum_{m \neq 0} \langle 0 | \mathcal{H}_{int} | m \rangle \langle m | \mathcal{H}_{int} | 0 \rangle \left[E_0 - E_m\right]^{-1}$, which falls off with respect to the separation distance like $U_{eff,static} \propto \left\|\vec{R}_2 - \vec{R}_1\right\|^{-6}$. This is the classical result obtained by F. London for short distance electrostatic fields. F. London employed quantum mechanical perturbation approach to reach his result on a static van der Waals interaction without retardation effect in 1930.

The electromagnetic interaction can only propagate as fast as the speed of light in a given medium. This retardation effect due to propagation time was included by Casimir and Polder in their consideration. It led to their surprising discovery that the interaction between molecules falls off like $\left\|\vec{R}_1 - \vec{R}_2\right\|^{-7}$. It became the now well known Casimir-Polder potential [2],

$$U_{eff,retarded} = -\frac{\hbar c}{4\pi}\left\|\vec{R}_2 - \vec{R}_1\right\|^{-7}\left\{23\left[\alpha_E^{(1)}\alpha_E^{(2)} + \alpha_M^{(1)}\alpha_M^{(2)}\right] - 7\left[\alpha_E^{(1)}\alpha_M^{(2)} + \alpha_M^{(1)}\alpha_E^{(2)}\right]\right\},$$

where $\alpha_E^{(i)}$ and $\alpha_M^{(i)}$ represents the electric and magnetic polarizability of ith particle (or molecule).

To understand the Casimir effect, the physics behind the Casimir-Polder (or retarded van der Waals) interaction is essential. In the expression of the induced dipole energy $\mathcal{H}_d = -\vec{p}_d \bullet \vec{E}/2$, we rewrite $\vec{p}_d = \alpha(\omega)\vec{E}_\omega$ for the Fourier component of the dipole moment induced by the Fourier component $\vec{E}_\omega$ of the field. Here $\alpha(\omega)$ is the polarizability. The induced dipole field energy becomes $\mathcal{H}_d = -\alpha(\omega)\vec{E}_\omega^\dagger \cdot \vec{E}_\omega/2$, where the $(\cdot)$ denotes the matrix multiplication

instead of the vector dot product $(\bullet)$. Summing over all possible modes and polarizations, the field energy due to the induced dipole becomes

$$\mathcal{H}_{d,1} = -\frac{1}{2}\sum_{\vec{k},\lambda} \alpha_1(\omega_k)\, \vec{E}^{\dagger}_{1,\vec{k},\lambda}\left(\vec{R}_1, t\right) \cdot \vec{E}_{1,\vec{k},\lambda}\left(\vec{R}_1, t\right),$$

where the subscripts (1) and $\left(1, \vec{k}, \lambda\right)$ denote that this is the energy associated with the induced dipole moment $\vec{p}_{d,1}$ at location $\vec{R}_1$ as shown in Figure 2.1. The total electric field $\vec{E}_{1,\vec{k},\lambda}\left(\vec{R}_1, t\right)$ in mode $\left(\vec{k}, \lambda\right)$ acting on $\vec{p}_{d,1}$ is given by

$$\vec{E}_{1,\vec{k},\lambda}\left(\vec{R}_1, t\right) = \vec{E}_{o,\vec{k},\lambda}\left(\vec{R}_1, t\right) + \vec{E}_{2,\vec{k},\lambda}\left(\vec{R}_1, t\right),$$

where $\vec{E}_{o,\vec{k},\lambda}\left(\vec{R}_1, t\right)$ is the vacuum-field at location $\vec{R}_1$ and $\vec{E}_{2,\vec{k},\lambda}\left(\vec{R}_1, t\right)$ is the induced dipole field at $\vec{R}_1$ due to the neighboring induced dipole $\vec{p}_{d,2}$ located at $\vec{R}_2$. The effective Hamiltonian becomes

$$\begin{aligned}\mathcal{H}_{d,1} = -\frac{1}{2}\sum_{\vec{k},\lambda} \Big\{ \alpha_1(\omega_k) \Big[&\vec{E}^{\dagger}_{o,\vec{k},\lambda}\left(\vec{R}_1, t\right) \cdot \vec{E}_{o,\vec{k},\lambda}\left(\vec{R}_1, t\right) + \vec{E}^{\dagger}_{2,\vec{k},\lambda}\left(\vec{R}_1, t\right) \cdot \vec{E}_{2,\vec{k},\lambda}\left(\vec{R}_1, t\right) \\ &+ \vec{E}^{\dagger}_{o,\vec{k},\lambda}\left(\vec{R}_1, t\right) \cdot \vec{E}_{2,\vec{k},\lambda}\left(\vec{R}_1, t\right) + \vec{E}^{\dagger}_{2,\vec{k},\lambda}\left(\vec{R}_1, t\right) \cdot \vec{E}_{o,\vec{k},\lambda}\left(\vec{R}_1, t\right) \Big] \Big\} \\ = \mathcal{H}_o + \mathcal{H}_{\vec{p}_{d,2}} &+ \mathcal{H}_{\vec{p}_{d,1},\vec{p}_{d,2}},\end{aligned}$$

where

$$\mathcal{H}_o = -\frac{1}{2}\sum_{\vec{k},\lambda} \alpha_1(\omega_k)\, \vec{E}^{\dagger}_{o,\vec{k},\lambda}\left(\vec{R}_1, t\right) \cdot \vec{E}_{o,\vec{k},\lambda}\left(\vec{R}_1, t\right),$$

$$\mathcal{H}_{\vec{p}_{d,2}} = -\frac{1}{2}\sum_{\vec{k},\lambda} \alpha_1(\omega_k)\, \vec{E}^{\dagger}_{2,\vec{k},\lambda}\left(\vec{R}_1, t\right) \cdot \vec{E}_{2,\vec{k},\lambda}\left(\vec{R}_1, t\right),$$

$$\mathcal{H}_{\vec{p}_{d,1},\vec{p}_{d,2}} = -\frac{1}{2}\sum_{\vec{k},\lambda} \alpha_1(\omega_k) \left[\vec{E}^{\dagger}_{o,\vec{k},\lambda}\left(\vec{R}_1, t\right) \cdot \vec{E}_{2,\vec{k},\lambda}\left(\vec{R}_1, t\right) + \vec{E}^{\dagger}_{2,\vec{k},\lambda}\left(\vec{R}_1, t\right) \cdot \vec{E}_{o,\vec{k},\lambda}\left(\vec{R}_1, t\right) \right].$$

Because only the interaction between the two induced dipoles is relevant to the Casimir effect, the $\mathcal{H}_{\vec{p}_{d,1},\vec{p}_{d,2}}$ term is considered solely here. In the language of field operators, the vacuum-field $\vec{E}_{o,\vec{k},\lambda}\left(\vec{R}_1, t\right)$ is expressed as a sum:

$$\vec{E}_{o,\vec{k},\lambda}\left(\vec{R}_1, t\right) = \vec{E}^{(+)}_{o,\vec{k},\lambda}\left(\vec{R}_1, t\right) + \vec{E}^{(-)}_{o,\vec{k},\lambda}\left(\vec{R}_1, t\right),$$

where

$$\vec{E}^{(+)}_{o,\vec{k},\lambda}\left(\vec{R}_1, t\right) \equiv i\sqrt{\frac{2\pi\hbar\omega_k}{V}} a_{\vec{k},\lambda}(0) \exp(-i\omega_k t) \exp\left(i\vec{k} \bullet \vec{R}_1\right) \hat{e}_{\vec{k},\lambda},$$

$$\vec{E}^{(-)}_{o,\vec{k},\lambda}\left(\vec{R}_1, t\right) \equiv -i\sqrt{\frac{2\pi\hbar\omega_k}{V}} a^{\dagger}_{\vec{k},\lambda}(0) \exp(i\omega_k t) \exp\left(-i\vec{k} \bullet \vec{R}_1\right) \hat{e}_{\vec{k},\lambda}.$$

In the above expressions, $a^{\dagger}_{\vec{k},\lambda}$ and $a_{\vec{k},\lambda}$ are the creation and annihilation operators respectively; and V, the quantization volume; $\hat{e}_{\vec{k},\lambda}$, the polarization. By convention, $\vec{E}^{(+)}_{o,\vec{k},\lambda}\left(\vec{R}_1, t\right)$ is called the positive frequency (annihilation) operator

and $\vec{E}^{(-)}_{o,\vec{k},\lambda}\left(\vec{R}_1,t\right)$ is called the negative frequency (creation) operator.

The field operator $\vec{E}_{2,\vec{k},\lambda}\left(\vec{R}_1,t\right)$ has the same form as the classical field of an induced electric dipole,

$$\vec{E}_{2,\vec{k},\lambda}\left(\vec{R}_1,t\right)=\left\{3\left[\hat{p}_{d,2}\bullet\hat{S}\right]\hat{S}-\hat{p}_{d,2}\right\}\left[\frac{1}{r^3}\left\|\vec{p}_{d,2}\left(t-r/c\right)\right\|+\frac{1}{cr^2}\left\|\dot{\vec{p}}_{d,2}\left(t-r/c\right)\right\|\right]$$
$$-\frac{1}{c^2r}\left\{\hat{p}_{d,2}-\left[\hat{p}_{d,2}\bullet\hat{S}\right]\hat{S}\right\}\left\|\ddot{\vec{p}}_{d,2}\left(t-r/c\right)\right\|,$$

where $r=\left\|\vec{R}_2-\vec{R}_1\right\|\equiv\left\|\vec{S}\right\|$, $\hat{S}=\left[\vec{R}_2-\vec{R}_1\right]/\left\|\vec{R}_2-\vec{R}_1\right\|$, $\hat{p}_{d,2}=\vec{p}_{d,2}/\left\|\vec{p}_{d,2}\right\|$ as shown in Figure 2.1, and c is the speed of light in vacuum. Because the dipole moment is expressed as $\vec{p}_d=\alpha\left(\omega\right)\vec{E}_\omega$, the appropriate dipole moment in the above expression for $\vec{E}_{2,\vec{k},\lambda}\left(\vec{R}_1,t\right)$ is to be replaced by

$$\vec{p}_{d,2}=\sum_{\vec{k},\lambda}\alpha_2\left(\omega_k\right)\left[\vec{E}^{(+)}_{o,\vec{k},\lambda}\left(\vec{R}_2,t\right)+\vec{E}^{(-)}_{o,\vec{k},\lambda}\left(\vec{R}_2,t\right)\right],$$

where $\alpha_2\left(\omega_k\right)$ is now the polarizability of the molecule or atom associated with the induced dipole moment $\vec{p}_{d,2}$ at the location $\vec{R}_2$. With this in place, $\vec{E}_{2,\vec{k},\lambda}\left(\vec{R}_1,t\right)$ is now a quantum mechanical operator.

The interaction Hamiltonian operator $\hat{\mathcal{H}}_{\vec{p}_{d,1},\vec{p}_{d,2}}$ can be written as

$$\hat{\mathcal{H}}_{\vec{p}_{d,1},\vec{p}_{d,2}}=-\frac{1}{2}\sum_{\vec{k},\lambda}\alpha_1\left(\omega_k\right)\left[\left\langle\vec{E}^{(+)}_{o,\vec{k},\lambda}\left(\vec{R}_1,t\right)\cdot\vec{E}_{2,\vec{k},\lambda}\left(\vec{R}_1,t\right)\right\rangle+\left\langle\vec{E}_{2,\vec{k},\lambda}\left(\vec{R}_1,t\right)\cdot\vec{E}^{(-)}_{o,\vec{k},\lambda}\left(\vec{R}_1,t\right)\right\rangle\right],$$

where we have taken into account the fact that $\vec{E}^{(+)}_{o,\vec{k},\lambda}\left(\vec{R}_2,t\right)|vac\rangle=\langle vac|\,\vec{E}^{(-)}_{o,\vec{k},\lambda}\left(\vec{R}_2,t\right)=0$. It was shown in [17] in great detail that the interaction energy is given by

$$U\left(r\right)\equiv\left\langle\mathcal{H}_{\vec{p}_{d,1},\vec{p}_{d,2}}\right\rangle=-\frac{2\pi\hbar}{V}\mathbb{R}_E\sum_{\vec{k},\lambda}k^3\omega_k\alpha_1\left(\omega_k\right)\alpha_2\left(\omega_k\right)\exp\left(-ikr\right)\exp\left(i\vec{k}\bullet\vec{r}\right)$$
$$\times\left[\left\{1-\left[\hat{e}_{\vec{k},\lambda}\bullet\hat{S}\right]^2\right\}\frac{1}{kr}+\left\{3\left[\hat{e}_{\vec{k},\lambda}\bullet\hat{S}\right]^2-1\right\}\left\{\frac{1}{k^3r^3}+\frac{i}{k^2r^2}\right\}\right].$$

In the limit of $r\ll c/\left|\omega_{mn}\right|$, where ω_{mn} is the transition frequency between the ground state and the first excited energy state, or the resonance frequency, the above result becomes

$$U\left(r\right)\cong-\left[\frac{3}{4}\hbar\omega_o\alpha^2\right]r^{-6},\qquad\alpha=2\left[3\hbar\omega_o\right]^{-1}\left\|\langle m\left|\vec{p}_d\right|0\rangle\right\|^2.$$

This was also the non-retarded van der Waals potential obtained by F. London. Here ω_o is the transition frequency, and α is the static ($\omega=0$) polarizability of an atom in the ground state. Once the retardation effect due to light propagation is taken into account, the Casimir-Polder potential becomes,

$$U\left(r\right)\cong-\left[\frac{23}{4\pi}\hbar c\alpha_1\left(\omega\right)\alpha_2\left(\omega\right)\right]r^{-7}.$$

What we try to emphasize in this brief derivation is that both retarded and non-retarded van der Waals interaction may be regarded as a consequence of the fluctuating vacuum-fields. It arises due to a non-vanishing correlation of the vacuum-fields over distance of $r=\left\|\vec{R}_2-\vec{R}_1\right\|$. The non-vanishing correlation here is defined by $\left\langle vac\left|\vec{E}^{(+)}_{o,\vec{k},\lambda}\left(\vec{R}_1,t\right)\cdot\vec{E}^{(-)}_{o,\vec{k},\lambda}\left(\vec{R}_2,t\right)\right|vac\right\rangle\neq0$. In more physical terms, the vacuum-fields induce fluctuating dipole moments in polarizable media. The correlated dipole-dipole interaction is the van der Waals interaction. If the retardation effect is taken into account, it is called the "Casimir-Polder" interaction.

In the Casimir-Polder picture, the Casimir force between two neutral parallel plates of infinite conductivity was

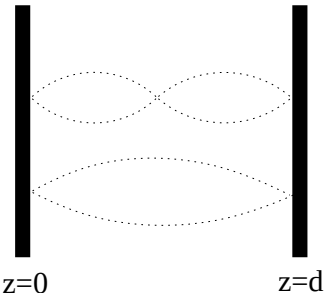

Figure 2.2.: A cross-sectional view of two infinite parallel conducting plates separated by a gap distance of $z = d$. The lowest first two wave modes are shown.

found by a simple summation of the pairwise intermolecular forces. It can be shown that such a procedure yields for the force between two parallel plates of infinite conductivity [17]

$$\vec{F}\,(d; L, c)_{Casimir-Polder} = -\frac{207\hbar c}{640\pi^2 d^4} L^2. \tag{2.10}$$

When this is compared with the force of equation (2.11) computed with Casimir's vacuum-field approach, which will be discussed in the next section, the agreement is within $\sim 20\%$ [17]. In other words, one can obtain a fairly reasonable estimate of the Casimir effect by simply adding up the pairwise intermolecular forces. The recent experimental verification of the Casimir-Polder force can be found in reference [19].

The discrepancy of $\sim 20\%$ between the two force results of equations (2.10) and (2.11) can be attributed to the fact that the force expression of equation (2.10) had been derived under the assumption that the intermolecular forces were additive in the sense that the force between two molecules is independent of the presence of a third molecule [17, 20]. The van der Waals forces are not however simply additive (see section 8.2 of reference [17]). And, the motivation behind the result of equation (2.10) is to illustrate the intrinsic connection between Casimir-Polder interaction and the Casimir effect, but without any rigor put into the derivation.

It is this discrepancy between the microscopic theories assuming additive intermolecular forces, and the experimental results reported in the early 1950s, that motivated Lifshitz in 1956 to develop a macroscopic theory of the forces between dielectrics [21, 22]. Lifshitz theory assumed that the dielectrics are characterized by randomly fluctuating sources. From the assumed delta-function correlation of these sources, the correlation functions for the field were calculated, and from these in turn the Maxwell stress tensor was determined. The force per unit area acting on the two dielectrics was then calculated as the zz component of the stress tensor. In the limiting case of perfect conductors, the Lifshitz theory correctly reduces to the Casimir force of equation (2.11).

2.3. Casimir Force Calculation Between Two Neutral Conducting Parallel Plates

Although the Casimir force may be regarded as a macroscopic manifestation of the retarded van der Waals force between two polarizable charge-neutral molecules (or atoms), it is most often alternatively derived by the consideration of the vacuum-field energy $\hbar\omega/2$ per mode of frequency ω rather than from the summation of the pairwise intermolecular forces. Three different methods widely used in Casimir force calculations are presented here. They are: (1) the Euler-Maclaurin sum approach, (2) the vacuum pressure approach by Milonni, Cook and Goggin, and lastly, (3) the source theory by Schwinger. The main purpose here is to exhibit their different calculational techniques.

2.3.1. Euler-Maclaurin Summation Approach

For pedagogical reasons and as a brief introduction to the technique, the Casimir's original configuration (two charge-neutral infinite parallel conducting plates) shown in Figure 2.2 is worked out in detail.

Since the electromagnetic fields are sinusoidal functions, and the tangential component of the electric fields vanish at the conducting surfaces, the functions $f_i(L_i)$ have the form $f_i(L_i) = \pi L_i^{-1}$. The wave numbers are given by $k_i'(n_i, L_i) = n_i f_i(L_i) = n_i \pi L_i^{-1}$. For $n_s = 0$ in equation (2.8), the ground state radiation energy is given by

$$\mathcal{H}'_{n_s,b} = \frac{1}{2}\hbar c \Theta_{k'} \sum_{n_1=0}^{\infty}\sum_{n_2=0}^{\infty}\sum_{n_3=0}^{\infty}\left\{\sum_{i=1}^{3} n_i^2 \pi^2 L_i^{-2}\right\}^{1/2}.$$

For the arrangement shown in Figure 2.2, the dimensions are such that $L_1 \gg L_3$ and $L_2 \gg L_3$, where (L_1, L_2, L_3) corresponds to (L_x, L_y, L_z). The area of the plates are given by $L_1 \times L_2$. The summation over n_1 and n_2 can be replaced by an integration,

$$\mathcal{H}'_{n_s,b} = \frac{1}{2}\hbar c L_1 L_2 \pi^{-2} \Theta_{k'} \int_0^{\infty}\int_0^{\infty}\sum_{n_3=0}^{\infty}\left\{[k_x']^2 + [k_y']^2 + n_3^2\pi^2 L_i^{-2}\right\}^{1/2} dk_x' dk_y'.$$

For simplicity and without any loss of generality, the designation of $L_1 = L_2 = L$ and $L_3 = d$ yields the result

$$\mathcal{H}'_{n_s,b}(d) = \frac{\Theta_{k'}}{2}\hbar c \frac{L^2}{\pi^2}\int_0^{\infty}\int_0^{\infty}\sum_{n_3=0}^{\infty}\left\{[k_x']^2 + [k_y']^2 + \frac{n_3^2\pi^2}{d^2}\right\}^{1/2} dk_x' dk_y'.$$

Here $\mathcal{H}'_{n_s,b}(d)$ denotes the vacuum electromagnetic field energy for the cavity when plate gap distance is d. In the limit the gap distance becomes arbitrarily large, the sum over n_3 is also replaced by an integral representation to yield

$$\mathcal{H}'_{n_s,b}(\infty) = \frac{\Theta_{k'}}{2}\hbar c \frac{L^2}{\pi^2}\lim_{d\to\infty}\left(\frac{d}{\pi}\int_0^{\infty}\int_0^{\infty}\int_0^{\infty}\left\{[k_x']^2 + [k_y']^2 + [k_z']^2\right\}^{1/2} dk_x' dk_y' dk_z'\right).$$

This is the electromagnetic field energy inside an infinitely large cavity, i.e., free space.

The work required to bring in the plates from an infinite separation to a final separation of d is then the potential energy,

$$\begin{aligned} U(d) &= \mathcal{H}'_{n_s,b}(d) - \mathcal{H}'_{n_s,b}(\infty) \\ &= \frac{\Theta_{k'}}{2}\hbar c \frac{L^2}{\pi^2}\left[\int_0^{\infty}\int_0^{\infty}\sum_{n_3=0}^{\infty}\left\{[k_x']^2 + [k_y']^2 + \frac{n_3^2\pi^2}{d^2}\right\}^{1/2} dk_x' dk_y' \right. \\ &\left. - \lim_{d\to\infty}\left(\frac{d}{\pi}\int_0^{\infty}\int_0^{\infty}\int_0^{\infty}\left\{[k_x']^2 + [k_y']^2 + [k_z']^2\right\}^{1/2} dk_x' dk_y' dk_z'\right)\right]. \end{aligned}$$

The result is a grossly divergent function. Nonetheless, with a proper choice of the cutoff function (or regularization function), a finite value for $U(d)$ can be obtained. In the polar coordinates representation (r, θ), we define $r^2 = [k_x']^2 + [k_y']^2$ and $dk_x' dk_y' = r dr d\theta$, then

$$\begin{aligned} U(d) = \frac{\Theta_{k'}\hbar c L^2}{2\pi^2}\left[\int_{\theta=0}^{\pi/2}\int_{r=0}^{\infty}\sum_{n_3=0}^{\infty}\sqrt{r^2 + \frac{n_3^2\pi^2}{d^2}}\, r dr d\theta \right. \\ \left. - \lim_{d\to\infty}\left(\frac{d}{\pi}\int_{k_z'=0}^{\infty}\int_{\theta=0}^{\pi/2}\int_{r=0}^{\infty}\sqrt{r^2 + [k_z']^2}\, r dr d\theta dk_z'\right)\right], \end{aligned}$$

where the integration over θ is done in the range $0 \le \theta \le \pi/2$ to ensure $k_x' \ge 0$ and $k_y' \ge 0$. For convenience, the integration over θ is carried out first,

$$U(d) = \frac{\Theta_{k'}\hbar c L^2}{4\pi}\left[\int_{r=0}^{\infty}\sum_{n_3=0}^{\infty}\sqrt{r^2 + \frac{n_3^2\pi^2}{d^2}}\, r dr - \lim_{d\to\infty}\left(\frac{d}{\pi}\int_{k_z'=0}^{\infty}\int_{r=0}^{\infty}\sqrt{r^2 + [k_z']^2}\, r dr dk_z'\right)\right].$$

As mentioned earlier, $U(d)$ in current form is grossly divergent. The need to regularize this divergent function through

some physically intuitive cutoff function is not a mere mathematical convenience, it is a must; otherwise, such a grossly divergent function is meaningless in physics. A cutoff (or regularizing) function in the form of $f(k') = f\left(\sqrt{r^2+[k'_z]^2}\right)$ (or $f(k') = f\left(\sqrt{r^2+n_3^2\pi^2d^{-2}}\right)$) such that $f(k') = 1$ for $k' \ll k'_{cutoff}$ and $f(k') = 0$ for $k' \gg k'_{cutoff}$ is chosen. Mathematically speaking, this cutoff function $f(k')$ is able to regularize the above divergent function. Physically, introduction of the cutoff takes care of the failure at small distance of the assumption that plates are perfectly conducting for short wavelengths. It is a good approximation to assume $k'_{cutoff} \sim 1/a_o$, where a_o is the Bohr radius. In this sense, one is inherently assuming that Casimir effect is primarily a low-frequency or long wavelength effect. Hence, with the cutoff function substituted in $U(d)$ above, the potential energy becomes

$$U(d) = \frac{\Theta_{k'}\hbar cL^2}{4\pi}\left[\sum_{n_3=0}^{\infty}\int_{r=0}^{\infty}\sqrt{r^2+\frac{n_3^2\pi^2}{d^2}}f\left(\sqrt{r^2+\frac{n_3^2\pi^2}{d^2}}\right)rdr - \lim_{d\to\infty}\left(\frac{d}{\pi}\int_{k'_z=0}^{\infty}\int_{r=0}^{\infty}\sqrt{r^2+[k'_z]^2}f\left(\sqrt{r^2+[k'_z]^2}\right)rdrdk'_z\right)\right].$$

The summation $\sum_{n_3=0}^{\infty}$ and the integral $\int_{r=0}^{\infty}$ in the first term on the right hand side can be interchanged. The interchange of sums and integrals is justified due to the absolute convergence in the presence of the cutoff function. In terms of the new definition for the integration variables $x = r^2d^2\pi^{-2}$ and $\kappa = k'_z d\pi^{-1}$, the above expression for $U(d)$ is rewritten as

$$\begin{aligned} U(d) &= \frac{1}{8}\Theta_{k'}\hbar cL^2\pi^2\left[\frac{1}{d^3}\sum_{n_3=0}^{\infty}\int_{x=0}^{\infty}\sqrt{x+n_3^2}f\left(\frac{\pi}{d}\sqrt{x+n_3^2}\right)dx - \lim_{d\to\infty}\left(\frac{1}{d^3}\int_{\kappa=0}^{\infty}\int_{x=0}^{\infty}\sqrt{x+\kappa^2}f\left(\frac{\pi}{d}\sqrt{x+\kappa^2}\right)dxd\kappa\right)\right] \\ &\equiv \frac{1}{8}\Theta_{k'}\hbar cL^2\pi^2\left[\frac{1}{2}F(0) + \sum_{n_3=1}^{\infty}F(n_3) - \int_{\kappa=0}^{\infty}F(\kappa)\,d\kappa\right], \end{aligned}$$

where

$$F(n_3) \equiv \frac{1}{d^3}\int_{x=0}^{\infty}\sqrt{x+n_3^2}f\left(\frac{\pi}{d}\sqrt{x+n_3^2}\right)dx,$$

and

$$F(\kappa) \equiv \lim_{d\to\infty}\left(\frac{1}{d^3}\int_{x=0}^{\infty}\sqrt{x+\kappa^2}f\left(\frac{\pi}{d}\sqrt{x+\kappa^2}\right)dx\right).$$

Then, according to the Euler-Maclaurin summation formula [23, 24],

$$\sum_{n_3=1}^{\infty}F(n_3) - \int_{\kappa=0}^{\infty}F(\kappa)\,d\kappa = -\frac{1}{2}F(0) - \frac{1}{12}\frac{dF(0)}{d\kappa} + \frac{1}{720}\frac{d^3F(0)}{d\kappa^3} + \cdots$$

for $F(\infty) \to 0$. Noting that from $F(\kappa) = \int_{\kappa^2}^{\infty}\sqrt{r}f\left(\frac{\pi}{d}\sqrt{r}\right)dr$ and $dF(\kappa)/d\kappa = -2\kappa^2 f\left(\frac{\pi}{d}\kappa\right)$, one can find $dF(0)/d\kappa = 0$, $d^3F(0)/d\kappa^3 = -4$, and all higher order derivatives vanish if one assumes that all derivatives of the cutoff function vanish at $\kappa = 0$. Finally, the result for the vacuum electromagnetic potential energy $U(d)$ becomes

$$U(d;L,c) = -\Theta_{k'}\frac{\hbar c\pi^2}{1440d^3}L^2.$$

This result is finite, and it is independent of the cutoff function as it should be. The corresponding Casimir force for

the two infinite parallel conducting plates is given by

$$\vec{F}\left(d;L,c\right)=-\frac{\partial U\left(d;L,c\right)}{\partial d}=-\Theta_{k'}\frac{3\hbar c\pi^2}{1440d^4}L^2.$$

The electromagnetic wave has two possible polarizations, $\Theta_{k'}=2$, therefore,

$$\vec{F}\left(d;L,c\right)=-\frac{\hbar c\pi^2}{240d^4}L^2. \tag{2.11}$$

This is the Casimir force between two uncharged parallel conducting plates [3].

It is to be noted that the Euler-Maclaurin summation approach discussed here is just one of the many techniques that can be used in calculating the Casimir force. One can also employ dimensional regularization to compute the Casimir force. This technique can be found in section 2.2 of the reference [14].

2.3.2. Vacuum Pressure Approach

The Casimir force between two perfectly conducting plates can also be calculated from the radiation pressure exerted by a plane wave incident normally on one of the plates. Here the radiation pressure is due to the vacuum electromagnetic fields. The technique discussed here is due to Milonni, Cook and Goggin [25].

The Casimir force is regarded as a consequence of the radiation pressure associated with the zero-point energy of $\hbar\omega/2$ per mode of the field. The main idea behind this techniques is that since the zero-point fields have the momentum $p_i'=\hbar k_i'/2$, the pressure exerted by an incident wave normal to the plates is twice the energy $\mathcal{H}$ per unit volume of the incident field. The pressure imparted to the plate is twice that of the incident wave for perfect conductors. If the wave has an angle of incidence θ_{inc}, the radiation pressure is

$$P=FA^{-1}=2\mathcal{H}\cos^2\theta_{inc}.$$

Two factors of $\cos\theta_{inc}$ appear here because (1) the normal component of the linear momentum imparted to the plate is proportional to $\cos\theta_{inc}$, and (2) the element of area A is increased by $1/\cos\theta_{inc}$ compared with the case of normal incidence. It can be shown then

$$P=2\mathcal{H}\cos^2\theta_{inc}=2\times\frac{1}{2}\times\frac{1}{2}\hbar\omega\times V^{-1}\times\cos^2\theta_{inc}=\frac{\hbar\omega}{2V}\left[k_z'\right]^2\left\|\vec{k'}\right\|^{-2},$$

where the factor of half have been inserted because the zero-point field energy of a mode of energy $\hbar\omega/2$ is divided equally between waves propagating toward and away from each of the plates. The $\cos\theta_{inc}$ factor have been rewritten using the fact that $k_z'=\vec{k'}\bullet\hat{e}_z=\left\|\vec{k'}\right\|\cos\theta_{inc}$, where $\hat{e}_z$ is the unit vector normal to the plate on the inside, $\left\|\vec{k'}\right\|=\omega/c$ and V is the quantization volume.

The successive reflections of the radiation off the plates act to push the plates apart through a pressure P. For large plates where k_x', k_y' take on a continuum of values and the component along the plate gap is $k_z'=n\pi/d$, where n is a positive integer, the total outward pressure on each plate over all possible modes can be written as

$$P_{out}=\frac{\Theta_{k'}\hbar c}{2\pi^2 d}\sum_{n=1}^{\infty}\int_{k_y'=0}^{\infty}\int_{k_x'=0}^{\infty}\frac{\left[n\pi/d\right]^2}{\sqrt{\left[k_x'\right]^2+\left[k_y'\right]^2+\left[n\pi/d\right]^2}}dk_x'dk_y',$$

where $\Theta_{k'}$ is the number of independent polarizations.

External to the plates, the allowed field modes take on a continuum of values. Therefore, by the replacement of $\sum_{n=1}^{\infty}\rightarrow\pi^{-1}d\int_{k_z'=0}^{\infty}$ in the above expression, the total inward pressure on each plate over all possible modes is given by

$$P_{in}=\frac{\Theta_{k'}\hbar c}{2\pi^3}\int_{k_z'=0}^{\infty}\int_{k_y'=0}^{\infty}\int_{k_x'=0}^{\infty}\frac{\left[k_z'\right]^2}{\sqrt{\left[k_x'\right]^2+\left[k_y'\right]^2+\left[k_z'\right]^2}}dk_x'dk_y'dk_z'.$$

Both P_{out} and P_{in} are infinite, but their difference has physical meaning. After some algebraic simplifications, the difference can be written as

$$P_{out} - P_{in} = \frac{\Theta_{k'}\pi^2\hbar c}{8d^4}\left[\sum_{n=1}^{\infty} n^2 \int_{x=0}^{\infty} \frac{dx}{\sqrt{x+n^2}} - \int_{u=0}^{\infty}\int_{x=0}^{\infty} \frac{u^2}{\sqrt{x+u^2}} dxdu\right].$$

An application of the Euler-Maclaurin summation formula [23, 24] leads to the Casimir's result

$$P_{out} - P_{in} = -\frac{\pi^2\hbar c}{240d^4},$$

where $\Theta_{k'} = 2$ for two possible polarizations for zero-point electromagnetic fields.

2.3.3. The Source Theory Approach

The Casimir effect can also be explained by the source theory of Schwinger [14, 15, 17]. An induced dipole $\vec{p}_d$ in a field $\vec{E}$ has an energy $\mathcal{H}_d = -\vec{p}_d \bullet \vec{E}/2$. The factor of one half comes from the fact that this is an induced dipole energy. When there are N dipoles per unit volume, the associated polarization is $\vec{P} = N\vec{p}_d$ and the expectation value of the energy in quantum theory is $\langle \mathcal{H}_d \rangle = -\int \left\langle \vec{p}_d \bullet \vec{E}/2 \right\rangle d^3\vec{R}$. Here the polarizability in $\vec{p}_d$ is left as a free parameter which needs to be determined from the experiment. The expectation value of the energy is then

$$\langle \mathcal{H}_d \rangle = -\frac{1}{2}\int \left\langle \vec{p}_d \bullet \vec{E}^{(+)} + \vec{E}^{(-)} \bullet \vec{p}_d \right\rangle d^3\vec{R},$$

where $\vec{E}^{(\pm)}\left(\vec{R},t\right) = \vec{E}_v^{(\pm)}\left(\vec{R},t\right) + \vec{E}_s^{(\pm)}\left(\vec{R},t\right)$. Here $\vec{E}_v^{(\pm)}$ is the vacuum-field and $\vec{E}_s^{(\pm)}$ is the field due to other sources. Since $\vec{E}_v^{(+)}\left(\vec{R},t\right)|vac\rangle = \langle vac|\,\vec{E}_v^{(-)}\left(\vec{R},t\right) = 0$, the above expectation value of the energy can be written as

$$\langle \mathcal{H}_d \rangle = -\frac{1}{2}\int \left\langle \vec{p}_d \bullet \vec{E}^{(+)} \right\rangle d^3\vec{R} + c.c., \tag{2.12}$$

where $c.c.$ denotes complex conjugation. From the fact that electric field operator can be written as an expansion in the mode functions $\vec{A}_\alpha\left(\vec{R}\right)$,

$$\vec{E}^{(+)} = i\sum_{\alpha}\sqrt{2\pi\hbar\omega_\alpha}\left[a_\alpha(t)\,\vec{A}_\alpha\left(\vec{R}\right) - a_\alpha^\dagger(t)\,\vec{A}_\alpha^*\left(\vec{R}\right)\right],$$

the Heisenberg equation of motion for $\dot{a}_\alpha(t)$ and $a_{\alpha,s}(t)$ are obtained as

$$\dot{a}_\alpha(t) = -i\omega_\alpha a_\alpha(t) + \sqrt{\frac{2\pi\omega_\alpha}{\hbar}}\int \vec{A}_\alpha^*\left(\vec{R}\right) \bullet \vec{p}_d\left(\vec{R},t\right) d^3\vec{R},$$

$$a_{\alpha,s}(t) = \sqrt{\frac{2\pi\omega_\alpha}{\hbar}}\int_0^t \exp\left(i\omega_\alpha\left[t'-t\right]\right)dt' \int \vec{A}_\alpha^*\left(\vec{R}\right) \bullet \vec{p}_d\left(\vec{R},t'\right) d^3\vec{R},$$

where $a_{\alpha,s}(t)$ is the source contribution part of $a_\alpha(t)$. The "positive frequency" or the photon annihilation part of $\vec{E}_s^{(+)}\left(\vec{R},t\right)$ can then be written as

$$\begin{aligned}\vec{E}_s^{(+)}\left(\vec{R},t\right) &= 2\pi i\sum_\alpha \omega_\alpha \vec{A}_\alpha\left(\vec{R}\right)\int_0^t \exp\left(i\omega_\alpha\left[t'-t\right]\right)dt'\int \vec{A}_\alpha^*\left(\vec{R}'\right)\bullet\vec{p}_d\left(\vec{R}',t'\right)d^3\vec{R}' \\ &= 2\pi i\int\int_0^t\sum_\alpha \omega_\alpha\vec{A}_\alpha\left(\vec{R}\right)\vec{A}_\alpha^*\left(\vec{R}'\right)\exp\left(i\omega_\alpha\left[t'-t\right]\right)\bullet\vec{p}_d\left(\vec{R}',t'\right)dt'd^3\vec{R}' \\ &\equiv 8\pi\int\int_0^t \overleftrightarrow{G^{(+)}}\left(\vec{R},\vec{R}';t,t'\right)\bullet\vec{p}_d\left(\vec{R}',t'\right)dt'd^3\vec{R}',\end{aligned}$$

where $\overleftrightarrow{G^{(+)}}\left(\vec{R},\vec{R}';t,t'\right)$ is a dyadic Green function

$$\overleftrightarrow{G^{(+)}}\left(\vec{R},\vec{R}';t,t'\right)=\frac{i}{4}\sum_\alpha\omega_\alpha\vec{A}_\alpha\left(\vec{R}\right)\vec{A}_\alpha^*\left(\vec{R}'\right)\exp\left(i\omega_\alpha\left[t'-t\right]\right). \tag{2.13}$$

Equations (2.12) and (2.13) lead to the result

$$\langle\mathcal{H}_d\rangle=-8\pi\mathbb{R}_E\int_{\vec{R}}\int_{\vec{R}'}\int_0^t\overleftrightarrow{G_{ij}^{(+)}}\left(\vec{R},\vec{R}';t,t'\right)\left\langle\vec{p}_{d,j}\left(\vec{R},t\right)\bullet\vec{p}_{d,i}\left(\vec{R}',t'\right)\right\rangle dt'd^3\vec{R}'d^3\vec{R},$$

where the summation over repeated indices is understood, and $\mathbb{R}_E$ denotes the real part. The above result is the energy of the induced dipoles in a medium due to the source fields produced by the dipoles. It can be further shown that for the infinitesimal variations in energy,

$$\langle\delta\mathcal{H}_d\rangle=-4\mathbb{R}_E\int_{\vec{R}}\int_{\vec{R}'}\int_0^t\int_0^\infty\Gamma_{ij}\left(\vec{R},\vec{R}',\omega\right)\left\langle\vec{p}_{d,j}\left(\vec{R},t\right)\bullet\vec{p}_{d,i}\left(\vec{R}',t'\right)\right\rangle\exp\left(i\omega\left[t'-t\right]\right)d\omega dt'd^3\vec{R}'d^3\vec{R},$$

where $\Gamma_{ij}\left(\vec{R},\vec{R}',\omega\right)$ is related to $\overleftrightarrow{G_{ij}^{(+)}}\left(\vec{R},\vec{R}';t,t'\right)$ through the relation

$$\overleftrightarrow{G^{(+)}}\left(\vec{R},\vec{R}';t,t'\right)=\frac{1}{2\pi}\int_0^\infty\Gamma_{ij}\left(\vec{R},\vec{R}',\omega\right)\exp\left(i\omega\left[t'-t\right]\right)d\omega.$$

The force per unit area can then be shown to be

$$F(d)=\frac{i\hbar}{8\pi^3}\int_0^\infty\int_{\vec{k}_\perp}\left[\varepsilon_2-\varepsilon_3\right]\Gamma_{jj}\left(d,d,\vec{k}_\perp,\omega\right)d^2\vec{k}_\perp d\omega, \tag{2.14}$$

where the factor $\left[\varepsilon_2-\varepsilon_3\right]\Gamma_{jj}\left(d,d,\vec{k}_\perp,\omega\right)$ is given by

$$\begin{aligned}\left[\varepsilon_2-\varepsilon_3\right]\Gamma_{jj}\left(d,d,\vec{k}_\perp,\omega\right) &= 2\left[K_3-K_2\right]+2K_3\left\{\left(\left[\frac{K_1+K_3}{K_1-K_3}\right]\left[\frac{K_2+K_3}{K_2-K_3}\right]\exp\left(2K_3d\right)-1\right)^{-1}\right. \\ &\left.+\left(\left[\frac{\varepsilon_3K_1+\varepsilon_1K_3}{\varepsilon_3K_1-\varepsilon_1K_3}\right]\left[\frac{\varepsilon_3K_2+\varepsilon_2K_3}{\varepsilon_3K_2-\varepsilon_2K_3}\right]\exp\left(2K_3d\right)-1\right)^{-1}\right\}.\end{aligned}$$

Here $K^2\equiv k_\perp^2-c^{-2}\omega^2\varepsilon(\omega)$ and ε_i is the dielectric constant corresponding to the region i. The plate configuration corresponding to the source theory description discussed above is illustrated in Figure 2.3.

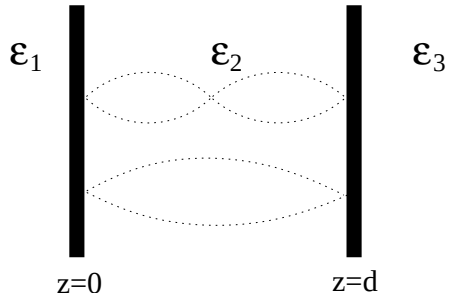

Figure 2.3.: A cross-sectional view of two infinite parallel conducting plates. The plates are separated by a gap distance of $z = d$. Also, the three regions have different dielectric constants $\varepsilon_i(\omega)$.

The expression of force, equation (2.14), is derived from the source theory of Schwinger, Milton and DeRaad [14, 15]. It reproduces the result of Lifshitz [21, 22], which is a generalization of the Casimir force involving perfectly conducting parallel plates to that involving dielectric media. The details of this brief outline of the source theory description can be found in references [14, 17].

3. Reflection Dynamics

Once the idea of physics of vacuum polarization is taken for granted, one can move forward to calculate the effective, temperature-averaged energy due to the dipole-dipole interactions with the time retardation effect folded into the van der Waals interaction. The energy between the dielectric or conducting media is then obtained from the allowed modes of electromagnetic waves determined by the Maxwell equations together with the electromagnetic boundary conditions, granted that the most significant zero-point electromagnetic field wavelengths determining the interaction are large when compared with the spacing of the lattice points in the media. Under such an assumption, the effect of all the multiple dipole scattering by atoms in the dielectric or conducting media is to simply enforce the macroscopic reflection laws of electromagnetic waves; and this allows the macroscopic electromagnetic theory to be used with impunity in calculation of the Casimir force, granted the classical electromagnetic fields have been quantized. The Casimir force is then simply obtained by taking the negative gradient of the energy in space.

In principle, the atomistic approach utilizing the Casimir-Polder interaction explains the Casimir effect observed between any system. Unfortunately, the pairwise summation of the intermolecular forces for systems containing large number of atoms can become very complicated. H. B. G. Casimir, realizing the linear relationship between the field and the polarization, devised an easier approach to the calculation of the Casimir effect for large systems such as two perfectly conducting parallel plates. This latter development is the description of the Euler-Maclaurin summation approach shown previously, in which the Casimir force have been found by utilizing the field boundary conditions only. The vacuum pressure approach originally introduced by Milonni, Cook and Goggin [25] is a simple elaboration of Casimir's latter invention utilizing the boundary conditions. The source theory description of Schwinger is an alternate explanation of the Casimir effect which can be inherently traced to the retarded van der Waals interaction.

Because all four approaches which were previously mentioned, (1) the Casimir-Polder interaction, (2) the Euler-Maclaurin summation, (3) the vacuum pressure and (4) the source theory, stem from the same physics of vacuum polarization, they are equivalent. The preference of one over another mainly depends on the geometry of the boundaries being investigated. For the type of physical arrangements of boundary configurations that are being considered in this thesis, the vacuum pressure approach provides the most natural route to the Casimir force calculation. The three physical arrangements for the boundary configurations considered in this thesis are: (1) the plate-hemisphere, (2) the hemisphere-hemisphere and (3) a sphere formed by brining two hemispheres together. Because the geometric configurations of items (2) and (3) are special versions of the more general, plate-hemisphere configuration, the basic reflection dynamics needed for the plate-hemisphere case is worked out first. The results can then be applied to the hemisphere-hemisphere and the sphere configurations later.

The vacuum-fields are subject to the appropriate boundary conditions. For boundaries made of perfect conductors, the transverse components of the electric field are zero at the surface. For this simplification, the skin depth of penetration is considered as zero. The plate-hemisphere under consideration is shown in Figure 3.1. The solutions to the vacuum-fields are that of the Cartesian version of the free Maxwell field vector potential differential equation $\nabla^2 \vec{A}\left(\vec{R}\right) - c^{-2}\partial_t^2 \vec{A}\left(\vec{R}\right) = 0$, where the Coulomb gauge $\vec{\nabla} \bullet \vec{A} = 0$ and the absence of the source $\Phi\left(\rho, \left\|\vec{R}\right\|\right) = 0$ have been imposed. The electric and the magnetic field component of the vacuum-field are given by $\vec{E} = -c^{-1}\partial_t \vec{A}$ and $\vec{B} = \vec{\nabla} \times \vec{A}$, where $\vec{A}$ is the free field vector potential. The zero value requirement for the transversal component of the electric field at the perfect conductor surface implies the solution for $\vec{E}$ is in the form of $\vec{E} \propto \sin\left(2\pi\lambda^{-1}\left\|\vec{L}\right\|\right)$, where λ is the wavelength and $\left\|\vec{L}\right\|$ is the path length between the boundaries. The wavelength is restricted by the condition $\lambda \leq 2\left\|\vec{R'}_2 - \vec{R'}_1\right\| \equiv 2\xi_2$, where $\vec{R'}_2$ and $\vec{R'}_1$ are two immediate reflection points in the hemisphere cavity of Figure 3.1. In order to compute the modes allowed inside the hemisphere resonator, a detailed knowledge of the reflections occurring in the hemisphere cavity is needed. This is described in the following section.

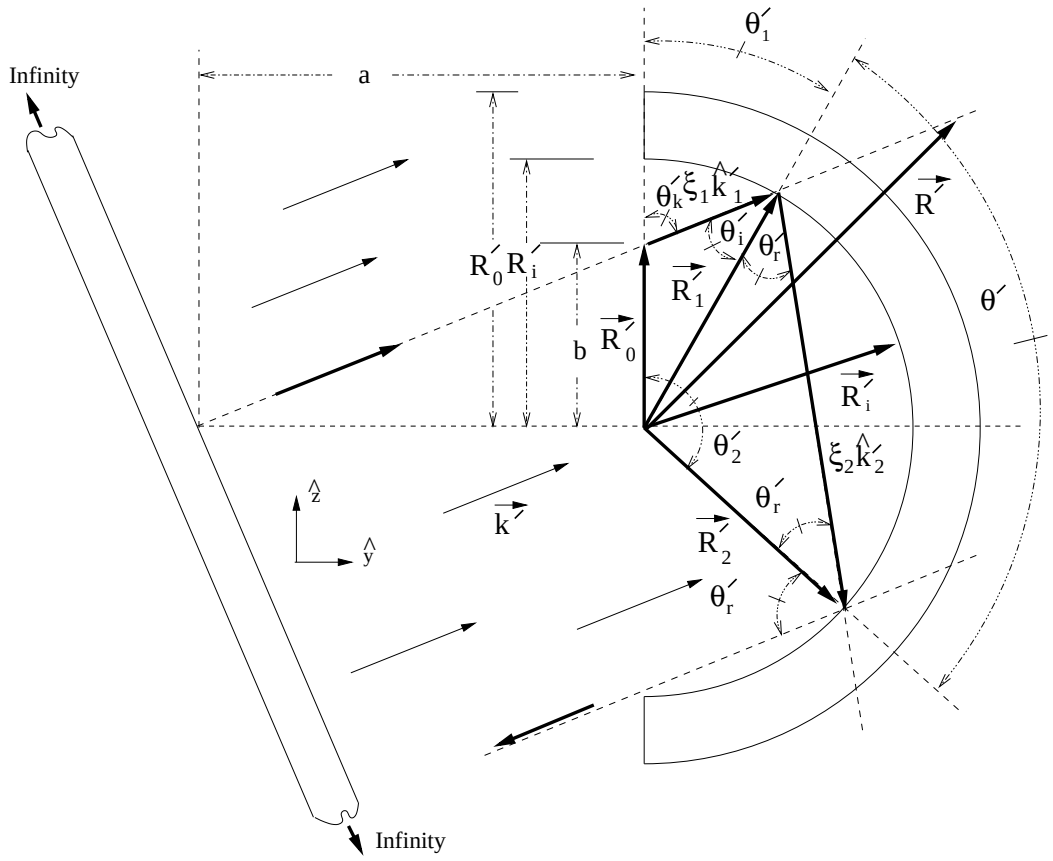

Figure 3.1.: The plane of incidence view of plate-hemisphere configuration. The waves that are supported through internal reflections in the hemisphere cavity must satisfy the relation $\lambda \leq 2\left\|\vec{R'}_2 - \vec{R'}_1\right\|$.

3.1. Reflection Points on the Surface of a Resonator

The wave vector directed along an arbitrary direction in Cartesian coordinates is written as

$$\vec{k'}_1\left(k'_{1,x}, k'_{1,y}, k'_{1,z}\right) = \sum_{i=1}^{3} k'_{1,i}\hat{e_i}, \qquad k'_{1,i} = \begin{cases} i = 1 \rightarrow k'_{1,x}, & \hat{e_1} = \hat{x}, \\ i = 2 \rightarrow k'_{1,y}, & \hat{e_2} = \hat{y} \\ i = 3 \rightarrow k'_{1,z}, & \hat{e_3} = \hat{z}. \end{cases} \tag{3.1}$$

Hence, the unit wave vector, $\hat{k'}_1 = \left\|\vec{k'}_1\right\|^{-1} \sum_{i=1}^{3} k'_{1,i}\hat{e_i}$. Define the initial position $\vec{R'}_0$ for the incident wave $\vec{k'}_1$,

$$\vec{R'}_0\left(r'_{0,x}, r'_{0,y}, r'_{0,z}\right) = \sum_{i=1}^{3} r'_{0,i}\hat{e_i}, \qquad r'_{0,i} = \begin{cases} i = 1 \rightarrow r'_{0,x}, \\ i = 2 \rightarrow r'_{0,y}, \\ i = 3 \rightarrow r'_{0,z}. \end{cases} \tag{3.2}$$

Here it should be noted that $\vec{R'}_0$ really has only components $r'_{0,x}$ and $r'_{0,z}$. But nevertheless, one can always set $r'_{0,y} = 0$ whenever needed. Since no particular wave vectors with specified wave lengths are prescribed initially, it is desirable to employ a parameterization scheme to represent these wave vectors. The line segment traced out by this

wave vector $\hat{k'}_1$ is formulated in the parametric form

$$\vec{R'}_1 = \xi_1 \hat{k'}_1 + \vec{R'}_0 = \sum_{i=1}^{3} \left[r'_{0,i} + \xi_1 \left\| \vec{k'}_1 \right\|^{-1} k'_{1,i} \right] \hat{e}_i, \tag{3.3}$$

where the variable ξ_1 is a positive definite parameter. The restriction $\xi_1 \geq 0$ is necessary because the direction of the wave propagation is set by $\hat{k'}_1$. Here $\vec{R'}_1$ is the first reflection point on the hemisphere. In terms of spherical coordinate variables, $\vec{R'}_1$ takes the form

$$\vec{R'}_1 \left(r'_i, \theta'_1, \phi'_1 \right) = r'_i \sum_{i=1}^{3} \Lambda'_{1,i} \hat{e}_i, \qquad \begin{cases} \Lambda'_{1,1} = \sin\theta'_1 \cos\phi'_1, \\ \Lambda'_{1,2} = \sin\theta'_1 \sin\phi'_1, \\ \Lambda'_{1,3} = \cos\theta'_1, \end{cases} \tag{3.4}$$

where r'_i is the hemisphere radius, θ'_1 and ϕ'_1 are the polar and the azimuthal angle respectively of $\vec{R'}_1$ at the first reflection point. Notice that subscript i of r'_i denotes "inner radius" not a summation index.

By combining equations (3.3) and (3.4), we can solve for the parameter ξ_1. It can be shown that

$$\xi_1 \equiv \xi_{1,p} = -\hat{k'}_1 \bullet \vec{R'}_0 + \sqrt{\left[\hat{k'}_1 \bullet \vec{R'}_0 \right]^2 + [r'_i]^2 - \left\| \vec{R'}_0 \right\|^2}, \tag{3.5}$$

where the positive root for ξ_1 have been chosen due to the restriction $\xi_1 \geq 0$. The detailed proof of equation (3.5) is given in Appendix A, where the same equation is designated as equation (A.11).

Substituting ξ_1 in equation (3.3), the first reflection point off the inner hemisphere surface is expressed as

$$\vec{R'}_1 \left(\xi_{1,p}; \vec{R'}_0, \hat{k'}_1 \right) = \sum_{i=1}^{3} \left[r'_{0,i} + \xi_{1,p} \left\| \vec{k'}_1 \right\|^{-1} k'_{1,i} \right] \hat{e}_i, \tag{3.6}$$

where $\xi_{1,p}$ is from equation (3.5).

The incoming wave vector $\vec{k'}_i$ can always be decomposed into parallel and perpendicular with respect to the local reflection surface components, $\vec{k'}_{i,\parallel}$ and $\vec{k'}_{i,\perp}$. It is shown in equation (A.14) of Appendix A that the reflected wave vector $\vec{k'}_r$ has the form $\vec{k'}_r = \alpha_{r,\perp} \left[\hat{n'} \times \vec{k'}_i \right] \times \hat{n'} - \alpha_{r,\parallel} \hat{n'} \bullet \vec{k'}_i \hat{n'}$, where the quantities $\alpha_{r,\parallel}$ and $\alpha_{r,\perp}$ are the reflection coefficients and $\hat{n'}$ is a unit surface normal. For the perfect reflecting surfaces, $\alpha_{r,\parallel} = \alpha_{r,\perp} = 1$. In component form, $\vec{k'}_r = \sum_{l=1}^{3} \left\{ \alpha_{r,\perp} \left[n'_n k'_{i,l} n'_n - n'_l k'_{i,n} n'_n \right] - \alpha_{r,\parallel} n'_n k'_{i,n} n'_l \right\} \hat{e}_l$, where it is understood that $\hat{n'}$ is already normalized and Einstein summation convention is applied to the index n. The second reflection point $\vec{R'}_2$ is found then by repeating the steps done for $\vec{R'}_1$ and by using the expression $\vec{k'}_r \equiv \vec{k'}_r / \left\| \vec{k'}_r \right\|$,

$$\vec{R'}_2 = \vec{R'}_1 + \xi_{2,p} \hat{k'}_r = \vec{R'}_1 + \xi_{2,p} \frac{\alpha_{r,\perp} \left[\hat{n'} \times \vec{k'}_i \right] \times \hat{n'} - \alpha_{r,\parallel} \hat{n'} \bullet \vec{k'}_i \hat{n'}}{\left\| \alpha_{r,\perp} \left[\hat{n'} \times \vec{k'}_i \right] \times \hat{n'} - \alpha_{r,\parallel} \hat{n'} \bullet \vec{k'}_i \hat{n'} \right\|},$$

where $\xi_{2,p}$ is the new positive definite parameter for the second reflection point.

The incidence plane of reflection is determined solely by the incident wave $\vec{k'}_i$ and the local normal $\vec{n'}_i$ of the reflecting surface. It is important to recognize the fact that the subsequent successive reflections of this incoming wave will be confined to this particular incident plane. This incident plane can be characterized by a unit normal vector. For the system shown in Figure 3.1, $\vec{k'}_i = \vec{k'}_1$ and $\vec{n'}_{n'_i,1} = -\xi_{1,p} \hat{k'}_1 - \vec{R'}_0$. The unit vector which represents the incident plane is given by $\hat{n'}_{p,1} = -\left\| \vec{n'}_{p,1} \right\|^{-1} \sum_{i=1}^{3} \epsilon_{ijk} k'_{1,j} r'_{0,k} \hat{e}_i$, where the summations over indices j and k are implicit. If the plane of incidence is represented by a scalar function $f\left(x', y', z'\right)$, then its unit normal vector $\hat{n'}_{p,1}$ will satisfy

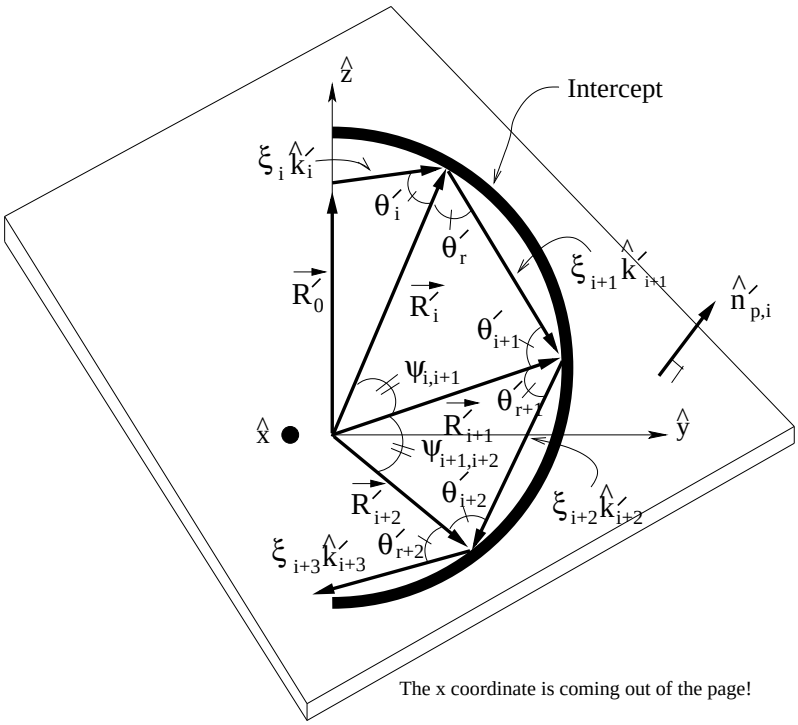

Figure 3.2.: The thick line shown here represents the intersection between hemisphere surface and the plane of incidence. The unit vector normal to the incident plane is given by $\hat{n'}_{p,1} = -\left\|\vec{n'}_{p,1}\right\|^{-1} \sum_{i=1}^{3} \epsilon_{ijk} k'_{1,j} r'_{0,k} \hat{e}_i$.

the relationship $\hat{n'}_{p,1} \propto \vec{\nabla}' f_{p,1}(x', y', z')$. It is shown from equation (A.43) of Appendix A that

$$f_{p,1}(\nu'_1, \nu'_2, \nu'_3) = -\left\|\vec{n'}_{p,1}\right\|^{-1} \sum_{i=1}^{3} \epsilon_{ijk} k'_{1,j} r'_{0,k} \nu'_i, \qquad i = \begin{cases} 1 \to \nu'_1 = x', \\ 2 \to \nu'_2 = y', \\ 3 \to \nu'_3 = z', \end{cases} \tag{3.7}$$

where $-\infty \leq \{\nu'_1 = x', \nu'_2 = y', \nu'_3 = z'\} \leq \infty$.

The surface of a sphere or hemisphere is defined through the relation $f_{hemi}(x', y', z') = [r'_i]^2 - \sum_{i=1}^{3} [\nu'_i]^2$, where r'_i is the radius of sphere and the subscript i denotes the inner surface. The intercept of interest is shown in Figure 3.2. The intersection between the hemisphere surface and the incidence plane $f_{p,1}(\nu'_1, \nu'_2, \nu'_3)$ is given by $f_{hemi}(x', y', z') - f_{p,1}(x', y', z') = 0$. After substitution of $f_{p,1}(x', y', z')$ and $f_{hemi}(x', y', z')$, we have

$$\sum_{i=1}^{3} \left\{ [\nu'_i]^2 - \left\|\vec{n'}_{p,1}\right\|^{-1} \epsilon_{ijk} k'_{1,j} r'_{0,k} \nu'_i \right\} - [r'_i]^2 = 0, \qquad i = \begin{cases} 1 \to \nu'_1 = x', \\ 2 \to \nu'_2 = y', \\ 3 \to \nu'_3 = z'. \end{cases}$$

The term $[r'_i]^2$ can be rewritten in the form $[r'_i]^2 = \sum_{i=1}^{3} \left[r'_{i,i}\right]^2$, where $r'_{i,1} = r'_{i,x'}$, $r'_{i,2} = r'_{i,y'}$ and $r'_{i,3} = r'_{i,z'}$. Solving for ν'_i, it can be shown from equation (A.51) of Appendix A that

$$\nu'_i = \frac{1}{2} \left\|\vec{n'}_{p,1}\right\|^{-1} \epsilon_{ijk} k'_{1,j} r'_{0,k} \pm \left\{ \left[\frac{1}{2} \left\|\vec{n'}_{p,1}\right\|^{-1} \epsilon_{ijk} k'_{1,j} r'_{0,k} \right]^2 + \left[r'_{i,i}\right]^2 \right\}^{1/2}, \qquad i = 1, 2, 3, \tag{3.8}$$

where ϵ_{ijk} is the Levi-Civita coefficient. The result for ν'_i shown above provide a set of discrete reflection points found by the intercept between the hemisphere and the plane of incidence.

Using spherical coordinate representations for the variables $r'_{i,1}$, $r'_{i,2}$ and $r'_{i,3}$, the initial reflection point $\vec{R'}_1$ can be

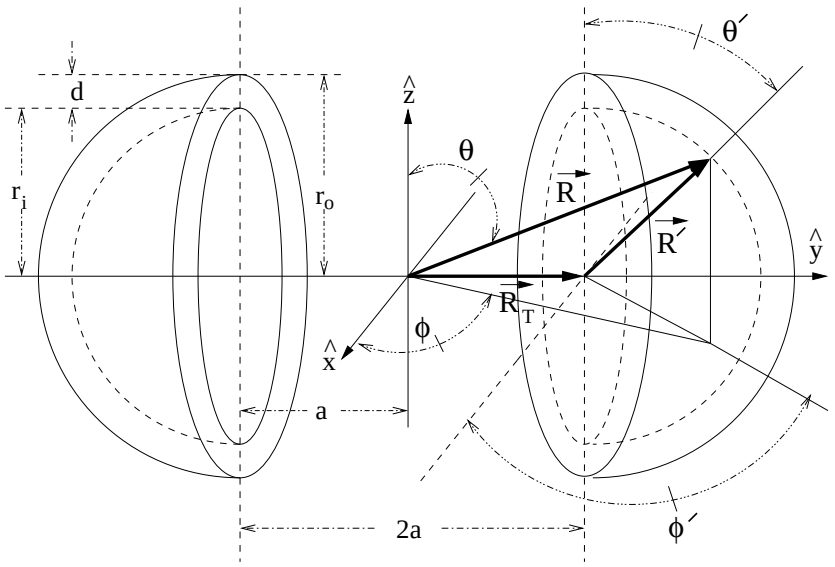

Figure 3.3.: The surface of the hemisphere-hemisphere configuration can be described relative to the system origin through $\vec{R}$, or relative to the hemisphere centers through $\vec{R}'$.

expressed in terms of the spherical coordinate variables $(r_i', \theta_1', \phi_1')$ (equation (A.109) of Appendix A),

$$\vec{R}'_1\,(r_i', \theta_1', \phi_1') = \sum_{i=1}^{3} \nu'_{1,i}\,(r_i', \theta_1', \phi_1')\,\hat{e}_i, \qquad i = \begin{cases} 1 \to \nu'_{1,1} = r_i' \sin\theta_1' \cos\phi_1', \\ 2 \to \nu'_{1,2} = r_i' \sin\theta_1' \sin\phi_1', \\ 3 \to \nu'_{1,3} = r_i' \cos\theta_1', \end{cases} \tag{3.9}$$

where r_i' is the hemisphere radius, ϕ_1' and θ_1', the polar and azimuthal angle, respectively. They are defined in equations (A.102), (A.103), (A.107) and (A.108) of Appendix A. Similarly, the second reflection point on the inner hemisphere surface is given by equation (A.151) of Appendix A:

$$\vec{R}'_2\,(r_i', \theta_2', \phi_2') = \sum_{i=1}^{3} \nu'_{2,i}\,(r_i', \theta_2', \phi_2')\,\hat{e}_i, \qquad i = \begin{cases} 1 \to \nu'_{2,1} = r_i' \sin\theta_2' \cos\phi_2', \\ 2 \to \nu'_{2,2} = r_i' \sin\theta_2' \sin\phi_2', \\ 3 \to \nu'_{2,3} = r_i' \cos\theta_2', \end{cases} \tag{3.10}$$

where the spherical angles ϕ_2' and θ_2' are defined in equations (A.143), (A.144), (A.148) and (A.149) of Appendix A. In general, leaving the details to Appendix A, the Nth reflection point inside the hemisphere is, from equation (A.162) of Appendix A,

$$\vec{R}'_N\,(r_i', \theta_N', \phi_N') = \sum_{i=1}^{3} \nu'_{N,i}\,(r_i', \theta_N', \phi_N')\,\hat{e}_i, \qquad i = \begin{cases} 1 \to \nu'_{N,1} = r_i' \sin\theta_N' \cos\phi_N', \\ 2 \to \nu'_{N,2} = r_i' \sin\theta_N' \sin\phi_N', \\ 3 \to \nu'_{N,3} = r_i' \cos\theta_N', \end{cases} \tag{3.11}$$

where the spherical angles θ_N' and ϕ_N' are defined in equations (A.158), (A.159), (A.160) and (A.161) of Appendix A. The details of all the work shown up to this point can be found in Appendix A.

The previously shown reflection points ($\vec{R}'_1$, $\vec{R}'_2$ and $\vec{R}'_N$) were described relative to the hemisphere center. In many cases, the preferred choice for the system origin, from which the variables are defined, depend on the physical arrangements of the system being considered. For a sphere, the natural choice for the origin is its center from which the spherical variables (r_i', θ', ϕ') are prescribed. For more complicated configuration shown in Figure 3.3, the preferred choice for origin really depends on the problem at hand. For this reason, a set of transformation rules between (r_i', θ', ϕ') and (r_i, θ, ϕ) is sought. Here the primed set is defined relative to the sphere center and the unprimed set is defined relative to the origin of the global configuration. In terms of the Cartesian variables, the two vectors $\vec{R}$ and $\vec{R}'$

describing an identical point on the hemisphere surface are expressed by

$$\vec{R}\left(\nu_1,\nu_2,\nu_3\right)=\sum_{i=1}^{3}\nu_i\hat{e_i},\qquad \vec{R}'\left(\nu_1',\nu_2',\nu_3'\right)=\sum_{i=1}^{3}\nu_i'\hat{e_i}, \tag{3.12}$$

where $(\nu_1,\nu_2,\nu_3)\rightarrow(x,y,z)$, $(\nu_1',\nu_2',\nu_3')\rightarrow(x',y',z')$ and $(\hat{e_1},\hat{e_2},\hat{e_3})\rightarrow(\hat{x},\hat{y},\hat{z})$. The vectors $\vec{R}$ and $\vec{R}'$ are connected through the relation $\vec{R}\left(\nu_1,\nu_2,\nu_3\right)=\sum_{i=1}^{3}\left[\nu_{T,i}+\nu_i'\right]\hat{e_i}$ with $\vec{R}_T\equiv\sum_{i=1}^{3}\nu_{T,i}\hat{e_i}$ which represents the position of hemisphere center relative to the system origin. As a result, we have $\sum_{i=1}^{3}\left[\nu_i-\nu_{T,i}-\nu_i'\right]\hat{e_i}=0$. In terms of the spherical coordinate representation for (ν_1,ν_2,ν_3) and (ν_1',ν_2',ν_3'), we can solve for θ and ϕ. As shown from equations (B.10) and (B.12) of Appendix B, the result is

$$\phi\equiv\grave{\phi}\left(r_i',\theta',\phi',\nu_{T,1},\nu_{T,2}\right)=\arctan\left(\frac{\nu_{T,2}+r_i'\sin\theta'\sin\phi'}{\nu_{T,1}+r_i'\sin\theta'\cos\phi'}\right), \tag{3.13}$$

$$\begin{aligned}\theta&\equiv\grave{\theta}\left(r_i',\theta',\phi',\vec{R}_T\right)\\&=\arctan\left(\frac{\left\{\nu_{T,1}+\nu_{T,2}+r_i'\sin\theta'\left[\cos\phi'+\sin\phi'\right]\right\}\left[\nu_{T,3}+r_i'\cos\theta'\right]^{-1}}{\cos\left(\arctan\left(\frac{\nu_{T,2}+r_i'\sin\theta'\sin\phi'}{\nu_{T,1}+r_i'\sin\theta'\cos\phi'}\right)\right)+\sin\left(\arctan\left(\frac{\nu_{T,2}+r_i'\sin\theta'\sin\phi'}{\nu_{T,1}+r_i'\sin\theta'\cos\phi'}\right)\right)}\right),\end{aligned} \tag{3.14}$$

where the notation $\grave{\phi}$ and $\grave{\theta}$ indicates that ϕ and θ are explicitly expressed in terms of the primed variables, respectively. It is to be noticed that for the configuration shown in Figure 3.3, the hemisphere center is only shifted along $\hat{y}$ by an amount of $\nu_{T,2}=a$, which leads to $\nu_{T,i\neq2}=0$. Nevertheless, the derivation have been done for the case where $\nu_{T,i}\neq0$, $i=1,2,3$ for the generalization purpose.

With the magnitude $\left\|\vec{R}\right\|=\left\{\sum_{i=1}^{3}\left[\nu_{T,i}+r_i'\Lambda_i'\right]^2\right\}^{1/2}$, where $\Lambda_1'\left(\theta',\phi'\right)=\sin\theta'\cos\phi'$, $\Lambda_2'\left(\theta',\phi'\right)=\sin\theta'\sin\phi'$ and $\Lambda_3'\left(\theta'\right)=\cos\theta'$, the vector $\vec{R}\left(r_i',\grave{\vec{\Lambda}},\vec{\Lambda}',\vec{R}_T\right)$ is given by equation (B.13) of Appendix B as

$$\vec{R}\left(r_i',\grave{\vec{\Lambda}},\vec{\Lambda}',\vec{R}_T\right)=\left\{\sum_{i=1}^{3}\left[\nu_{T,i}+r_i'\Lambda_i'\right]^2\right\}^{1/2}\sum_{i=1}^{3}\grave{\Lambda}_i\hat{e_i},\qquad\begin{cases}\grave{\Lambda}_1\left(\grave{\theta},\grave{\phi}\right)=\sin\grave{\theta}\cos\grave{\phi},\\ \grave{\Lambda}_2\left(\grave{\theta},\grave{\phi}\right)=\sin\grave{\theta}\sin\grave{\phi},\\ \grave{\Lambda}_3\left(\grave{\theta}\right)=\cos\grave{\theta}.\end{cases} \tag{3.15}$$

The details of this section can be found in Appendices A and B.

3.2. Selected Configurations

Having found all of the wave reflection points in the hemisphere resonator, the net momentum imparted on both the inner and outer surfaces by the incident wave is computed for three configurations: (1) the sphere, (2) the hemisphere-hemisphere and (3) the plate-hemisphere. The surface element that is being impinged upon by an incident wave would experience the net momentum change in an amount proportional to $\triangle\vec{k'}_{inner}\left(;\vec{R'}_{s,1},\vec{R'}_{s,0}\right)$ on the inner side, and $\triangle\vec{k'}_{outer}\left(;\vec{R'}_{s,1}+a\hat{R'}_{s,1}\right)$ on the outer side of the surface. The quantities $\triangle\vec{k'}_{inner}$ and $\triangle\vec{k'}_{outer}$ are due to the contribution from a single mode of wave traveling in particular direction. The notation $\left(;\vec{R'}_{s,1},\vec{R'}_{s,0}\right)$ of $\triangle\vec{k'}_{inner}$ denotes that it is defined in terms of the initial reflection point $\vec{R'}_{s,1}$ on the surface and the initial crossing point $\vec{R'}_{s,0}$ of the hemisphere opening (or the sphere cross-section). The notation $\left(;\vec{R'}_{s,1}+a\hat{R'}_{s,1}\right)$ of $\triangle\vec{k'}_{outer}$ implies the outer surface reflection point. The total resultant imparted momentum on the hemisphere or sphere is found by summing over all modes of wave, over all directions.

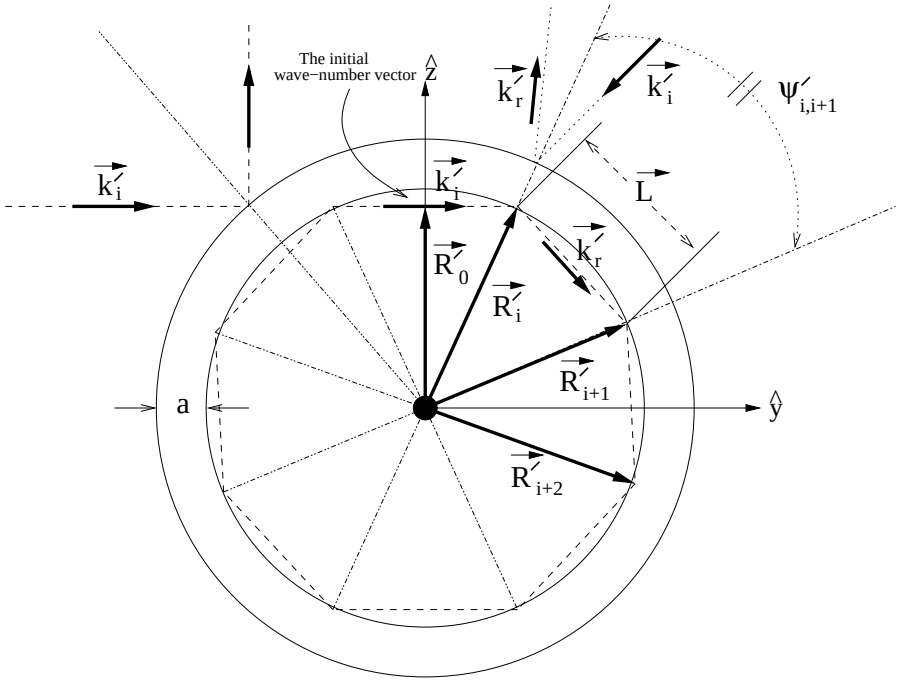

Figure 3.4.: Inside the cavity, an incident wave $\vec{k'}_i$ on first impact point $\vec{R'}_i$ induces a series of reflections that propagate throughout the entire inner cavity. Similarly, a wave $\vec{k'}_i$ incident on the impact point $\vec{R'}_i + a\hat{R'}_i$, where a is the thickness of the sphere, induces reflected wave of magnitude $\left\|\vec{k'}_i\right\|$. The resultant wave direction in the external region is along $\vec{R'}_i$ and the resultant wave direction in the resonator is along $-\vec{R'}_i$ due to the fact there is exactly another wave vector traveling in opposite direction in both regions. In both cases, the reflected and incident waves have equal magnitude due to the fact that the sphere is assumed to be a perfect conductor.

3.2.1. Hollow Spherical Shell

A sphere formed by bringing in two hemispheres together is shown in Figure 3.4. The resultant change in wave vector direction upon reflection at the inner surface of the sphere is from the equation (C.4) of Appendix C1,

$$\triangle\vec{k'}_{inner}\left(;\vec{R'}_{s,1},\vec{R'}_{s,0}\right) = -\frac{4n\pi\cos\theta_{inc}}{\left\|\vec{R}_{s,2}\left(r'_i,\vec{\Lambda}'_{s,2}\right)-\vec{R}_{s,1}\left(r'_i,\vec{\Lambda}'_{s,1}\right)\right\|}\hat{R'}_{s,1}, \qquad \begin{cases} 0\le\theta_{inc}<\pi/2, \\ n=1,2,\cdots, \end{cases} \tag{3.16}$$

where θ_{inc} is from equation (A.115); $\vec{R}_{s,1}\left(r'_i,\vec{\Lambda}'_{s,1}\right)$ and $\vec{R}_{s,2}\left(r'_i,\vec{\Lambda}'_{s,2}\right)$ follow the generic form shown in the equation (C.1) of Appendix C1,

$$\vec{R}_{s,N}\left(r'_i,\vec{\Lambda}'_{s,N}\right) = r'_i\sum_{i=1}^{3}\Lambda'_{s,N,i}\hat{e}_i, \qquad \begin{cases} \Lambda'_{s,N,1}\left(\theta'_{s,N},\phi'_{s,N}\right)=\sin\theta'_{s,N}\cos\phi'_{s,N}, \\ \Lambda'_{s,N,2}\left(\theta'_{s,N},\phi'_{s,N}\right)=\sin\theta'_{s,N}\sin\phi'_{s,N}, \\ \Lambda'_{s,N,3}\left(\theta'_{s,N}\right)=\cos\theta'_{s,N}. \end{cases} \tag{3.17}$$

Here the label s have been attached to denote a sphere and the obvious index changes in the spherical variables $\theta'_{s,N}$ and $\phi'_{s,N}$ are understood from the set of equations (A.158), (A.159), (A.160) and (A.161).

Similarly, the resultant change in wave vector direction upon reflection at the outer surface of the sphere is from equation (C.5) of Appendix C1,

$$\triangle\vec{k'}_{outer}\left(;\vec{R'}_{s,1}+a\hat{R'}_{s,1}\right) = 4\left\|\vec{k'}_{i,f}\right\|\cos\theta_{inc}\hat{R'}_{s,1}, \qquad \begin{cases} 0\le\theta_{inc}<\pi/2, \\ n=1,2,\cdots. \end{cases} \tag{3.18}$$

The details of this section can be found in Appendix C1.

3.2.2. Hemisphere-Hemisphere

For the hemisphere, the changes in wave vector directions after the reflection at a point $\hat{R'}_{h,1}$ inside the resonator, or after the reflection at location $\vec{R'}_{h,1} + a\hat{R'}_{h,1}$ outside the hemisphere, can be found from equations (3.16) and (3.18) with obvious subscript changes,

$$\triangle\vec{k'}_{inner}\left(;\vec{R'}_{h,1},\vec{R'}_{h,0}\right) = -\frac{4n\pi\cos\theta_{inc}}{\left\|\vec{R}_{h,2}\left(r'_i,\vec{\Lambda}'_{h,2}\right)-\vec{R}_{h,1}\left(r'_i,\vec{\Lambda}'_{h,1}\right)\right\|}\hat{R'}_{h,1}, \qquad \left\{\begin{array}{c} 0\le\theta_{inc}<\pi/2, \\ n=1,2,\cdots; \end{array}\right. \tag{3.19}$$

$$\triangle\vec{k'}_{outer}\left(;\vec{R'}_{h,1}+a\hat{R'}_{h,1}\right) = 4\left\|\vec{k'}_{i,f}\right\|\cos\theta_{inc}\hat{R'}_{h,1}, \qquad \left\{\begin{array}{c} 0\le\theta_{inc}<\pi/2, \\ n=1,2,\cdots, \end{array}\right. \tag{3.20}$$

where the reflection location $\vec{R}_{h,N}\left(r'_i,\dot{\vec{\Lambda}}_{h,N},\vec{\Lambda}'_{h,N},\vec{R}_{T,h}\right)$ follows the generic form as shown in equation (C.6) of Appendix C2,

$$\vec{R}_{h,N}\left(r'_i,\dot{\vec{\Lambda}}_{h,N},\vec{\Lambda}'_{h,N},\vec{R}_{T,h}\right) = \left\{\sum_{i=1}^{3}\left[\nu_{T,h,i}+r'_i\Lambda'_{h,N,i}\right]^2\right\}^{1/2}\sum_{i=1}^{3}\dot{\Lambda}_{h,N,i}\hat{e}_i. \tag{3.21}$$

In the above equation, the subscript h denotes the hemisphere; and

$$\left\{\begin{array}{r} \dot{\Lambda}_{h,N,1}\left(\dot{\theta}_{h,N},\dot{\phi}_{h,N}\right) = \sin\dot{\theta}_{h,N}\cos\dot{\phi}_{h,N}, \\ \dot{\Lambda}_{h,N,2}\left(\dot{\theta}_{h,N},\dot{\phi}_{h,N}\right) = \sin\dot{\theta}_{h,N}\sin\dot{\phi}_{h,N}, \\ \dot{\Lambda}_{h,N,3}\left(\dot{\theta}_{h,N}\right) = \cos\dot{\theta}_{h,N}. \end{array}\right.$$

The expressions for $\Lambda'_{h,N,i}$, $i=1,2,3$, are defined identically in form. The angular variables in spherical coordinates, $\dot{\theta}_{h,N}$ and $\dot{\phi}_{h,N}$, can be obtained from equations (3.13) and (3.14), where the obvious notational changes are understood. The implicit angular variables, $\theta'_{h,N}$ and $\phi'_{h,N}$, are the sets defined in Appendix A, equations (A.158) and (A.159) for $\theta'_{s,N}$, and the sets from equations (A.160) and (A.161) for $\phi'_{s,N}$.

Unlike the sphere situation, the initial wave vector could eventually escape the hemisphere resonator after some maximum number of reflections. It is shown in the Appendix C2 that this maximum number for internal reflection is given by equation (C.8),

$$N_{h,max} = \left[\mathbb{Z}_{h,max}\right]_G, \tag{3.22}$$

where the greatest integer function $\left[\mathbb{Z}_{h,max}\right]_G$ is defined in equation (C.7) of Appendix C2,

$$\mathbb{Z}_{h,max} = \frac{1}{\pi-2\theta_{inc}}\left[\pi-\arccos\left(\frac{1}{2}\left\{r'_i\left\|\vec{R'}_0\right\|^{-1}+\left[r'_i\right]^{-1}\left\|\vec{R'}_0\right\|-\left[r'_i\left\|\vec{R'}_0\right\|\right]^{-1}\xi_{1,p}^2\right\}\right)\right]. \tag{3.23}$$

Here $\xi_{1,p}$ is given in equation (3.5) and θ_{inc} is from equation (A.115).

The above results of $\triangle\vec{k'}_{inner}\left(;\vec{R'}_{h,1},\vec{R'}_{h,0}\right)$ and $\triangle\vec{k'}_{outer}\left(;\vec{R'}_{h,1}+a\hat{R'}_{h,1}\right)$ have been derived based on the fact that there are multiple internal reflections. For a sphere, the multiple internal reflections are inherent. However, for a hemisphere, it is not necessarily true that all incoming waves would result in multiple internal reflections. Naturally, the criteria for multiple internal reflections are in order. If the initial direction of the incoming wave vector, $\hat{k'}_1$, is given, the internal reflections can be either single or multiple depending upon the location of the entry point in the cavity, $\vec{R'}_0$. As shown in Figure 3.5, these are two reflection dynamics where the dashed vectors represent the single reflection case and the non-dashed vectors represent multiple reflections case. Because the whole process occurs in the same plane of incidence, the vector $\vec{R'}_f = -\lambda_0\vec{R'}_0$ where $\lambda_0 > 0$. The multiple or single internal reflection criteria

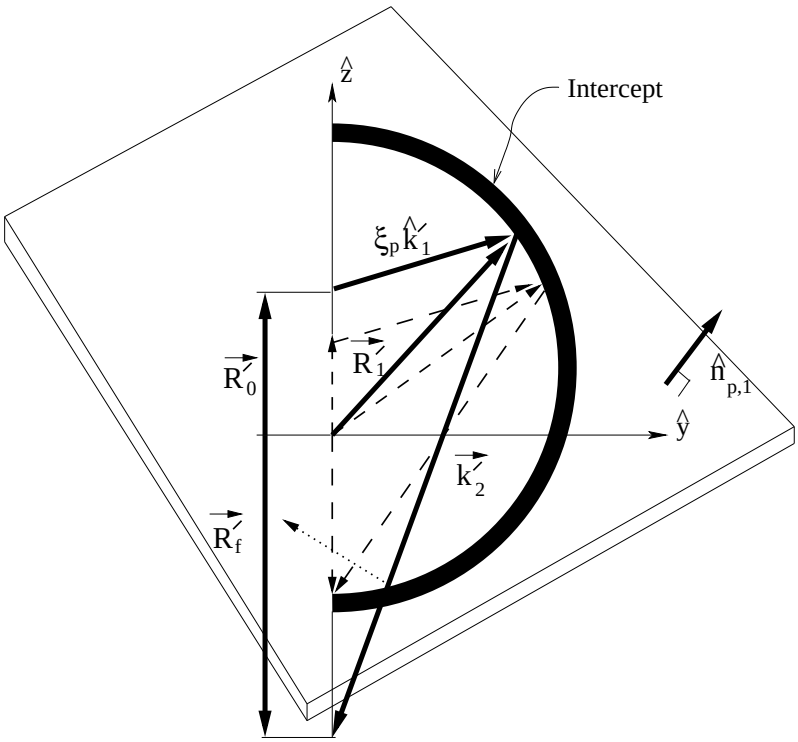

Figure 3.5.: The dashed line vectors represent the situation where only single internal reflection occurs. The dark line vectors represent the situation where multiple internal reflections occur.

can be summarized by the relation found in equation (C.21) of Appendix C2:

$$\left\|\vec{R'}_f\right\| = \frac{1}{2}\left\|\vec{R'}_0\right\|\left[\sum_{n=1}^{3} k'_{1,n}\right]\left\{\sum_{j=1}^{3}\sum_{l=1}^{3}\left[\left\|\vec{k'}_1\right\|^2 - k'_{1,l}\sum_{m=1}^{3} k'_{1,m}\right] r'_{0,l}r'_{0,j}\right\}^{-1}\sum_{l=1}^{3}\left\{k'_{1,l}\left[r'_i\right]^2 - \left[r'_{0,l}\right]^2\right.$$
$$\left. +2\vec{R'}_0 \bullet \vec{k'}_1 r'_{0,l} - \left\|\vec{R'}_0\right\|^2 k'_{1,l} - 2r'_{0,l}\left[\sum_{l=1}^{3} k'_{1,l}\right]^{-1}\sum_{i=1}^{3}\left[\left\|\vec{k'}_1\right\|^2 - k'_{1,i}\sum_{m=1}^{3} k'_{1,m}\right] r'_{0,i}\right\}. \tag{3.24}$$

Finally, because the hemisphere opening has a radius r'_i, the following criteria are concluded:

$$\begin{cases} \left\|\vec{R'}_f\right\| < r'_i, & Single - Internal - Reflection, \\ \left\|\vec{R'}_f\right\| \geq r'_i, & Multiple - Internal - Reflections, \end{cases} \tag{3.25}$$

where $\left\|\vec{R'}_f\right\|$ is defined in equation (3.24). The details of this section can be found in Appendix C2.

3.2.3. Plate-Hemisphere

A surface is represented by a unit vector $\hat{n'}_p$, which is normal to the surface locally. For the circular plate shown in Figure 3.6, its orthonormal triad $\left(\hat{n'}_p, \hat{\theta'}_p, \hat{\phi'}_p\right)$ has the form

$$\hat{n'}_p = \sum_{i=1}^{3}\Lambda'_{p,i}\hat{e}_i, \qquad \hat{\theta'}_p = \sum_{i=1}^{3}\frac{\partial\Lambda'_{p,i}}{\partial\theta'_p}\hat{e}_i, \qquad \hat{\phi'}_p = \sum_{i=1}^{3}\frac{1}{\sin\theta'_p}\frac{\partial\Lambda'_{p,i}}{\partial\phi'_p}\hat{e}_i,$$

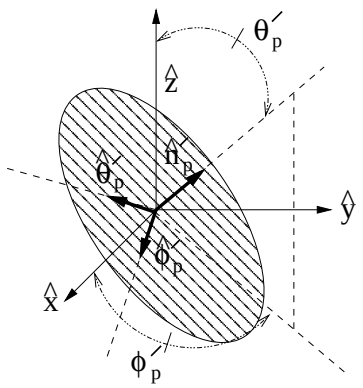

Figure 3.6.: The orientation of a disk is given through the surface unit normal $\hat{n'}_p$. The disk is spanned by the two unit vectors $\hat{\theta'}_p$ and $\hat{\phi'}_p$.

where $\Lambda'_{p,1}\left(\theta'_p,\phi'_p\right)=\sin\theta'_p\cos\phi'_p$, $\Lambda'_{p,2}\left(\theta'_p,\phi'_p\right)=\sin\theta'_p\sin\phi'_p$ and $\Lambda'_{p,3}\left(\theta'_p\right)=\cos\theta'_p$.

For the plate-hemisphere configuration shown in Figure 3.7, it can be shown that the element $\vec{R}_p$ on the plane and its velocity $d\vec{R}_p/dt$ are given by (see equation (3.27) and (C.30) in Appendix C3:

$$\vec{R}_p\left(\grave{\vec{\Lambda}}_p,\vec{\Lambda}'_p,\vec{R}_{T,p}\right)=\left\{\sum_{i=1}^{3}\left[\nu_{T,p,i}+\nu'_{p,\theta'_p}\frac{\partial\Lambda'_{p,i}}{\partial\theta'_p}+\frac{\nu'_{p,\phi'_p}}{\sin\theta'_p}\frac{\partial\Lambda'_{p,i}}{\partial\phi'_p}\right]^2\right\}^{1/2}\sum_{i=1}^{3}\grave{\Lambda}_{p,i}\hat{e}_i, \tag{3.26}$$

$$\begin{aligned}\dot{\vec{R}}_p\equiv\frac{d\vec{R}_p}{dt}=&\left\{\sum_{i=1}^{3}\left[\nu_{T,p,i}+\nu'_{p,\theta'_p}\frac{\partial\Lambda'_{p,i}}{\partial\theta'_p}+\frac{\nu'_{p,\phi'_p}}{\sin\theta'_p}\frac{\partial\Lambda'_{p,i}}{\partial\phi'_p}\right]^2\right\}^{-1/2}\sum_{j=1}^{3}\sum_{k=1}^{3}\left(\left[\nu_{T,p,k}+\nu'_{p,\theta'_p}\frac{\partial\Lambda'_{p,k}}{\partial\theta'_p}\right.\right.\\&\left.+\frac{\nu'_{p,\phi'_p}}{\sin\theta'_p}\frac{\partial\Lambda'_{p,k}}{\partial\phi'_p}\right]\left[\dot{\nu}_{T,p,k}+\left\{\nu'_{p,\theta'_p}\frac{\partial^2\Lambda'_{p,k}}{\partial\left[\theta'_p\right]^2}+\frac{\nu'_{p,\phi'_p}}{\sin\theta'_p}\left(\frac{\partial^2\Lambda'_{p,k}}{\partial\theta'_p\partial\phi'_p}-\cot\theta'_p\frac{\partial\Lambda'_{p,k}}{\partial\phi'_p}\right)\right\}\dot{\theta'}_p\right.\\&+\left\{\nu'_{p,\theta'_p}\frac{\partial^2\Lambda'_{p,k}}{\partial\phi'_p\partial\theta'_p}+\frac{\nu'_{p,\phi'_p}}{\sin\theta'_p}\frac{\partial^2\Lambda'_{p,k}}{\partial\left[\phi'_p\right]^2}\right\}\dot{\phi'}_p+\dot{\nu'}_{p,\theta'_p}\frac{\partial\Lambda'_{p,k}}{\partial\theta'_p}+\frac{\dot{\nu'}_{p,\phi'_p}}{\sin\theta'_p}\frac{\partial\Lambda'_{p,k}}{\partial\phi'_p}\left.\right]\grave{\Lambda}_{p,j}\\&\left.+\sum_{i=1}^{3}\left[\nu_{T,p,i}+\nu'_{p,\theta'_p}\frac{\partial\Lambda'_{p,i}}{\partial\theta'_p}+\frac{\nu'_{p,\phi'_p}}{\sin\theta'_p}\frac{\partial\Lambda'_{p,i}}{\partial\phi'_p}\right]^2\left[\frac{\partial\grave{\Lambda}_{p,j}}{\partial\grave{\theta}_p}\frac{\partial\grave{\theta}_p}{\partial\phi'_p}\dot{\theta'}_p+\frac{\partial\grave{\Lambda}_{p,j}}{\partial\grave{\phi}_p}\frac{\partial\grave{\phi}_p}{\partial\phi'_p}\dot{\phi'}_p\right]\right)\hat{e}_j,\end{aligned} \tag{3.27}$$

where $\left(\grave{\Lambda}_{p,1},\grave{\Lambda}_{p,2},\grave{\Lambda}_{p,3}\right)$ is defined in equation (C.31) and the angles $\grave{\phi}_p$ and $\grave{\theta}_p$ are defined in equations (C.27) and (C.28) of Appendix C3. The subscript p of $\grave{\phi}_p$ and $\grave{\theta}_p$ indicates that these are spherical variables for the points on the plate of Figure 3.7, not that of the hemisphere. It is also understood that $\Lambda'_{p,3}$ and $\grave{\Lambda}_{p,3}$ are independent of ϕ'_p and $\grave{\phi}_p$, respectively. Therefore, their differentiation with respect to ϕ'_p and $\grave{\phi}_p$ respectively vanishes. The quantities $\dot{\theta'}_p$ and $\dot{\phi'}_p$ are the angular frequencies, and $\dot{\nu}_{T,p,i}$ is the translation speed of the plate relative to the system origin. The quantities $\dot{\nu'}_{p,\theta'_p}$ and $\dot{\nu'}_{p,\phi'_p}$ are the lattice vibrations along the directions $\hat{\theta'}_p$ and $\hat{\phi'}_p$ respectively. For the static plate without lattice vibrations, $\dot{\nu'}_{p,\theta'_p}$ and $\dot{\nu'}_{p,\phi'_p}$ vanishes.

In the cross-sectional view of the plate-hemisphere system shown in Figure 3.8, the initial wave vector $\vec{k'}_i$ traveling toward the hemisphere would go through a complex series of reflections according to the law of reflection and finally exit the cavity. It would then continue toward the plate, and depending on the orientation of plate at the time of impact, the wave-vector, now reflecting off the plate, would either escape to infinity or re-enter the hemisphere. The process repeats successively. In order to determine whether the wave that just escaped from the hemisphere cavity can reflect

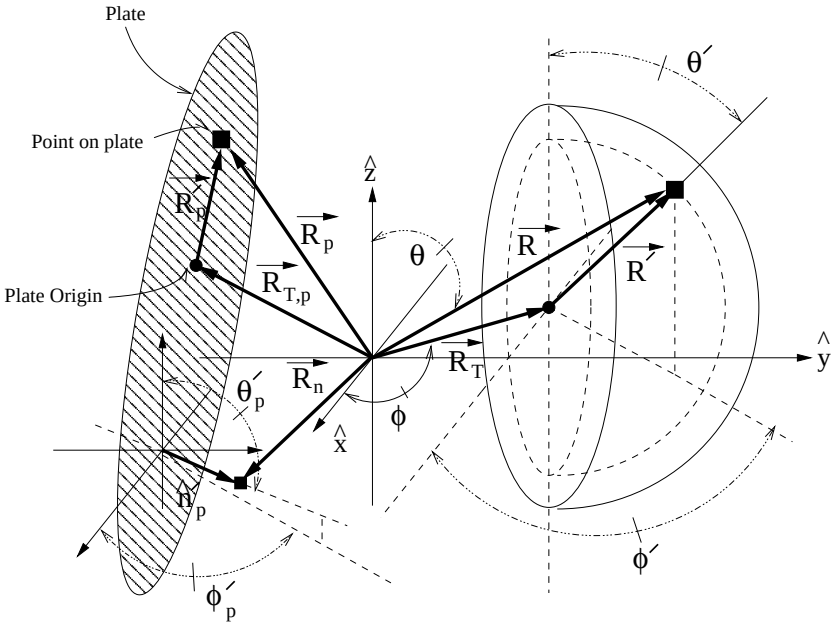

Figure 3.7.: The plate-hemisphere configuration.

back from the plate and re-enter the hemisphere or escape to infinity, the exact location of reflection on the plate must be known. This reflection point on the plate is found to be, from equation (C.54) of Appendix C3,

$$\vec{R}_p = \left\{ \sum_{s=1}^{3} \left[\frac{\partial \Lambda'_{p,s}}{\partial \phi'_p} - \frac{\sum_{i=1}^{3} \frac{\partial \Lambda'_{p,i}}{\partial \phi'_p} \left[\Lambda'_{p,i} + \left\| \vec{n'}_{p,1} \right\|^{-1} \epsilon_{ijk} k'_{1,j} r'_{0,k} \right]}{\sum_{l=1}^{3} \frac{\partial \Lambda'_{p,l}}{\partial \theta'_p} \left[\Lambda'_{p,l} + \left\| \vec{n'}_{p,1} \right\|^{-1} \epsilon_{lmn} k'_{1,m} r'_{0,n} \right]} \frac{\partial \Lambda'_{p,s}}{\partial \theta'_p} \right]^2 \right\}^{1/2}$$
$$\times \left[C_\beta^{-1} C_\gamma^{-1} A_\gamma A_\beta + \gamma_o C_\beta^{-1} C_\gamma^{-1} B_\gamma A_\beta + C_\beta^{-1} B_\zeta B_\beta \right] \sum_{i=1}^{3} \grave{\Lambda}_{p,i} \hat{e}_i, \tag{3.28}$$

where the translation parameter $\nu_{T,p,j} = 0$ and the terms $(A_\zeta, B_\zeta, C_\zeta)$, $(A_\gamma, B_\gamma, C_\gamma)$, $(A_\beta, B_\beta, C_\beta)$ and γ_o are defined in equations (C.46), (C.49), (C.50) and (C.52) of Appendix C3. It is to be noticed that for a situation where the translation parameter $\nu_{T,p,j} = 0$, $\grave{\Lambda}$ becomes identical to Λ' in form. Results for $\grave{\Lambda}$ can be obtained from Λ' by a simple replacement of primed variables with the unprimed ones.

Leaving the details to the relevant Appendix, the criterion whether the wave reflecting off the plate at location $\vec{R}_p$ can re-enter the hemisphere cavity or simply escape to infinity is found from the result shown in equation (C.58) of Appendix C3,

$$\xi_{\kappa,i} = \left(\nu_{T,h,i} + r'_{0,i} - \left\{ \sum_{s=1}^{3} \left[\frac{\partial \Lambda'_{p,s}}{\partial \phi'_p} - \frac{\sum_{i=1}^{3} \frac{\partial \Lambda'_{p,i}}{\partial \phi'_p} \left[\Lambda'_{p,i} + \left\| \vec{n'}_{p,1} \right\|^{-1} \epsilon_{ijk} k'_{1,j} r'_{0,k} \right]}{\sum_{l=1}^{3} \frac{\partial \Lambda'_{p,l}}{\partial \theta'_p} \left[\Lambda'_{p,l} + \left\| \vec{n'}_{p,1} \right\|^{-1} \epsilon_{lmn} k'_{1,m} r'_{0,n} \right]} \frac{\partial \Lambda'_{p,s}}{\partial \theta'_p} \right]^2 \right\}^{1/2} \right.$$
$$\times \left[C_\beta^{-1} C_\gamma^{-1} A_\gamma A_\beta + \gamma_o C_\beta^{-1} C_\gamma^{-1} B_\gamma A_\beta + C_\beta^{-1} B_\zeta B_\beta \right] \grave{\Lambda}_{p,i} \left(\sum_{k=1}^{3} \left\{ \alpha_{r,\perp} \left[k_{N_{h,max}+1,i} n'_{p,k} n'_{p,k} \right. \right. \right.$$
$$\left. \left. \left. - n'_{p,i} k_{N_{h,max}+1,k} n'_{p,k} \right] - \alpha_{r,\parallel} n'_{p,k} k_{N_{h,max}+1,k} n'_{p,i} \right\} \right)^{-1}, \tag{3.29}$$

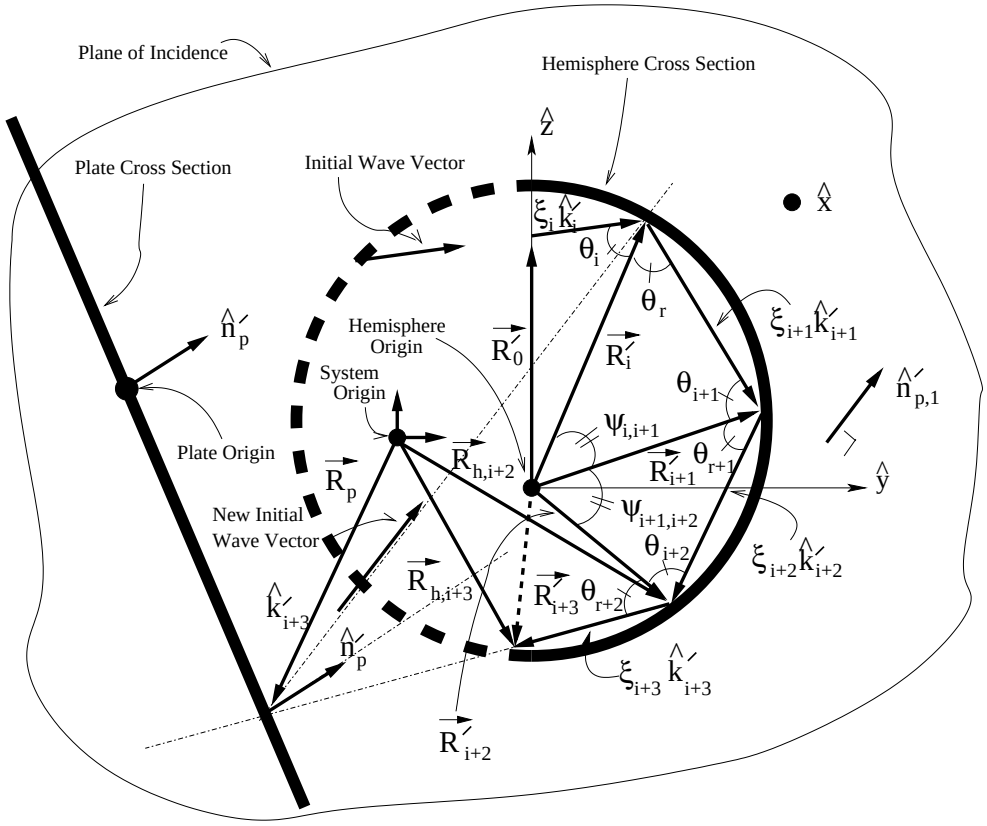

Figure 3.8.: The intersection between oscillating plate, hemisphere and the plane of incidence whose normal is $\hat{n'}_{p,1} = -\left\|\vec{n'}_{p,1}\right\|^{-1} \sum_{i=1}^{3} \epsilon_{ijk} k'_{1,j} r'_{0,k} \hat{e}_i$.

where $i = 1, 2, 3$ and $\xi_{\kappa,i}$ is the component of the scale vector $\vec{\xi}_\kappa = \sum_{i=1}^{3} \xi_{\kappa,i} \hat{e}_i$ explained in the Appendix C3.

In the above re-entry criteria, it should be noticed that $\vec{R}_0 \leq r'_i$. This implies $r'_{0,i} \leq r'_i$, where r'_i is the radius of hemisphere. It is then concluded that all waves re-entering the hemisphere cavity would satisfy the condition $\xi_{\kappa,1} = \xi_{\kappa,2} = \xi_{\kappa,3}$. On the other hand, those waves that escapes to infinity cannot have all three $\xi_{\kappa,i}$ equal to a single constant. The re-entry condition $\xi_{\kappa,1} = \xi_{\kappa,2} = \xi_{\kappa,3}$ is just another way of stating the existence of a parametric line along the vector $\vec{k}_{r,N_{h,max}+1}$ that happens to pierce through the hemisphere opening. In case such a line does not exist, the initial wave direction has to be rotated into a new direction such that there is a parametric line that pierces through the hemisphere opening. That is why all three $\xi_{\kappa,i}$ values cannot be equal to a single constant. The re-entry criteria are summarized here for bookkeeping purpose:

$$\begin{cases} \xi_{\kappa,1} = \xi_{\kappa,2} = \xi_{\kappa,3} \rightarrow Wave - ReEnters - Hemisphere, \\ \qquad ELSE \rightarrow Wave - Escapes - to - Infinity, \end{cases} \tag{3.30}$$

where $ELSE$ is the case where $\xi_{\kappa,1} = \xi_{\kappa,2} = \xi_{\kappa,3}$ cannot be satisfied. The details of this section can be found in Appendix C3.

3.3. Dynamical Casimir Force

The phenomenon of Casimir effect is inherently a dynamical effect due to the fact that it involves radiation, rather than static fields. One of my original objectives in studying the Casimir effect was to investigate the physical implications of vacuum-fields on movable boundaries. Consider the two parallel plates configuration of charge-neutral, perfect conductors shown in Figure 3.9. Because there are more wave modes in the outer region of the parallel plate res-

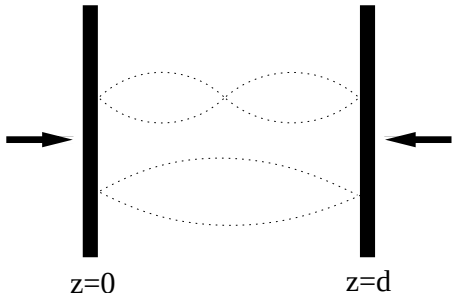

Figure 3.9.: Because there are more vacuum-field modes in the external regions, the two charge-neutral conducting plates are accelerated inward till the two finally stick.

onator, two loosely restrained (or unfixed in position) plates will accelerate inward until they finally meet. The energy conservation would require that the energy initially confined in the resonator when the two plates were separated be transformed into the heat energy that acts to raise the temperatures of the two plates.

Davies in 1975 [26], followed by Unruh in 1976 [27], have asked the similar question and came to a conclusion that when an observer is moving with a constant acceleration in vacuum, the observer perceives himself to be immersed in a thermal bath at the temperature $T = \hbar\ddot{R}/\left[2\pi ck'\right]$, where $\ddot{R}$ is the acceleration of the observer and k', the wave number. The details of the Unruh-Davies effect can also be found in the reference [17]. The other work that dealt with the concept of dynamical Casimir effect is due to Schwinger in his proposals [14, 16] to explain the phenomenon of sonoluminescense. Sonoluminescense is a phenomenon in which when a small air bubble filled with noble gas is under a strong acoustic-field pressure, the bubble will emit an intense flash of light in the optical range.

Although the name "dynamical Casimir effect" have been introduced by Schwinger, the motivation and derivation behind the dynamical Casimir force in this thesis did not stem from that of Schwinger's work. Therefore, the dynamical Casimir force here should not have any resemblance to Schwinger's work to the best of my knowledge. I have only found out of Schwinger's proposals on sonoluminescense after my work on dynamical Casimir force have already begun. The terminology "dynamical Casimir force" seemed to be appealing enough, I have personally used it at the beginning of my work. After discovering Schwinger's work on sonoluminescense, I have learned that Schwinger had already introduced the terminology "dynamical Casimir effect" in his papers. My original development to the dynamical Casimir force formalism is briefly presented in the following sections. The details of the derivations pertaining to the dynamical Casimir force can be found in Appendix D.

3.3.1. Formalism of Zero-Point Energy and its Force

For massless fields, the energy-momentum relation is $\mathcal{H}'_{n_s} \equiv E_{Total} = pc$, where p is the momentum, c the speed of light, and $\mathcal{H}'_{n_s}$ is the quantized field energy for the harmonic fields of equation (2.8) for the bounded space, or equation (2.9) for the free space. For the bounded space, the quantized field energy $\mathcal{H}'_{n_s} \equiv \mathcal{H}'_{n_s,b}$ of equation (2.8) is a function of the wave number $k'_i(n_i)$, which in turn is a function of the wave mode value n_i and the boundary functional $f_i(L_i)$, where L_i is the gap distance in the direction of $\vec{L}_i = \left[\vec{R'}_2 \bullet \hat{e}_i - \vec{R'}_1 \bullet \hat{e}_i\right]\hat{e}_i$. Here $\vec{R'}_1$ and $\vec{R'}_2$ are the position vectors for the involved boundaries. As an illustration with the two plate configuration shown in Figure 3.9, $\vec{R'}_1$ may represent the plate positioned at $z = 0$ and $\vec{R'}_2$ may correspond to the plate at the position $z = d$. When the position of these boundaries are changing in time, the quantized field energy $\mathcal{H}'_{n_s} \equiv \mathcal{H}'_{n_s,b}$ will be modified accordingly because the wave number functional $k'_i(n_i)$ is varying in time,

$$\frac{dk'_i}{dt} = \frac{\partial k'_i}{\partial n_i}\frac{dn_i}{dt}f_i(L_i) + n_i\frac{\partial f_i}{\partial L_i}\frac{dL_i}{dt} = f_i(L_i)\frac{\partial k'_i}{\partial n_i}\dot{n}_i + n_i\frac{\partial f_i}{\partial L_i}\dot{L}_i.$$

Here the term proportional to $\dot{n}_i$ refers to the case where the boundaries remain fixed throughout all times but the number of wave modes in the resonator are being driven by some active external influence. The term proportional to $\dot{L}_i$ represents the changes in the number of wave modes due to the moving boundaries.

For an isolated system, there are no external influences, hence $\dot{n}_i = 0$. Then, the dynamical force arising from the

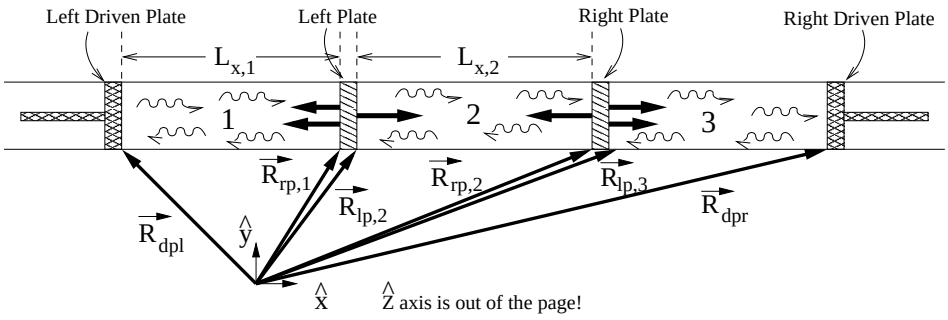

Figure 3.10.: A one dimensional driven parallel plates configuration.

fact that the time variation of the boundaries is given by equation (D.17) of Appendix D1,

$$\vec{\mathcal{F}'}_\alpha = \sum_{i=1}^{3} \left\{ n_i \frac{\partial f_i}{\partial L_i} \left[C_{\alpha,5} \frac{\partial^2 \mathcal{H}'_{n_s}}{\partial \left[k'_i\right]^2} + (1-\delta_{i\alpha}) \left(C_{\alpha,6} - C_{\alpha,7} \left[n_s + \frac{1}{2} \right] k'_i \right) \left[n_s + \frac{1}{2} \right] \right] \dot{L}_i \right.$$
$$\left. + \sum_{j=1}^{3} (1-\delta_{ij})\, C_{\alpha,5} n_j \frac{\partial f_j}{\partial L_j} \frac{\partial^2 \mathcal{H}'_{n_s}}{\partial k'_j \partial k'_i} \dot{L}_j \right\} \hat{e_\alpha}, \tag{3.31}$$

where $C_{\alpha,1}$, $C_{\alpha,2}$, $C_{\alpha,3}$, $C_{\alpha,4}$, $C_{\alpha,5}$, $C_{\alpha,6}$ and $C_{\alpha,7}$ are defined in equations (D.6), (D.9), (D.14), (D.15) and (D.16) of Appendix D1.

The force shown in the above expression vanishes for the one dimensional case. This is an expected result. To understand why the force vanishes, we have to refer to the starting point equation (D.4) in the Appendix D1. The summation there obviously runs only once to arrive at the expression, $\partial \mathcal{H}'_{n_s} / \partial k'_i = \left[n_s + \frac{1}{2} \right] \hbar c$. This is a classic situation where the problem has been over specified. For the **3D** case, equation (D.4) is a combination of two constraints, $\sum_{i=1}^{3} \left[p'_i\right]^2$ and $\mathcal{H}'_{n_s}$. For the one dimensional case, there is only one constraint, $\mathcal{H}'_{n_s}$. Therefore, equation (D.4) becomes an over specification. In order to avoid the problem caused by over specifications in this formulation, the one dimensional force expression can be obtained directly by differentiating equation (D.1) instead of using the above formulation for the three dimensional case. The **1D** dynamical force expression for an isolated, non-driven systems then becomes (see equation (D.18) of Appendix D1)

$$\vec{\mathcal{F}'} = \frac{n}{c} \frac{\partial f}{\partial L} \frac{\partial \mathcal{H}'_{n_s}}{\partial k'} \dot{L} \hat{e}, \tag{3.32}$$

where $\vec{\mathcal{F}'}$ is an one dimensional force. Here the subscript α of $\vec{\mathcal{F}'}_\alpha$ have been dropped for simplicity, since it is a one dimensional force. The details of this section can be found in Appendix D1.

3.3.2. Equations of Motion for the Driven Parallel Plates

The Unruh-Davies effect states that heating up of an accelerating conductor plate is proportional to its acceleration through the relation $T = \hbar \ddot{R} / \left[2\pi c k'\right]$, where $\ddot{R}$ is the plate acceleration. A one dimensional system of two parallel plates, shown in Figure 3.10, can be used as a simple model to demonstrate the complicated sonoluminescense phenomenon for a bubble subject to a strong acoustic field.

The dynamical force for the **1D**, linear coupled system can be expressed with equation (3.32),

$$\ddot{R}_1 - \eta_1 \dot{R}_1 - \eta_2 \dot{R}_2 = \xi_{rp}, \qquad \ddot{R}_2 - \eta_3 \dot{R}_2 - \eta_4 \dot{R}_1 = \xi_{lp}, \tag{3.33}$$

where the quantities $\eta_1, \eta_2, \eta_3, \eta_4, \xi_{rp}, \xi_{lp}, R_1, R_2$ are defined in equation (D.31) of Appendix D2. Here R_1 represents the center of mass position for the "Right Plate" and R_2 represents the center of mass position for the "Left Plate" as illustrated in Figure 3.10. With a slight modification, equation (3.33) for this linear coupled system can be written in

the matrix form, (see equations (D.33), (D.34) and (D.35) of Appendix D2):

$$R_1 = \int_{t_0}^{t} R_3 dt', \qquad R_2 = \int_{t_0}^{t} R_4 dt',$$

and

$$\underbrace{\begin{bmatrix} \dot{R}_3 \\ \dot{R}_4 \end{bmatrix}}_{\vec{\dot{R}}_\eta} = \underbrace{\begin{bmatrix} \eta_1 & \eta_2 \\ \eta_4 & \eta_3 \end{bmatrix}}_{\widetilde{M}_\eta} \cdot \underbrace{\begin{bmatrix} R_3 \\ R_4 \end{bmatrix}}_{\vec{R}_\eta} + \underbrace{\begin{bmatrix} \xi_{rp} \\ \xi_{lp} \end{bmatrix}}_{\vec{\xi}}, \tag{3.34}$$

where

$$\begin{cases} \dot{R}_1 = R_3, \qquad \dot{R}_2 = R_4, \\ \dot{R}_3 = \ddot{R}_1 = \xi_{rp} + \eta_1 \dot{R}_1 + \eta_2 \dot{R}_2 = \xi_{rp} + \eta_1 R_3 + \eta_2 R_4, \\ \dot{R}_4 = \ddot{R}_2 = \xi_{lp} + \eta_3 \dot{R}_2 + \eta_4 \dot{R}_1 = \xi_{lp} + \eta_3 R_4 + \eta_4 R_3. \end{cases}$$

The matrix equation has the solutions given by equations (D.51) and (D.52) of Appendix D2:

$$\begin{aligned} \dot{R}_{rp,cm,\alpha}(t) = & \left[\frac{\lambda_4(;t_0) - \eta_1(;t_0)}{\lambda_3(;t_0) - \eta_1(;t_0)} - 1\right]^{-1} \frac{\psi_{11}(t,t_0)\,\dot{R}_{rp,cm,\alpha}(t_0) + \psi_{12}(t,t_0)\,\dot{R}_{lp,cm,\alpha}(t_0)}{\exp\left(\left[\lambda_3(;t_0) + \lambda_4(;t_0)\right] t_0\right)} \\ & + \psi_{11}(t,t_0) \int_{t_0}^{t} \frac{\psi_{22}(t',t_0)\,\xi_{rp}(t') - \psi_{12}(t',t_0)\,\xi_{lp}(t')}{\psi_{11}(t',t_0)\,\psi_{22}(t',t_0) - \psi_{12}(t',t_0)\,\psi_{21}(t',t_0)} dt' + \psi_{12}(t,t_0) \\ & \times \int_{t_0}^{t} \frac{\psi_{11}(t',t_0)\,\xi_{lp}(t') - \psi_{21}(t',t_0)\,\xi_{rp}(t')}{\psi_{11}(t',t_0)\,\psi_{22}(t',t_0) - \psi_{12}(t',t_0)\,\psi_{21}(t',t_0)} dt', \end{aligned} \tag{3.35}$$

$$\begin{aligned} \dot{R}_{lp,cm,\alpha}(t) = & \left[\frac{\lambda_4(;t_0) - \eta_1(;t_0)}{\lambda_3(;t_0) - \eta_1(;t_0)} - 1\right]^{-1} \frac{\psi_{21}(t,t_0)\,\dot{R}_{rp,cm,\alpha} + \psi_{22}(t,t_0)\,\dot{R}_{lp,cm,\alpha}(t_0)}{\exp\left(\left[\lambda_3(;t_0) + \lambda_4(;t_0)\right] t_0\right)} \\ & + \psi_{21}(t,t_0) \int_{t_0}^{t} \frac{\psi_{22}(t',t_0)\,\xi_{rp}(t') - \psi_{12}(t',t_0)\,\xi_{lp}(t')}{\psi_{11}(t',t_0)\,\psi_{22}(t',t_0) - \psi_{12}(t',t_0)\,\psi_{21}(t',t_0)} dt' + \psi_{22}(t,t_0) \\ & \times \int_{t_0}^{t} \frac{\psi_{11}(t',t_0)\,\xi_{lp}(t') - \psi_{21}(t',t_0)\,\xi_{rp}(t')}{\psi_{11}(t',t_0)\,\psi_{22}(t',t_0) - \psi_{12}(t',t_0)\,\psi_{21}(t',t_0)} dt', \end{aligned} \tag{3.36}$$

where the terms λ_3 and λ_4 are defined in equation (D.37); and $\psi_{11}(t,t_0)$, $\psi_{12}(t,t_0)$, $\psi_{21}(t,t_0)$ and $\psi_{22}(t,t_0)$ are defined in equations (D.43) through (D.46) in Appendix D2. The quantities $\dot{R}_{rp,cm,\alpha}$ and $\dot{R}_{lp,cm,\alpha}$ are the speed of the center of mass of "Right Plate" and the speed of the center of mass of the "Left Plate," respectively, and α defines the particular basis direction.

The corresponding positions $R_{rp,cm,\alpha}(t)$ and $R_{lp,cm,\alpha}(t)$ are found by integrating equations (3.35) and (3.36) with respect to time,

$$\begin{aligned} R_{rp,cm,\alpha}(t) = & \left[\frac{\lambda_4(;t_0) - \eta_1(;t_0)}{\lambda_3(;t_0) - \eta_1(;t_0)} - 1\right]^{-1} \int_{t_0}^{t} \left[\frac{\psi_{11}(\tau,t_0)\,\dot{R}_{rp,cm,\alpha}(t_0) + \psi_{12}(\tau,t_0)\,\dot{R}_{lp,cm,\alpha}(t_0)}{\exp\left(\left[\lambda_3(;t_0) + \lambda_4(;t_0)\right] t_0\right)} \right. \\ & + \psi_{11}(\tau,t_0) \int_{t_0}^{\tau} \frac{\psi_{22}(t',t_0)\,\xi_{rp}(t') - \psi_{12}(t',t_0)\,\xi_{lp}(t')}{\psi_{11}(t',t_0)\,\psi_{22}(t',t_0) - \psi_{12}(t',t_0)\,\psi_{21}(t',t_0)} dt' + \psi_{12}(\tau,t_0) \\ & \left. \times \int_{t_0}^{\tau} \frac{\psi_{11}(t',t_0)\,\xi_{lp}(t') - \psi_{21}(t',t_0)\,\xi_{rp}(t')}{\psi_{11}(t',t_0)\,\psi_{22}(t',t_0) - \psi_{12}(t',t_0)\,\psi_{21}(t',t_0)} dt' \right] d\tau + R_{rp,cm,\alpha}(t_0), \end{aligned} \tag{3.37}$$

$$R_{lp,cm,\alpha}(t) = \left[\frac{\lambda_4(;t_0)-\eta_1(;t_0)}{\lambda_3(;t_0)-\eta_1(;t_0)}-1\right]^{-1}\int_{t_0}^{t}\left[\frac{\psi_{21}(\tau,t_0)\,\dot{R}_{rp,cm,\alpha}(t_0)+\psi_{22}(\tau,t_0)\,\dot{R}_{lp,cm,\alpha}(t_0)}{\exp\left(\left[\lambda_3(;t_0)+\lambda_4(;t_0)\right]t_0\right)}\right.$$
$$+\psi_{21}(\tau,t_0)\int_{t_0}^{\tau}\frac{\psi_{22}(t',t_0)\,\xi_{rp}(t')-\psi_{12}(t',t_0)\,\xi_{lp}(t')}{\psi_{11}(t',t_0)\,\psi_{22}(t',t_0)-\psi_{12}(t',t_0)\,\psi_{21}(t',t_0)}dt'+\psi_{22}(\tau,t_0)$$
$$\left.\times\int_{t_0}^{\tau}\frac{\psi_{11}(t',t_0)\,\xi_{lp}(t')-\psi_{21}(t',t_0)\,\xi_{rp}(t')}{\psi_{11}(t',t_0)\,\psi_{22}(t',t_0)-\psi_{12}(t',t_0)\,\psi_{21}(t',t_0)}dt'\right]d\tau+R_{lp,cm,\alpha}(t_0)\,. \tag{3.38}$$

The remaining integrations are straightforward and the explicit forms will not be shown here.

One may argue that for the static case, $\dot{R}_{rp,cm,\alpha}(t_0)$ and $\dot{R}_{lp,cm,\alpha}(t_0)$ must be zero because the conductors seem to be fixed in position. This argument is flawed, for any wall totally fixed in position upon impact would require an infinite amount of energy. One has to consider the conservation of momentum simultaneously. The wall has to have moved by the amount $\triangle R_{wall}=\dot{R}_{wall}\triangle t$, where $\triangle t$ is the total duration of impact, and $\dot{R}_{wall}$ is calculated from the momentum conservation and it is non-zero. The same argument can be applied to the apparatus shown in Figure 3.10. For that system

$$\|\vec{p}_{virtual-photon}\|=\frac{1}{c}\mathcal{H}'_{n_s,\Re}(t_0)\,,\qquad\begin{cases}\dot{R}_{rp,cm,\alpha}(t_0)=\left\|\dot{\vec{R}}_{lp,3}(t_0)+\dot{\vec{R}}_{rp,2}(t_0)\right\|,\\ \dot{R}_{lp,cm,\alpha}(t_0)=\left\|\dot{\vec{R}}_{rp,1}(t_0)+\dot{\vec{R}}_{lp,2}(t_0)\right\|.\end{cases}$$

For simplicity, assuming that the impact is always only in the normal direction,

$$\dot{R}_{rp,cm,\alpha}(t_0)=\frac{2}{m_{rp}c}\left\|\mathcal{H}'_{n_s,3}(t_0)-\mathcal{H}'_{n_s,2}(t_0)\right\|,\qquad\dot{R}_{lp,cm,\alpha}(t_0)=\frac{2}{m_{lp}c}\left\|\mathcal{H}'_{n_s,1}(t_0)-\mathcal{H}'_{n_s,2}(t_0)\right\|,$$

where the differences under the magnitude symbol imply field energies from different regions counteract the other. The details of this section can be found in Appendix D2.

4. Results and Outlook

The results for the sign of Casimir force on non-planar geometric configurations considered in this thesis will eventually be compared with the classic repulsive result obtained by Boyer decades earlier. For this reason, it is worth reviewing Boyer's original configuration as shown in Figure 4.1.

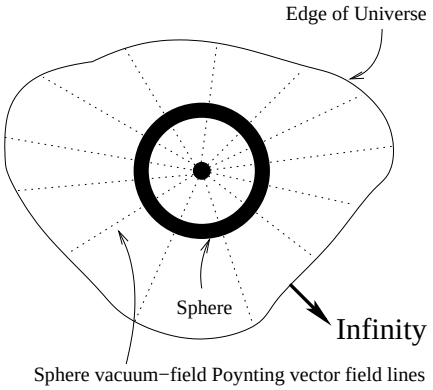

Figure 4.1.: Boyer's configuration is such that a sphere is the only matter in the entire universe. His universe extends to the infinity, hence there are no boundaries. The sense of vacuum-field energy flow is along the radial vector $\hat{r}$, which is defined with respect to the sphere center.

T. H. Boyer in 1968 obtained a repulsive Casimir force result for his charge-neutral, hollow spherical shell of a perfect conductor [4]. For simplicity, his sphere is the only object in the entire universe and, therefore, no external boundaries such as laboratory walls, etc., were defined in his problem. Furthermore, the zero-point energy flow is always perpendicular to his sphere. Such restriction can be a very stringent condition for the material property that a sphere has to meet. For example, if one were to look at Boyer's sphere, he would not see the whole sphere; but instead, he would see a small spot on the surface of a sphere that happens to be in his line of sight. This happens because the sphere in Boyer's configuration can only radiate in a direction normal to the surface. One could equivalently argue that Boyer's sphere only responds to the approaching radiation at normal angles of incidence with respect to the surface of the sphere. When the Casimir force is computed for such restricted radiation energy flow, the result is repulsive. This can be attributed to the fact that closer to the sphere origin, the spherically symmetric radiation energy flow becomes more dense and this density decreases as it gets further away from the sphere center. As an illustration, Boyer's sphere is shown in Figure 4.1. For the rest of the thesis, "Boyer's sphere" would be strictly referred to as the sphere made of such material property that it only radiates or responds to vacuum-field radiations at normal angle of incidence with respect to its surface.

The formation of a sphere by bringing together two nearby hemispheres satisfying the material property of Boyer's sphere is illustrated in Figure 4.2. Since Boyer's material property only allow radiation in the normal direction to its surface, the radiation associated with each hemisphere would necessarily go through the corresponding hemisphere centers. For clarity, let us define the unit radial basis vector associated with the left and right hemispheres by $\hat{r}_L$ and $\hat{r}_R$, respectively. If the hemispheres are made of normal conductors the radiation from one hemisphere entering the other hemisphere cavity would go through a complex series of reflections before escaping the cavity. Here, a conductor with Boyer's stringent material property is not considered normal. Conductors that are normal also radiate in directions non-normal to their surface, whereas Boyer's conductor can only radiate normal to its surface. Due to the fact that Boyer's conducting materials can only respond to radiation impinging at a normal angle of incidence with respect to its surface, all of the incoming radiation at oblique angles of incidence with respect to the local surface normal is absorbed by the host hemisphere. This suggests that for the hemisphere-hemisphere arrangement made of

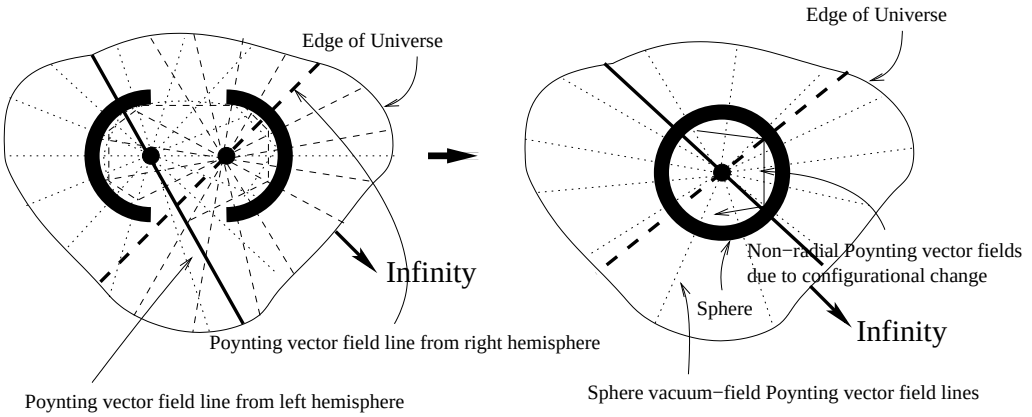

Figure 4.2.: Manufactured sphere, in which two hemispheres are brought together, results in small non-spherically symmetric vacuum-field radiation inside the cavity due to the configuration change. For the hemispheres made of Boyer's material, these fields in the resonator will eventually get absorbed by the conductor resulting in heating of the hemispheres.

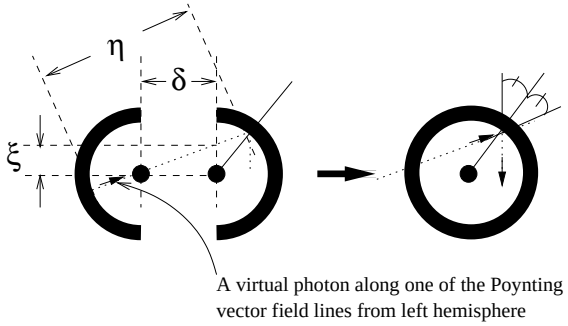

Figure 4.3.: The process in which a configuration change from hemisphere-hemisphere to sphere inducing virtual photon in the direction other than $\hat{r}$ is shown. The virtual photon here is referred to as the quanta of energy associated with the zero-point radiation.

Boyer's material shown in Figure 4.2, the temperature of the two hemispheres would rise indefinitely over time. This does not happen with ordinary conductors. This suggests that Boyer's conducting material, of which his sphere is made, is completely hypothetical. Precisely because of this material assumption, Boyer's Casimir force is repulsive.

For the moment, let us relax the stringent Boyer's material property for the hemispheres to that of ordinary conductors. For the hemispheres made of ordinary conducting materials, there would result a series of reflections in one hemisphere cavity due to those radiations entering the cavity from nearby hemisphere. For simplicity, the ordinary conducting material referred to here is that of perfect conductors without Boyer's hypothetical material property requirement. Furthermore, only the radiation emanating normally with respect to its surface is considered. The idea is to illustrate that the "normally emanated radiation" from one hemisphere results in elaboration of the effects of "obliquely emanated radiation" on another hemisphere cavity. Here the obliquely emanated radiation means those radiation emanating from a surface not along the local normal of the surface.

When two such hemispheres are brought together to form a sphere, there would exist some radiation trapped in the sphere of which the radiation energy flow lines are not spherically symmetric with respect to the sphere center. To see how a mere change in configuration invokes such non-spherically symmetric energy flow, consider the illustration shown in Figure 4.3. For clarity, only one "normally emanated radiation" energy flow line from the left hemisphere is shown. When one brings together the two hemispheres just in time before that quantum of energy escapes the hemisphere cavity to the right, the trapped energy quantum would continuously go through series of complex reflections in the cavity obeying the reflection law. But how fast or how slow one brings in two hemispheres is irrelevant in

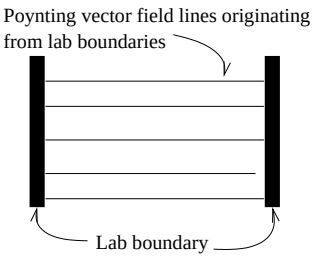

Figure 4.4.: A realistic laboratory has boundaries, e.g., walls. These boundaries have effect similar to the field modes between two parallel plates. In **3D**, the effects are similar to that of a cubical laboratory, etc.

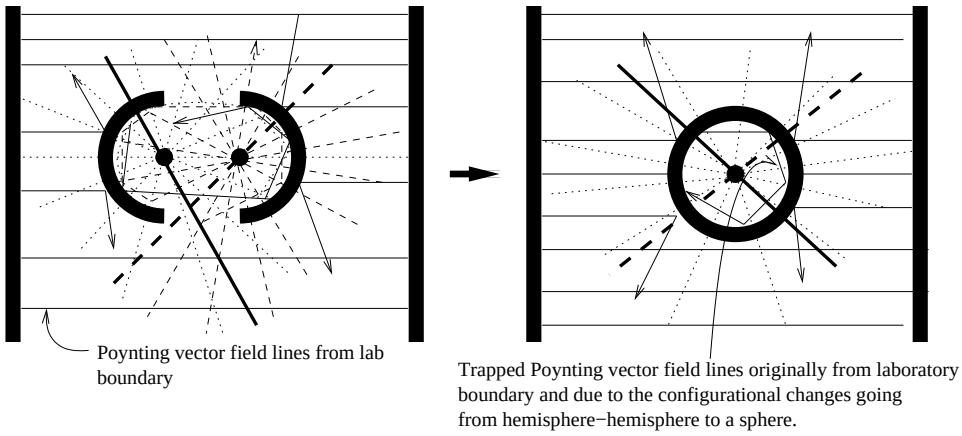

Figure 4.5.: The schematic of sphere manufacturing process in a realistic laboratory.

invoking such non-spherically symmetric energy flow because the gap δ can be chosen arbitrarily. Therefore, there would always be a stream of energy quanta crossing the hemisphere opening with $\xi \neq 0$ as shown in Figure 4.3. In other words, there is always a time interval $\triangle t$ within which the hemispheres are separated by an amount δ before closure. The quanta of vacuum-field radiation energy created within that time interval $\triangle t$ would always be satisfying the condition $\xi \neq 0$, and this results in reflections at oblique angle of incidence with respect to the local normal of the walls of inner sphere cavity. Only when the two hemispheres are finally closed, would then $\xi = 0$ and the radiation energy produced in the sphere after that point would be spherically symmetric and the reflections would be normal to the surface. However, those trapped quantum of energy that were produced prior to the closure of the two hemispheres would always be reflecting from the inner sphere surface at oblique angles of incidence.

Unlike Boyer's ideal laboratory, realistic laboratories have boundaries made of ordinary material as illustrated in Figure 4.4. One must then take into account, when calculating the Casimir force, the vacuum-field radiation pressure contributions from the involved conductors, as well as those contributions from the boundaries such as laboratory walls, etc. We will examine the physics of placing two hemispheres inside the laboratory.

For simplicity, the boundaries of the laboratory as shown in Figure 4.5 are assumed to be simple cubical. Normally, the dimension of conductors considered in Casimir force experiment is in the ranges of microns. When this is compared with the size of the laboratory boundaries such as the walls, the walls of the laboratory can be treated as a set of infinite parallel plates and the vacuum-fields inside the the laboratory can be treated as simple plane waves with impunity.

The presence of laboratory boundaries induce reflection of energy flow similar to that between the two parallel plate arrangement. When the two hemisphere arrangement shown in Figure 4.2 is placed in such a laboratory, the result is to elaborate the radiation pressure contributions from obliquely incident radiations on external surfaces of the two hemispheres. If the two hemispheres are made of conducting material satisfying Boyer's material property, the vacuum-field radiation impinging on hemisphere surfaces at oblique angles of incidence would cause heating of the hemispheres. It means that Boyer's hemispheres placed in a realistic laboratory would continue to rise in temperature

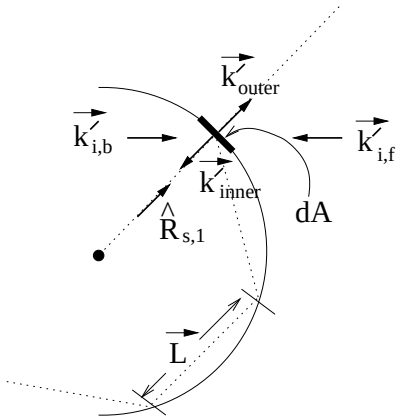

Figure 4.6.: The vacuum-field wave vectors $\vec{k'}_{i,b}$ and $\vec{k'}_{i,f}$ impart a net momentum of the magnitude $\|\vec{p}_{net}\| = \hbar \left\| \vec{k'}_{i,b} - \vec{k'}_{i,f} \right\| /2$ on differential patch of an area dA on a conducting spherical surface.

as a function of time. However, this does not happen with ordinary conductors.

If the two hemispheres are made of ordinary perfect conducting materials, the reflections of radiation at oblique angles of incidence from the laboratory boundaries would elaborate on the radiation pressure acting on the external surfaces of two hemispheres at oblique angles of incidence. Because Boyer's sphere only radiates in the normal direction to its surface, or only responds to impinging radiation at normal incidence with respect to the sphere surface, the extra vacuum-field radiation pressures considered here, i.e., the ones involving oblique angles of incidence, are missing in his Casimir force calculation for the sphere.

4.1. Results

T. H. Boyer in 1968 have shown that for a charge-neutral, perfect conductor of hollow spherical shell, the sign of the Casimir force is positive, which means the force is repulsive. He reached this conclusion by assuming that all vacuum-field radiation energy flows for his sphere are spherically symmetric with respect to its center. In other words, only the wave vectors that are perpendicular to his sphere surface were included in the Casimir force calculation. In the following sections, the non-perpendicular wave vector contributions to the Casimir force that were not accounted for in Boyer's work are considered.

4.1.1. Hollow Spherical Shell

As shown in Figure 4.6, the vacuum-field radiation imparts upon a differential patch of an area dA on the inner wall of the conducting spherical cavity a net momentum of the amount

$$\triangle\vec{p}_{inner} = -\frac{1}{2}\hbar\triangle\vec{k'}_{inner}\left(;\vec{R'}_{s,1},\vec{R'}_{s,0}\right) = \frac{2n\pi\hbar\cos\theta_{inc}}{\left\|\vec{R}_{s,2}\left(r'_i,\vec{\Lambda}'_{s,2}\right)-\vec{R}_{s,1}\left(r'_i,\vec{\Lambda}'_{s,1}\right)\right\|}\hat{R'}_{s,1}, \qquad \begin{cases} 0 \le \theta_{inc} < \pi/2, \\ n = 1,2,3,\cdots, \end{cases}$$

where $\triangle\vec{k'}_{inner}\left(;\vec{R'}_{s,1},\vec{R'}_{s,0}\right)$ is from equation (3.16). The angle of incidence θ_{inc} is from equation (A.115); $\vec{R}_{s,1}\left(r'_i,\vec{\Lambda}'_{s,1}\right)$ and $\vec{R}_{s,2}\left(r'_i,\vec{\Lambda}'_{s,2}\right)$ follow the generic form shown in equation (3.17).

Similarly, the vacuum-field radiation imparts upon a differential patch of an area dA on the outer surface of the conducting spherical shell a net momentum of the amount

$$\triangle\vec{p}_{outer} = -\frac{1}{2}\hbar\triangle\vec{k'}_{outer}\left(;\vec{R'}_{s,1}+a\hat{R'}_{s,1}\right) = -2\hbar\left\|\vec{k'}_{i,f}\right\|\cos\theta_{inc}\hat{R'}_{s,1}, \qquad \begin{cases} 0 \le \theta_{inc} < \pi/2, \\ n = 1,2,3,\cdots, \end{cases}$$

where $\triangle\vec{k'}_{outer}\left(;\vec{R'}_{s,1}+a\hat{R'}_{s,1}\right)$ is from equation (3.18).

The net average force per unit time, per initial wave vector direction, acting on differential element patch of an area dA is given by

$$\vec{\mathcal{F}}_{s,avg}=\lim_{\triangle t\to 1}\left(\frac{\triangle\vec{p}_{outer}}{\triangle t}+\frac{\triangle\vec{p}_{inner}}{\triangle t}\right)$$

or

$$\vec{\mathcal{F}}_{s,avg}=2\hbar\cos\theta_{inc}\left[\frac{n\pi}{\left\|\vec{R}_{s,2}\left(r'_i,\vec{\Lambda}'_{s,2}\right)-\vec{R}_{s,1}\left(r'_i,\vec{\Lambda}'_{s,1}\right)\right\|}-\left\|\vec{k'}_{i,f}\right\|\right]\hat{R'}_{s,1},\qquad\begin{cases}0\le\theta_{inc}<\pi/2,\\ n=1,2,3,\cdots.\end{cases}$$

Notice that $\vec{\mathcal{F}}_{s,avg}$ is called a force per initial wave vector direction because it is computed for $\vec{k'}_{i,b}$ and $\vec{k'}_{i,f}$ along specific initial directions. Here $\vec{k'}_{i,b}$ denotes a particular initial wave vector $\vec{k'}_i$ entering the resonator at $\vec{R}_{s,0}$ as shown in Figure 3.4. The subscript b for $\vec{k'}_{i,b}$ denotes the bounded space inside the resonator. The $\vec{k'}_{i,f}$ denotes a particular initial wave vector $\vec{k'}_i$ impinging upon the surface of the unbounded region of sphere at point $\vec{R'}_{s,1}+a\hat{R'}_{s,1}$ as shown in Figure 3.4. The subscript f for $\vec{k'}_{i,f}$ denotes the free space external to the resonator.

Because the wave vector $\vec{k'}_{i,f}$ resides in free or unbounded space, its magnitude $\left\|\vec{k'}_{i,f}\right\|$ can take on a continuum of allowed modes, whereas $\left\|\vec{k'}_{i,b}\right\|$ have been restricted by $\left\|\vec{L}\right\|=\left\|\vec{R}_{s,2}\left(r'_i,\vec{\Lambda}'_{s,2}\right)-\vec{R}_{s,1}\left(r'_i,\vec{\Lambda}'_{s,1}\right)\right\|$ of equation (C.2). The free space limit is the case where the radius of the sphere becomes very large. Therefore, by designating $\left\|\vec{k'}_{i,f}\right\|$ as

$$\left\|\vec{k'}_{i,f}\right\|=\lim_{r'_i\to\infty}\frac{n\pi}{\left\|\vec{R}_{s,2}\left(r'_i,\vec{\Lambda}'_{s,2}\right)-\vec{R}_{s,1}\left(r'_i,\vec{\Lambda}'_{s,1}\right)\right\|},$$

and summing over all allowed modes, the total average force per unit time, per initial wave vector direction, per unit area is given by

$$\vec{\mathcal{F}}_{s,avg}=\left[\sum_{n=1}^{\infty}\frac{n\pi 2\hbar\cos\theta_{inc}}{\left\|\vec{R}_{s,2}\left(r'_i,\vec{\Lambda}'_{s,2}\right)-\vec{R}_{s,1}\left(r'_i,\vec{\Lambda}'_{s,1}\right)\right\|}-\lim_{r'_i\to\infty}\sum_{n=1}^{\infty}\frac{n\pi 2\hbar\cos\theta_{inc}}{\left\|\vec{R}_{s,2}\left(r'_i,\vec{\Lambda}'_{s,2}\right)-\vec{R}_{s,1}\left(r'_i,\vec{\Lambda}'_{s,1}\right)\right\|}\right]\hat{R'}_{s,1}.$$

In the limit $r'_i\to\infty$, the second summation to the right can be replaced by an integration, $\sum_{n=1}^{\infty}\to\int_0^{\infty}dn$. Hence, we have

$$\vec{\mathcal{F}}_{s,avg}=\left[\sum_{n=1}^{\infty}\frac{2\hbar n\pi\cos\theta_{inc}}{\left\|\vec{R}_{s,2}\left(r'_i,\vec{\Lambda}'_{s,2}\right)-\vec{R}_{s,1}\left(r'_i,\vec{\Lambda}'_{s,1}\right)\right\|}-\lim_{r'_i\to\infty}\int_0^{\infty}\frac{2\hbar n\pi\cos\theta_{inc}}{\left\|\vec{R}_{s,2}\left(r'_i,\vec{\Lambda}'_{s,2}\right)-\vec{R}_{s,1}\left(r'_i,\vec{\Lambda}'_{s,1}\right)\right\|}dn\right]\hat{R'}_{s,1},$$

or with the following substitutions,

$$k'_{i,f}\equiv\frac{n\pi}{\left\|\vec{R}_{s,2}\left(r'_i,\vec{\Lambda}'_{s,2}\right)-\vec{R}_{s,1}\left(r'_i,\vec{\Lambda}'_{s,1}\right)\right\|},\qquad dn=\frac{1}{\pi}\left\|\vec{R}_{s,2}\left(r'_i,\vec{\Lambda}'_{s,2}\right)-\vec{R}_{s,1}\left(r'_i,\vec{\Lambda}'_{s,1}\right)\right\|dk'_{i,f},$$

the total average force per unit time, per initial wave vector direction, per unit area is written as

$$\begin{aligned}\vec{\mathcal{F}}_{s,avg}=2\hbar\cos\theta_{inc}\Bigg[&\sum_{n=1}^{\infty}\frac{n\pi}{\left\|\vec{R}_{s,2}\left(r'_i,\vec{\Lambda}'_{s,2}\right)-\vec{R}_{s,1}\left(r'_i,\vec{\Lambda}'_{s,1}\right)\right\|}\\&-\frac{1}{\pi}\lim_{r'_i\to\infty}\left\|\vec{R}_{s,2}\left(r'_i,\vec{\Lambda}'_{s,2}\right)-\vec{R}_{s,1}\left(r'_i,\vec{\Lambda}'_{s,1}\right)\right\|\int_0^{\infty}k'_{i,f}dk'_{i,f}\Bigg]\hat{R'}_{s,1},\end{aligned}\tag{4.1}$$

where $0 \leq \theta_{inc} < \pi/2$ and $n = 1, 2, 3, \cdots$. The total average vacuum-field radiation force per unit time acting on the uncharged conducting spherical shell is therefore

$$\vec{F}_{s,total} = \sum_{\left\{\vec{k'}_{i,b}, \vec{k'}_{i,f}, \vec{R'}_{s,0}\right\}} \int_S \vec{\mathcal{F}}_{s,avg} \bullet d\vec{S}_{sphere}$$

or

$$\vec{F}_{s,total} = \sum_{\left\{\vec{k'}_{i,b}, \vec{k'}_{i,f}, \vec{R'}_{s,0}\right\}} \int_S \left[\sum_{n=1}^{\infty} \frac{2n\pi\hbar\cos\theta_{inc}}{\left\| \vec{R}_{s,2}\left(r'_i, \vec{\Lambda}'_{s,2}\right) - \vec{R}_{s,1}\left(r'_i, \vec{\Lambda}'_{s,1}\right) \right\|} - \frac{2\hbar}{\pi}\cos\theta_{inc} \right.$$
$$\left. \times \lim_{r'_i \to \infty} \left\| \vec{R}_{s,2}\left(r'_i, \vec{\Lambda}'_{s,2}\right) - \vec{R}_{s,1}\left(r'_i, \vec{\Lambda}'_{s,1}\right) \right\| \int_0^{\infty} k'_{i,f} dk'_{i,f} \right] \hat{R'}_{s,1} \bullet d\vec{S}_{sphere}, \tag{4.2}$$

where $d\vec{S}_{sphere}$ is a differential surface element of a sphere and the integration $\int_S$ is over the spherical surface. The term $\vec{R'}_{s,0}$ is the initial crossing point inside the sphere as defined in equation (3.2). The notation $\sum_{\left\{\vec{k'}_{i,b}, \vec{k'}_{i,f}, \vec{R'}_{s,0}\right\}}$ imply the summation over all initial wave vector directions for both inside $\left(\vec{k'}_{i,b}\right)$ and outside $\left(\vec{k'}_{i,f}\right)$ of the sphere, over all crossing points given by $\vec{R'}_{s,0}$.

It is easy to see that $\vec{\mathcal{F}}_{s,avg}$ of equation (4.1) is an "unregularized" **1D** Casimir force expression for the parallel plates (see the vacuum pressure approach by Milonni, Cook and Goggin [25]). It becomes more apparent with the substitution $\triangle t = d/c$. An application of the Euler-Maclaurin summation formula [23, 24] leads to the regularized, finite force expression. The force $\vec{\mathcal{F}}_{s,avg}$ is attractive because

$$\cos\theta_{inc} > 0$$

and

$$\sum_{n=1}^{\infty} \frac{n\pi}{\left\| \vec{R}_{s,2}\left(r'_i, \vec{\Lambda}'_{s,2}\right) - \vec{R}_{s,1}\left(r'_i, \vec{\Lambda}'_{s,1}\right) \right\|} < \frac{1}{\pi} \lim_{r'_i \to \infty} \left\| \vec{R}_{s,2}\left(r'_i, \vec{\Lambda}'_{s,2}\right) - \vec{R}_{s,1}\left(r'_i, \vec{\Lambda}'_{s,1}\right) \right\| \int_0^{\infty} k'_{i,f} dk'_{i,f},$$

where $\left\| \vec{R}_{s,2}\left(r'_i, \vec{\Lambda}'_{s,2}\right) - \vec{R}_{s,1}\left(r'_i, \vec{\Lambda}'_{s,1}\right) \right\|$ is a constant for a given initial wave $\vec{k'}_{i,b}$ and the initial crossing point $\vec{R'}_{s,0}$ in the cross-section of a sphere (or hemisphere). The total average force $\vec{F}_{s,total}$, which is really the sum of $\vec{\mathcal{F}}_{s,avg}$ over all $\vec{R'}_{s,0}$ and all initial wave directions, is therefore also attractive. For the sphere configuration of Figure 3.4, where the energy flow direction is not restricted to the direction of local surface normal, the Casimir force problem becomes an extension of infinite set of parallel plates of a unit area.

4.1.2. Hemisphere-Hemisphere and Plate-Hemisphere

Similarly, for the hemisphere-hemisphere and plate-hemisphere configurations, the expression for the total average force per unit time, per initial wave vector direction, per unit area is identical to that of the hollow spherical shell with modifications,

$$\vec{\mathcal{F}}_{h,avg} = 2\hbar\cos\theta_{inc} \left[\sum_{n=1}^{\infty} \frac{n\pi}{\left\| \vec{R}_{h,2}\left(r'_i, \vec{\Lambda}'_{h,2}\right) - \vec{R}_{h,1}\left(r'_i, \vec{\Lambda}'_{h,1}\right) \right\|} \right.$$
$$\left. - \frac{1}{\pi} \lim_{r'_i \to \infty} \left\| \vec{R}_{h,2}\left(r'_i, \vec{\Lambda}'_{h,2}\right) - \vec{R}_{h,1}\left(r'_i, \vec{\Lambda}'_{h,1}\right) \right\| \int_0^{\infty} k'_{i,f} dk'_{i,f} \right] \hat{R'}_{h,1}, \tag{4.3}$$

where $\theta_{inc} \leq \pi/2$ and $n = 1, 2, 3, \cdots$. The incidence angle θ_{inc} is from equation (A.115); $\vec{R}_{h,1}\left(r'_i, \vec{\Lambda}'_{h,1}\right)$ and $\vec{R}_{h,2}\left(r'_i, \vec{\Lambda}'_{h,2}\right)$ follow the generic form shown in equation (3.21). This force is attractive for the same reasons as

discussed previously for the hollow spherical shell case. The total radiation force averaged over unit time, over all possible initial wave vector directions, acting on the uncharged conducting hemisphere-hemisphere (plate-hemisphere) surface is given by

$$\vec{F}_{h,total} = \sum_{\left\{\vec{k'}_{i,b},\vec{k'}_{i,f},\vec{R'}_{h,0}\right\}} \int_S \left[\sum_{n=1}^{\infty} \frac{2n\pi\hbar\cos\theta_{inc}}{\left\| \vec{R}_{h,2}\left(r'_i,\vec{\Lambda}'_{h,2}\right) - \vec{R}_{h,1}\left(r'_i,\vec{\Lambda}'_{h,1}\right)\right\|} - \frac{2\hbar}{\pi}\cos\theta_{inc} \right.$$
$$\left. \times \lim_{r'_i\to\infty} \left\| \vec{R}_{h,2}\left(r'_i,\vec{\Lambda}'_{h,2}\right) - \vec{R}_{h,1}\left(r'_i,\vec{\Lambda}'_{h,1}\right)\right\| \int_0^{\infty} k'_{i,f}dk'_{i,f} \right] \hat{R'}_{h,1} \bullet d\vec{S}_{hemisphere}, \tag{4.4}$$

where $d\vec{S}_{hemisphere}$ is now a differential surface element of a hemisphere and the integration $\int_S$ is over the surface of the hemisphere. The term $\vec{R'}_{h,0}$ is the initial crossing point of the hemisphere opening as defined in equation (3.2). The notation $\sum_{\left\{\vec{k'}_{i,b},\vec{k'}_{i,f},\vec{R'}_{h,0}\right\}}$ imply the summation over all initial wave vector directions for both inside $\left(\vec{k'}_{i,b}\right)$ and outside $\left(\vec{k'}_{i,f}\right)$ of the hemisphere-hemisphere (or the plate-hemisphere) resonator, over all crossing points given by $\vec{R'}_{h,0}$.

It should be remarked that for the plate-hemisphere configuration, the total average radiation force remains identical to that of the hemisphere-hemisphere configuration only for the case where the gap distance between plate and the center of hemisphere is more than the hemisphere radius r'_i. When the plate is placed closer, the boundary quantization length $\left\|\vec{L}\right\|$ must be chosen carefully to be either

$$\left\|\vec{L}\right\| = \left\| \vec{R}_{h,2}\left(r'_i,\vec{\Lambda}'_{h,2}\right) - \vec{R}_{h,1}\left(r'_i,\vec{\Lambda}'_{h,1}\right)\right\|$$

or

$$\left\|\vec{L}\right\| = \left\| \vec{R}_{p}\left(r'_i,\vec{\Lambda}'_{p}\right) - \vec{R}_{h,N_{h,max}}\left(r'_i,\vec{\Lambda}'_{h,N_{h,max}}\right)\right\|.$$

They are illustrated in Figure 3.8. The proper one to use is the smaller of the two. Here $\vec{R}_p\left(r'_i,\vec{\Lambda}'_p\right)$ is from equation (C.54) of Appendix C3 and $N_{h,max}$ is defined in equation (C.8) of Appendix C2.

4.2. Interpretation of the Result

Because only the specification of boundary is needed in Casimir's vacuum-field approach as opposed to the use of a polarizability parameter in Casimir-Polder interaction picture, the Casimir force is sometimes regarded as a configurational force. On the other hand, the Casimir effect can be thought of as a macroscopic manifestation of the retarded van der Waals interaction. And the Casimir force can be equivalently approximated by a summation of the constituent molecular forces employing Casimir-Polder interaction. This practice inherently relies on the material properties of the involved conductors through the use of polarizability parameters. In this respect, the Casimir force can be regarded as a material dependent force.

Boyer's material property is such that the atoms in his conducting sphere are arranged in such manner to respond only to the impinging radiation at local normal angle of incidence to the sphere surface, and they also radiate only along the direction of local normal to its surface. When the Casimir force is calculated for a sphere made of Boyer's fictitious material, the force is repulsive. Also, in Boyer's original work, the laboratory boundary did not exist. When Boyer's sphere is placed in a realistic laboratory, the net Casimir force acting on his sphere becomes attractive because the majority of the radiation from the laboratory boundaries acts to apply inward pressure on the external surface of sphere when the angle of incidence is oblique with respect to the local normal. If the sphere is made of ordinary perfect conductors, the impinging radiation at oblique angles of incidence would be reflected. In such cases the total radiation pressure applied to the external local-sphere-surface is twice the pressure exerted by the incident wave, which is the force found in equation (4.2) of the previous section. However, Boyer's sphere cannot radiate along the direction that is not normal to the local-sphere-surface. Therefore, the total pressure applied to Boyer's sphere is half of the force given in equation (4.2) of the previous section. This peculiar incapability of emission of a Boyer's sphere would lead to

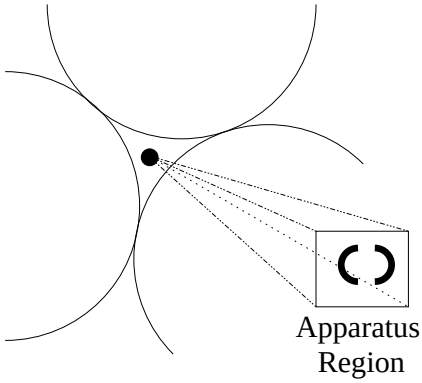

Figure 4.7.: To deflect away as much possible the vacuum-field radiation emanating from the laboratory boundaries, the walls, floor and ceiling are constructed with some optimal curvature to be determined. The apparatus is then placed within the "Apparatus Region."

the absorption of the energy and would cause a rise in the temperature for the sphere. Nonetheless, the extra pressure due to the waves of oblique angle of incidence is large enough to change the Casimir force for Boyer's sphere from being repulsive to attractive. The presence of the laboratory boundaries only act to enhance the attractive aspect of the Casimir force on a sphere. The fact that Boyer's sphere cannot irradiate along the direction that is not normal to the local-sphere-surface, whereas ordinary perfect conductors irradiate in all directions, implies that his sphere is made of extraordinarily hypothetical material, and this may be the reason why the repulsive Casimir force have not been experimentally observed to date.

In conclusion, (1) the Casimir force is both boundary and material property dependent. The particular shape of the conductor, e.g. sphere, only introduces the preferred direction for radiation. For example, radiations in direction normal to the local surface has bigger magnitude than those radiating in other directions. This preference for the direction of radiation is intrinsically connected to the preferred directions for the lattice vibrations. And, the characteristic of lattice vibrations is intrinsically connected to the property of material. (2) Boyer's sphere is made of extraordinary conducting material, which is why his Casimir force is repulsive. (3) When the radiation pressures of all angles of incidence are included in the Casimir force calculation, the force is attractive for a charge-neutral sphere made of ordinary perfect conductor.

4.3. Suggestions on the Detection of Repulsive Casimir Force for a Sphere

The first step in detecting the repulsive Casimir force for a spherical configuration is to find a conducting material that most closely resembles the Boyer's material to construct two hemispheres. It has been discussed previously that even Boyer's sphere can produce attractive Casimir force when the radiation pressures due to oblique incidence waves are included in the calculation. Therefore, the geometry of the laboratory boundaries have to be chosen to deflect away as much as possible the oblique incident wave as illustrated in Figure 4.7. Once these conditions are met, the experiment can be conducted in the region labeled "Apparatus Region" to observe Boyer's repulsive force.

4.4. Outlook

The Casimir effect has influence in broad range of physics. Here, we list one such phenomenon known as "sonoluminescense," and, finally conclude with the Casimir oscillator.

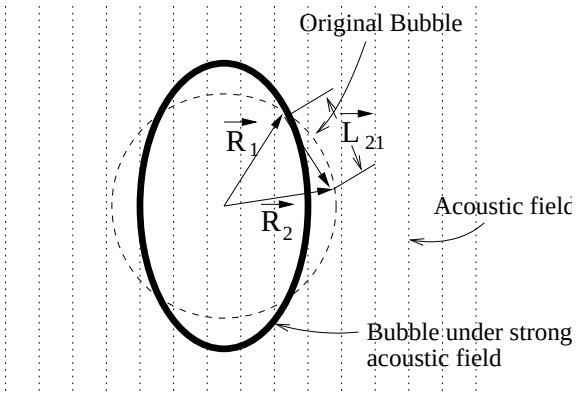

Figure 4.8.: The original bubble shape shown in dotted lines and the deformed bubble in solid line under strong acoustic field.

4.4.1. Sonoluminescense

The phenomenon of sonoluminescense remains a poorly understood subject to date [28, 29]. When a small air bubble of radius $\sim 10^{-3}\, cm$ is injected into water and subjected to a strong acoustic field of $\sim 20\, kHz$ under pressure roughly $\sim 1\, atm$, the bubble emits an intense flash of light in the optical range, with total energy of roughly $\sim 10^{7}\, eV$. This emission of light occurs at minimum bubble radius of roughly $\sim 10^{-4}\, cm$. The flash duration has been determined to be on the order of $100\, ps$ [30, 31, 32]. It is to be emphasized that small amounts of noble gases are necessary in the bubble for sonoluminescense.

The bubble in sonoluminescense experiment can be thought of as a deformed sphere under strong acoustic pressure. The dynamical Casimir effect arises due to the deformation of the shape; therefore, introducing a modification to $\vec{L}_{21} = \left\| \vec{R}_2 - \vec{R}_1 \right\|$ from that of the original bubble shape. Here $\vec{L}_{21}$ is the path length for the reflecting wave in the original bubble shape. In general $\vec{L}_{21} \equiv \vec{L}_{21}(t) = \left\| \vec{R}_2 (r_i(t), \theta(t), \phi(t)) - \vec{R}_1 (r_i(t), \theta(t), \phi(t)) \right\|$. From the relations found in this thesis work for the reflection points $\vec{R}_1 (r_i(t), \theta(t), \phi(t))$ and $\vec{R}_N (r_i(t), \theta(t), \phi(t))$, together with the dynamical Casimir force expression of equation (3.31), the amount of initial radiation energy converted into heat energy during the deformation process can be found. The bubble deformation process shown in Figure 4.8 is a three dimensional heat generation problem. Current investigation seeks to determine if the temperature can be raised sufficiently to cause deuterium-tritium (D-T) fusion, which could provide an alternative approach to achieve energy generation by this D-T reaction (threshold $\sim 17\, KeV$) [33]. Its theoretical treatment is similar to that discussed on the **1D** problem shown in Figure 3.9.

4.4.2. Casimir Oscillator

If one can create a laboratory as shown in Figure 4.7, and place in the laboratory hemispheres made of Boyer's material, then the hemisphere-hemisphere system will execute an oscillatory motion. When two such hemispheres are separated, the allowed wave modes in the hemisphere-hemisphere confinement would no longer follow Boyer's spherical Bessel function restriction. Instead it will be strictly constrained by the functional relation of $\left\| \vec{R}_2 - \vec{R}_1 \right\|$, where $\vec{R}_1$ and $\vec{R}_2$ are two neighboring reflection points. Only when the two hemispheres are closed, would the allowed wave modes obey Boyer's spherical Bessel function restriction.

Assuming that hemispheres are made of Boyer's material and the laboratory environment is that shown in Figure 4.7, the two closed hemispheres would be repulsing because Boyer's Casimir force is repulsive. Once the two hemispheres are separated, the allowed wave modes are governed by the internal reflections at oblique angle of incidence. Since the hemispheres made of Boyer's material are "infinitely unresponsive" to oblique incidence waves, all these temporary non-spherical symmetric waves would be absorbed by the Boyer's hemispheres and the hemispheres would heat up. The two hemispheres would then attract each other and the oscillation cycle repeats. Such a mechanical system may have application.

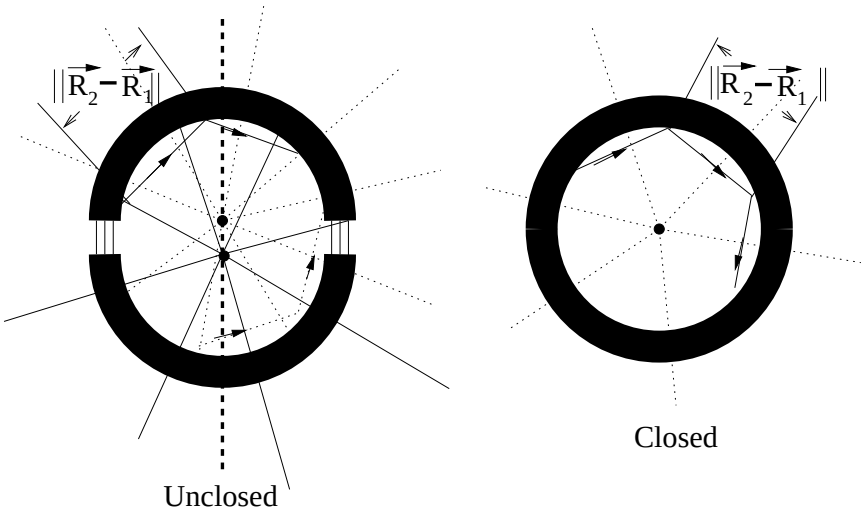

Figure 4.9.: The vacuum-field radiation energy flows are shown for closed and unclosed hemispheres. For the hemispheres made of Boyer's material, the non-radial wave would be absorbed by the hemispheres.

Appendices

These are my original derivations and developments that were too tedious and lengthy to be included in the main body of the thesis. There are five appendices: (1) Appendix A, (2) Appendix B, (3) Appendix C, (4) Appendix D and Appendix E. The appendices C and D are further divided into subparts C.1, C.2, C.3, D.1 and D.2. The title and the layout of the appendices closely follow the main body of the thesis. Finally, the appendix E have been added to provide further list of references pertaining to the Casimir effect, but which were not explicitly used by this thesis.

A. Reflection Points on the Surface of a Resonator

In this appendix, the original derivations and developments of this thesis pertaining to the reflection dynamics are included. It is referenced by the text of this thesis to supply all the details.

For the configuration shown in Figure 3.1, the wave vector directed along an arbitrary direction in Cartesian coordinates is written as

$$\vec{k'}_1\left(k'_{1,x},k'_{1,y},k'_{1,z}\right)=\sum_{i=1}^{3}k'_{1,i}\hat{e_i},\qquad k'_{1,i}=\begin{cases} i=1\rightarrow k'_{1,x}, & \hat{e_1}=\hat{x},\\ i=2\rightarrow k'_{1,y}, & \hat{e_2}=\hat{y}\\ i=3\rightarrow k'_{1,z}, & \hat{e_3}=\hat{z}.\end{cases} \tag{A.1}$$

The unit wave vector is given by

$$\hat{k'}_1=\left\|\vec{k'}_1\right\|^{-1}\sum_{i=1}^{3}k'_{1,i}\hat{e_i}. \tag{A.2}$$

The initial crossing position $\vec{R'}_0$ of hemisphere opening for the incident wave $\vec{k'}_1$ is defined as

$$\vec{R'}_0\left(r'_{0,x},r'_{0,y},r'_{0,z}\right)=\sum_{i=1}^{3}r'_{0,i}\hat{e_i},\qquad r'_{0,i}=\begin{cases} i=1\rightarrow r'_{0,x},\\ i=2\rightarrow r'_{0,y},\\ i=3\rightarrow r'_{0,z}.\end{cases} \tag{A.3}$$

It should be noticed here that $\vec{R'}_0$ has only two components, $r'_{0,x}$ and $r'_{0,z}$. But nevertheless, one can always set $r'_{0,y}=0$ whenever needed. Since no particular wave with certain wavelength is prescribed initially, it is desirable to employ a parameterization scheme to represent these wave vectors. The line segment traced out by the wave vector $\hat{k'}_1$ is formulated in the parametric form

$$\vec{R'}_1=\xi_1\hat{k'}_1+\vec{R'}_0=\sum_{i=1}^{3}\left[r'_{0,i}+\xi_1\left\|\vec{k'}_1\right\|^{-1}k'_{1,i}\right]\hat{e_i}, \tag{A.4}$$

where the real variable ξ_1 is a positive definite parameter. The restriction $\xi_1\geq 0$ is a necessary condition since the direction of the wave propagation is set by $\hat{k'}_1$. Here $\vec{R'}_1$ denotes the first reflection point on the hemisphere. In terms of spherical coordinates, $\vec{R'}_1$ takes the form

$$\vec{R'}_1\left(r'_i,\theta'_1,\phi'_1\right)=r'_i\sum_{i=1}^{3}\Lambda'_{1,i}\hat{e_i},\qquad \begin{cases}\Lambda'_{1,1}=\sin\theta'_1\cos\phi'_1,\\ \Lambda'_{1,2}=\sin\theta'_1\sin\phi'_1,\\ \Lambda'_{1,3}=\cos\theta'_1,\end{cases} \tag{A.5}$$

where r'_i is the hemisphere radius, θ'_1 and ϕ'_1 are the polar and azimuthal angles respectively of the first reflection point $\vec{R'}_1$. The subscript i of r'_i denotes "inner radius" and it is not a summation index. Equations (A.4) and (A.5) are combined as

$$\sum_{i=1}^{3}\left[r'_{0,i}+\xi_1\left\|\vec{k'}_1\right\|^{-1}k'_{1,i}-r'_i\Lambda_{1,i}\right]\hat{e_i}=0. \tag{A.6}$$

Because the basis vectors $\hat{e_i}$ are independent of each other, the above relations are only satisfied when each coefficients

of $\hat{e}_i$ vanish independently,

$$r'_{0,i} + \xi_1 \left\| \vec{k'}_1 \right\|^{-1} k'_{1,i} - r'_i \Lambda_{1,i} = 0, \qquad i = 1, 2, 3. \tag{A.7}$$

The three terms $\Lambda_{1,i=1}$, $\Lambda_{1,i=2}$ and $\Lambda_{1,i=3}$ satisfy an identity

$$\sum_{i=1}^{3} \Lambda_{1,i}^2 = 1. \tag{A.8}$$

From equation (A.7), $\Lambda_{1,i}^2$ is computed for each i :

$$\Lambda_{1,i}^2 = [r'_i]^{-2} \left\{ \left[r'_{0,i}\right]^2 + \xi_1^2 \left\| \vec{k'}_1 \right\|^{-2} \left[k'_{1,i}\right]^2 + 2 r'_{0,i} \xi_1 \left\| \vec{k'}_1 \right\|^{-1} k'_{1,i} \right\}, \qquad i = 1, 2, 3.$$

Substituting the above result of $\Lambda_{1,i}^2$ into equation (A.8) and after rearrangement, one obtains

$$\xi_1^2 \sum_{i=1}^{3} \left\| \vec{k'}_1 \right\|^{-2} \left[k'_{1,i}\right]^2 + 2\xi_1 \left\| \vec{k'}_1 \right\|^{-1} \sum_{i=1}^{3} r'_{0,i} k'_{1,i} + \sum_{i=1}^{3} \left[r'_{0,i}\right]^2 - [r'_i]^2 = 0. \tag{A.9}$$

Further simplifying, it becomes

$$\xi_1^2 + 2\hat{k'}_1 \bullet \vec{R'}_0 \xi_1 + \left\| \vec{R'}_0 \right\|^2 - [r'_i]^2 = 0. \tag{A.10}$$

There are two roots,

$$\xi_{1,a} = -\hat{k'}_1 \bullet \vec{R'}_0 - \sqrt{\left[\hat{k'}_1 \bullet \vec{R'}_0\right]^2 + [r'_i]^2 - \left\| \vec{R'}_0 \right\|^2}$$

and

$$\xi_{1,b} = -\hat{k'}_1 \bullet \vec{R'}_0 + \sqrt{\left[\hat{k'}_1 \bullet \vec{R'}_0\right]^2 + [r'_i]^2 - \left\| \vec{R'}_0 \right\|^2}.$$

The root to be used should have a positive value. For the wave reflected within the hemisphere, $\vec{R'}_0 \leq r'_i$,

$$\sqrt{\left[\hat{k'}_1 \bullet \vec{R'}_0\right]^2 + [r'_i]^2 - \left\| \vec{R'}_0 \right\|^2} \geq \left| \hat{k'}_1 \bullet \vec{R'}_0 \right| \geq -\hat{k'}_1 \bullet \vec{R'}_0$$

where the equality $\left| \hat{k'}_1 \bullet \vec{R'}_0 \right| = -\hat{k'}_1 \bullet \vec{R'}_0$ happens when $\hat{k'}_1 \bullet \vec{R'}_0 \leq 0$. Therefore, $\xi_{1,a} \leq 0$ and $\xi_{1,b} \geq 0$; the positive root $\xi_{1,b}$ should be selected. For bookkeeping purposes, $\xi_{1,b}$ is designated as $\xi_{1,p}$:

$$\xi_{1,p} = -\hat{k'}_1 \bullet \vec{R'}_0 + \sqrt{\left[\hat{k'}_1 \bullet \vec{R'}_0\right]^2 + [r'_i]^2 - \left\| \vec{R'}_0 \right\|^2}. \tag{A.11}$$

Using this positive root, the first reflection point of the inner hemisphere is found to be

$$\vec{R'}_1 \left(\xi_{1,p}; \vec{R'}_0, \hat{k'}_1 \right) = \sum_{i=1}^{3} \left[r'_{0,i} + \xi_{1,p} \left\| \vec{k'}_1 \right\|^{-1} k'_{1,i} \right] \hat{e}_i. \tag{A.12}$$

The incident wave $\vec{k'}_i$, shown in Figure A.1 and where i here stands for incident wave, can always be decomposed

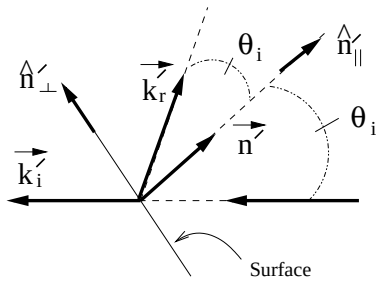

Figure A.1.: A simple reflection of incoming wave $\vec{k'}_i$ from the surface defined by a local normal $\vec{n'}$.

into components parallel and perpendicular to the vector $\vec{n'}$ normal to the reflecting surface,

$$\vec{k'}_i = \vec{k'}_{i,\parallel} + \vec{k'}_{i,\perp} = \frac{\vec{n'} \bullet \vec{k'}_i}{\vec{n'} \bullet \vec{n'}} \vec{n'} + \frac{\left[\vec{n'} \times \vec{k'}_i\right] \times \vec{n'}}{\vec{n'} \bullet \vec{n'}}.$$

If the local normal $\hat{n'}$ is already normalized to unity, the above expression reduces to

$$\vec{k'}_i = \hat{n'} \bullet \vec{k'}_i \hat{n'} + \left[\hat{n'} \times \vec{k'}_i\right] \times \hat{n'}. \tag{A.13}$$

Here the angle between $\vec{k'}_i$ and $\hat{n'}$ is $\pi - \theta_i$. The action of reflection only modifies $\vec{k'}_{i,\parallel}$ in the reflected wave. The reflected wave part of $\vec{k'}_i$ in equation (A.13) is

$$\vec{k'}_r = \alpha_{r,\perp} \vec{k'}_{i,\perp} - \alpha_{r,\parallel} \vec{k'}_{i,\parallel} = \alpha_{r,\perp} \left[\hat{n'} \times \vec{k'}_i\right] \times \hat{n'} - \alpha_{r,\parallel} \hat{n'} \bullet \vec{k'}_i \hat{n'}, \tag{A.14}$$

where $\vec{k'}_{i,\parallel}$ have been rotated by 180^o on the plane of incidence. The new quantities $\alpha_{r,\parallel}$ and $\alpha_{r,\perp}$ are the reflection coefficients. For a perfect reflecting surfaces, $\alpha_{r,\parallel} = \alpha_{r,\perp} = 1$. Because of the frequent usage of the component for $\vec{k'}_r$, equation (A.14) is also written in component form. The component of the double cross product $\left[\hat{n'} \times \vec{k'}_i\right] \times \hat{n'}$ is computed first,

$$\begin{aligned}
\left\{\left[\hat{n'} \times \vec{k'}_i\right] \times \hat{n'}\right\}_l &= \epsilon_{lmn} \left[\hat{n'} \times \vec{k'}_i\right]_m n'_n = \epsilon_{lmn}\epsilon_{mqr} n'_q k'_{i,r} n'_n = \epsilon_{nlm}\epsilon_{qrm} n'_q k'_{i,r} n'_n \\
&= \left[\delta_{nq}\delta_{lr} - \delta_{nr}\delta_{lq}\right] n'_q k'_{i,r} n'_n = \delta_{nq}\delta_{lr} n'_q k'_{i,r} n'_n - \delta_{nr}\delta_{lq} n'_q k'_{i,r} n'_n \\
&= n'_n k'_{i,l} n'_n - n'_l k'_{i,n} n'_n
\end{aligned}$$

or

$$\left[\hat{n'} \times \vec{k'}_i\right] \times \hat{n'} = \sum_{l=1}^{3} \left[n'_n k'_{i,l} n'_n - n'_l k'_{i,n} n'_n\right] \hat{e}_l, \tag{A.15}$$

where the summation over the index n is implicit. In component form, $\vec{k'}_r$ is hence expressed as

$$\vec{k'}_r = \sum_{l=1}^{3} \left\{\alpha_{r,\perp} \left[n'_n k'_{i,l} n'_n - n'_l k'_{i,n} n'_n\right] - \alpha_{r,\parallel} n'_n k'_{i,n} n'_l\right\} \hat{e}_l, \tag{A.16}$$

where it is understood $\hat{n'}$ is already normalized.

The second reflection point $\vec{R'}_2$ is found by repeating the steps done for $\vec{R'}_1$,

$$\vec{R'}_2 = \vec{R'}_1 + \xi_{2,p}\hat{k'}_r = \vec{R'}_1 + \xi_{2,p}\frac{\alpha_{r,\perp}\left[\hat{n'}\times\vec{k'}_i\right]\times\hat{n'} - \alpha_{r,\parallel}\hat{n'}\bullet\vec{k'}_i\hat{n'}}{\left\|\alpha_{r,\perp}\left[\hat{n'}\times\vec{k'}_i\right]\times\hat{n'} - \alpha_{r,\parallel}\hat{n'}\bullet\vec{k'}_i\hat{n'}\right\|},$$

where $\xi_{2,p}$ is the new positive parameter corresponding to the second reflection point. The procedure can be repeated for any reflection point. Although this technique is sound, it can be noticed immediately that the technique suffers from the lack of elegance. For this reason, the scalar field technique will be exclusively used in studying the reflection dynamics. For a simple plane, the scalar field function can be inferred rather intuitively. However, for more complex surfaces, one has to work it out to get the corresponding scalar field. For the purpose of generalization of the technique to any arbitrary surfaces, we derive the scalar field functional for the plane in great detail.

In simple reflection dynamics, there exists a plane of incidence in which all reflections occur. The plane of incidence is determined by the incident wave $\vec{k'}_i$ and the local surface normal $\vec{n'}_i$. For the system shown in Figure 3.1, $\vec{k'}_i$ and $\vec{n'}_i$ are given by

$$\vec{k'}_i = \vec{k'}_1, \qquad \vec{n'}_{n'_i,1} \equiv -\vec{R'}_1\left(\xi_{1,p};\vec{R'}_0,\hat{k'}_1\right) = -\xi_{1,p}\hat{k'}_1 - \vec{R'}_0.$$

The normal to the incidence plane is characterized by the cross product,

$$\vec{n'}_{p,1} = \vec{k'}_1\times\vec{n'}_{n'_i,1} = \vec{k'}_1\times\left[-\xi_{1,p}\hat{k'}_1 - \vec{R'}_0\right] = -\vec{k'}_1\times\vec{R'}_0 = -\sum_{i=1}^{3}\epsilon_{ijk}k'_{1,j}r'_{0,k}\hat{e_i},$$

where the summation over the indices j and k are implicit. The normal to the incidence plane is normalized as

$$\hat{n'}_{p,1} = -\left\|\vec{n'}_{p,1}\right\|^{-1}\sum_{i=1}^{3}\epsilon_{ijk}k'_{1,j}r'_{0,k}\hat{e_i}. \tag{A.17}$$

In order to take advantage of the information given above, the concept of scalar fields in mathematical sense is in order. A functional $f\left(x',y',z'\right)$ is a scalar field if to each point (x',y',z') of a region in space, there corresponds a number λ. The study of a scalar field is a study of scalar valued functions of three variables. Scalar fields are connected to its normals, e.g., equation (A.17), through the relation

$$\hat{n'}_{p,1} \propto \vec{\nabla}' f_{p,1}\left(x',y',z'\right) = \sum_{i=1}^{3}\hat{e_i}\frac{\partial}{\partial\nu'_i}f_{p,1}\left(x',y',z'\right), \qquad i = \begin{cases} 1\rightarrow\nu'_1 = x', \\ 2\rightarrow\nu'_2 = y', \\ 3\rightarrow\nu'_3 = z'. \end{cases} \tag{A.18}$$

Introducing a constant proportionality factor $\beta_{p,1}$, equation (A.18) becomes

$$\hat{n'}_{p,1} = \beta_{p,1}\sum_{i=1}^{3}\hat{e_i}\frac{\partial}{\partial\nu'_i}f_{p,1}\left(x',y',z'\right). \tag{A.19}$$

The proportionality factor $\beta_{p,1}$ is intrinsically connected to the normalization of $\vec{\nabla}' f_{p,1}$. Because the vector $\hat{n'}_{p,1}$ is a unit vector, its magnitude squared is

$$\beta_{p,1}^2\sum_{i=1}^{3}\left[\frac{\partial}{\partial\nu'_i}f_{p,1}\left(x',y',z'\right)\right]^2 = 1 \quad\rightarrow\quad \beta_{p,1} = \pm\left\{\sum_{i=1}^{3}\left[\frac{\partial}{\partial\nu'_i}f_{p,1}\left(x',y',z'\right)\right]^2\right\}^{-1/2}.$$

In equation (A.19), the directions for vectors $\hat{n'}_{p,1}$ and $\vec{\nabla}' f_{p,1}$ are intrinsically built in. Therefore, the proportionality

factor $\beta_{p,1}$ has to be a positive quantity,

$$\beta_{p,1} = \left\{ \sum_{i=1}^{3} \left[\frac{\partial}{\partial \nu_i'} f_{p,1}\left(x', y', z'\right) \right]^2 \right\}^{-1/2}. \tag{A.20}$$

Unfortunately, the exact form of the proportionality coefficient $\beta_{p,1}$ requires the knowledge of $f_{p,1}$, which is yet to be determined. However, we can use it formally for now until the solution for $f_{p,1}$ is found.

Substituting the gradient function $\vec{\nabla}' f_{p,1}$ into equation (A.19), and using equations (A.17) and (A.19), one arrives at

$$\sum_{i=1}^{3} \left[\frac{\partial}{\partial \nu_i'} f_{p,1}\left(x', y', z'\right) + \beta_{p,1}^{-1} \left\| \vec{n'}_{p,1} \right\|^{-1} \epsilon_{ijk} k'_{1,j} r'_{0,k} \right] \hat{e}_i = 0, \qquad i = \begin{cases} 1 \to \nu_1' = x', \\ 2 \to \nu_2' = y', \\ 3 \to \nu_3' = z'. \end{cases} \tag{A.21}$$

Because the basis vectors $\hat{e}_i$ are linearly independent, the equation for each component is obtained as

$$\frac{\partial}{\partial \nu_i'} f_{p,1}\left(\alpha, \beta, \gamma\right) + \beta_{p,1}^{-1} \left\| \vec{n'}_{p,1} \right\|^{-1} \epsilon_{ijk} k'_{1,j} r'_{0,k} = 0, \qquad i = \begin{cases} 1 \to \nu_1' = x' = \alpha, \\ 2 \to \nu_2' = y' = \beta, \\ 3 \to \nu_3' = z' = \gamma. \end{cases} \tag{A.22}$$

Integrating both sides of equation (A.22) over the variable $\nu_i' = \alpha$,

$$\int_{\alpha_0}^{\alpha} \frac{\partial}{\partial \alpha'} f_{p,1}\left(\alpha', \beta, \gamma\right) d\alpha' = -\int_{\alpha_0}^{\alpha} \beta_{p,1}^{-1} \left\| \vec{n'}_{p,1} \right\|^{-1} \epsilon_{\alpha' jk} k'_{1,j} r'_{0,k} d\alpha',$$

where the dummy variable α' is introduced for integration purpose. The terms $\epsilon_{\alpha' jk} k'_{1,j} r'_{0,k}$, $\beta_{p,1}$ and $\left\| \vec{n'}_{p,1} \right\|$ are independent of the dummy variable α', and they can be moved out of the integrand,

$$\int_{\alpha_0}^{\alpha} \frac{\partial}{\partial \alpha'} f_{p,1}\left(\alpha', \beta, \gamma\right) d\alpha' = -\beta_{p,1}^{-1} \left\| \vec{n'}_{p,1} \right\|^{-1} \epsilon_{\alpha jk} k'_{1,j} r'_{0,k} \int_{\alpha_0}^{\alpha} d\alpha'. \tag{A.23}$$

Because the total differential of $f_{p,1}$ is given by

$$df_{p,1} = \frac{\partial f_{p,1}}{\partial \alpha'} d\alpha' + \frac{\partial f_{p,1}}{\partial \beta} d\beta + \frac{\partial f_{p,1}}{\partial \gamma} d\gamma, \qquad \alpha' \neq \beta \neq \gamma, \tag{A.24}$$

the term $\left[\partial f_{p,1}/\partial \alpha'\right] d\alpha'$ can be written as

$$\frac{\partial f_{p,1}}{\partial \alpha'} d\alpha' = df_{p,1} - \frac{\partial f_{p,1}}{\partial \beta} d\beta - \frac{\partial f_{p,1}}{\partial \gamma'} d\gamma.$$

The integration over the variable $\nu_i' = \alpha$ in equation (A.23), with variables $\nu_i' \neq \alpha$ fixed, can be carried out with

$$d\beta = d\gamma = 0, \qquad \frac{\partial}{\partial \alpha'} f_{p,1}\left(\alpha', \beta, \gamma\right) d\alpha' = df_{p,1}\left(\alpha', \beta, \gamma\right) \tag{A.25}$$

as

$$\int_{\alpha_0}^{\alpha} df_{p,1}\left(\alpha', \beta, \gamma\right) = -\beta_{p,1}^{-1} \left\| \vec{n'}_{p,1} \right\|^{-1} \epsilon_{\alpha jk} k'_{1,j} r'_{0,k} \int_{\alpha_0}^{\alpha} d\alpha'$$

to give

$$f_{p,1}\left(\alpha, \beta, \gamma\right) = \beta_{p,1}^{-1} \left\| \vec{n'}_{p,1} \right\|^{-1} \epsilon_{\alpha jk} k'_{1,j} r'_{0,k} \left[\alpha_0 - \alpha\right] + f_{p,1}\left(\alpha_0, \beta, \gamma\right). \tag{A.26}$$

The two terms $\left[\epsilon_{\alpha jk} k'_{1,j} r'_{0,k} / \left\{ \beta_{p,1} \left\| \vec{n'}_{p,1} \right\| \right\}\right] \alpha_0$ and $f_{p,1}\left(\alpha_0, \beta, \gamma\right)$ are independent of α. These terms can only

assume values of $\nu_i' = \beta$ or $\nu_i' = \gamma$. By re-designating α independent terms,

$$h_{p,1}(\beta,\gamma) = \beta_{p,1}^{-1}\left\|\vec{n'}_{p,1}\right\|^{-1}\epsilon_{\alpha jk}k'_{1,j}r'_{0,k}\alpha_0 + f_{p,1}(\alpha_0,\beta,\gamma), \tag{A.27}$$

equation (A.26) can be rewritten for bookkeeping purposes as

$$f_{p,1}(\alpha,\beta,\gamma) = h_{p,1}(\beta,\gamma) - \beta_{p,1}^{-1}\left\|\vec{n'}_{p,1}\right\|^{-1}\epsilon_{\alpha jk}k'_{1,j}r'_{0,k}\alpha. \tag{A.28}$$

Substituting the result into equation (A.22) and performing a differentiation with respect to the variable $\nu_i' = \beta$ gives

$$\frac{\partial}{\partial\beta}\left[h_{p,1}(\beta,\gamma) - \beta_{p,1}^{-1}\left\|\vec{n'}_{p,1}\right\|^{-1}\epsilon_{\alpha jk}k'_{1,j}r'_{0,k}\alpha\right] + \beta_{p,1}^{-1}\left\|\vec{n'}_{p,1}\right\|^{-1}\epsilon_{\beta jk}k'_{1,j}r'_{0,k} = 0$$

or

$$\frac{\partial}{\partial\beta}h_{p,1}(\beta,\gamma) = -\beta_{p,1}^{-1}\left\|\vec{n'}_{p,1}\right\|^{-1}\epsilon_{\beta jk}k'_{1,j}r'_{0,k}.$$

The integration of both sides with respect to the variable $\nu_i' = \beta$ yields the result

$$\int_{\beta_0}^{\beta}\frac{\partial}{\partial\beta'}h_{p,1}(\beta',\gamma)\,d\beta' = -\int_{\beta_0}^{\beta}\beta_{p,1}^{-1}\left\|\vec{n'}_{p,1}\right\|^{-1}\epsilon_{\beta' jk}k'_{1,j}r'_{0,k}d\beta' = -\beta_{p,1}^{-1}\left\|\vec{n'}_{p,1}\right\|^{-1}\epsilon_{\beta jk}k'_{1,j}r'_{0,k}\int_{\beta_0}^{\beta}d\beta',$$

where the dummy variable β' is introduced for integration purpose and the terms $\epsilon_{\beta jk}k'_{1,j}r'_{0,k}$, $\beta_{p,1}$ and $\left\|\vec{n'}_{p,1}\right\|$ have been taken out of the integrand because they are independent of β'. Following the same procedure used in equations (A.24) through (A.25), the integrand $[\partial h_{p,1}/\partial\beta']\,d\beta'$ on the left hand side of the integral is

$$\frac{\partial}{\partial\beta'}h_{p,1}(\beta',\gamma)\,d\beta' = dh_{p,1}(\beta',\gamma).$$

Consequently, $h_{p,1}(\beta,\gamma)$ is given by

$$h_{p,1}(\beta,\gamma) = \beta_{p,1}^{-1}\left\|\vec{n'}_{p,1}\right\|^{-1}\epsilon_{\beta jk}k'_{1,j}r'_{0,k}[\beta_0 - \beta] + h_{p,1}(\beta_0,\gamma). \tag{A.29}$$

The two terms $\left[\epsilon_{\beta jk}k'_{1,j}r'_{0,k}/\left\{\beta_{p,1}\left\|\vec{n'}_{p,1}\right\|\right\}\right]\beta_0$ and $h_{p,1}(\beta_0,\gamma)$ are independent of β. The β independent terms can be re-designated as

$$g_{p,1}(\gamma) = \beta_{p,1}^{-1}\left\|\vec{n'}_{p,1}\right\|^{-1}\epsilon_{\beta jk}k'_{1,j}r'_{0,k}\beta_0 + h_{p,1}(\beta_0,\gamma). \tag{A.30}$$

For bookkeeping purposes, equation (A.29) is rewritten as

$$h_{p,1}(\beta,\gamma) = g_{p,1}(\gamma) - \beta_{p,1}^{-1}\left\|\vec{n'}_{p,1}\right\|^{-1}\epsilon_{\beta jk}k'_{1,j}r'_{0,k}\beta. \tag{A.31}$$

Substitution of $h_{p,1}(\beta,\gamma)$ into equation (A.28) gives

$$f_{p,1}(\alpha,\beta,\gamma) = g_{p,1}(\gamma) - \beta_{p,1}^{-1}\left\|\vec{n'}_{p,1}\right\|^{-1}\left[\epsilon_{\beta jk}k'_{1,j}r'_{0,k}\beta + \epsilon_{\alpha jk}k'_{1,j}r'_{0,k}\alpha\right]. \tag{A.32}$$

Once more substituting $f_{p,1}(\alpha,\beta,\gamma)$ into equation (A.22), and performing the differentiation with respect to the variable $\nu_i' = \gamma$, where $\gamma \neq \alpha \neq \beta$, we obtain

$$\frac{d}{d\gamma}\left[g_{p,1}(\gamma) - \beta_{p,1}^{-1}\left\|\vec{n'}_{p,1}\right\|^{-1}\left\{\epsilon_{\beta jk}k'_{1,j}r'_{0,k}\beta + \epsilon_{\alpha jk}k'_{1,j}r'_{0,k}\right\}\alpha\right] + \beta_{p,1}^{-1}\left\|\vec{n'}_{p,1}\right\|^{-1}\epsilon_{\gamma jk}k'_{1,j}r'_{0,k} = 0$$

or

$$\frac{d}{d\gamma}g_{p,1}\left(\gamma\right)=-\beta_{p,1}^{-1}\left\|\vec{n'}_{p,1}\right\|^{-1}\epsilon_{\gamma jk}k'_{1,j}r'_{0,k},$$

where the differentiation have been changed from ∂ to d because $g_{p,1}$ is a function of single variable. The integration of both sides with respect to the variable $\nu'_i=\gamma$ then gives

$$\int_{\gamma_0}^{\gamma}\frac{d}{d\gamma'}g_{p,1}\left(\gamma'\right)d\gamma'=-\int_{\gamma_0}^{\gamma}\beta_{p,1}^{-1}\left\|\vec{n'}_{p,1}\right\|^{-1}\epsilon_{\gamma' jk}k'_{1,j}r'_{0,k}d\gamma'=-\beta_{p,1}^{-1}\left\|\vec{n'}_{p,1}\right\|^{-1}\epsilon_{\gamma jk}k'_{1,j}r'_{0,k}\int_{\gamma_0}^{\gamma}d\gamma',$$

where the dummy variable γ' have been introduced for integration purpose and the terms $\epsilon_{\gamma jk}k'_{1,j}r'_{0,k}$, $\beta_{p,1}$ and $\left\|\vec{n'}_{p,1}\right\|$ have been taken out of the integrand because they are independent of γ'. Knowing $\left[dg_{p,1}/d\gamma'\right]d\gamma'=dg_{p,1}$, the integration is carried out to yield

$$g_{p,1}\left(\gamma\right)=\beta_{p,1}^{-1}\left\|\vec{n'}_{p,1}\right\|^{-1}\epsilon_{\gamma jk}k'_{1,j}r'_{0,k}\left[\gamma_0-\gamma\right]+g_{p,1}\left(\gamma_0\right). \tag{A.33}$$

The two terms $\left[\epsilon_{\gamma jk}k'_{1,j}r'_{0,k}/\left\{\beta_{p,1}\left\|\vec{n'}_{p,1}\right\|\right\}\right]\gamma_0$ and $g_{p,1}\left(\gamma_0\right)$ are independent of γ. The γ independent terms are re-designated as

$$b_0=\beta_{p,1}^{-1}\left\|\vec{n'}_{p,1}\right\|^{-1}\epsilon_{\gamma jk}k'_{1,j}r'_{0,k}\gamma_0+g_{p,1}\left(\gamma_0\right). \tag{A.34}$$

For bookkeeping purposes, equation (A.33) is rewritten as

$$g_{p,1}\left(\gamma\right)=b_0-\beta_{p,1}^{-1}\left\|\vec{n'}_{p,1}\right\|^{-1}\epsilon_{\gamma jk}k'_{1,j}r'_{0,k}\gamma. \tag{A.35}$$

Substituting $g_{p,1}\left(\gamma\right)$ in equation (A.32), the result for $f_{p,1}\left(\alpha,\beta,\gamma\right)$ is found to be

$$f_{p,1}\left(\alpha,\beta,\gamma\right)=b_0-\beta_{p,1}^{-1}\left\|\vec{n'}_{p,1}\right\|^{-1}\sum_{i=1}^{3}\epsilon_{ijk}k'_{1,j}r'_{0,k}\nu'_i,\qquad i=\begin{cases}1\rightarrow\nu'_1=\alpha=x',\\2\rightarrow\nu'_2=\beta=y',\\3\rightarrow\nu'_3=\gamma=z'.\end{cases} \tag{A.36}$$

The cross product expressed in terms of the Levi-Civita symbol is expanded to give

$$\epsilon_{x' jk}k'_{1,j}r'_{0,k}=k'_{1,j=y'}r'_{0,k=z'}-k'_{1,k=z'}r'_{0,j=y'}, \tag{A.37}$$

$$\epsilon_{y' jk}k'_{1,j}r'_{0,k}=k'_{1,j=z'}r'_{0,k=x'}-k'_{1,k=x'}r'_{0,k=z'}, \tag{A.38}$$

$$\epsilon_{z' jk}k'_{1,j}r'_{0,k}=k'_{1,j=x'}r'_{0,k=y'}-k'_{1,k=y'}r'_{0,j=x'}. \tag{A.39}$$

It is important to understand that the functional $f_{p,1}$ in equation (A.36) is a scalar field description of an infinite family of parallel planes characterized by the normal given in equation (A.17),

$$\hat{n'}_{p,1}=-\left\|\vec{n'}_{p,1}\right\|^{-1}\sum_{i=1}^{3}\epsilon_{ijk}k'_{1,j}r'_{0,k}\hat{e_i}.$$

Because the normal $\hat{n'}_{p,1}$ is a cross product of the two vectors $\vec{k'}_1$ and $\vec{R'}_0$, the surface represented by the scalar field $f_{p,1}$ is a plane spanned by all the scattered wave vectors. The graphical plot of the functional $f_{p,1}$ is illustrated in Figure A.2. The three coefficients,

$$\epsilon_{\alpha jk}k'_{1,j}r'_{0,k},\qquad\epsilon_{\beta jk}k'_{1,j}r'_{0,k},\qquad\epsilon_{\gamma jk}k'_{1,j}r'_{0,k},$$

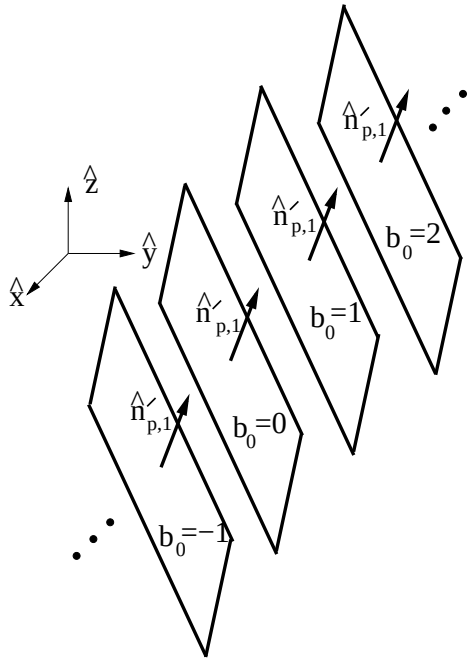

Figure A.2.: Parallel planes characterized by a normal $\hat{n'}_{p,1} = -\left\|\vec{n'}_{p,1}\right\|^{-1} \sum_{i=1}^{3} \epsilon_{ijk} k'_{1,j} r'_{0,k} \hat{e}_i$.

of the independent variables α, β and γ define the slopes along the respective bases $\hat{\alpha}$, $\hat{\beta}$ and $\hat{\gamma}$. The integration constant b_0 provides infinite set of parallel planes whose common normal is $\hat{n'}_{p,1}$. For what is concerned with here, only one of them containing the coordinate origin is required. It is convenient to choose the plane with $b_0 = 0$. With the plane of $b_0 = 0$ chosen, the scalar field of equation (A.36) is rewritten for the sake of bookkeeping purposes:

$$f_{p,1}(\alpha,\beta,\gamma) = -\beta_{p,1}^{-1}\left\|\vec{n'}_{p,1}\right\|^{-1} \sum_{i=1}^{3} \epsilon_{ijk} k'_{1,j} r'_{0,k} \nu'_i, \qquad i = \begin{cases} 1 \to \nu'_1 = \alpha = x', \\ 2 \to \nu'_2 = \beta = y', \\ 3 \to \nu'_3 = \gamma = z'. \end{cases} \tag{A.40}$$

where $-\infty \leq \{\alpha,\beta,\gamma\} \leq \infty$.

As mentioned before, $f_{p,1}$ of equation (A.40) is a scalar field where $\vec{k'}_1$ and $\vec{R'}_0$ are the two initially known vectors which span locally the reflection surface. Other than $\vec{k'}_1$ and $\vec{R'}_0$, any member vectors of the spanning set for the incidence plane can also be used to determine the orientation of a surface. Then it is always true that

$$f_{p,1}\left(\alpha,\beta,\gamma;\vec{k'}_1,\vec{R'}_0\right) = f_{p,2}\left(\alpha,\beta,\gamma;\vec{k'}_2,\vec{R'}_1\right) = \cdots = f_{p,N}\left(\alpha,\beta,\gamma;\vec{k'}_N,\vec{R'}_N\right), \tag{A.41}$$

where the integer index N of $\vec{k'}_N$ is used to enumerate the sequence of reflections; and the integer index N of $\vec{R'}_N$ is used to enumerate the sequence of reflection points.

What is still yet undetermined in equation (A.40) is the proportionality factor $\beta_{p,1}$. From equation (A.20), the $\beta_{p,1}$ has an algebraic definition

$$\beta_{p,1} = \left\{\sum_{i=1}^{3}\left[\frac{\partial}{\partial\nu'_i} f_{p,1}(\alpha,\beta,\gamma)\right]^2\right\}^{-1/2}, \qquad i = \begin{cases} 1 \to \nu'_1 = \alpha, \\ 2 \to \nu'_2 = \beta, \\ 3 \to \nu'_3 = \gamma. \end{cases}$$

The partial derivatives $\partial f_{p,1}/\partial \nu_i'$ are calculated with the solution of $f_{p,1}$ in equation (A.40),

$$\frac{\partial}{\partial \nu_i'} f_{p,1}(\alpha,\beta,\gamma) = -\beta_{p,1}^{-1} \left\| \vec{n'}_{p,1} \right\|^{-1} \frac{\partial}{\partial \nu_i'} \sum_{i=1}^{3} \epsilon_{ijk} k'_{1,j} r'_{0,k} \nu_i' = -\beta_{p,1}^{-1} \left\| \vec{n'}_{p,1} \right\|^{-1} \epsilon_{ijk} k'_{1,j} r'_{0,k};$$

which reduces to

$$\beta_{p,1} \left[1 - \left\| \vec{n'}_{p,1} \right\| \left\{ \sum_{i=1}^{3} \left[\epsilon_{ijk} k'_{1,j} r'_{0,k} \right]^2 \right\}^{-1/2} \right] = 0. \tag{A.42}$$

The two possible solutions are either $\beta_{p,1} = 0$, or the term enclosed in the outermost square bracket must vanish. Because $\beta_{p,1} = 0$ is a useless trivial solution, the second solution has to be adopted. Since $\left\| \vec{n'}_{p,1} \right\| = \left\{ \sum_{i=1}^{3} \left[\epsilon_{ijk} k'_{1,j} r'_{0,k} \right]^2 \right\}^{1/2}$, the equation (A.42) is already satisfied for any value of $\beta_{p,1}$. Therefore, $\beta_{p,1}$ is an arbitrary quantity, and it is simply chosen to be unity which makes the gradient function $\vec{\nabla}' f_{p,1}$ automatically normalized. The scalar field solution $f_{p,1}$ of equation (A.40) is now restated with $\beta_{p,1} = 1$,

$$f_{p,1}(\alpha,\beta,\gamma) = -\left\| \vec{n'}_{p,1} \right\|^{-1} \sum_{i=1}^{3} \epsilon_{ijk} k'_{1,j} r'_{0,k} \nu_i', \qquad i = \begin{cases} 1 \to \nu_1' = \alpha = x', \\ 2 \to \nu_2' = \beta = y', \\ 3 \to \nu_3' = \gamma = z', \end{cases} \tag{A.43}$$

where $-\infty \leq \{\nu_1' = \alpha = x', \nu_2' = \beta = y', \nu_3' = \gamma = z'\} \leq \infty$.

The intercept between the plane of incidence, defined by equation (A.43), and the hemisphere is found through the algebraic relation

$$x'^2 + y'^2 + z'^2 = \left[r_i' \right]^2,$$

which can be written as

$$\left[r_i' \right]^2 - \sum_{i=1}^{3} \left[\nu_i' \right]^2 = 0, \qquad i = \begin{cases} 1 \to \nu_1' = x', \\ 2 \to \nu_2' = y', \\ 3 \to \nu_3' = z', \end{cases} \tag{A.44}$$

where the r_i' is the radius of sphere and the index i denotes the radius of the inner surface. The intercept of interest is shown in Figure 3.2.

One may be tempted to incorporate the surface vibration into equation (A.44) through a slight modification

$$\left[r_i'(t) \right]^2 - \sum_{i=1}^{3} \left[\nu_i' \right]^2 = 0,$$

where the vibration have been introduced through the time variations in radius. Some have employed such a model in describing the "Casimir radiation," as well as the phenomenon of sonoluminescense mainly due to its simplicity from the mathematical point of view [14, 29]. In general, if one wishes to incorporate the vibration of a surface, the description of such system could be represented in the form

$$\left[r_i'(\theta', \phi', t) \right]^2 - \sum_{i=1}^{3} \left[\nu_i'(\theta', \phi') \right]^2 = 0.$$

Since the radius function varies with θ', ϕ' and t, its treatment has to be postponed until the surface function can be found in later sections. In the present discussion, the hemisphere is regarded as having no vibration.

Returning from the above short digression, the surface function of the sphere is expressed as the null function from

equation (A.44),

$$f_{hemi}\left(x',y',z'\right)=\left[r_i'\right]^2-\sum_{i=1}^{3}\left[\nu_i'\right]^2=0,\qquad i=\begin{cases}1\rightarrow\nu_1'=x',\\2\rightarrow\nu_2'=y',\\3\rightarrow\nu_3'=z'.\end{cases}\tag{A.45}$$

The intersection between the two surfaces, the plane of incidence defined in equation (A.43) and the hemisphere defined in equation (A.45), is found through the relation

$$f_{p,1}\left(x',y',z'\right)-f_{hemi}\left(x',y',z'\right)=0,\tag{A.46}$$

which is equivalent to setting the scalar function $f_{p,1}\left(x',y',z'\right)=0$. Substituting expressions for $f_{p,1}\left(x',y',z'\right)$ and $f_{hemi}\left(x',y',z'\right)$ given in equations (A.43) and (A.45), we arrive at

$$\sum_{i=1}^{3}\left\{\left[\nu_i'\right]^2-\left\|\vec{n'}_{p,1}\right\|^{-1}\epsilon_{ijk}k_{1,j}'r_{0,k}'\nu_i'\right\}-\left[r_i'\right]^2=0,\qquad i=\begin{cases}1\rightarrow\nu_1'=\alpha=x',\\2\rightarrow\nu_2'=\beta=y',\\3\rightarrow\nu_3'=\gamma=z'.\end{cases}\tag{A.47}$$

It is convenient to rewrite $\left[r_i'\right]^2$ in the form

$$\left[r_i'\right]^2=\left[r_{i,x'}'\right]^2+\left[r_{i,y'}'\right]^2+\left[r_{i,z'}'\right]^2=\sum_{i=1}^{3}\left[r_{i,i}'\right]^2,\qquad i=\begin{cases}1\rightarrow r_{i,1}'=r_{i,x'}',\\2\rightarrow r_{i,2}'=r_{i,y'}',\\3\rightarrow r_{i,3}'=r_{i,z'}'.\end{cases}\tag{A.48}$$

Equation (A.47) can then be written as

$$\sum_{i=1}^{3}\left\{\left[\nu_i'\right]^2-\left\|\vec{n'}_{p,1}\right\|^{-1}\epsilon_{ijk}k_{1,j}'r_{0,k}'\nu_i'-\left[r_{i,i}'\right]^2\right\}=0,\qquad i=\begin{cases}1\rightarrow\nu_1'=\alpha=x';r_{i,1}'=r_{i,x'}',\\2\rightarrow\nu_2'=\beta=y';r_{i,2}'=r_{i,y'}',\\3\rightarrow\nu_3'=\gamma=z';r_{i,3}'=r_{i,z'}'.\end{cases}\tag{A.49}$$

Since the first two terms are already known, we can set each braced term equal to zero,

$$\left[\nu_i'\right]^2-\left\|\vec{n'}_{p,1}\right\|^{-1}\epsilon_{ijk}k_{1,j}'r_{0,k}'\nu_i'-\left[r_{i,i}'\right]^2=0,\qquad i=1,2,3.\tag{A.50}$$

The above relation, equation (A.50), is valid in determining the set of discrete reflection points. The solutions of this quadratic equation are

$$\nu_i'=\frac{1}{2}\left\|\vec{n'}_{p,1}\right\|^{-1}\epsilon_{ijk}k_{1,j}'r_{0,k}'\pm\left\{\left[\frac{1}{2}\left\|\vec{n'}_{p,1}\right\|^{-1}\epsilon_{ijk}k_{1,j}'r_{0,k}'\right]^2+\left[r_{i,i}'\right]^2\right\}^{1/2},\qquad i=1,2,3,\tag{A.51}$$

where the summation over the indices j and k is implicit. The restriction of ν_i' being real imposes the condition

$$\left[\frac{1}{2}\left\|\vec{n'}_{p,1}\right\|^{-1}\epsilon_{ijk}k_{1,j}'r_{0,k}'\right]^2+\left[r_{i,i}'\right]^2\geq 0,\qquad i=1,2,3.\tag{A.52}$$

In spherical coordinates, the three radial vector components $r_{i,1}'$, $r_{i,2}'$ and $r_{i,3}'$ are

$$r_{i,1}'=r_i'\sin\theta'\cos\phi',\qquad r_{i,2}'=r_i'\sin\theta'\sin\phi',\qquad r_{i,3}'=r_i'\cos\theta',\tag{A.53}$$

where $r_{i,1}'=r_{i,x'}'$, $r_{i,2}'=r_{i,y'}'$ and $r_{i,3}'=r_{i,z'}'$. Here the terms r_i', θ' and ϕ' are the usual radial length, the polar and the azimuthal angle. This guarantees that $\vec{R}'=\sum_{i=1}^{3}r_{i,i}'\hat{e}_i$ is on the sphere, and justifies the step taken in equation (A.50) since we are only interested in the conditions of the discriminants expressed by equation (A.52). With $r_{i,i}'$

redefined in terms of spherical coordinates, the reality condition of ν_i' in equation (A.52) becomes

$$\left[\frac{1}{2}\left\|\vec{n'}_{p,1}\right\|^{-1}\epsilon_{1jk}k'_{1,j}r'_{0,k}\right]^2+\left[r'_i\right]^2\sin^2\theta'\cos^2\phi'\geq 0, \tag{A.54}$$

$$\left[\frac{1}{2}\left\|\vec{n'}_{p,1}\right\|^{-1}\epsilon_{2jk}k'_{1,j}r'_{0,k}\right]^2+\left[r'_i\right]^2\sin^2\theta'\sin^2\phi'\geq 0, \tag{A.55}$$

$$\left[\frac{1}{2}\left\|\vec{n'}_{p,1}\right\|^{-1}\epsilon_{3jk}k'_{1,j}r'_{0,k}\right]^2+\left[r'_i\right]^2\cos^2\theta'\geq 0. \tag{A.56}$$

Equations (A.54) through (A.56) provide allowed range of ν_i' to ensure its value being real. The solution of equation (A.56) is

$$\cos^2\theta'\geq-\left[\frac{1}{2r'_i}\left\|\vec{n'}_{p,1}\right\|^{-1}\epsilon_{3jk}k'_{1,j}r'_{0,k}\right]^2, \tag{A.57}$$

which leads to two inequalities,

$$\cos\theta'\geq i\frac{1}{2r'_i}\left\|\vec{n'}_{p,1}\right\|^{-1}\epsilon_{3jk}k'_{1,j}r'_{0,k},\qquad \cos\theta'\leq -i\frac{1}{2r'_i}\left\|\vec{n'}_{p,1}\right\|^{-1}\epsilon_{3jk}k'_{1,j}r'_{0,k}. \tag{A.58}$$

These two inequalities cannot be satisfied simultaneously by the two vectors $\vec{R'}_0$ and $\vec{k'}_1$. We have to look for $\sin\theta'$ by combining equations (A.54) and (A.55) to give

$$\frac{1}{4}\left\|\vec{n'}_{p,1}\right\|^{-2}\left\{\left[\epsilon_{1jk}k'_{1,j}r'_{0,k}\right]^2+\left[\epsilon_{2mn}k'_{1,m}r'_{0,n}\right]^2\right\}+\left[r'_i\right]^2\sin^2\theta'\geq 0,$$

which yields

$$\sin^2\theta'\geq-\frac{1}{4}\left[r'_i\right]^{-2}\left\|\vec{n'}_{p,1}\right\|^{-2}\left\{\left[\epsilon_{1jk}k'_{1,j}r'_{0,k}\right]^2+\left[\epsilon_{2mn}k'_{1,m}r'_{0,n}\right]^2\right\}. \tag{A.59}$$

The solutions are again two inequalities,

$$\sin\theta'\geq\frac{i}{2r'_i}\left\|\vec{n'}_{p,1}\right\|^{-1}\left\{\left[\epsilon_{1jk}k'_{1,j}r'_{0,k}\right]^2+\left[\epsilon_{2mn}k'_{1,m}r'_{0,n}\right]^2\right\}, \tag{A.60}$$

$$\sin\theta'\leq-\frac{i}{2r'_i}\left\|\vec{n'}_{p,1}\right\|^{-1}\left\{\left[\epsilon_{1jk}k'_{1,j}r'_{0,k}\right]^2+\left[\epsilon_{2mn}k'_{1,m}r'_{0,n}\right]^2\right\}, \tag{A.61}$$

which cannot be simultaneously satisfied by the vectors $\vec{R'}_0$ and $\vec{k'}_1$. We have to combine equations (A.57) and (A.59) to give

$$\tan^2\theta'\geq\left[\epsilon_{3qr}k'_{1,q}r'_{0,r}\right]^{-2}\left\{\left[\epsilon_{1jk}k'_{1,j}r'_{0,k}\right]^2+\left[\epsilon_{2mn}k'_{1,m}r'_{0,n}\right]^2\right\}, \tag{A.62}$$

which leads to another two inequalities,

$$\tan\theta'\geq\left[\epsilon_{3qr}k'_{1,q}r'_{0,r}\right]^{-1}\left\{\left[\epsilon_{1jk}k'_{1,j}r'_{0,k}\right]^2+\left[\epsilon_{2mn}k'_{1,m}r'_{0,n}\right]^2\right\}^{1/2}, \tag{A.63}$$

$$\tan\theta'\leq-\left[\epsilon_{3qr}k'_{1,q}r'_{0,r}\right]^{-1}\left\{\left[\epsilon_{1jk}k'_{1,j}r'_{0,k}\right]^2+\left[\epsilon_{2mn}k'_{1,m}r'_{0,n}\right]^2\right\}^{1/2}. \tag{A.64}$$

In the specified range for θ', $0 \leq \theta' \leq \pi$, the tangent function has the limits

$$\lim_{\varepsilon \to 0} \left(0 \leq \theta' \leq \frac{1}{2}\pi - |\varepsilon| \right) \Rightarrow 0 \leq \tan\theta' \leq \infty, \tag{A.65}$$

$$\lim_{\varepsilon \to 0} \left(\frac{1}{2}\pi + |\varepsilon| \leq \theta' \leq \pi \right) \Rightarrow -\infty \leq \tan\theta' \leq 0, \tag{A.66}$$

where ε is infinitesimal quantity introduced for limiting purposes. Since there is no guarantee that $\epsilon_{3qr} k'_{1,q} r'_{0,r} > 0$ in equations (A.63) and (A.64), one has to consider both cases where $\epsilon_{3qr} k'_{1,q} r'_{0,r} > 0$ and $\epsilon_{3qr} k'_{1,q} r'_{0,r} < 0$. Therefore, for the positive denominator case where $\epsilon_{3qr} k'_{1,q} r'_{0,r} > 0$, we have

$$\begin{cases} \epsilon_{3qr} k'_{1,q} r'_{0,r} \geq 0, \qquad \lim_{\varepsilon \to 0} \left(0 \leq \theta' \leq \frac{1}{2}\pi - |\varepsilon| \right), \\ 0 \leq \left(\tan\theta' \geq \left[\epsilon_{3qr} k'_{1,q} r'_{0,r} \right]^{-1} \left\{ \left[\epsilon_{1jk} k'_{1,j} r'_{0,k} \right]^2 + \left[\epsilon_{2mn} k'_{1,m} r'_{0,n} \right]^2 \right\}^{1/2} \right) \leq \infty; \end{cases} \tag{A.67}$$

$$\begin{cases} \epsilon_{3qr} k'_{1,q} r'_{0,r} \geq 0, \qquad \lim_{\varepsilon \to 0} \left(\frac{1}{2}\pi + |\varepsilon| \leq \theta' \leq \pi \right), \\ -\infty \leq \left(\tan\theta' \leq -\left[\epsilon_{3qr} k'_{1,q} r'_{0,r} \right]^{-1} \left\{ \left[\epsilon_{1jk} k'_{1,j} r'_{0,k} \right]^2 + \left[\epsilon_{2mn} k'_{1,m} r'_{0,n} \right]^2 \right\}^{1/2} \right) \leq 0. \end{cases} \tag{A.68}$$

For the negative denominator case where $\epsilon_{3qr} k'_{1,q} r'_{0,r} < 0$, we rewrite equations (A.63) and (A.64) in the form

$$\epsilon_{3qr} k'_{1,q} r'_{0,r} \leq 0 \quad \Rightarrow \quad -\left| \epsilon_{3qr} k'_{1,q} r'_{0,r} \right| \leq 0,$$

$$\tan\theta' \geq -\left| \epsilon_{3qr} k'_{1,q} r'_{0,r} \right|^{-1} \left\{ \left[\epsilon_{1jk} k'_{1,j} r'_{0,k} \right]^2 + \left[\epsilon_{2mn} k'_{1,m} r'_{0,n} \right]^2 \right\}^{1/2}, \tag{A.69}$$

$$\tan\theta' \leq \left| \epsilon_{3qr} k'_{1,q} r'_{0,r} \right|^{-1} \left\{ \left[\epsilon_{1jk} k'_{1,j} r'_{0,k} \right]^2 + \left[\epsilon_{2mn} k'_{1,m} r'_{0,n} \right]^2 \right\}^{1/2}. \tag{A.70}$$

The tangent function in the domain $0 \leq \theta' \leq \pi$ has a discontinuity at $\theta' = \pi/2$, the inequality (A.69) has the limit $0 \geq \tan\theta' \geq -\infty$, and the inequality (A.70) has the limit $\infty \geq \tan\theta' \geq 0$. Therefore, the limits for a negative denominator case where $\epsilon_{3qr} k'_{1,q} r'_{0,r} < 0$,

$$\begin{cases} \epsilon_{3qr} k'_{1,q} r'_{0,r} \leq 0, \qquad \lim_{\varepsilon \to 0} \left(0 \leq \theta' \leq \frac{1}{2}\pi - |\varepsilon| \right), \\ 0 \leq \left(\tan\theta' \leq \left| \epsilon_{3qr} k'_{1,q} r'_{0,r} \right|^{-1} \left\{ \left[\epsilon_{1jk} k'_{1,j} r'_{0,k} \right]^2 + \left[\epsilon_{2mn} k'_{1,m} r'_{0,n} \right]^2 \right\}^{1/2} \right) \leq \infty; \end{cases} \tag{A.71}$$

$$\begin{cases} \epsilon_{3qr} k'_{1,q} r'_{0,r} \leq 0, \qquad \lim_{\varepsilon \to 0} \left(\frac{1}{2}\pi + |\varepsilon| \leq \theta' \leq \pi \right), \\ -\infty \leq \left(\tan\theta' \geq -\left| \epsilon_{3qr} k'_{1,q} r'_{0,r} \right|^{-1} \left\{ \left[\epsilon_{1jk} k'_{1,j} r'_{0,k} \right]^2 + \left[\epsilon_{2mn} k'_{1,m} r'_{0,n} \right]^2 \right\}^{1/2} \right) \leq 0. \end{cases} \tag{A.72}$$

Comparing equations (A.67), (A.68), (A.71) and (A.72), we see that two of them are identical when rewritten in terms of the later convention where $\epsilon_{3qr} k'_{1,q} r'_{0,r} \leq 0$ is expressed as $-\left| \epsilon_{3qr} k'_{1,q} r'_{0,r} \right| \leq 0$. The two tangent function inequality limits are summarized below for bookkeeping purposes:

$$\begin{cases} \lim_{\varepsilon \to 0} \left(0 \leq \theta' \leq \frac{1}{2}\pi - |\varepsilon| \right), \\ 0 \leq \left(\tan\theta' \leq \left| \epsilon_{3qr} k'_{1,q} r'_{0,r} \right|^{-1} \left\{ \left[\epsilon_{1jk} k'_{1,j} r'_{0,k} \right]^2 + \left[\epsilon_{2mn} k'_{1,m} r'_{0,n} \right]^2 \right\}^{1/2} \right) \leq \infty; \end{cases} \tag{A.73}$$

$$\left\{ \begin{array}{c} \lim_{\varepsilon\to 0}\left(\frac{1}{2}\pi+|\varepsilon|\le\theta'\le\pi\right), \\ -\infty\le\left(\tan\theta'\ge-\left|\epsilon_{3qr}k'_{1,q}r'_{0,r}\right|^{-1}\left\{\left[\epsilon_{1jk}k'_{1,j}r'_{0,k}\right]^2+\left[\epsilon_{2mn}k'_{1,m}r'_{0,n}\right]^2\right\}^{1/2}\right)\le 0. \end{array}\right. \tag{A.74}$$

The corresponding arguments for inequalities in (A.73) and (A.74) are

$$\left\{ \begin{array}{c} \lim_{\varepsilon\to 0}\left(0\le\theta'\le\frac{1}{2}\pi-|\varepsilon|\right), \\ \theta'=\arctan\left(\left|\epsilon_{3qr}k'_{1,q}r'_{0,r}\right|^{-1}\left\{\left[\epsilon_{1jk}k'_{1,j}r'_{0,k}\right]^2+\left[\epsilon_{2mn}k'_{1,m}r'_{0,n}\right]^2\right\}^{1/2}\right); \end{array}\right. \tag{A.75}$$

$$\left\{ \begin{array}{c} \lim_{\varepsilon\to 0}\left(\frac{1}{2}\pi+|\varepsilon|\le\theta'\le\pi\right), \\ \theta'=\arctan\left(-\left|\epsilon_{3qr}k'_{1,q}r'_{0,r}\right|^{-1}\left\{\left[\epsilon_{1jk}k'_{1,j}r'_{0,k}\right]^2+\left[\epsilon_{2mn}k'_{1,m}r'_{0,n}\right]^2\right\}^{1/2}\right). \end{array}\right. \tag{A.76}$$

The spherical coordinate representation is incomplete without the azimuthal angle ϕ'. We have to solve for the allowed range for the azimuthal angle ϕ' by combining equations (A.54) and (A.55). From equation (A.54), we have

$$\cos^2\phi'\ge-\left[\frac{1}{2}\left\|\vec{n'}_{p,1}\right\|^{-1}\epsilon_{1jk}k'_{1,j}r'_{0,k}\right]^2\left[r'_i\sin^2\theta'\right]^{-2}$$

and from equation (A.55),

$$\sin^2\phi'\ge-\left[\frac{1}{2}\left\|\vec{n'}_{p,1}\right\|^{-1}\epsilon_{2jk}k'_{1,j}r'_{0,k}\right]^2\left[r'_i\sin^2\theta'\right]^{-2}.$$

They are combined to give

$$\tan^2\phi'=\frac{\sin^2\phi'}{\cos^2\phi'}\ge\left[\epsilon_{1jk}k'_{1,j}r'_{0,k}\right]^{-2}\left[\epsilon_{2mn}k'_{1,m}r'_{0,n}\right]^2. \tag{A.77}$$

The two inequalities are derived from the last equation,

$$\tan\phi'\ge\left[\epsilon_{1jk}k'_{1,j}r'_{0,k}\right]^{-1}\epsilon_{2mn}k'_{1,m}r'_{0,n},\qquad\tan\phi'\le-\left[\epsilon_{1jk}k'_{1,j}r'_{0,k}\right]^{-1}\epsilon_{2mn}k'_{1,m}r'_{0,n}. \tag{A.78}$$

In the range of ϕ', $0\le\phi'\le 2\pi$, the tangent function has the limits

$$\lim_{\varepsilon\to 0}\left(0\le\phi'\le\frac{1}{2}\pi-|\varepsilon|\right)\Rightarrow\left[0\le\tan\phi'\le\infty\right], \tag{A.79}$$

$$\lim_{\varepsilon\to 0}\left(\frac{1}{2}\pi+|\varepsilon|\le\phi'\le\pi-\varepsilon\right)\Rightarrow\left[-\infty\le\tan\phi'\le 0\right], \tag{A.80}$$

$$\lim_{\varepsilon\to 0}\left(\pi+|\varepsilon|\le\phi'\le\frac{3}{2}\pi-|\varepsilon|\right)\Rightarrow\left[0\le\tan\phi'\le\infty\right], \tag{A.81}$$

$$\lim_{\varepsilon\to 0}\left(\frac{3}{2}\pi+|\varepsilon|\le\phi'<2\pi-|\varepsilon|\right)\Rightarrow\left[-\infty\le\tan\phi'<0\right], \tag{A.82}$$

where ε is an infinitesimal number used in the limiting process. Because discontinuities occur at $\phi'=\pi/2$ and $\phi'=3\pi/2$, the inequalities (A.78) has the limits

$$0\le\left(\tan\phi'\ge\left[\epsilon_{1jk}k'_{1,j}r'_{0,k}\right]^{-1}\epsilon_{2mn}k'_{1,m}r'_{0,n}\right)\le\infty,$$

and

$$-\infty \leq \left(\tan\phi' \leq -\left[\epsilon_{1jk}k'_{1,j}r'_{0,k}\right]^{-1}\epsilon_{2mn}k'_{1,m}r'_{0,n}\right) \leq 0.$$

The ranges for inequalities in (A.79) through (A.82) can now be expressed explicitly as

$$\begin{cases} \lim_{\varepsilon\to 0}\left(0 \leq \phi' \leq \frac{1}{2}\pi - |\varepsilon|\right), \qquad \lim_{\varepsilon\to 0}\left(\pi + |\varepsilon| \leq \phi' \leq \frac{3}{2}\pi - |\varepsilon|\right), \\ 0 \leq \left(\tan\phi' \geq \left[\epsilon_{1jk}k'_{1,j}r'_{0,k}\right]^{-1}\epsilon_{2mn}k'_{1,m}r'_{0,n}\right) \leq \infty; \end{cases} \tag{A.83}$$

$$\begin{cases} \lim_{\varepsilon\to 0}\left(\frac{1}{2}\pi + |\varepsilon| \leq \phi' \leq \pi - \varepsilon\right), \qquad \lim_{\varepsilon\to 0}\left(\frac{3}{2}\pi + |\varepsilon| \leq \phi' < 2\pi - |\varepsilon|\right), \\ -\infty \leq \left(\tan\phi' \leq -\left[\epsilon_{1jk}k'_{1,j}r'_{0,k}\right]^{-1}\epsilon_{2mn}k'_{1,m}r'_{0,n}\right) < 0. \end{cases} \tag{A.84}$$

The solutions for ϕ' are

$$\begin{cases} \lim_{\varepsilon\to 0}\left(0 \leq \phi' \leq \frac{1}{2}\pi - |\varepsilon|\right), \qquad \lim_{\varepsilon\to 0}\left(\pi + |\varepsilon| \leq \phi' \leq \frac{3}{2}\pi - |\varepsilon|\right), \\ \phi' = \arctan\left(\left[\epsilon_{1jk}k'_{1,j}r'_{0,k}\right]^{-1}\epsilon_{2mn}k'_{1,m}r'_{0,n}\right); \end{cases} \tag{A.85}$$

$$\begin{cases} \lim_{\varepsilon\to 0}\left(\frac{1}{2}\pi + |\varepsilon| \leq \phi' \leq \pi - \varepsilon\right), \qquad \lim_{\varepsilon\to 0}\left(\frac{3}{2}\pi + |\varepsilon| \leq \phi' < 2\pi - |\varepsilon|\right), \\ \phi' = \arctan\left(-\left[\epsilon_{1jk}k'_{1,j}r'_{0,k}\right]^{-1}\epsilon_{2mn}k'_{1,m}r'_{0,n}\right). \end{cases} \tag{A.86}$$

In order to have ν'_i values being real, the allowed range of θ' is determined by equations (A.75) and (A.76) and the allowed range of ϕ' is determined by equations (A.85) and (A.86). Having found valid ranges of θ' and ϕ' in which ν'_i is real, the task is now shifted in locating reflection points on the inner hemisphere surface in spherical coordinates. To distinguish one reflection point from the other, the notation ν'_i is modified to $\nu'_i \to \nu'_{1,i}$ in equation (A.51). The first index 1 of $\nu'_{1,i}$ denotes the first reflection point. In this notation, the second reflection point would be $\nu'_{2,i}$ and the Nth reflection point, $\nu'_{N,i}$. Then equation (A.53) is used to rewrite $r'_{i,i}$ in terms of spherical coordinates. The Cartesian coordinate variables x', y' and z' in equation (A.51) are expressed as

$$\nu'_{1,1} \equiv x'_1 = \frac{1}{2}\left\|\vec{n'}_{p,1}\right\|^{-1}\epsilon_{1jk}k'_{1,j}r'_{0,k} \pm \left\{\left[\frac{1}{2}\left\|\vec{n'}_{p,1}\right\|^{-1}\epsilon_{1jk}k'_{1,j}r'_{0,k}\right]^2 + [r'_i]^2\sin^2\theta'_1\cos^2\phi'_1\right\}^{1/2}, \tag{A.87}$$

$$\nu'_{1,2} \equiv y'_1 = \frac{1}{2}\left\|\vec{n'}_{p,1}\right\|^{-1}\epsilon_{2jk}k'_{1,j}r'_{0,k} \pm \left\{\left[\frac{1}{2}\left\|\vec{n'}_{p,1}\right\|^{-1}\epsilon_{2jk}k'_{1,j}r'_{0,k}\right]^2 + [r'_i]^2\sin^2\theta'_1\sin^2\phi'_1\right\}^{1/2}, \tag{A.88}$$

$$\nu'_{1,3} \equiv z'_1 = \frac{1}{2}\left\|\vec{n'}_{p,1}\right\|^{-1}\epsilon_{3jk}k'_{1,j}r'_{0,k} \pm \left\{\left[\frac{1}{2}\left\|\vec{n'}_{p,1}\right\|^{-1}\epsilon_{3jk}k'_{1,j}r'_{0,k}\right]^2 + [r'_i]^2\cos^2\theta'_1\right\}^{1/2}. \tag{A.89}$$

Although the first reflection point on hemisphere is fully described by $\vec{R'}_1$ in equation (A.12), it is not convenient to use $\vec{R'}_1$ in its current form. The most effective representation of $\vec{R'}_1$ is in spherical coordinates. We set $\theta' = \theta'_1$ and $\phi' = \phi'_1$ that describe the same reflection point $\vec{R'}_1$ on the hemisphere. The subscript on the angular variables θ'_1 and ϕ'_1 denotes first reflection point on the hemisphere surface. In terms of Cartesian variables x', y' and z', the first reflection point on hemisphere is given by

$$\vec{R'}_1\left(x'_1, y'_1, z'_1\right) = \sum_{i=1}^{3}\nu'_{1,i}\hat{e}_i, \qquad i = \begin{cases} 1 \to \nu'_{1,1} = x'_1, \\ 2 \to \nu'_{1,2} = y'_1, \\ 3 \to \nu'_{1,3} = z'_1. \end{cases} \tag{A.90}$$

The same point on the hemisphere, defined by equation (A.90), can be expressed in terms of a parametric representation

of equation (A.12),

$$\vec{R'}_1\left(\xi_{1,p};\vec{R'}_0,\hat{k'}_1\right)=\sum_{i=1}^{3}\left[r'_{0,i}+\xi_{1,p}\left\|\vec{k'}_1\right\|^{-1}k'_{1,i}\right]\hat{e_i}=\sum_{i=1}^{3}\Upsilon_{1,i}\hat{e_i}, \tag{A.91}$$

where

$$\Upsilon_{1,i}=r'_{0,i}+\xi_{1,p}\left\|\vec{k'}_1\right\|^{-1}k'_{1,i},\qquad i=1,2,3. \tag{A.92}$$

Both representations, $\vec{R'}_1\left(x'_1,y'_1,z'_1\right)$ and $\vec{R'}_1\left(\xi_{1,p};\vec{R'}_0,\hat{k'}_1\right)$, describe the same point on the hemisphere. Therefore, we have

$$\vec{R'}_1\left(x'_1,y'_1,z'_1\right)=\vec{R'}_1\left(\xi_{1,p};\vec{R'}_0,\hat{k'}_1\right)\quad\rightarrow\quad\sum_{i=1}^{3}\left[\nu_{1,i}-\Upsilon_{1,i}\right]\hat{e_i}=0.$$

The components of the last equation are

$$\nu'_{1,i}-\Upsilon_{1,i}=0,\qquad i=1,2,3. \tag{A.93}$$

Substituting expression of $\nu'_{1,i}$ from equations (A.87), (A.88) and (A.89) into the above equation, we obtain

$$\frac{1}{2}\left\|\vec{n'}_{p,1}\right\|^{-1}\epsilon_{1jk}k'_{1,j}r'_{0,k}\pm\left\{\left[\frac{1}{2}\left\|\vec{n'}_{p,1}\right\|^{-1}\epsilon_{1jk}k'_{1,j}r'_{0,k}\right]^2+\left[r'_i\right]^2\sin^2\theta'_1\cos^2\phi'_1\right\}^{1/2}-\Upsilon_{1,1}=0, \tag{A.94}$$

$$\frac{1}{2}\left\|\vec{n'}_{p,1}\right\|^{-1}\epsilon_{2jk}k'_{1,j}r'_{0,k}\pm\left\{\left[\frac{1}{2}\left\|\vec{n'}_{p,1}\right\|^{-1}\epsilon_{2jk}k'_{1,j}r'_{0,k}\right]^2+\left[r'_i\right]^2\sin^2\theta'_1\sin^2\phi'_1\right\}^{1/2}-\Upsilon_{1,2}=0, \tag{A.95}$$

$$\frac{1}{2}\left\|\vec{n'}_{p,1}\right\|^{-1}\epsilon_{3jk}k'_{1,j}r'_{0,k}\pm\left\{\left[\frac{1}{2}\left\|\vec{n'}_{p,1}\right\|^{-1}\epsilon_{3jk}k'_{1,j}r'_{0,k}\right]^2+\left[r'_i\right]^2\cos^2\theta'_1\right\}^{1/2}-\Upsilon_{1,3}=0, \tag{A.96}$$

where $\Upsilon_{1,i}$ is defined in equation (A.92). To solve for θ'_1, equation (A.96) is first rearranged,

$$\pm\left\{\left[\frac{1}{2}\left\|\vec{n'}_{p,1}\right\|^{-1}\epsilon_{3jk}k'_{1,j}r'_{0,k}\right]^2+\left[r'_i\right]^2\cos^2\theta'_1\right\}^{1/2}=\Upsilon_{1,3}-\frac{1}{2}\left\|\vec{n'}_{p,1}\right\|^{-1}\epsilon_{3jk}k'_{1,j}r'_{0,k}.$$

Square both sides and solve for $\cos^2\theta'_1$, the result is

$$\cos^2\theta'_1=\left[r'_i\right]^{-2}\left[\Upsilon_{1,3}^2-\Upsilon_{1,3}\left\|\vec{n'}_{p,1}\right\|^{-1}\epsilon_{3jk}k'_{1,j}r'_{0,k}\right]. \tag{A.97}$$

For reasons discussed earlier, θ'_1 information from the sine function is also needed. Following the earlier procedures, equations (A.94) and (A.95) are combined to yield the relation,

$$\begin{aligned}&\frac{1}{2}\left\|\vec{n'}_{p,1}\right\|^{-1}\epsilon_{1jk}k'_{1,j}r'_{0,k}\pm\left\{\left[\frac{1}{2}\left\|\vec{n'}_{p,1}\right\|^{-1}\epsilon_{1jk}k'_{1,j}r'_{0,k}\right]^2+\left[r'_i\right]^2\sin^2\theta'_1\cos^2\phi'_1\right\}^{1/2}-\Upsilon_{1,1}\\&+\frac{1}{2}\left\|\vec{n'}_{p,1}\right\|^{-1}\epsilon_{2mn}k'_{1,m}r'_{0,n}\pm\left\{\left[\frac{1}{2}\left\|\vec{n'}_{p,1}\right\|^{-1}\epsilon_{2mn}k'_{1,m}r'_{0,n}\right]^2+\left[r'_i\right]^2\sin^2\theta'_1\sin^2\phi'_1\right\}^{1/2}-\Upsilon_{1,2}=0,\end{aligned}$$

The equation is not easy to solve for $\sin^2\phi_1'$. Fortunately, there is another way to extract the sine function which requires the knowledge of ϕ_1'. The solution of θ_1' is postponed until a solution of ϕ_1' is found. To solve for ϕ_1', it is desirable to solve for $\cos^2\phi_1'$ and $\sin^2\phi_1'$ from equations (A.94) and (A.95) first. Rearranging equation (A.94),

$$\pm\left\{\left[\frac{1}{2}\left\|\vec{n'}_{p,1}\right\|^{-1}\epsilon_{1jk}k'_{1,j}r'_{0,k}\right]^2+\left[r_i'\right]^2\sin^2\theta_1'\cos^2\phi_1'\right\}^{1/2}=\Upsilon_{1,1}-\frac{1}{2}\left\|\vec{n'}_{p,1}\right\|^{-1}\epsilon_{1jk}k'_{1,j}r'_{0,k},$$

and followed by squaring both sides, then $\cos^2\phi_1'$ can be found to be

$$\cos^2\phi_1'=\left[r_i'\sin\theta_1'\right]^{-2}\left[\Upsilon_{1,1}^2-\Upsilon_{1,1}\left\|\vec{n'}_{p,1}\right\|^{-1}\epsilon_{1jk}k'_{1,j}r'_{0,k}\right]. \tag{A.98}$$

Similarly, rearranging equation (A.95),

$$\pm\left\{\left[\frac{1}{2}\left\|\vec{n'}_{p,1}\right\|^{-1}\epsilon_{2jk}k'_{1,j}r'_{0,k}\right]^2+\left[r_i'\right]^2\sin^2\theta_1'\sin^2\phi_1'\right\}^{1/2}=\Upsilon_{1,2}-\frac{1}{2}\left\|\vec{n'}_{p,1}\right\|^{-1}\epsilon_{2jk}k'_{1,j}r'_{0,k}$$

and squaring both sides, then $\sin^2\phi_1'$ can be found to be

$$\sin^2\phi_1'=\left[r_i'\sin\theta_1'\right]^{-2}\left[\Upsilon_{1,2}^2-\Upsilon_{1,2}\left\|\vec{n'}_{p,1}\right\|^{-1}\epsilon_{2jk}k'_{1,j}r'_{0,k}\right]. \tag{A.99}$$

Finally, $\tan^2\phi_1'$ can be obtained by combining equations (A.99) and (A.98),

$$\tan^2\phi_1'=\left[\Upsilon_{1,1}^2-\Upsilon_{1,1}\left\|\vec{n'}_{p,1}\right\|^{-1}\epsilon_{1jk}k'_{1,j}r'_{0,k}\right]^{-1}\left[\Upsilon_{1,2}^2-\Upsilon_{1,2}\left\|\vec{n'}_{p,1}\right\|^{-1}\epsilon_{2mn}k'_{1,m}r'_{0,n}\right]. \tag{A.100}$$

Finally, the azimuthal angle ϕ_1' is found to be

$$\phi_1'=\arctan\left(\pm\left[\frac{\Upsilon_{1,2}^2-\Upsilon_{1,2}\left\|\vec{n'}_{p,1}\right\|^{-1}\epsilon_{2mn}k'_{1,m}r'_{0,n}}{\Upsilon_{1,1}^2-\Upsilon_{1,1}\left\|\vec{n'}_{p,1}\right\|^{-1}\epsilon_{1jk}k'_{1,j}r'_{0,k}}\right]^{1/2}\right). \tag{A.101}$$

The restriction of ϕ_1' being real imposes the condition

$$\frac{\Upsilon_{1,2}^2-\Upsilon_{1,2}\left\|\vec{n'}_{p,1}\right\|^{-1}\epsilon_{2mn}k'_{1,m}r'_{0,n}}{\Upsilon_{1,1}^2-\Upsilon_{1,1}\left\|\vec{n'}_{p,1}\right\|^{-1}\epsilon_{1jk}k'_{1,j}r'_{0,k}}\geq\varsigma$$

or

$$\Upsilon_{1,2}^2-\Upsilon_{1,2}\left\|\vec{n'}_{p,1}\right\|^{-1}\epsilon_{2mn}k'_{1,m}r'_{0,n}\geq\varsigma\Upsilon_{1,1}^2-\varsigma\Upsilon_{1,1}\left\|\vec{n'}_{p,1}\right\|^{-1}\epsilon_{1jk}k'_{1,j}r'_{0,k},$$

where $\varsigma\geq 0$. Following equations (A.77) through (A.86), the following results are obtained:

$$\begin{cases}\lim_{\varepsilon\to 0}\left(0\leq\phi_1'\leq\frac{1}{2}\pi-|\varepsilon|\right), \qquad \lim_{\varepsilon\to 0}\left(\pi+|\varepsilon|\leq\phi_1'\leq\frac{3}{2}\pi-|\varepsilon|\right),\\ \phi_1'=\arctan\left(\left[\frac{\Upsilon_{1,2}^2-\Upsilon_{1,2}\left\|\vec{n'}_{p,1}\right\|^{-1}\epsilon_{2mn}k'_{1,m}r'_{0,n}}{\Upsilon_{1,1}^2-\Upsilon_{1,1}\left\|\vec{n'}_{p,1}\right\|^{-1}\epsilon_{1jk}k'_{1,j}r'_{0,k}}\right]^{1/2}\right);\end{cases} \tag{A.102}$$

$$\begin{cases}\lim_{\varepsilon\to 0}\left(\frac{1}{2}\pi+|\varepsilon|\leq\phi_1'\leq\pi-\varepsilon\right), \qquad \lim_{\varepsilon\to 0}\left(\frac{3}{2}\pi+|\varepsilon|\leq\phi_1'<2\pi-|\varepsilon|\right),\\ \phi_1'=\arctan\left(-\left[\frac{\Upsilon_{1,2}^2-\Upsilon_{1,2}\left\|\vec{n'}_{p,1}\right\|^{-1}\epsilon_{2mn}k'_{1,m}r'_{0,n}}{\Upsilon_{1,1}^2-\Upsilon_{1,1}\left\|\vec{n'}_{p,1}\right\|^{-1}\epsilon_{1jk}k'_{1,j}r'_{0,k}}\right]^{1/2}\right).\end{cases} \tag{A.103}$$

Having found the solution for ϕ'_1, we can proceed to finalize the task of solving for the polar angle θ'_1. Combining the results for $\cos^2\phi'_1$ and $\sin^2\phi'_1$ found in equations (A.98) and (A.99), $\sin^2\theta'_1$ can be found to be

$$\sin^2\theta'_1 = [r'_i]^{-2}\left[\Upsilon^2_{1,1}+\Upsilon^2_{1,2}-\left\|\vec{n'}_{p,1}\right\|^{-1}\left\{\Upsilon_{1,1}\epsilon_{1jk}k'_{1,j}r'_{0,k}+\Upsilon_{1,2}\epsilon_{2mn}k'_{1,m}r'_{0,n}\right\}\right]. \tag{A.104}$$

Finally, $\tan^2\theta'_1$ is constructed with equations (A.97) and (A.104),

$$\tan^2\theta'_1 = \frac{\Upsilon^2_{1,1}+\Upsilon^2_{1,2}-\left\|\vec{n'}_{p,1}\right\|^{-1}\left\{\Upsilon_{1,1}\epsilon_{1jk}k'_{1,j}r'_{0,k}+\Upsilon_{1,2}\epsilon_{2mn}k'_{1,m}r'_{0,n}\right\}}{\Upsilon^2_{1,3}-\Upsilon_{1,3}\left\|\vec{n'}_{p,1}\right\|^{-1}\epsilon_{3qr}k'_{1,q}r'_{0,r}}. \tag{A.105}$$

Then θ'_1 is given by

$$\theta'_1 = \arctan\left(\pm\left[\frac{\Upsilon^2_{1,1}+\Upsilon^2_{1,2}-\left\|\vec{n'}_{p,1}\right\|^{-1}\left\{\Upsilon_{1,1}\epsilon_{1jk}k'_{1,j}r'_{0,k}+\Upsilon_{1,2}\epsilon_{2mn}k'_{1,m}r'_{0,n}\right\}}{\Upsilon^2_{1,3}-\Upsilon_{1,3}\left\|\vec{n'}_{p,1}\right\|^{-1}\epsilon_{3qr}k'_{1,q}r'_{0,r}}\right]^{1/2}\right). \tag{A.106}$$

Following equations (A.62) through (A.76), we arrive at

$$\begin{cases} \lim_{\varepsilon\to 0}\left(0\le\theta'_1\le\frac{1}{2}\pi-|\varepsilon|\right), \\ \theta'_1 = \arctan\left(\left[\frac{\Upsilon^2_{1,1}+\Upsilon^2_{1,2}-\left\|\vec{n'}_{p,1}\right\|^{-1}\left\{\Upsilon_{1,1}\epsilon_{1jk}k'_{1,j}r'_{0,k}+\Upsilon_{1,2}\epsilon_{2mn}k'_{1,m}r'_{0,n}\right\}}{\Upsilon^2_{1,3}-\Upsilon_{1,3}\left\|\vec{n'}_{p,1}\right\|^{-1}\epsilon_{3qr}k'_{1,q}r'_{0,r}}\right]^{1/2}\right); \end{cases} \tag{A.107}$$

$$\begin{cases} \lim_{\varepsilon\to 0}\left(\frac{1}{2}\pi+|\varepsilon|\le\theta'_1\le\pi\right), \\ \theta'_1 = \arctan\left(-\left[\frac{\Upsilon^2_{1,1}+\Upsilon^2_{1,2}-\left\|\vec{n'}_{p,1}\right\|^{-1}\left\{\Upsilon_{1,1}\epsilon_{1jk}k'_{1,j}r'_{0,k}+\Upsilon_{1,2}\epsilon_{2mn}k'_{1,m}r'_{0,n}\right\}}{\Upsilon^2_{1,3}-\Upsilon_{1,3}\left\|\vec{n'}_{p,1}\right\|^{-1}\epsilon_{3qr}k'_{1,q}r'_{0,r}}\right]^{1/2}\right). \end{cases} \tag{A.108}$$

The allowed angular values are all defined now: ϕ'_1 by equations (A.102) and (A.103); and θ'_1 by equations (A.107) and (A.108). The initial reflection point on the inner hemisphere surface can be calculated by the equation:

$$\vec{R'}_1\left(r'_i,\theta'_1,\phi'_1\right) = \sum_{i=1}^{3}\nu'_{1,i}\left(r'_i,\theta'_1,\phi'_1\right)\hat{e}_i, \qquad i=\begin{cases} 1\to\nu'_{1,1}=r'_i\sin\theta'_1\cos\phi'_1, \\ 2\to\nu'_{1,2}=r'_i\sin\theta'_1\sin\phi'_1, \\ 3\to\nu'_{1,3}=r'_i\cos\theta'_1. \end{cases} \tag{A.109}$$

We still have to determine the maximum wavelength that can fit the hemispherical cavity. It is determined from the distance between two immediate reflection points once they are found. We have to find expression describing the second reflection point $\vec{R'}_2$. In Figure 3.2, the angle $\psi_{1,2}$ satisfies the relation

$$\psi_{1,2}+\theta_2+\theta_r=\pi. \tag{A.110}$$

Angles θ_2 and θ_r are equal due to the law of reflection, consequently

$$\theta_2=\theta_r=\theta_1, \qquad \psi_{1,2}=\pi-2\theta_i. \tag{A.111}$$

It is important not to confuse the angle θ_i above with that of spherical polar angle θ_i which was previously denoted with an index i to indicate particular reflection point $\vec{R'}_i$. The θ_i in equation (A.111) is an angle of incidence, not a polar angle. In order to avoid any further confusion in notation, equation (A.111) is restated with modifications applied to the indexing convention for angle of incidence,

$$\theta_{i+1}=\theta_r=\theta_{inc}, \qquad \psi_{i,i+1}=\pi-2\theta_{inc}. \tag{A.112}$$

A. Reflection Points on the Surface of a Resonator

The relation that connects angle of incidence to known quantities $\vec{k'}_1$ and $\vec{R'}_1$ is

$$\vec{k'}_1 \bullet \vec{R'}_1 = \sum_{i=1}^{3} k'_{1,i}\nu'_{1,i} = r'_i \left\|\vec{k'}_1\right\| \cos\theta_{inc},$$

where $\left\|\vec{R'}_1\right\| = r'_i$, and the index i is not summed over. The incident angle θ_{inc} is given by

$$\theta_{inc} = \arccos\left(\left[r'_i \left\|\vec{k'}_1\right\|\right]^{-1} \sum_{i=1}^{3} k'_{1,i}\nu'_{1,i}\right). \tag{A.113}$$

Substituting the explicit expression of $\nu'_{1,i}$:

$$\nu'_{1,1} = x'_1 = r'_i \sin\theta'_1 \cos\phi'_1, \qquad \nu'_{1,2} = y'_1 = r'_i \sin\theta'_1 \sin\phi'_1, \qquad \nu'_{1,3} = z'_1 = r'_i \cos\theta'_1, \tag{A.114}$$

into equation (A.113), the incident angle is evaluated as

$$\theta_{inc} = \arccos\left(\frac{\sin\theta'_1\left[k'_{x'_1}\cos\phi'_1 + k'_{y'_1}\sin\phi'_1\right] + k'_{z'_1}\cos\theta'_1}{\sqrt{\left[k'_{x'_1}\right]^2 + \left[k'_{y'_1}\right]^2 + \left[k'_{z'_1}\right]^2}}\right), \tag{A.115}$$

where $k'_{1,1} = k'_{x'_1}$, $k'_{1,2} = k'_{y'_1}$ and $k'_{1,3} = k'_{z'_1}$. The second reflection point $\vec{R'}_2$ has the form

$$\vec{R'}_2\left(\nu'_{2,1}, \nu'_{2,2}, \nu'_{2,3}\right) = \sum_{i=1}^{3} \nu'_{2,i}\left(\nu'_{1,1}, \nu'_{1,2}, \nu'_{1,3}\right)\hat{e}_i, \qquad i = \begin{cases} 1 \to \nu'_{2,1} = x'_2, & \nu'_{1,1} = x'_1, \\ 2 \to \nu'_{2,2} = y'_2, & \nu'_{1,2} = y'_1, \\ 3 \to \nu'_{2,3} = z'_2, & \nu'_{1,3} = z'_1. \end{cases} \tag{A.116}$$

The relation that connects two vectors $\vec{R'}_1$ and $\vec{R'}_2$ is

$$\vec{R'}_1 \bullet \vec{R'}_2 = \left[r'_i\right]^2 \cos\psi_{1,2}, \tag{A.117}$$

where $\left\|\vec{R'}_1\right\| = \left\|\vec{R'}_2\right\| = r'_i$ for a rigid hemisphere. Equivalently, this expression can be evaluated using $\psi_{1,2}$, given in equation (A.112), as

$$\left[r'_i\right]^2 \cos\left(\pi - 2\theta_{inc}\right) - \sum_{i=1}^{3} \nu'_{1,i}\nu'_{2,i} = 0. \tag{A.118}$$

Equation (A.118) serves as one of the two needed relations. The other relation can be found from the cross product of $\vec{R'}_1$ and $\vec{R'}_2$,

$$\vec{R'}_1 \times \vec{R'}_2 = \sum_{i=1}^{3} \epsilon_{ijk}\nu'_{1,j}\nu'_{2,k}\hat{e_i}. \tag{A.119}$$

Since $\vec{R'}_1$ and $\vec{R'}_2$ span the plane of incidence whose unit normal is given by equation (A.17),

$$\hat{n'}_{p,1} = -\left\|\vec{n'}_{p,1}\right\|^{-1} \sum_{i=1}^{3} \epsilon_{ijk}k'_{1,j}r'_{0,k}\hat{e_i},$$

the cross product of $\vec{R'}_1$ and $\vec{R'}_2$ can be equivalently expressed as

$$\vec{R'}_1 \times \vec{R'}_2 = -\Gamma_{1,2} \left\| \vec{n'}_{p,1} \right\|^{-1} \sum_{i=1}^{3} \epsilon_{ijk} k'_{1,j} r'_{0,k} \hat{e}_i, \tag{A.120}$$

where $\Gamma_{1,2}$ is a proportionality factor. The factor $\Gamma_{1,2}$ can be found simply by noticing

$$\vec{R'}_1 \times \vec{R'}_2 = \Gamma_{1,2} \hat{n'}_{p,1} \quad \rightarrow \quad \left\| \vec{R'}_1 \times \vec{R'}_2 \right\| = \Gamma_{1,2} \left\| \hat{n'}_{p,1} \right\| = \Gamma_{1,2},$$

which leads to

$$\Gamma_{1,2} = \left\| \vec{R'}_1 \times \vec{R'}_2 \right\| = [r'_i]^2 \sin(\pi - 2\theta_{inc}). \tag{A.121}$$

Equations (A.119) and (A.120) are combined as

$$\sum_{i=1}^{3} \left[\epsilon_{ijk} \nu'_{1,j} \nu'_{2,k} + \Gamma_{1,2} \left\| \vec{n'}_{p,1} \right\|^{-1} \epsilon_{ijk} k'_{1,j} r'_{0,k} \right] \hat{e}_i = 0. \tag{A.122}$$

The individual component equation is written

$$\epsilon_{ijk} \nu'_{1,j} \nu'_{2,k} + \Gamma_{1,2} \left\| \vec{n'}_{p,1} \right\|^{-1} \epsilon_{ijk} k'_{1,j} r'_{0,k} = 0, \qquad i = 1,2,3. \tag{A.123}$$

Equations (A.123) and (A.118) together provide the needed relations to specify the second reflection point $\vec{R'}_2$ in terms of the known quantities, $\vec{R'}_0$, $\vec{k'}_1$ and $\vec{R'}_1$. It is convenient to expand equations (A.118) and (A.123) as

$$\overbrace{[r'_i]^2 \cos(\pi - 2\theta_{inc})}^{-[d\Gamma_{1,2}/d\theta_{inc}]/2} - \nu'_{1,1}\nu'_{2,1} - \nu'_{1,2}\nu'_{2,2} - \nu'_{1,3}\nu'_{2,3} = 0, \tag{A.124}$$

$$\nu'_{1,2}\nu'_{2,3} - \nu'_{1,3}\nu'_{2,2} + \Gamma_{1,2} \left\| \vec{n'}_{p,1} \right\|^{-1} \epsilon_{1jk} k'_{1,j} r'_{0,k} = 0, \tag{A.125}$$

$$\nu'_{1,3}\nu'_{2,1} - \nu'_{1,1}\nu'_{2,3} + \Gamma_{1,2} \left\| \vec{n'}_{p,1} \right\|^{-1} \epsilon_{2jk} k'_{1,j} r'_{0,k} = 0, \tag{A.126}$$

$$\nu'_{1,1}\nu'_{2,2} - \nu'_{1,2}\nu'_{2,1} + \Gamma_{1,2} \left\| \vec{n'}_{p,1} \right\|^{-1} \epsilon_{3jk} k'_{1,j} r'_{0,k} = 0. \tag{A.127}$$

Equations (A.124) and (A.125) are added to yield

$$\nu'_{1,1}\nu'_{2,1} + \left[\nu'_{1,2} + \nu'_{1,3}\right] \nu'_{2,2} + \left[\nu'_{1,3} - \nu'_{1,2}\right] \nu_{2,3} = \Gamma_{1,2} \left\| \vec{n'}_{p,1} \right\|^{-1} \epsilon_{1jk} k'_{1,j} r'_{0,k} - \frac{1}{2} \frac{d\Gamma_{1,2}}{d\theta_{inc}}. \tag{A.128}$$

Equations (A.124) and (A.126) are added to give

$$\left[\nu'_{1,1} - \nu'_{1,3}\right] \nu'_{2,1} + \nu'_{1,2}\nu'_{2,2} + \left[\nu'_{1,3} + \nu'_{1,1}\right] \nu'_{2,3} = \Gamma_{1,2} \left\| \vec{n'}_{p,1} \right\|^{-1} \epsilon_{2jk} k'_{1,j} r'_{0,k} - \frac{1}{2} \frac{d\Gamma_{1,2}}{d\theta_{inc}}. \tag{A.129}$$

Similarly, equations (A.124) and (A.127) are combined to give

$$\left[\nu'_{1,1} + \nu'_{1,2}\right] \nu'_{2,1} + \left[\nu'_{1,2} - \nu'_{1,1}\right] \nu'_{2,2} + \nu'_{1,3}\nu'_{2,3} = \Gamma_{1,2} \left\| \vec{n'}_{p,1} \right\|^{-1} \epsilon_{3jk} k'_{1,j} r'_{0,k} - \frac{1}{2} \frac{d\Gamma_{1,2}}{d\theta_{inc}}. \tag{A.130}$$

Define the quantities

$$\begin{cases} \alpha_1 = \nu'_{1,2} + \nu'_{1,3}, & \alpha_2 = \nu'_{1,3} - \nu'_{1,2}, & \zeta_1 = \Gamma_{1,2} \left\| \vec{n}'_{p,1} \right\|^{-1} \epsilon_{1jk} k'_{1,j} r'_{0,k} - \frac{1}{2} \frac{d\Gamma_{1,2}}{d\theta_{inc}}, \\ \alpha_3 = \nu'_{1,1} - \nu'_{1,3}, & \alpha_4 = \nu'_{1,3} + \nu'_{1,1}, & \zeta_2 = \Gamma_{1,2} \left\| \vec{n}'_{p,1} \right\|^{-1} \epsilon_{2jk} k'_{1,j} r'_{0,k} - \frac{1}{2} \frac{d\Gamma_{1,2}}{d\theta_{inc}}, \\ \alpha_5 = \nu'_{1,1} + \nu'_{1,2}, & \alpha_6 = \nu'_{1,2} - \nu'_{1,1}, & \zeta_3 = \Gamma_{1,2} \left\| \vec{n}'_{p,1} \right\|^{-1} \epsilon_{3jk} k'_{1,j} r'_{0,k} - \frac{1}{2} \frac{d\Gamma_{1,2}}{d\theta_{inc}}, \end{cases} \tag{A.131}$$

where $\Gamma_{1,2}$ is defined in equation (A.121). Equations (A.128), (A.129) and (A.130) form a reduced set

$$\nu'_{1,1}\nu'_{2,1} + \alpha_1\nu'_{2,2} + \alpha_2\nu'_{2,3} = \zeta_1, \qquad \alpha_3\nu'_{2,1} + \nu'_{1,2}\nu'_{2,2} + \alpha_4\nu'_{2,3} = \zeta_2, \qquad \alpha_5\nu'_{2,1} + \alpha_6\nu'_{2,2} + \nu'_{1,3}\nu'_{2,3} = \zeta_3 \ .$$

In matrix form it reads

$$\underbrace{\begin{bmatrix} \nu'_{1,1} & \alpha_1 & \alpha_2 \\ \alpha_3 & \nu'_{1,2} & \alpha_4 \\ \alpha_5 & \alpha_6 & \nu'_{1,3} \end{bmatrix}}_{\widetilde{M}_0} \cdot \begin{bmatrix} \nu'_{2,1} \\ \nu'_{2,2} \\ \nu'_{2,3} \end{bmatrix} = \begin{bmatrix} \zeta_1 \\ \zeta_2 \\ \zeta_3 \end{bmatrix}, \tag{A.132}$$

and its determinant is expressed as

$$\det\left(\widetilde{M}_0\right) = \left[\nu'_{1,1} + \nu'_{1,2} + \nu'_{1,3}\right] \left\{ \left[\nu'_{1,1}\right]^2 + \left[\nu'_{1,2}\right]^2 + \left[\nu'_{1,3}\right]^2 \right\} = \left[r'_i\right]^2 \left[\nu'_{1,1} + \nu'_{1,2} + \nu'_{1,3}\right]. \tag{A.133}$$

Three new matrices are then defined here as

$$\widetilde{M}_1 = \begin{bmatrix} \zeta_1 & \alpha_1 & \alpha_2 \\ \zeta_2 & \nu'_{1,2} & \alpha_4 \\ \zeta_3 & \alpha_6 & \nu'_{1,3} \end{bmatrix}, \qquad \widetilde{M}_2 = \begin{bmatrix} \nu'_{1,1} & \zeta_1 & \alpha_2 \\ \alpha_3 & \zeta_2 & \alpha_4 \\ \alpha_5 & \zeta_3 & \nu'_{1,3} \end{bmatrix}, \qquad \widetilde{M}_3 = \begin{bmatrix} \nu'_{1,1} & \alpha_1 & \zeta_1 \\ \alpha_3 & \nu'_{1,2} & \zeta_2 \\ \alpha_5 & \alpha_6 & \zeta_3 \end{bmatrix}.$$

The variables $\nu'_{2,1}$, $\nu'_{2,2}$ and $\nu'_{2,3}$ are solved with the Cramer's Rule as

$$\nu'_{2,1} = \det\left(\widetilde{M}_1\right) / \det\left(\widetilde{M}_0\right), \qquad \nu'_{2,2} = \det\left(\widetilde{M}_2\right) / \det\left(\widetilde{M}_0\right), \qquad \nu'_{2,3} = \det\left(\widetilde{M}_3\right) / \det\left(\widetilde{M}_0\right).$$

Explicitly, they are given by

$$\begin{aligned} \grave{\nu}'_{2,1} \equiv \nu'_{2,1} = \Big(& \nu'_{1,1}\left[\nu'_{1,1} - \nu'_{1,2} + \nu'_{1,3}\right]\zeta_1 + \left\{ \nu'_{1,1}\left[\nu'_{1,2} - \nu'_{1,3}\right] - \left[\nu'_{1,2}\right]^2 - \left[\nu'_{1,3}\right]^2 \right\}\zeta_2 \\ & + \left\{ \nu'_{1,1}\left[\nu'_{1,2} + \nu'_{1,3}\right] + \left[\nu'_{1,2}\right]^2 + \left[\nu'_{1,3}\right]^2 \right\}\zeta_3 \Big) \left[\nu'_{1,1} + \nu'_{1,2} + \nu'_{1,3}\right]^{-1} \left[r'_i\right]^{-2}, \end{aligned} \tag{A.134}$$

$$\begin{aligned} \grave{\nu}'_{2,2} \equiv \nu'_{2,2} = \Big(& \left\{ \nu'_{1,2}\left[\nu'_{1,1} + \nu'_{1,3}\right] + \left[\nu'_{1,1}\right]^2 + \left[\nu'_{1,3}\right]^2 \right\}\zeta_1 + \left\{ \nu'_{1,2}\left[\nu'_{1,1} - \nu'_{1,3}\right] + \left[\nu'_{1,2}\right]^2 \right\}\zeta_2 \\ & + \left\{ \nu'_{1,2}\left[\nu'_{1,3} - \nu'_{1,1}\right] - \left[\nu'_{1,1}\right]^2 - \left[\nu'_{1,3}\right]^2 \right\}\zeta_3 \Big) \left[\nu'_{1,1} + \nu'_{1,2} + \nu'_{1,3}\right]^{-1} \left[r'_i\right]^{-2}, \end{aligned} \tag{A.135}$$

$$\begin{aligned} \grave{\nu}'_{2,3} \equiv \nu'_{2,3} = \Big(& \left\{ \left[\nu'_{1,1} - \nu'_{1,2}\right]\nu'_{1,3} - \left[\nu'_{1,1}\right]^2 - \left[\nu'_{1,2}\right]^2 \right\}\zeta_1 + \left\{ \left[\nu'_{1,1} + \nu'_{1,2}\right]\nu'_{1,3} + \left[\nu'_{1,1}\right]^2 + \left[\nu'_{1,2}\right]^2 \right\}\zeta_2 \\ & + \left\{ \left[\nu'_{1,2} - \nu'_{1,1}\right]\nu'_{1,3} + \left[\nu'_{1,3}\right]^2 \right\}\zeta_3 \Big) \left[\nu'_{1,1} + \nu'_{1,2} + \nu'_{1,3}\right]^{-1} \left[r'_i\right]^{-2}, \end{aligned} \tag{A.136}$$

where

$$\nu'_{1,1} + \nu'_{1,2} + \nu'_{1,3} \neq 0, \qquad \begin{bmatrix} \nu'_{1,1} = x'_1\left(r'_i, \theta_1, \phi_1\right) \\ \nu'_{1,2} = y'_1\left(r'_i, \theta_1, \phi_1\right) \\ \nu'_{1,3} = z'_1\left(r'_i, \theta_1, \phi_1\right) \end{bmatrix}, \qquad \begin{bmatrix} \nu'_{2,1}\left(\nu'_{1,1}, \nu'_{1,2}, \nu'_{1,3}\right) = x'_2 \\ \nu'_{2,2}\left(\nu'_{1,1}, \nu'_{1,2}, \nu'_{1,3}\right) = y'_2 \\ \nu'_{2,3}\left(\nu'_{1,1}, \nu'_{1,2}, \nu'_{1,3}\right) = z'_2 \end{bmatrix}. \tag{A.137}$$

In the above set of equations, $\grave{\nu}'_{2,i}$ has been used to indicate that $\nu'_{2,i}$ is now expressed explicitly in terms of the Cartesian coordinates $\left(\nu'_{1,1}, \nu'_{1,2}, \nu'_{1,3}\right)$ instead of spherical coordinates corresponding to the second reflection point, (r'_i, θ_2, ϕ_2) . The second reflection point inside the hemisphere is then from equation (A.116),

$$\vec{R}'_2\left(\grave{\nu}'_{2,1}, \grave{\nu}'_{2,2}, \grave{\nu}'_{2,3}\right) = \sum_{i=1}^{3} \grave{\nu}'_{2,i}\hat{e}_i,$$

where $\grave{\nu}'_{2,i}$, $i = 1, 2, 3$ are given in equations (A.134) through (A.136) with restriction given in equation (A.137). In general, all subsequent reflection points $\vec{R}'_N$ can be expressed in generic form

$$\vec{R}'_N\left(\grave{\nu}'_{N,1}, \grave{\nu}'_{N,2}, \grave{\nu}'_{N,3}\right) = \sum_{i=1}^{3} \grave{\nu}'_{N,i}\hat{e}_i$$

through iterative applications of the result $\grave{\nu}'_{2,i}$, $i = 1, 2, 3$. This however proves to be very inefficient technique. A better way is to express $\vec{R}'_N$ in terms of spherical coordinates. Because $\vec{R}'_2$ belongs to a spanning set for the plane of incidence whose unit normal is $\hat{n'}_{p,1}$ defined in equation (A.17), the component relations $\grave{\nu}'_{2,i}$ of equations (A.134), (A.135) and (A.136) satisfy the intercept relation given in equation (A.51),

$$\grave{\nu}'_{2,i} = \frac{1}{2}\left\|\vec{n'}_{p,1}\right\|^{-1}\epsilon_{ijk}k'_{1,j}r'_{0,k} \pm \left\{\left[\frac{1}{2}\left\|\vec{n'}_{p,1}\right\|^{-1}\epsilon_{ijk}k'_{1,j}r'_{0,k}\right]^2 + \left[r'_{i,i}\right]^2\right\}^{1/2}, \qquad i = 1, 2, 3,$$

where $r'_{i,1} = r'_i \sin\theta'_2 \cos\phi'_2$, $r'_{i,2} = r'_i \sin\theta'_2 \sin\phi'_2$ and $r'_{i,3} = r'_i \cos\theta'_2$. Here the subscript 2 of angular variables θ'_2 and ϕ'_2 denote the second reflection point. In terms of the angular variables, using the above expression for $\grave{\nu}'_{2,i}$, the $\grave{\nu}'_{2,1}$, $\grave{\nu}'_{2,2}$ and $\grave{\nu}'_{2,3}$ are expressed as

$$\mp\left\{\left[\frac{1}{2}\left\|\vec{n'}_{p,1}\right\|^{-1}\epsilon_{1jk}k'_{1,j}r'_{0,k}\right]^2 + [r'_i]^2\sin^2\theta'_2\cos^2\phi'_2\right\}^{1/2} = \frac{1}{2}\left\|\vec{n'}_{p,1}\right\|^{-1}\epsilon_{1jk}k'_{1,j}r'_{0,k} - \grave{\nu}'_{2,1}, \tag{A.138}$$

$$\mp\left\{\left[\frac{1}{2}\left\|\vec{n'}_{p,1}\right\|^{-1}\epsilon_{2jk}k'_{1,j}r'_{0,k}\right]^2 + [r'_i]^2\sin^2\theta'_2\sin^2\phi'_2\right\}^{1/2} = \frac{1}{2}\left\|\vec{n'}_{p,1}\right\|^{-1}\epsilon_{2jk}k'_{1,j}r'_{0,k} - \grave{\nu}'_{2,2}, \tag{A.139}$$

$$\mp\left\{\left[\frac{1}{2}\left\|\vec{n'}_{p,1}\right\|^{-1}\epsilon_{3jk}k'_{1,j}r'_{0,k}\right]^2 + [r'_i]^2\cos^2\theta'_2\right\}^{1/2} = \frac{1}{2}\left\|\vec{n'}_{p,1}\right\|^{-1}\epsilon_{3jk}k'_{1,j}r'_{0,k} - \grave{\nu}'_{2,3}. \tag{A.140}$$

Square both sides of equation (A.138), $\cos^2\phi'_2$ can be solved as

$$\cos^2\phi'_2 = [r'_i\sin\theta'_2]^{-2}\left\{\left[\frac{1}{2}\left\|\vec{n'}_{p,1}\right\|^{-1}\epsilon_{1jk}k'_{1,j}r'_{0,k} - \grave{\nu}'_{2,1}\right]^2 - \left[\frac{1}{2}\left\|\vec{n'}_{p,1}\right\|^{-1}\epsilon_{1jk}k'_{1,j}r'_{0,k}\right]^2\right\}. \tag{A.141}$$

Similarly, square both sides of equation (A.139), $\sin^2\phi'_2$ can be solved as

$$\sin^2\phi'_2 = [r'_i\sin\theta'_2]^{-2}\left\{\left[\frac{1}{2}\left\|\vec{n'}_{p,1}\right\|^{-1}\epsilon_{2jk}k'_{1,j}r'_{0,k} - \grave{\nu}'_{2,2}\right]^2 - \left[\frac{1}{2}\left\|\vec{n'}_{p,1}\right\|^{-1}\epsilon_{2jk}k'_{1,j}r'_{0,k}\right]^2\right\}. \tag{A.142}$$

The last two equations are divided to give

$$\tan^2\phi_2' = \frac{\left[\frac{1}{2}\left\|\vec{n'}_{p,1}\right\|^{-1}\epsilon_{2mn}k'_{1,m}r'_{0,n} - \grave{\nu}'_{2,2}\right]^2 - \left[\frac{1}{2}\left\|\vec{n'}_{p,1}\right\|^{-1}\epsilon_{2mn}k'_{1,m}r'_{0,n}\right]^2}{\left[\frac{1}{2}\left\|\vec{n'}_{p,1}\right\|^{-1}\epsilon_{1jk}k'_{1,j}r'_{0,k} - \grave{\nu}'_{2,1}\right]^2 - \left[\frac{1}{2}\left\|\vec{n'}_{p,1}\right\|^{-1}\epsilon_{1jk}k'_{1,j}r'_{0,k}\right]^2}.$$

The azimuthal angle ϕ_2' is obtained as

$$\phi_2' = \arctan\left(\pm\left\{\frac{\left[\frac{1}{2}\left\|\vec{n'}_{p,1}\right\|^{-1}\epsilon_{2mn}k'_{1,m}r'_{0,n} - \grave{\nu}'_{2,2}\right]^2 - \left[\frac{1}{2}\left\|\vec{n'}_{p,1}\right\|^{-1}\epsilon_{2mn}k'_{1,m}r'_{0,n}\right]^2}{\left[\frac{1}{2}\left\|\vec{n'}_{p,1}\right\|^{-1}\epsilon_{1jk}k'_{1,j}r'_{0,k} - \grave{\nu}'_{2,1}\right]^2 - \left[\frac{1}{2}\left\|\vec{n'}_{p,1}\right\|^{-1}\epsilon_{1jk}k'_{1,j}r'_{0,k}\right]^2}\right\}^{1/2}\right).$$

Following the procedures used in equations (A.77) through (A.86), the following results are arrived at

$$\begin{cases} \lim_{\varepsilon\to 0}\left(0 \le \phi_2' \le \frac{1}{2}\pi - |\varepsilon|\right), \qquad \lim_{\varepsilon\to 0}\left(\pi + |\varepsilon| \le \phi_2' \le \frac{3}{2}\pi - |\varepsilon|\right), \\ \phi_2' = \arctan\left(\left\{\frac{\left[\frac{1}{2}\left\|\vec{n'}_{p,1}\right\|^{-1}\epsilon_{2mn}k'_{1,m}r'_{0,n} - \grave{\nu}'_{2,2}\right]^2 - \left[\frac{1}{2}\left\|\vec{n'}_{p,1}\right\|^{-1}\epsilon_{2mn}k'_{1,m}r'_{0,n}\right]^2}{\left[\frac{1}{2}\left\|\vec{n'}_{p,1}\right\|^{-1}\epsilon_{1jk}k'_{1,j}r'_{0,k} - \grave{\nu}'_{2,1}\right]^2 - \left[\frac{1}{2}\left\|\vec{n'}_{p,1}\right\|^{-1}\epsilon_{1jk}k'_{1,j}r'_{0,k}\right]^2}\right\}^{1/2}\right); \end{cases} \tag{A.143}$$

$$\begin{cases} \lim_{\varepsilon\to 0}\left(\frac{1}{2}\pi + |\varepsilon| \le \phi_2' \le \pi - \varepsilon\right), \qquad \lim_{\varepsilon\to 0}\left(\frac{3}{2}\pi + |\varepsilon| \le \phi_2' < 2\pi - |\varepsilon|\right), \\ \phi_2' = \arctan\left(-\left\{\frac{\left[\frac{1}{2}\left\|\vec{n'}_{p,1}\right\|^{-1}\epsilon_{2mn}k'_{1,m}r'_{0,n} - \grave{\nu}'_{2,2}\right]^2 - \left[\frac{1}{2}\left\|\vec{n'}_{p,1}\right\|^{-1}\epsilon_{2mn}k'_{1,m}r'_{0,n}\right]^2}{\left[\frac{1}{2}\left\|\vec{n'}_{p,1}\right\|^{-1}\epsilon_{1jk}k'_{1,j}r'_{0,k} - \grave{\nu}'_{2,1}\right]^2 - \left[\frac{1}{2}\left\|\vec{n'}_{p,1}\right\|^{-1}\epsilon_{1jk}k'_{1,j}r'_{0,k}\right]^2}\right\}^{1/2}\right). \end{cases} \tag{A.144}$$

The solution for ϕ_2' forms a generic structure for any subsequent reflection points on the inner hemisphere surface. The Nth azimuthal angle ϕ_N' is found following a prescribed sequential steps

$$\phi_1' \to \phi_2' \to \phi_3' \to \cdots \to \phi_{N-1}' \to \phi_N'. \tag{A.145}$$

By reversing the direction of sequence, ϕ_N' can be expressed in terms of the initial azimuthal angle ϕ_1', $\phi_N' = \phi_N'\left(\phi_1'\right)$. The polar angle θ_2' of the second reflection point can be found by squaring equation (A.140), which yields

$$\cos^2\theta_2' = [r_i']^{-2}\left\{\left[\frac{1}{2}\left\|\vec{n'}_{p,1}\right\|^{-1}\epsilon_{3jk}k'_{1,j}r'_{0,k} - \grave{\nu}'_{2,3}\right]^2 - \left[\frac{1}{2}\left\|\vec{n'}_{p,1}\right\|^{-1}\epsilon_{3jk}k'_{1,j}r'_{0,k}\right]^2\right\}. \tag{A.146}$$

Add together equations (A.141) and (A.142), $\sin\theta_2'$ can be solved as

$$\begin{aligned}\sin^2\theta_2' = [r_i']^{-2}\Bigg\{&\left[\frac{1}{2}\left\|\vec{n'}_{p,1}\right\|^{-1}\epsilon_{1jk}k'_{1,j}r'_{0,k} - \grave{\nu}'_{2,1}\right]^2 - \left[\frac{1}{2}\left\|\vec{n'}_{p,1}\right\|^{-1}\epsilon_{1jk}k'_{1,j}r'_{0,k}\right]^2 \\ &+ \left[\frac{1}{2}\left\|\vec{n'}_{p,1}\right\|^{-1}\epsilon_{2mn}k'_{1,m}r'_{0,n} - \grave{\nu}'_{2,2}\right]^2 - \left[\frac{1}{2}\left\|\vec{n'}_{p,1}\right\|^{-1}\epsilon_{2mn}k'_{1,m}r'_{0,n}\right]^2\Bigg\}.\end{aligned} \tag{A.147}$$

Finally, by dividing equations (A.146) and (A.147), we get

$$\begin{aligned}\tan^2\theta_2' = &\left\{\left[\frac{1}{2}\left\|\vec{n'}_{p,1}\right\|^{-1}\epsilon_{1jk}k'_{1,j}r'_{0,k}-\dot{\nu}'_{2,1}\right]^2-\left[\frac{1}{2}\left\|\vec{n'}_{p,1}\right\|^{-1}\epsilon_{1jk}k'_{1,j}r'_{0,k}\right]^2\right.\\ &\left.+\left[\frac{1}{2}\left\|\vec{n'}_{p,1}\right\|^{-1}\epsilon_{2mn}k'_{1,m}r'_{0,n}-\dot{\nu}'_{2,2}\right]^2-\left[\frac{1}{2}\left\|\vec{n'}_{p,1}\right\|^{-1}\epsilon_{2mn}k'_{1,m}r'_{0,n}\right]^2\right\}\\ &\times\left\{\left[\frac{1}{2}\left\|\vec{n'}_{p,1}\right\|^{-1}\epsilon_{3qr}k'_{1,q}r'_{0,r}-\dot{\nu}'_{2,3}\right]^2-\left[\frac{1}{2}\left\|\vec{n'}_{p,1}\right\|^{-1}\epsilon_{3qr}k'_{1,q}r'_{0,r}\right]^2\right\}^{-1}.\end{aligned}$$

The polar angle θ_2' is given by

$$\begin{aligned}\theta_2' = \arctan\Bigg(&\pm\left\{\left[\frac{1}{2}\left\|\vec{n'}_{p,1}\right\|^{-1}\epsilon_{1jk}k'_{1,j}r'_{0,k}-\dot{\nu}'_{2,1}\right]^2-\left[\frac{1}{2}\left\|\vec{n'}_{p,1}\right\|^{-1}\epsilon_{1jk}k'_{1,j}r'_{0,k}\right]^2\right.\\ &\left.+\left[\frac{1}{2}\left\|\vec{n'}_{p,1}\right\|^{-1}\epsilon_{2mn}k'_{1,m}r'_{0,n}-\dot{\nu}'_{2,2}\right]^2-\left[\frac{1}{2}\left\|\vec{n'}_{p,1}\right\|^{-1}\epsilon_{2mn}k'_{1,m}r'_{0,n}\right]^2\right\}^{1/2}\\ &\times\left\{\left[\frac{1}{2}\left\|\vec{n'}_{p,1}\right\|^{-1}\epsilon_{3qr}k'_{1,q}r'_{0,r}-\dot{\nu}'_{2,3}\right]^2-\left[\frac{1}{2}\left\|\vec{n'}_{p,1}\right\|^{-1}\epsilon_{3qr}k'_{1,q}r'_{0,r}\right]^2\right\}^{-1/2}\Bigg).\end{aligned}$$

Following the procedures given in equations (A.62) through (A.76), the following results are obtained

$$\begin{cases}\lim_{\varepsilon\to 0}\left(0\le\theta_2'\le\frac{1}{2}\pi-|\varepsilon|\right),\\ \theta_2' = \arctan\Bigg(\left\{\left[\frac{1}{2}\left\|\vec{n'}_{p,1}\right\|^{-1}\epsilon_{1jk}k'_{1,j}r'_{0,k}-\dot{\nu}'_{2,1}\right]^2-\left[\frac{1}{2}\left\|\vec{n'}_{p,1}\right\|^{-1}\epsilon_{1jk}k'_{1,j}r'_{0,k}\right]^2\right.\\ \quad\left.+\left[\frac{1}{2}\left\|\vec{n'}_{p,1}\right\|^{-1}\epsilon_{2mn}k'_{1,m}r'_{0,n}-\dot{\nu}'_{2,2}\right]^2-\left[\frac{1}{2}\left\|\vec{n'}_{p,1}\right\|^{-1}\epsilon_{2mn}k'_{1,m}r'_{0,n}\right]^2\right\}^{1/2}\\ \quad\times\left\{\left[\frac{1}{2}\left\|\vec{n'}_{p,1}\right\|^{-1}\epsilon_{3qr}k'_{1,q}r'_{0,r}-\dot{\nu}'_{2,3}\right]^2-\left[\frac{1}{2}\left\|\vec{n'}_{p,1}\right\|^{-1}\epsilon_{3qr}k'_{1,q}r'_{0,r}\right]^2\right\}^{-1/2}\Bigg);\end{cases}\tag{A.148}$$

$$\begin{cases}\lim_{\varepsilon\to 0}\left(\frac{1}{2}\pi+|\varepsilon|\le\theta_2'\le\pi\right),\\ \theta_2' = \arctan\Bigg(-\left\{\left[\frac{1}{2}\left\|\vec{n'}_{p,1}\right\|^{-1}\epsilon_{1jk}k'_{1,j}r'_{0,k}-\dot{\nu}'_{2,1}\right]^2-\left[\frac{1}{2}\left\|\vec{n'}_{p,1}\right\|^{-1}\epsilon_{1jk}k'_{1,j}r'_{0,k}\right]^2\right.\\ \quad\left.+\left[\frac{1}{2}\left\|\vec{n'}_{p,1}\right\|^{-1}\epsilon_{2mn}k'_{1,m}r'_{0,n}-\dot{\nu}'_{2,2}\right]^2-\left[\frac{1}{2}\left\|\vec{n'}_{p,1}\right\|^{-1}\epsilon_{2mn}k'_{1,m}r'_{0,n}\right]^2\right\}^{1/2}\\ \quad\times\left\{\left[\frac{1}{2}\left\|\vec{n'}_{p,1}\right\|^{-1}\epsilon_{3qr}k'_{1,q}r'_{0,r}-\dot{\nu}'_{2,3}\right]^2-\left[\frac{1}{2}\left\|\vec{n'}_{p,1}\right\|^{-1}\epsilon_{3qr}k'_{1,q}r'_{0,r}\right]^2\right\}^{-1/2}\Bigg).\end{cases}\tag{A.149}$$

The above result of θ_2' forms a generic structure for any subsequent reflection points on the inner hemisphere surface. The Nth polar angle θ_N' can be obtained by following the sequential steps

$$\theta_1'\to\theta_2'\to\theta_3'\to\cdots\to\theta_{N-1}'\to\theta_N'.\tag{A.150}$$

Equivalently, reversing the direction of sequence, θ_N' can be expressed as a function of the initial polar angle θ_1', $\theta_N' = \theta_N'(\theta_1')$. With angular variable ϕ_2' defined in equations (A.143) and (A.144), and θ_2' defined in equations

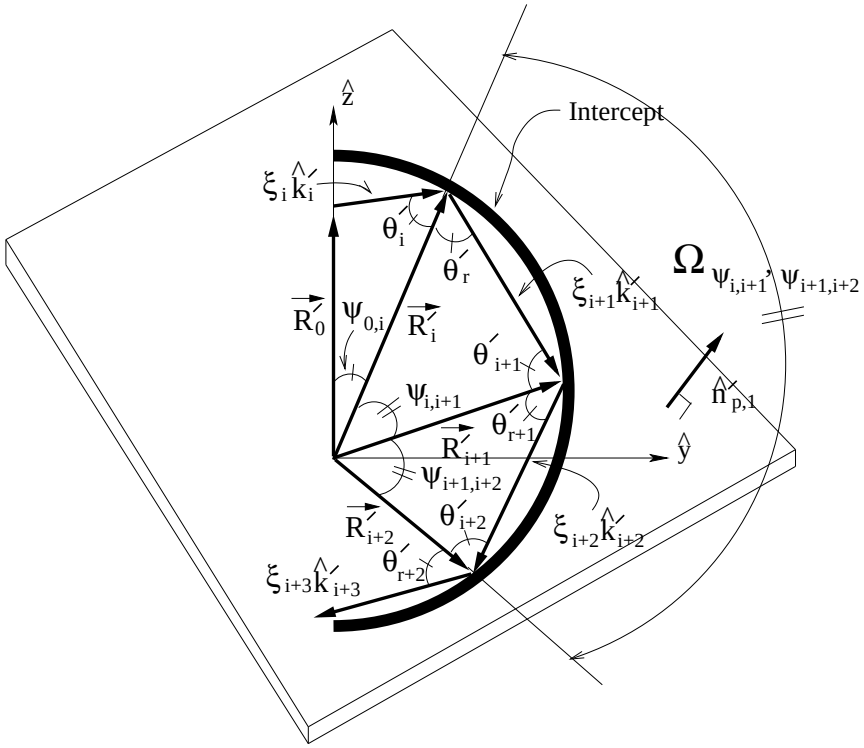

Figure A.3.: The two immediate neighboring reflection points $\vec{R}'_1$ and $\vec{R}'_2$ are connected through the angle $\psi_{1,2}$. Similarly, the two distant neighbor reflection points $\vec{R}'_i$ and $\vec{R}'_{i+2}$ are connected through the angle $\Omega_{\psi_{i,i+1},\psi_{i+1,i+2}}$.

(A.148) and (A.149), the second reflection point on the inner hemisphere surface is given by

$$\vec{R}'_2\left(r'_i,\theta'_2,\phi'_2\right)=\sum_{i=1}^{3}\nu'_{2,i}\left(r'_i,\theta'_2,\phi'_2\right)\hat{e}_i,\qquad i=\left\{\begin{array}{l}1\rightarrow\nu'_{2,1}=r'_i\sin\theta'_2\cos\phi'_2,\\ 2\rightarrow\nu'_{2,2}=r'_i\sin\theta'_2\sin\phi'_2,\\ 3\rightarrow\nu'_{2,3}=r'_i\cos\theta'_2.\end{array}\right. \tag{A.151}$$

As shown in Figure A.3, two reflection points $\vec{R}'_1$ and $\vec{R}'_2$ are related through $\psi_{1,2}$, which is the angle measured between the two. Since $\vec{R}'_j$, where the index $j=1,2,\cdots,N_{max}$ and N_{max} is the last count of reflection before a repeat in cycle, belongs to a spanning set for a plane of incidence whose unit normal is $\hat{n}'_{p,1}$ given in equation (A.17), all reflections occur on the same plane of incidence. The task of determining the Nth subsequent reflection point $\vec{R}'_N$ is therefore particularly simple. The needed connection formulae between the initial reflection point $\vec{R}'_1$ and the Nth subsequent reflection point $\vec{R}'_N$ is found through both scalar and vector cross product relations similar to those given in equations (A.117) and (A.119). In order to generalize the previous result for $\vec{R}'_2$ to $\vec{R}'_N$, recall the set from equations (A.117) and (A.119),

$$\left.\begin{array}{c}\vec{R}'_1\bullet\vec{R}'_2\\ \vec{R}'_1\times\vec{R}'_2\end{array}\right\}\quad\Leftrightarrow\quad\left\{\begin{array}{c}\left[r'_i\right]^2\cos\psi_{1,2}-\sum_{i=1}^{3}\nu'_{1,i}\nu'_{2,i}=0,\\ \sum_{i=1}^{3}\left[\epsilon_{ijk}\nu'_{1,j}\nu'_{2,k}+\Gamma_{1,2}\left\|\vec{n}'_{p,1}\right\|^{-1}\epsilon_{ijk}k'_{1,j}r'_{0,k}\right]\hat{e}_i=0,\end{array}\right. \tag{A.152}$$

where $\Gamma_{1,2}=\left[r'_i\right]^2\sin\psi_{1,2}$ and $\psi_{1,2}=\pi-2\theta_{inc}$. Because $\vec{R}'_N\in\left\{S:\hat{n}'_{p,1}\right\}$, it is true that

$$\vec{R}'_1\times\vec{R}'_N\propto\vec{R}'_1\times\vec{R}'_2.$$

Therefore, we can write

$$\vec{R'}_1 \times \vec{R'}_N = \Gamma'_{1,N}\vec{R'}_1 \times \vec{R'}_2 = \Gamma'_{1,N}\Gamma_{1,2}\hat{n'}_{p,1} = \Gamma_{1,N}\hat{n'}_{p,1},$$

where $\Gamma_{1,N} = \Gamma'_{1,N}\Gamma_{1,2}$ is a proportionality factor. Comparing the results,

$$\left\{\vec{R'}_1 \times \vec{R'}_N = \Gamma_{1,N}\hat{n'}_{p,1}\right\} \quad \rightleftharpoons \quad \left\{\vec{R'}_1 \times \vec{R'}_2 = \Gamma_{1,2}\hat{n'}_{p,1}\right\},$$

one obtains a set of relations similar to equation (A.152) for $\vec{R'}_N$,

$$\left.\begin{array}{c}\vec{R'}_1 \bullet \vec{R'}_N \\ \vec{R'}_1 \times \vec{R'}_N\end{array}\right\} \quad \Leftrightarrow \quad \left\{\begin{array}{c}[r'_i]^2 \cos\psi_{1,N} - \sum_{i=1}^{3}\nu'_{1,i}\nu'_{N,i} = 0, \\ \sum_{i=1}^{3}\left[\epsilon_{ijk}\nu'_{1,j}\nu'_{N,k} + \Gamma_{1,N}\left\|\vec{n'}_{p,1}\right\|^{-1}\epsilon_{ijk}k'_{1,j}r'_{0,k}\right]\hat{e}_i = 0.\end{array}\right. \tag{A.153}$$

In the above expression the index N on $\nu'_{N,i}$ and $\nu'_{N,k}$ denotes components corresponding to $\vec{R'}_N$ and $\psi_{1,N}$ is the angle measured between $\vec{R'}_1$ and $\vec{R'}_N$. The proportionality factor $\Gamma_{1,N}$ is found to be

$$\vec{R'}_1 \times \vec{R'}_N = \Gamma_{1,N}\hat{n'}_{p,1} \quad \rightarrow \quad \left\|\vec{R'}_1 \times \vec{R'}_N\right\| = \Gamma_{1,N}\left\|\hat{n'}_{p,1}\right\| = \Gamma_{1,N},$$

which yields

$$\Gamma_{1,N} = \left\|\vec{R'}_1 \times \vec{R'}_N\right\| = [r'_i]^2 \sin\psi_{1,N}.$$

The angle $\psi_{1,N}$ is contained in $\Omega_{\psi_{1,2},\psi_{N-1,N}}$ as shown in Figure A.3,

$$\Omega_{\vec{R'}_1,\vec{R'}_N} \equiv \Omega_{\psi_{1,2},\psi_{N-1,N}} = \psi_{1,2} + \psi_{2,3} + \cdots + \psi_{N-2,N-1} + \psi_{N-1,N}. \tag{A.154}$$

For each $\psi_{i,i+1}$, the sum of inner angles of a triangle gives

$$\left\{\begin{array}{c}\psi_{1,2} + \theta_2 + \theta_r = \pi, \\ \psi_{2,3} + \theta_3 + \theta_{r+1} = \pi, \\ \vdots \\ \psi_{N-2,N-1} + \theta_{N-1} + \theta_{r+N-2} = \pi, \\ \psi_{N-1,N} + \theta_N + \theta_{r+N-1} = \pi.\end{array}\right.$$

The law of reflection gives

$$\theta_2 = \theta_3 = \cdots = \theta_{N-1} = \theta_N = \theta_r = \theta_{r+1} = \cdots = \theta_{r+N-2} = \theta_{r+N-1} = \theta_{inc}.$$

Hence, the angles $\psi_{i,i+1}$ are found to be

$$\psi_{1,2} = \psi_{2,3} = \cdots = \psi_{N-2,N-1} = \psi_{N-1,N} = \pi - 2\theta_{inc}. \tag{A.155}$$

The angle $\Omega_{\psi_{1,2},\psi_{N-1,N}}$ is expressed as

$$\Omega_{\psi_{1,2},\psi_{N-1,N}} = \psi_{1,2} + \psi_{2,3} + \cdots + \psi_{N-1,N} = [\pi - 2\theta_{inc}] + [\pi - 2\theta_{inc}] + \cdots + [\pi - 2\theta_{inc}]$$

or

$$\psi_{1,N} \equiv \Omega_{\psi_{1,2},\psi_{N-1,N}} = [N-1]\,[\pi - 2\theta_{inc}]\,. \tag{A.156}$$

Hence for $\Gamma_{1,N}$, we have the result:

$$\Gamma_{1,N} = [r'_i]^2 \sin\left([N-1]\,[\pi - 2\theta_{inc}]\right). \tag{A.157}$$

The angular variables θ'_N and ϕ'_N corresponding to Nth reflection point $\vec{R}'_N$ are given as

$$\begin{cases} \lim_{\varepsilon\to 0}\left(0 \le \theta'_N \le \frac{1}{2}\pi - |\varepsilon|\right), \qquad N \ge 2, \\ \theta'_{N\ge 2} = \arctan\left(\left\{\left[\frac{1}{2}\left\|\vec{n'}_{p,1}\right\|^{-1}\epsilon_{1jk}k'_{1,j}r'_{0,k} - \grave{\nu}'_{N,1}\right]^2 - \left[\frac{1}{2}\left\|\vec{n'}_{p,1}\right\|^{-1}\epsilon_{1jk}k'_{1,j}r'_{0,k}\right]^2\right. \right. \\ \quad \left. + \left[\frac{1}{2}\left\|\vec{n'}_{p,1}\right\|^{-1}\epsilon_{2mn}k'_{1,m}r'_{0,n} - \grave{\nu}'_{N,2}\right]^2 - \left[\frac{1}{2}\left\|\vec{n'}_{p,1}\right\|^{-1}\epsilon_{2mn}k'_{1,m}r'_{0,n}\right]^2\right\}^{1/2} \\ \quad \left. \times\left\{\left[\frac{1}{2}\left\|\vec{n'}_{p,1}\right\|^{-1}\epsilon_{3qr}k'_{1,q}r'_{0,r} - \grave{\nu}'_{N,3}\right]^2 - \left[\frac{1}{2}\left\|\vec{n'}_{p,1}\right\|^{-1}\epsilon_{3qr}k'_{1,q}r'_{0,r}\right]^2\right\}^{-1/2}\right); \end{cases} \tag{A.158}$$

$$\begin{cases} \lim_{\varepsilon\to 0}\left(\frac{1}{2}\pi + |\varepsilon| \le \theta'_N \le \pi\right), \qquad N \ge 2, \\ \theta'_{N\ge 2} = \arctan\left(-\left\{\left[\frac{1}{2}\left\|\vec{n'}_{p,1}\right\|^{-1}\epsilon_{1jk}k'_{1,j}r'_{0,k} - \grave{\nu}'_{N,1}\right]^2 - \left[\frac{1}{2}\left\|\vec{n'}_{p,1}\right\|^{-1}\epsilon_{1jk}k'_{1,j}r'_{0,k}\right]^2\right. \right. \\ \quad \left. + \left[\frac{1}{2}\left\|\vec{n'}_{p,1}\right\|^{-1}\epsilon_{2mn}k'_{1,m}r'_{0,n} - \grave{\nu}'_{N,2}\right]^2 - \left[\frac{1}{2}\left\|\vec{n'}_{p,1}\right\|^{-1}\epsilon_{2mn}k'_{1,m}r'_{0,n}\right]^2\right\}^{1/2} \\ \quad \left. \times\left\{\left[\frac{1}{2}\left\|\vec{n'}_{p,1}\right\|^{-1}\epsilon_{3qr}k'_{1,q}r'_{0,r} - \grave{\nu}'_{N,3}\right]^2 - \left[\frac{1}{2}\left\|\vec{n'}_{p,1}\right\|^{-1}\epsilon_{3qr}k'_{1,q}r'_{0,r}\right]^2\right\}^{-1/2}\right). \end{cases} \tag{A.159}$$

$$\begin{cases} \lim_{\varepsilon\to 0}\left(0 \le \phi'_N \le \frac{1}{2}\pi - |\varepsilon|\right), \qquad \lim_{\varepsilon\to 0}\left(\pi + |\varepsilon| \le \phi'_N \le \frac{3}{2}\pi - |\varepsilon|\right), \qquad N \ge 2, \\ \phi'_{N\ge 2} = \arctan\left(\left\{\frac{\left[\frac{1}{2}\left\|\vec{n'}_{p,1}\right\|^{-1}\epsilon_{2mn}k'_{1,m}r'_{0,n} - \grave{\nu}'_{N,2}\right]^2 - \left[\frac{1}{2}\left\|\vec{n'}_{p,1}\right\|^{-1}\epsilon_{2mn}k'_{1,m}r'_{0,n}\right]^2}{\left[\frac{1}{2}\left\|\vec{n'}_{p,1}\right\|^{-1}\epsilon_{1jk}k'_{1,j}r'_{0,k} - \grave{\nu}'_{N,1}\right]^2 - \left[\frac{1}{2}\left\|\vec{n'}_{p,1}\right\|^{-1}\epsilon_{1jk}k'_{1,j}r'_{0,k}\right]^2}\right\}^{1/2}\right); \end{cases} \tag{A.160}$$

$$\begin{cases} \lim_{\varepsilon\to 0}\left(\frac{1}{2}\pi + |\varepsilon| \le \phi'_N \le \pi - \varepsilon\right), \qquad \lim_{\varepsilon\to 0}\left(\frac{3}{2}\pi + |\varepsilon| \le \phi'_N < 2\pi - |\varepsilon|\right), \qquad N \ge 2, \\ \phi'_{N\ge 2} = \arctan\left(-\left\{\frac{\left[\frac{1}{2}\left\|\vec{n'}_{p,1}\right\|^{-1}\epsilon_{2mn}k'_{1,m}r'_{0,n} - \grave{\nu}'_{N,2}\right]^2 - \left[\frac{1}{2}\left\|\vec{n'}_{p,1}\right\|^{-1}\epsilon_{2mn}k'_{1,m}r'_{0,n}\right]^2}{\left[\frac{1}{2}\left\|\vec{n'}_{p,1}\right\|^{-1}\epsilon_{1jk}k'_{1,j}r'_{0,k} - \grave{\nu}'_{N,1}\right]^2 - \left[\frac{1}{2}\left\|\vec{n'}_{p,1}\right\|^{-1}\epsilon_{1jk}k'_{1,j}r'_{0,k}\right]^2}\right\}^{1/2}\right), \end{cases} \tag{A.161}$$

where $\left\{\grave{\nu}'_{N,i} : i = 1,2,3\right\}$ are given in equations (A.134), (A.135) and (A.136) together with the modification $\grave{\nu}'_{2,i} \to \grave{\nu}'_{N,i}$, $\zeta_1(\Gamma_{1,2}) \to \zeta_1(\Gamma_{1,N})$, $\zeta_2(\Gamma_{1,2}) \to \zeta_2(\Gamma_{1,N})$ and $\zeta_3(\Gamma_{1,2}) \to \zeta_3(\Gamma_{1,N})$, where $\Gamma_{1,N}$ is given in equation (A.157). With angular variable $\theta'_{N\ge 2}$ defined in equations (A.158) and (A.159) and $\phi'_{N\ge 2}$ defined in equations (A.160) and (A.161), the Nth reflection point on the inner hemisphere surface is given by

$$\vec{R}'_N(r'_i,\theta'_N,\phi'_N) = \sum_{i=1}^{3}\nu'_{N,i}(r'_i,\theta'_N,\phi'_N)\,\hat{e}_i, \qquad i = \begin{cases} 1 \to \nu'_{N,1} = r'_i\sin\theta'_N\cos\phi'_N, \\ 2 \to \nu'_{N,2} = r'_i\sin\theta'_N\sin\phi'_N, \\ 3 \to \nu'_{N,3} = r'_i\cos\theta'_N, \end{cases} \tag{A.162}$$

where the initial reflection point $\vec{R}'_1$ is given in equation (A.109).

For a sphere, the maximum number of reflections are given by the equation

$$N_{s,max}\psi_{N-2,N-1} = 2\pi,$$

where $\psi_{N-2,N-1}$ is the angle between two neighboring reflection points $\vec{R}'_{N-1}$ and $\vec{R}'_{N-2}$; the subscript $N_{s,max}$ denotes the maximum number of reflection points for a sphere. The above result is a statement that the sum of all angles is equal to 2π. Application of the rule shown in equation (A.155) for $\psi_{N-2,N-1}$ gives

$$N_{max}\left[\pi - 2\theta_{inc}\right] = 2\pi \quad \to \quad N_{s,max} = \frac{2\pi}{\pi - 2\theta_{inc}}, \tag{A.163}$$

where θ_{inc} is given in equation (A.115). In explicit form $N_{s,max}$ is given by

$$N_{s,max} = 2\pi \left[\pi - 2 \arccos \left(\frac{\sin\theta_1' \left[k_{x_1'}' \cos\phi_1' + k_{y_1'}' \sin\phi_1' \right] + k_{z_1'}' \cos\theta_1'}{\sqrt{\left[k_{x_1'}' \right]^2 + \left[k_{y_1'}' \right]^2 + \left[k_{z_1'}' \right]^2}} \right) \right]^{-1} . \tag{A.164}$$

B. Mapping Between Sets (r, θ, ϕ) and (r', θ', ϕ')

In this appendix, the original derivations and developments pertaining to the mapping between the sets (r, θ, ϕ) and (r', θ', ϕ') used in this thesis are described in detail.

For a sphere, the natural choice for origin is the sphere center from which the spherical coordinates (r'_i, θ', ϕ') are prescribed. For more complicated configurations, as shown in Figure 3.3, the preferred choice for the origin depends upon the problem in hand. For this reason, this section is devoted in deriving a set of transformations between (r'_i, θ', ϕ') and (r_i, θ, ϕ) , where the primed set is defined relative to the sphere center, and the unprimed set is defined relative to the global configuration origin. In Cartesian coordinates, the two vectors $\vec{R}$ and $\vec{R}'$ describing an identical point on the hemisphere surface are expressed as

$$\vec{R}\left(\nu_1, \nu_2, \nu_3\right) = \sum_{i=1}^{3} \nu_i \hat{e_i}, \qquad \vec{R}'\left(\nu'_1, \nu'_2, \nu'_3\right) = \sum_{i=1}^{3} \nu'_i \hat{e_i}, \tag{B.1}$$

where

$$\left[\begin{array}{c} \nu_1 = x \\ \nu_2 = y \\ \nu_3 = z \end{array}\right], \qquad \left[\begin{array}{c} \nu'_1 = x' \\ \nu'_2 = y' \\ \nu'_3 = z' \end{array}\right], \qquad \left[\begin{array}{c} \hat{e_1} = \hat{x} \\ \hat{e_2} = \hat{y} \\ \hat{e_3} = \hat{z} \end{array}\right].$$

Here $\vec{R}$ and $\vec{R}'$ are the position vectors of the same location relative to the system origin and the hemisphere center, respectively. The two vectors are related through a translation,

$$\vec{R}\left(\nu_1, \nu_2, \nu_3\right) = \vec{R}_T\left(\nu_{T,1}, \nu_{T,2}, \nu_{T,3}\right) + \vec{R}'\left(\nu'_1, \nu'_2, \nu'_3\right) = \sum_{i=1}^{3} \left[\nu_{T,i} + \nu'_i\right] \hat{e_i}, \tag{B.2}$$

where $\vec{R}_T = \sum_{i=1}^{3} \nu_{T,i} \hat{e_i}$ is the position of hemisphere center relative to the system origin. Equation (B.2) can be written as

$$\sum_{i=1}^{3} \left[\nu_i - \nu_{T,i} - \nu'_i\right] \hat{e_i} = 0. \tag{B.3}$$

and the component equations are

$$\nu_i - \nu_{T,i} - \nu'_i = 0, \qquad i = 1, 2, 3. \tag{B.4}$$

It is to be emphasized that in the configuration shown in Figure 3.3, the hemisphere center is only shifted along $\hat{y}$ by the distance $\nu_{T,2} = a$, therefore $\nu_{T,i\neq 2} = 0$. Nevertheless, the derivation is done for the case where $\nu_{T,i} \neq 0$, $i = 1, 2, 3$ for general purpose. In explicit forms, they are written as

$$\nu_1 - \nu_{T,1} - \nu'_1 = 0, \qquad \nu_2 - \nu_{T,2} - \nu'_2 = 0, \qquad \nu_3 - \nu_{T,3} - \nu'_3 = 0. \tag{B.5}$$

In spherical coordinates,

$$\left[\begin{array}{c} \nu_1 = r_i \sin\theta \cos\phi = r_i \Lambda_1\left(\theta, \phi\right) \\ \nu_2 = r_i \sin\theta \sin\phi = r_i \Lambda_2\left(\theta, \phi\right) \\ \nu_3 = r_i \cos\theta = r_i \Lambda_3\left(\theta\right) \end{array}\right], \qquad \left[\begin{array}{c} \nu'_1 = r'_i \sin\theta' \cos\phi' = r'_i \Lambda'_1\left(\theta', \phi'\right) \\ \nu'_2 = r'_i \sin\theta' \sin\phi' = r'_i \Lambda'_2\left(\theta', \phi'\right) \\ \nu'_3 = r'_i \cos\theta' = r'_i \Lambda'_3\left(\theta'\right) \end{array}\right], \tag{B.6}$$

equation (B.5) is written as

$$r_i \sin\theta \cos\phi - \nu_{T,1} - r'_i \sin\theta' \cos\phi' = 0, \tag{B.7}$$

$$r_i \sin\theta \sin\phi - \nu_{T,2} - r'_i \sin\theta' \sin\phi' = 0, \tag{B.8}$$

$$r_i \cos\theta - \nu_{T,3} - r'_i \cos\theta' = 0, \tag{B.9}$$

where the Cartesian variables $\{\nu_i, \nu'_i : i = 1, 2, 3\}$ were expressed in terms of the spherical coordinates. The $\cos\phi$ and $\sin\phi$ functions are obtained from equations (B.7) and (B.8),

$$\cos\phi = \frac{\nu_{T,1} + r'_i \sin\theta' \cos\phi'}{r_i \sin\theta}, \qquad \sin\phi = \frac{\nu_{T,2} + r'_i \sin\theta' \sin\phi'}{r_i \sin\theta}.$$

The azimuthal angle ϕ is given by

$$\phi \equiv \grave{\phi}\left(r'_i, \theta', \phi', \nu_{T,1}, \nu_{T,2}\right) = \arctan\left(\frac{\nu_{T,2} + r'_i \sin\theta' \sin\phi'}{\nu_{T,1} + r'_i \sin\theta' \cos\phi'}\right), \tag{B.10}$$

where the notation $\grave{\phi}$ indicates that ϕ is explicitly expressed in terms of primed variables. Combining equations (B.7) and (B.8), we have

$$r_i \sin\theta \left[\cos\phi + \sin\phi\right] - \nu_{T,1} - \nu_{T,2} - r'_i \sin\theta' \left[\cos\phi' + \sin\phi'\right] = 0$$

which leads to

$$\sin\theta = \frac{\nu_{T,1} + \nu_{T,2} + r'_i \sin\theta' \left[\cos\phi' + \sin\phi'\right]}{r_i \left[\cos\phi + \sin\phi\right]}.$$

From equation (B.9), we have

$$\cos\theta = r_i^{-1} \left[\nu_{T,3} + r'_i \cos\theta'\right].$$

Combining the above results for $\sin\theta$ and $\cos\theta$; and, solving for the argument θ,

$$\theta = \arctan\left(\frac{\nu_{T,1} + \nu_{T,2} + r'_i \sin\theta' \left[\cos\phi' + \sin\phi'\right]}{\left[\cos\phi + \sin\phi\right]\left[\nu_{T,3} + r'_i \cos\theta'\right]}\right), \tag{B.11}$$

where ϕ is to be substituted in from equation (B.10). For convenience, the above result for θ is rewritten explicitly in terms of primed variables,

$$\grave{\theta}\left(r'_i, \theta', \phi', \vec{R}_T\right) = \arctan\left(\frac{\left\{\nu_{T,1} + \nu_{T,2} + r'_i \sin\theta' \left[\cos\phi' + \sin\phi'\right]\right\}\left[\nu_{T,3} + r'_i \cos\theta'\right]^{-1}}{\cos\left(\arctan\left(\frac{\nu_{T,2} + r'_i \sin\theta' \sin\phi'}{\nu_{T,1} + r'_i \sin\theta' \cos\phi'}\right)\right) + \sin\left(\arctan\left(\frac{\nu_{T,2} + r'_i \sin\theta' \sin\phi'}{\nu_{T,1} + r'_i \sin\theta' \cos\phi'}\right)\right)}\right). \tag{B.12}$$

Here the notation $\grave{\theta}$ indicates that θ is explicitly expressed in terms of primed variables. The magnitude of a vector describing hemisphere relative to system origin is found from equation (B.2),

$$r_i\left(r'_i, \vec{\Lambda}', \vec{R}_T\right) \equiv \left\|\vec{R}\right\| = \left\{\sum_{i=1}^{3} \left[\nu_{T,i} + r'_i \Lambda'_i\right]^2\right\}^{1/2}, \qquad \begin{cases} \Lambda'_1\left(\theta', \phi'\right) = \sin\theta' \cos\phi', \\ \Lambda'_2\left(\theta', \phi'\right) = \sin\theta' \sin\phi', \\ \Lambda'_3\left(\theta'\right) = \cos\theta'. \end{cases}$$

In terms of spherical coordinates, the position vector is expressed as

$$\vec{R}\left(r'_i, \grave{\vec{\Lambda}}, \vec{\Lambda}', \vec{R}_T\right) = \left\{\sum_{i=1}^{3} \left[\nu_{T,i} + r'_i \Lambda'_i\right]^2\right\}^{1/2} \sum_{i=1}^{3} \grave{\Lambda}_i \hat{e}_i, \qquad \begin{cases} \grave{\Lambda}_1\left(\grave{\theta}, \grave{\phi}\right) = \sin\grave{\theta} \cos\grave{\phi}, \\ \grave{\Lambda}_2\left(\grave{\theta}, \grave{\phi}\right) = \sin\grave{\theta} \sin\grave{\phi}, \\ \grave{\Lambda}_3\left(\grave{\theta}\right) = \cos\grave{\theta}. \end{cases} \tag{B.13}$$

C. Selected Configurations

In this appendix, the original derivations and developments in the thesis pertaining to the selected configurations: (1) the hollow spherical shell, (2) the hemisphere-hemisphere and (3) the plate-hemisphere are described in detail.

C.1. Hollow Spherical Shell

For the reflection problem in a sphere as shown in Figure 3.4, the natural choice for a system origin is that of the sphere center, $\vec{R}' = 0$. The Nth reflection point inside the sphere is given by equation (A.162) as

$$\vec{R'}_{s,N}\left(r'_i, \theta'_{s,N}, \phi'_{s,N}\right) = \sum_{i=1}^{3} \nu'_{s,N,i}\left(r'_i, \theta'_{s,N}, \phi'_{s,N}\right)\hat{e}_i, \qquad \begin{cases} \nu'_{s,N,1} = r'_i \sin\theta'_{s,N}\cos\phi'_{s,N}, \\ \nu'_{s,N,2} = r'_i \sin\theta'_{s,N}\sin\phi'_{s,N}, \\ \nu'_{s,N,3} = r'_i \cos\theta'_{s,N}, \end{cases}$$

where the label s have been attached to denote the sphere. Keeping in mind the obvious index changes, the angular variable $\theta'_{s,N}$ is defined in equations (A.158) and (A.159), and $\phi'_{s,N}$, in equations (A.160) and (A.161). Staying with the notation of equation (B.13), $\vec{R'}_{s,N}$ is rewritten as

$$\vec{R}_{s,N}\left(r'_i, \vec{\Lambda}'_{s,N}\right) = r'_i \sum_{i=1}^{3} \Lambda'_{s,N,i}\hat{e_i}, \qquad \begin{cases} \Lambda'_{s,N,1}\left(\theta'_{s,N}, \phi'_{s,N}\right) = \sin\theta'_{s,N}\cos\phi'_{s,N}, \\ \Lambda'_{s,N,2}\left(\theta'_{s,N}, \phi'_{s,N}\right) = \sin\theta'_{s,N}\sin\phi'_{s,N}, \\ \Lambda'_{s,N,3}\left(\theta'_{s,N}\right) = \cos\theta'_{s,N}, \end{cases} \tag{C.1}$$

where the relations $\nu_{T,s,i} = 0$, and $\sum_{i=1}^{3}\left[\Lambda'_{s,N,i}\right]^2 = 1$ are used.

The maximum number of internal reflections for a spherical cavity before a repeat in cycle is given by equation (A.163),

$$N_{s,max} = \frac{2\pi}{\pi - 2\theta_{inc}},$$

where θ_{inc} is given in equation (A.115).

The distance $\left\|\vec{L}\right\|$ between two immediate neighboring reflection points on a sphere is

$$\left\|\vec{L}\right\| = \left\|\vec{R}_{s,2}\left(r'_i, \vec{\Lambda}'_{s,2}\right) - \vec{R}_{s,1}\left(r'_i, \vec{\Lambda}'_{s,1}\right)\right\|. \tag{C.2}$$

It should be noted that

$$\left\|\vec{R}_{s,2} - \vec{R}_{s,1}\right\| = \left\|\vec{R}_{s,j} - \vec{R}_{s,j-1}\right\|, \qquad j = 3, \cdots, N_{s,max}. \tag{C.3}$$

The only reason that $\vec{R}_{s,1}$ and $\vec{R}_{s,2}$ are used is for the purpose of convenience.

To compute the resultant wave vector, $\vec{k'}_{inner}$, acting at the point $\vec{R'}_{s,1}$, the incident wave is first decomposed into components parallel and perpendicular to the inner surface normal vector, $-\hat{R'}_{s,1}$,

$$\vec{k'}_{i,+} \equiv \vec{k'}_i = \vec{k'}_{i\parallel} + \vec{k'}_{i\perp} = \left[\vec{k'}_i \bullet \hat{R'}_{s,1}\right]\hat{R'}_{s,1} + \left[\hat{R'}_{s,1} \times \vec{k'}_i\right] \times \hat{R'}_{s,1},$$

where the subscript $(+)$ of $\vec{k'}_{i,+}$ denotes the particular contribution where the incident wave $\vec{k'}_i$ is approaching $\vec{R'}_{s,1}$ from $\vec{R'}_{s,0}$. From equation (A.14) of Appendix A, the corresponding reflected wave vector can be expressed in terms

of the incident wave as

$$\begin{aligned}\vec{k'}_{r,+} \equiv \vec{k'}_r &= \left[\hat{R'}_{s,1} \times \left\{\left[\vec{k'}_i \bullet \hat{R'}_{s,1}\right] \hat{R'}_{s,1} + \left[\hat{R'}_{s,1} \times \vec{k'}_i\right] \times \hat{R'}_{s,1}\right\}\right] \times \hat{R'}_{s,1} \\ &- \hat{R'}_{s,1} \bullet \left\{\left[\vec{k'}_i \bullet \hat{R'}_{s,1}\right] \hat{R'}_{s,1} + \left[\hat{R'}_{s,1} \times \vec{k'}_i\right] \times \hat{R'}_{s,1}\right\} \hat{R'}_{s,1} \\ &= \left[\hat{R'}_{s,1} \times \left[\vec{k'}_i \bullet \hat{R'}_{s,1}\right] \hat{R'}_{s,1} + \hat{R'}_{s,1} \times \left\{\left[\hat{R'}_{s,1} \times \vec{k'}_i\right] \times \hat{R'}_{s,1}\right\}\right] \times \hat{R'}_{s,1} \\ &- \left[\hat{R'}_{s,1} \bullet \left[\vec{k'}_i \bullet \hat{R'}_{s,1}\right] \hat{R'}_{s,1} + \hat{R'}_{s,1} \bullet \left\{\left[\hat{R'}_{s,1} \times \vec{k'}_i\right] \times \hat{R'}_{s,1}\right\}\right] \hat{R'}_{s,1},\end{aligned}$$

where $\alpha_{r,\perp} = \alpha_{r,\parallel} = 1$ and $\hat{n'} \to -\hat{R'}_{s,1}$. Because $\hat{R'}_{s,1} \perp \left\{\left[\hat{R'}_{s,1} \times \vec{k'}_i\right] \times \hat{R'}_{s,1}\right\}$ and $\hat{R'}_{s,1} \parallel \left[\vec{k'}_i \bullet \hat{R'}_{s,1}\right] \hat{R'}_{s,1}$, the above expression is simplified to

$$\vec{k'}_{r,+} = \left[\hat{R'}_{s,1} \times \left\{\left[\hat{R'}_{s,1} \times \vec{k'}_i\right] \times \hat{R'}_{s,1}\right\}\right] \times \hat{R'}_{s,1} - \left[\vec{k'}_i \bullet \hat{R'}_{s,1}\right] \hat{R'}_{s,1}.$$

The changes in resultant wave vector $\vec{k'}_{inner}$ at the point $\vec{R'}_{s,1}$ due to $\vec{k'}_{i,+}$ at location $\vec{R'}_{s,0}$ is given by

$$\begin{aligned}\triangle\vec{k'}_{inner,+}\left(;\vec{R'}_{s,1},\vec{R'}_{s,0}\right) &= \vec{k'}_{r,+} - \vec{k'}_{i,+} \\ &= \left[\hat{R'}_{s,1} \times \left\{\left[\hat{R'}_{s,1} \times \vec{k'}_i\right] \times \hat{R'}_{s,1}\right\}\right] \times \hat{R'}_{s,1} \\ &- \left[\hat{R'}_{s,1} \times \vec{k'}_i\right] \times \hat{R'}_{s,1} - 2\left[\vec{k'}_i \bullet \hat{R'}_{s,1}\right] \hat{R'}_{s,1} \\ &= -2\left[\vec{k'}_i \bullet \hat{R'}_{s,1}\right] \hat{R'}_{s,1},\end{aligned}$$

where $\left[\hat{R'}_{s,1} \times \left\{\left[\hat{R'}_{s,1} \times \vec{k'}_i\right] \times \hat{R'}_{s,1}\right\}\right] \times \hat{R'}_{s,1} = \left[\hat{R'}_{s,1} \times \vec{k'}_i\right] \times \hat{R'}_{s,1}$.

For the incident wave traveling in the opposite direction, i.e., approaching $\vec{R'}_{s,1}$ from $\vec{R'}_{s,2}$, one has

$$\vec{k'}_{i,-} \equiv -\vec{k'}_r = -\vec{k'}_{r,+}, \qquad \vec{k'}_{r,-} \equiv -\vec{k'}_i = -\vec{k'}_{i,+},$$

where the subscript $(-)$ on $\vec{k'}_{i,-}$ denotes the particular contribution where the incident wave $\vec{k'}_i$ is approaching $\vec{R'}_{s,1}$ from $\vec{R'}_{s,2}$. In this case, the changes in the resultant wave vector $\vec{k'}_{inner}$ at the point $\vec{R'}_{s,1}$ due to $\vec{k'}_{i,-}$ at the location $\vec{R'}_{s,0}$ is given by

$$\triangle\vec{k'}_{inner,-}\left(;\vec{R'}_{s,1},\vec{R'}_{s,0}\right) = \vec{k'}_{r,-} - \vec{k'}_{i,-} = -\vec{k'}_{i,+} + \vec{k'}_{r,+} = \triangle\vec{k'}_{inner,+}\left(;\vec{R'}_{s,1},\vec{R'}_{s,0}\right).$$

The resultant wave vector $\vec{k'}_{inner}$ acting at the point $\vec{R'}_{s,1}$ due to incident wave approaching $\vec{R'}_{s,1}$ from $\vec{R'}_{s,0}$ and the other incident wave approaching $\vec{R'}_{s,1}$ from $\vec{R'}_{s,2}$ is therefore

$$\begin{aligned}\triangle\vec{k'}_{inner}\left(;\vec{R'}_{s,1},\vec{R'}_{s,0}\right) &\equiv \triangle\vec{k'}_{inner,+}\left(;\vec{R'}_{s,1},\vec{R'}_{s,0}\right) + \triangle\vec{k'}_{inner,-}\left(;\vec{R'}_{s,1},\vec{R'}_{s,0}\right) \\ &= -4\left[\vec{k'}_{i,b} \bullet \hat{R'}_{s,1}\right] \hat{R'}_{s,1},\end{aligned}$$

where the subscript b of $\vec{k'}_{i,b}$ denotes the wave vector for ambient fields inside cavity.

The wave number $\left\|\vec{k'}_{i,b}\right\|$ that can be fit in the bounded space of a resonator is restricted by the boundary condition

$$\left\|\vec{k'}_{i,b}\right\| = n\pi \left\|\vec{L}\right\|^{-1} = n\pi \left\|\vec{R}_{s,2}\left(r'_i,\vec{\Lambda}'_{s,2}\right) - \vec{R}_{s,1}\left(r'_i,\vec{\Lambda}'_{s,1}\right)\right\|^{-1}.$$

The scalar product of $\vec{k'}_{i,b}$ and $\hat{R'}_{s,1}$ is

$$\vec{k'}_{i,b} \bullet \hat{R'}_{s,1} = \left\| \vec{k'}_{i,b} \right\| \cos\theta_{inc},$$

where the angle between the two vectors $\vec{k'}_{i,b}$ and $\vec{R}_{s,1}$ is equal to the angle of incidence θ_{inc}, as shown in equation (A.115). The momentum transfer is proportional to

$$\triangle\vec{k'}_{inner}\left(;\vec{R'}_{s,1},\vec{R'}_{s,0}\right) = -\frac{4n\pi\cos\theta_{inc}}{\left\|\vec{R}_{s,2}\left(r'_i,\vec{\Lambda}'_{s,2}\right)-\vec{R}_{s,1}\left(r'_i,\vec{\Lambda}'_{s,1}\right)\right\|}\hat{R'}_{s,1}, \qquad \left\{\begin{array}{c} 0\le\theta_{inc}<\pi/2, \\ n=1,2,\cdots. \end{array}\right. \tag{C.4}$$

Similarly, the resultant wave vector $\vec{k'}_{outer}$ acting at point $\vec{R'}_{s,1}+a\hat{R'}_{s,1}$ on the outer spherical surface, where a is the sphere thickness parameter, is given by

$$\triangle\vec{k'}_{outer}\left(;\vec{R'}_{s,1}+a\hat{R'}_{s,1}\right) = -4\left[\vec{k'}_{i,f}\bullet\hat{R'}_{s,1}\right]\hat{R'}_{s,1},$$

where the subscript f of $\vec{k'}_{i,f}$ denotes the wave vector of the ambient fields in free space, and the factor 4 is due to the fact there are two incidence wave vectors from opposite directions. The free space wave number $\left\|\vec{k'}_{i,f}\right\|$ has no quantization restriction due to the boundary. And, the scalar product of $\vec{k'}_{i,f}$ and $\hat{R'}_{s,1}$ is

$$\vec{k'}_{i,f}\bullet\hat{R'}_{s,1} = \left\|\vec{k'}_{i,f}\right\|\cos\left(\pi-\theta_{inc}\right) = -\left\|\vec{k'}_{i,f}\right\|\cos\theta_{inc}\hat{R'}_{s,1}.$$

The momentum transfer is proportional to

$$\triangle\vec{k'}_{outer}\left(;\vec{R'}_{s,1}+a\hat{R'}_{s,1}\right) = 4\left\|\vec{k'}_{i,f}\right\|\cos\theta_{inc}\hat{R'}_{s,1}, \qquad \left\{\begin{array}{c} 0\le\theta_{inc}<\pi/2, \\ n=1,2,\cdots. \end{array}\right. \tag{C.5}$$

C.2. Hemisphere-Hemisphere

For the hemisphere-hemisphere configuration, the preferred choice for a system origin is that of $\vec{R}=0$. The Nth internal reflection point is given by equation (B.13),

$$\vec{R}_{h,N}\left(r'_i,\grave{\vec{\Lambda}}_{h,N},\vec{\Lambda}'_{h,N},\vec{R}_{T,h}\right) = \left\{\sum_{i=1}^{3}\left[\nu_{T,h,i}+r'_i\Lambda'_{h,N,i}\right]^2\right\}^{1/2}\sum_{i=1}^{3}\grave{\Lambda}_{h,N,i}\hat{e_i}, \tag{C.6}$$

where the label h denotes hemisphere; and

$$\left\{\begin{array}{r} \grave{\Lambda}_{h,N,1}\left(\grave{\theta}_{h,N},\grave{\phi}_{h,N}\right) = \sin\grave{\theta}_{h,N}\cos\grave{\phi}_{h,N}, \\ \grave{\Lambda}_{h,N,2}\left(\grave{\theta}_{h,N},\grave{\phi}_{h,N}\right) = \sin\grave{\theta}_{h,N}\sin\grave{\phi}_{h,N}, \\ \grave{\Lambda}_{h,N,3}\left(\grave{\theta}_{h,N}\right) = \cos\grave{\theta}_{h,N}. \end{array}\right.$$

The definitions for $\Lambda'_{h,N,i}$, $i=1,2,3$ are identical in form. The angular variables $\left(\grave{\theta}_{h,N},\grave{\phi}_{h,N}\right)$ are given in equations (B.10) and (B.12), where the obvious notational changes are understood. The implicit angular variable $\theta'_{s,N}$ is defined in equations (A.158) and (A.159); and $\phi'_{s,N}$, defined in equations (A.160) and (A.161).

We have to determine the maximum number of internal reflections of the wave in the hemisphere cavity before its escape. Three vectors $\vec{R'}_0$, $\xi_i\hat{k'}_i$ and $\vec{R'}_{h,i}\equiv\vec{R'}_i$ shown in Figure A.3 satisfy the relation

$$\vec{R'}_{h,i=1}-\vec{R'}_0 = \xi_{i=1}\hat{k'}_{i=1},$$

where the notation h of $\vec{R'}_{h,i=1}$ denotes the hemisphere. The path length squared is given by

$$\left\|\vec{R'}_{h,i=1}-\vec{R'}_0\right\|^2=\left\|\vec{R'}_{h,1}\right\|^2+\left\|\vec{R'}_0\right\|^2-2\vec{R'}_{h,1}\bullet\vec{R'}_0=[r'_i]^2+\left\|\vec{R'}_0\right\|^2-2r'_i\left\|\vec{R'}_0\right\|\cos\psi_{0,1}.$$

Since $\left\|\vec{R'}_{h,i=1}-\vec{R'}_0\right\|^2=\left\|\xi_{i=1}\hat{k'}_{i=1}\right\|^2=\xi_1^2$, the angle $\psi_{0,1}$ is found from the last equation to be

$$\psi_{0,1}=\arccos\left(\frac{1}{2}\left\{r'_i\left\|\vec{R'}_0\right\|^{-1}+[r'_i]^{-1}\left\|\vec{R'}_0\right\|-\left[r'_i\left\|\vec{R'}_0\right\|\right]^{-1}\xi_1^2\right\}\right),$$

where $\xi_1=\xi_{1,p}$ is given in equation (A.11). The angle $\psi_{1,2}$ measured between the two vectors $\vec{R'}_{h,1}$ and $\vec{R'}_{h,2}$ is

$$\psi_{1,2}=\arccos\left([r'_i]^{-2}\,\vec{R'}_{h,1}\bullet\vec{R'}_{h,2}\right)=\arccos\left(\sum_{i=1}^{3}\Lambda'_{h,1,i}\Lambda'_{h,2,i}\right),$$

where $\vec{R'}_{h,1}$ and $\vec{R'}_{h,2}$ have been explicitly written for $N=1,2$ in equation (C.1), or equivalently,

$$\psi_{1,2}=\pi-2\theta_{inc}$$

from equation (A.112). Because a hemisphere is just a sphere halve, it is convenient to define a quantity

$$\mathbb{Z}_{h,max}=\frac{1}{\psi_{1,2}}\left[\pi-\psi_{0,1}\right],$$

or in explicit expression,

$$\mathbb{Z}_{h,max}=\frac{1}{\pi-2\theta_{inc}}\left[\pi-\arccos\left(\frac{1}{2}\left\{r'_i\left\|\vec{R'}_0\right\|^{-1}+[r'_i]^{-1}\left\|\vec{R'}_0\right\|-\left[r'_i\left\|\vec{R'}_0\right\|\right]^{-1}\xi_{1,p}^2\right\}\right)\right],\qquad\text{(C.7)}$$

where $\xi_{1,p}$ is given in equation (A.11) and θ_{inc} is given in equation (A.115). The maximum number of internal reflections is then simply

$$N_{h,max}=\left[\mathbb{Z}_{h,max}\right]_G,\qquad\text{(C.8)}$$

where the notation $\left[\mathbb{Z}_{h,max}\right]_G$ is the greatest integer of $\mathbb{Z}_{h,max}$ and it is defined in equation (C.7).

The distance $\left\|\vec{L}\right\|$ between the two immediate neighboring reflection points of the hemisphere is

$$\left\|\vec{L}\right\|=\left\|\vec{R}_{h,2}\left(r'_i,\grave{\Lambda}_{h,2},\vec{\Lambda}'_{h,2},\vec{R}_{T,h}\right)-\vec{R}_{h,1}\left(r'_i,\grave{\Lambda}_{h,1},\vec{\Lambda}'_{h,1},\vec{R}_{T,h}\right)\right\|.\qquad\text{(C.9)}$$

It should be noted that

$$\left\|\vec{R}_{h,2}-\vec{R}_{h,1}\right\|=\left\|\vec{R}_{h,j}-\vec{R}_{h,j-1}\right\|,\qquad j=3,\cdots,N_{h,max}\qquad\text{(C.10)}$$

and the only reason that $\vec{R}_{h,1}$ and $\vec{R}_{h,2}$ are used is for the purpose of convenience.

The change in wave vector direction upon reflection at the point $\hat{R'}_{h,1}$ inside the resonator, or at the location $\vec{R'}_{h,1}+a\hat{R'}_{h,1}$ outside of the hemisphere, is given by results found for the sphere case, equations (C.4) and (C.5), with obvious subscript changes,

$$\triangle\vec{k'}_{inner}\left(;\vec{R'}_{h,1},\vec{R'}_{h,0}\right)=-\frac{4n\pi\cos\theta_{inc}}{\left\|\vec{R}_{h,2}\left(r'_i,\vec{\Lambda}'_{h,2}\right)-\vec{R}_{h,1}\left(r'_i,\vec{\Lambda}'_{h,1}\right)\right\|}\hat{R'}_{h,1},\qquad\left\{\begin{array}{c}0\le\theta_{inc}<\pi/2,\\ n=1,2,\cdots\end{array}\right.\qquad\text{(C.11)}$$

and

$$\triangle\vec{k'}_{outer}\left(;\vec{R'}_{h,1}+a\hat{R'}_{h,1}\right)=4\left\|\vec{k'}_{i,f}\right\|\cos\theta_{inc}\hat{R'}_{h,1},\qquad\left\{\begin{array}{c}0\leq\theta_{inc}<\pi/2,\\ n=1,2,\cdots.\end{array}\right. \tag{C.12}$$

The above results on $\triangle\vec{k'}_{inner}\left(;\vec{R'}_{h,1},\vec{R'}_{h,0}\right)$ and $\triangle\vec{k'}_{outer}\left(;\vec{R'}_{h,1}+a\hat{R'}_{h,1}\right)$ have been derived based upon the fact that there are multiple internal reflections. For a sphere, the multiple internal reflections are inherent. However, for a hemisphere, it is not necessarily true that all incoming waves would result in multiple internal reflections. The criteria for multiple internal reflections are to be established. For a given initial incoming wave vector $\hat{k'}_1$, there can be multiple or single internal reflections depending upon the location of point of entry into the cavity, $\vec{R'}_0$. Shown in Figure 3.5 are the two such reflections dynamics where the dashed vectors represent the single reflection case and the non-dashed vectors represent the multiple reflection case. Because all the processes occur in the same plane of incidence, the relationship $\vec{R'}_f=-\lambda_0\vec{R'}_0$ with $\lambda_0\geq 0$ has to be true. Therefore, we will have

$$\vec{R'}_1=\vec{R'}_0+\xi_p\hat{k'}_1,\qquad\vec{R'}_f\equiv-\lambda_0\vec{R'}_0=\vec{R'}_1+\vec{k'}_2. \tag{C.13}$$

After eliminating $\vec{R'}_1$ from the last two equations, we find

$$\vec{R'}_0=-\left[1+\lambda_0\right]^{-1}\left[\xi_p\hat{k'}_1+\vec{k'}_2\right]. \tag{C.14}$$

The direction of the reflected wave vector $\vec{k'}_2$ cannot be arbitrary because it has to obey the reflection law. The relationship between the directions of an incident and the associated reflection wave is shown in equation (A.14). Designating $\hat{n'}=-\vec{R'}_1/r'_i$, $\vec{k'}_r\rightarrow\vec{k'}_2$ and $\vec{k'}_i\rightarrow\vec{k'}_1$, the reflected wave vector $\vec{k'}_2$ can be written in the form

$$\vec{k'}_2\propto\alpha_{r,\perp}\left[r'_i\right]^{-2}\left[\vec{R'}_1\times\vec{k'}_1\right]\times\vec{R'}_1-\alpha_{r,\parallel}\left[r'_i\right]^{-2}\vec{R'}_1\bullet\vec{k'}_1\vec{R'}_1$$

or, introducing a proportionality factor λ_2, it becomes

$$\vec{k'}_2=\lambda_2\alpha_{r,\perp}\left[r'_i\right]^{-2}\left[\vec{R'}_1\times\vec{k'}_1\right]\times\vec{R'}_1-\lambda_2\alpha_{r,\parallel}\left[r'_i\right]^{-2}\vec{R'}_1\bullet\vec{k'}_1\vec{R'}_1.$$

The goal is to relate $\vec{R'}_f$, or λ_0, in terms of $\vec{R'}_0$. Substituting the expression for $\vec{R'}_1$ from equation (C.13), we arrive at

$$\begin{aligned}\vec{k'}_2=&-\xi_p^2\lambda_2\alpha_{r,\parallel}\left[r'_i\right]^{-2}\vec{k'}_1+\xi_p\lambda_2\left[r'_i\right]^{-2}\left\{\alpha_{r,\perp}\left[\vec{R'}_0\times\vec{k'}_1\right]\times\hat{k'}_1-\alpha_{r,\parallel}\left[\vec{R'}_0\bullet\vec{k'}_1\hat{k'}_1+\left\|\vec{k'}_1\right\|\vec{R'}_0\right]\right\}\\&+\lambda_2\left[r'_i\right]^{-2}\left\{\alpha_{r,\perp}\left[\vec{R'}_0\times\vec{k'}_1\right]\times\vec{R'}_0-\alpha_{r,\parallel}\vec{R'}_0\bullet\vec{k'}_1\vec{R'}_0\right\}.\end{aligned} \tag{C.15}$$

Finally, equations (C.14) and (C.15) are combined to yield

$$\begin{aligned}&\xi_p^2\alpha_{r,\parallel}\vec{k'}_1-\xi_p\left\{\alpha_{r,\perp}\left[\vec{R'}_0\times\vec{k'}_1\right]\times\hat{k'}_1-\alpha_{r,\parallel}\left[\vec{R'}_0\bullet\vec{k'}_1\hat{k'}_1+\left\|\vec{k'}_1\right\|\vec{R'}_0\right]+\lambda_2^{-1}\left[r'_i\right]^2\hat{k'}_1\right\}\\&\qquad+\alpha_{r,\parallel}\vec{R'}_0\bullet\vec{k'}_1\vec{R'}_0-\alpha_{r,\perp}\left[\vec{R'}_0\times\vec{k'}_1\right]\times\vec{R'}_0-\lambda_2^{-1}\left[r'_i\right]^2\left[1+\lambda_0\right]\vec{R'}_0=0.\end{aligned} \tag{C.16}$$

Utilizing the formula $\left[\vec{A}\times\vec{B}\right]\times\vec{C}=\sum_{l=1}^{3}\left\{\left[\vec{A}\bullet\vec{C}\right]B_l-\left[\vec{B}\bullet\vec{C}\right]A_l\right\}\hat{e}_l$, the cross product are evaluated as

$$\left\{\begin{array}{c}\left[\vec{R'}_0\times\vec{k'}_1\right]\times\hat{k'}_1\equiv\left\|\vec{k'}_1\right\|^{-1}\left[\vec{R'}_0\times\vec{k'}_1\right]\times\vec{k'}_1=\sum_{l=1}^{3}\left\{\left\|\vec{k'}_1\right\|^{-1}\left[\vec{R'}_0\bullet\vec{k'}_1\right]k'_{1,l}-\left\|\vec{k'}_1\right\|r'_{0,l}\right\}\hat{e}_l,\\ \left[\vec{R'}_0\times\vec{k'}_1\right]\times\vec{R'}_0=\sum_{l=1}^{3}\left\{\left\|\vec{R'}_0\right\|^2k'_{1,l}-\left[\vec{k'}_1\bullet\vec{R'}_0\right]r'_{0,l}\right\}\hat{e}_l,\\ \vec{k'}_1=\sum_{l=1}^{3}k'_{1,l}\hat{e}_l,\qquad\vec{R'}_0=\sum_{l=1}^{3}r'_{0,l}\hat{e}_l.\end{array}\right.$$

Rewriting equation (C.16) then

$$\sum_{l=1}^{3}\Bigg\{\xi_p^2\alpha_{r,\parallel}k'_{1,l}+\xi_p\Bigg(\alpha_{r,\parallel}\left[\vec{R'}_0\bullet\vec{k'}_1\left\|\vec{k'}_1\right\|^{-1}k'_{1,l}+\left\|\vec{k'}_1\right\|r'_{0,l}\right]-\alpha_{r,\perp}\left[\vec{R'}_0\bullet\vec{k'}_1\left\|\vec{k'}_1\right\|^{-1}k'_{1,l}\\ -\left\|\vec{k'}_1\right\|r'_{0,l}\right]-\lambda_2^{-1}\left[r'_i\right]^2\left\|\vec{k'}_1\right\|^{-1}k'_{1,l}\Bigg)+\alpha_{r,\parallel}\vec{R'}_0\bullet\vec{k'}_1r'_{0,l}-\alpha_{r,\perp}\\ \times\left[\left\|\vec{R'}_0\right\|^2k'_{1,l}-\vec{k'}_1\bullet\vec{R'}_0r'_{0,l}\right]-\lambda_2^{-1}\left[r'_i\right]^2\left[1+\lambda_0\right]r'_{0,l}\Bigg\}\hat{e}_l=0,$$

which leads to the component equations

$$\xi_p^2\alpha_{r,\parallel}k'_{1,l}+\xi_p\Bigg(\alpha_{r,\parallel}\left[\vec{R'}_0\bullet\vec{k'}_1\left\|\vec{k'}_1\right\|^{-1}k'_{1,l}+\left\|\vec{k'}_1\right\|r'_{0,l}\right]-\alpha_{r,\perp}\left[\vec{R'}_0\bullet\vec{k'}_1\left\|\vec{k'}_1\right\|^{-1}k'_{1,l}\\ -\left\|\vec{k'}_1\right\|r'_{0,l}\right]-\lambda_2^{-1}\left[r'_i\right]^2\left\|\vec{k'}_1\right\|^{-1}k'_{1,l}\Bigg)+\alpha_{r,\parallel}\vec{R'}_0\bullet\vec{k'}_1r'_{0,l}-\alpha_{r,\perp}\\ \times\left[\left\|\vec{R'}_0\right\|^2k'_{1,l}-\vec{k'}_1\bullet\vec{R'}_0r'_{0,l}\right]-\lambda_2^{-1}\left[r'_i\right]^2\left[1+\lambda_0\right]r'_{0,l}=0,$$

where $l=1,2,3$. For an isotropic system, $\alpha_{r,\perp}=\alpha_{r,\parallel}=\alpha_r$, the last equation reduces to

$$\xi_p^2\alpha_rk'_{1,l}+\xi_p\left[2\alpha_r\left\|\vec{k'}_1\right\|r'_{0,l}-\lambda_2^{-1}\left[r'_i\right]^2\left\|\vec{k'}_1\right\|^{-1}k'_{1,l}\right]\\ +2\alpha_r\vec{R'}_0\bullet\vec{k'}_1r'_{0,l}-\alpha_r\left\|\vec{R'}_0\right\|^2k'_{1,l}-\lambda_2^{-1}\left[r'_i\right]^2\left[1+\lambda_0\right]r'_{0,l}=0,$$

where $l=1,2,3$. Because there are three such relations of the above, all three component equations are added to yield

$$\xi_p^2+\xi_p\left[\sum_{l=1}^{3}k'_{1,l}\right]^{-1}\sum_{l=1}^{3}\left[2\left\|\vec{k'}_1\right\|r'_{0,l}-\lambda_2^{-1}\left[r'_i\right]^2\left\|\vec{k'}_1\right\|^{-1}k'_{1,l}\right]\\ +\left[\sum_{l=1}^{3}k'_{1,l}\right]^{-1}\sum_{l=1}^{3}\left\{2\vec{R'}_0\bullet\vec{k'}_1r'_{0,l}-\left\|\vec{R'}_0\right\|^2k'_{1,l}-\lambda_2^{-1}\left[r'_i\right]^2\left[1+\lambda_0\right]r'_{0,l}\right\}=0, \tag{C.17}$$

where the both sides of the above equation have been multiplied by $\left[\sum_{l=1}^{3}k'_{1,l}\right]^{-1}$ and $\alpha_r=1$ have been chosen for simplicity. Since ξ_p is just a positive root of ξ_1 of equation (A.9), it satisfies the equation

$$\overbrace{\xi_1^2\sum_{l=1}^{3}\left\|\vec{k'}_1\right\|^{-2}\left[k'_{1,l}\right]^2}^{1}+2\xi_1\left\|\vec{k'}_1\right\|^{-1}\sum_{l=1}^{3}r'_{0,l}k'_{1,l}+\sum_{l=1}^{3}\left[r'_{0,l}\right]^2-\left[r'_i\right]^2=0,$$

where the index i have been changed to l in equation (A.9). The reflection coefficient α_r have been set to a unity in equation (C.17) for the very reason that $\alpha_r=1$ had been already imposed in the above relation, the equation (A.9). Because $\xi_1\equiv\xi_p$, and the fact that coefficient of $\xi_p^2=\xi_1^2=1$ in equations (A.9) and (C.17), the two polynomials must be identical. Therefore, subtracting equation (A.9) from equation (C.17), we obtain

$$\xi_p\Bigg\{\left[\sum_{l=1}^{3}k'_{1,l}\right]^{-1}\sum_{l=1}^{3}\left[2\left\|\vec{k'}_1\right\|r'_{0,l}-\lambda_2^{-1}\left[r'_i\right]^2\left\|\vec{k'}_1\right\|^{-1}k'_{1,l}\right]-2\left\|\vec{k'}_1\right\|^{-1}\sum_{l=1}^{3}r'_{0,l}k'_{1,l}\Bigg\}+\left[r'_i\right]^2\\ +\left[\sum_{l=1}^{3}k'_{1,l}\right]^{-1}\sum_{l=1}^{3}\left\{2\vec{R'}_0\bullet\vec{k'}_1r'_{0,l}-\left\|\vec{R'}_0\right\|^2k'_{1,l}-\lambda_2^{-1}\left[r'_i\right]^2\left[1+\lambda_0\right]r'_{0,l}-\left[r'_{0,l}\right]^2\right\}=0.$$

Because ξ_p is a particular value for the root of ξ_1, for the case where $\xi_p \neq 0$, the above equation is satisfied only when the coefficients of the different powers of ξ_p vanish independently. This is another way of stating that each coefficients of the different powers of ξ_p in equations (A.9) and (C.17) must be proportional to each other. For the situation here, they must be identical due to the fact that coefficients of $\xi_p^2 = \xi_1^2 = 1$. Hence, we have the conditions:

$$\begin{cases} \left[\sum_{l=1}^{3} k'_{1,l}\right]^{-1} \sum_{l=1}^{3} \left[2\left\|\vec{k'}_1\right\| r'_{0,l} - \lambda_2^{-1}\left[r'_i\right]^2 \left\|\vec{k'}_1\right\|^{-1} k'_{1,l}\right] - 2\left\|\vec{k'}_1\right\|^{-1} \sum_{l=1}^{3} r'_{0,l} k'_{1,l} = 0, \\ \left[r'_i\right]^2 + \left[\sum_{l=1}^{3} k'_{1,l}\right]^{-1} \sum_{l=1}^{3} \left\{2\vec{R'}_0 \bullet \vec{k'}_1 r'_{0,l} - \left\|\vec{R'}_0\right\|^2 k'_{1,l} - \lambda_2^{-1}\left[r'_i\right]^2 [1+\lambda_0]\, r'_{0,l} - \left[r'_{0,l}\right]^2\right\} = 0. \end{cases} \tag{C.18}$$

From the first expression of equation (C.18), we find

$$\lambda_2^{-1} = 2\left[r'_i\right]^{-2} \left[\sum_{l=1}^{3} k'_{1,l}\right]^{-1} \sum_{l=1}^{3} \left[\left\|\vec{k'}_1\right\|^2 - k'_{1,l} \sum_{m=1}^{3} k'_{1,m}\right] r'_{0,l}. \tag{C.19}$$

Solving for λ_0 from the second expression of equation (C.18), we have

$$\lambda_0 = \frac{\sum_{l=1}^{3} \left\{k'_{1,l} + 2\vec{R'}_0 \bullet \vec{k'}_1 r'_{0,l}\left[r'_i\right]^{-2} - \left\|\vec{R'}_0\right\|^2 k'_{1,l}\left[r'_i\right]^{-2} - \lambda_2^{-1} r'_{0,l} - \left[r'_{0,l}\right]^2 \left[r'_i\right]^{-2}\right\}}{\lambda_2^{-1} \sum_{l=1}^{3} r'_{0,l}}$$

or, substituting the expression of λ_2^{-1} given in equation (C.19), we have the result:

$$\begin{aligned} \lambda_0 = \frac{1}{2}\left[\sum_{n=1}^{3} k'_{1,n}\right] \left\{\sum_{j=1}^{3}\sum_{l=1}^{3} \left[\left\|\vec{k'}_1\right\|^2 - k'_{1,l}\sum_{m=1}^{3} k'_{1,m}\right] r'_{0,l} r'_{0,j}\right\}^{-1} \sum_{l=1}^{3} \left\{k'_{1,l}\left[r'_i\right]^2 - \left[r'_{0,l}\right]^2\right. \\ \left. + 2\vec{R'}_0 \bullet \vec{k'}_1 r'_{0,l} - \left\|\vec{R'}_0\right\|^2 k'_{1,l} - 2r'_{0,l}\left[\sum_{l=1}^{3} k'_{1,l}\right]^{-1} \sum_{i=1}^{3} \left[\left\|\vec{k'}_1\right\|^2 - k'_{1,i}\sum_{m=1}^{3} k'_{1,m}\right] r'_{0,i}\right\}. \end{aligned} \tag{C.20}$$

Referring back to Figure 3.5, the term λ_0 is connected to $\vec{R'}_f$ through the relation $\vec{R'}_f \equiv -\lambda_0 \vec{R'}_0$. Therefore, the criterion for waves to have multiple or single internal reflection is contained in the controlled quantity λ_0. The vector $\vec{R'}_0$ is a quantity that must be specified initially. Because λ_0 is a positive definite scalar, we can rewrite it as

$$\lambda_0 = \left\|\vec{R'}_f\right\| \left\|\vec{R'}_0\right\|^{-1} = \left\|\vec{R'}_f\right\| \left\{\sum_{i=1}^{3} \left[r'_{0,i}\right]^2\right\}^{-1/2}.$$

Substituting the above definition of λ_0 into equation (C.20), the quantity $\left\|\vec{R'}_f\right\|$ can be solved as

$$\begin{aligned} \left\|\vec{R'}_f\right\| = \frac{1}{2}\left\|\vec{R'}_0\right\| \left[\sum_{n=1}^{3} k'_{1,n}\right] \left\{\sum_{j=1}^{3}\sum_{l=1}^{3} \left[\left\|\vec{k'}_1\right\|^2 - k'_{1,l}\sum_{m=1}^{3} k'_{1,m}\right] r'_{0,l} r'_{0,j}\right\}^{-1} \sum_{l=1}^{3} \left\{k'_{1,l}\left[r'_i\right]^2 - \left[r'_{0,l}\right]^2\right. \\ \left. + 2\vec{R'}_0 \bullet \vec{k'}_1 r'_{0,l} - \left\|\vec{R'}_0\right\|^2 k'_{1,l} - 2r'_{0,l}\left[\sum_{l=1}^{3} k'_{1,l}\right]^{-1} \sum_{i=1}^{3} \left[\left\|\vec{k'}_1\right\|^2 - k'_{1,i}\sum_{m=1}^{3} k'_{1,m}\right] r'_{0,i}\right\}. \end{aligned} \tag{C.21}$$

Because the hemisphere opening has a radius r'_i, the following criteria are concluded:

$$\begin{cases} \left\|\vec{R'}_f\right\| < r'_i, & Single - Internal - Reflection, \\ \left\|\vec{R'}_f\right\| \geq r'_i, & Multiple - Internal - Reflections, \end{cases} \tag{C.22}$$

where $\left\|\vec{R'}_f\right\|$ is given in equation (C.21) and r'_i is the radius of a hemisphere.

C.3. Plate-Hemisphere

The description of a surface is a study of the orientation of its local normal $\hat{n'}_p$, which is shown in Figure 3.6. In spherical coordinates, the unit vectors $\hat{n'}_p$, $\hat{\theta'}_p$ and $\hat{\phi'}_p$ are expressed as

$$\hat{n'}_p = \sum_{i=1}^{3} \Lambda'_{p,i}\hat{e}_i, \qquad \hat{\theta'}_p = \sum_{i=1}^{3} \frac{\partial \Lambda'_{p,i}}{\partial \theta'_p}\hat{e}_i, \qquad \hat{\phi'}_p = \sum_{i=1}^{3} \frac{1}{\sin\theta'_p}\frac{\partial \Lambda'_{p,i}}{\partial \phi'_p}\hat{e}_i, \tag{C.23}$$

where

$$\Lambda'_{p,1}\left(\theta'_p, \phi'_p\right) = \sin\theta'_p\cos\phi'_p, \qquad \Lambda'_{p,2}\left(\theta'_p, \phi'_p\right) = \sin\theta'_p\sin\phi'_p, \qquad \Lambda'_{p,3}\left(\theta'_p\right) = \cos\theta'_p. \tag{C.24}$$

It is easy to show that the set of unit vectors $\left(\hat{n'}_p, \hat{\theta'}_p, \hat{\phi'}_p\right)$ forms an orthonormal coordinates. Therefore, the points on plane can be described by a **2D** coordinate system made of $\hat{\theta'}_p$ and $\hat{\phi'}_p$,

$$\vec{R'}_p = \nu'_{p,\theta'_p}\hat{\theta'}_p + \nu'_{p,\phi'_p}\hat{\phi'}_p = \sum_{i=1}^{3}\left[\nu'_{p,\theta'_p}\frac{\partial \Lambda'_{p,i}}{\partial \theta'_p} + \frac{\nu'_{p,\phi'_p}}{\sin\theta'_p}\frac{\partial \Lambda'_{p,i}}{\partial \phi'_p}\right]\hat{e}_i. \tag{C.25}$$

If the plane's orientation constantly changes in time about its origin, the points on the plane experience the velocity $d\vec{R'}_p/dt$,

$$\begin{aligned}\dot{\vec{R}}'_p \equiv \frac{d\vec{R'}_p}{dt} = \sum_{i=1}^{3}\Bigg[&\dot{\nu'}_{p,\theta'_p}\frac{\partial \Lambda'_{p,i}}{\partial \theta'_p} + \left\{\nu'_{p,\theta'_p}\frac{\partial^2 \Lambda'_{p,i}}{\partial\left[\theta'_p\right]^2} + \frac{\nu'_{p,\phi'_p}}{\sin\theta'_p}\left(\frac{\partial^2 \Lambda'_{p,i}}{\partial\theta'_p\partial\phi'_p} - \cot\theta'_p\frac{\partial \Lambda'_{p,i}}{\partial \phi'_p}\right)\right\}\dot{\theta'}_p \\ &+\frac{\dot{\nu'}_{p,\phi'_p}}{\sin\theta'_p}\frac{\partial \Lambda'_{p,i}}{\partial \phi'_p} + \left\{\nu'_{p,\theta'_p}\frac{\partial^2 \Lambda'_{p,i}}{\partial\phi'_p\partial\theta'_p} + \frac{\nu'_{p,\phi'_p}}{\sin\theta'_p}\frac{\partial^2 \Lambda'_{p,i}}{\partial\left[\phi'_p\right]^2}\right\}\dot{\phi'}_p\Bigg]\hat{e}_i,\end{aligned} \tag{C.26}$$

where $\dot{\theta'}_p$, $\dot{\phi'}_p$ are the angular frequencies and $\dot{\nu'}_{p,\theta'_p}$, $\dot{\nu'}_{p,\phi'_p}$ are the lattice vibrations along the directions $\hat{\theta'}_p$ and $\hat{\phi'}_p$, respectively. Here, it is understood that $\Lambda'_{p,3}$ is independent of ϕ'_p. Therefore, the differentiation of $\Lambda'_{p,3}$ with respect to the ϕ'_p vanishes. For the static plate in which there are no lattice vibrations, $\dot{\nu'}_{p,\theta'_p}$ and $\dot{\nu'}_{p,\phi'_p}$ vanishes.

For the case of plate-hemisphere configuration shown in Figure 3.7, the points on the plate are represented by the vector $\vec{R}_p$ relative to the system origin. Making the correspondence in equation (B.2), $\vec{R} \to \vec{R}_n$, $\vec{R}_T \to \vec{R}_{T,p}$ and $\vec{R'} \to \hat{n'}_p$, the two angular variable sets $\left(\theta'_p, \phi'_p\right)$ and (θ, ϕ) are connected through the relations given in equations (B.10) and (B.12) with $r'_i \to 1$. Here $r'_i \to 1$ because $\left\|\hat{n'}_p\right\| = 1$. Therefore, we obtain

$$\grave{\phi}_p\left(\theta'_p, \phi'_p, \nu_{T,p,1}, \nu_{T,p,2}\right) = \arctan\left(\frac{\nu_{T,p,2} + \sin\theta'_p\sin\phi'_p}{\nu_{T,p,1} + \sin\theta'_p\cos\phi'_p}\right), \tag{C.27}$$

$$\grave{\theta}_p\left(\theta'_p, \phi'_p, \vec{R}_{T,p}\right) = \arctan\left(\frac{\left\{\nu_{T,p,1} + \nu_{T,p,2} + \sin\theta'_p\left[\cos\phi'_p + \sin\phi'_p\right]\right\}\left[\nu_{T,p,3} + \cos\theta'_p\right]^{-1}}{\cos\left(\arctan\left(\frac{\nu_{T,p,2}+\sin\theta'_p\sin\phi'_p}{\nu_{T,p,1}+\sin\theta'_p\cos\phi'_p}\right)\right) + \sin\left(\arctan\left(\frac{\nu_{T,p,2}+\sin\theta'_p\sin\phi'_p}{\nu_{T,p,1}+\sin\theta'_p\cos\phi'_p}\right)\right)}\right), \tag{C.28}$$

where the subscript p of $\grave{\phi}_p$ and $\grave{\theta}_p$ indicates that these are the spherical variables for the points on the plate shown in Figure 3.7, and they are not that of the hemisphere. The vector $\vec{R}_p$ becomes

$$\vec{R}_p = \vec{R}_{T,p}\left(\nu_{T,p,1}, \nu_{T,p,2}, \nu_{T,p,3}\right) + \vec{R'}_p = \sum_{i=1}^{3}\left[\nu_{T,p,i} + \nu'_{p,\theta'_p}\frac{\partial \Lambda'_{p,i}}{\partial \theta'_p} + \frac{\nu'_{p,\phi'_p}}{\sin\theta'_p}\frac{\partial \Lambda'_{p,i}}{\partial \phi'_p}\right]\hat{e}_i. \tag{C.29}$$

The magnitude $\left\|\vec{R}_p\right\|$ is given by

$$r_p\left(\vec{\Lambda}'_p, \vec{R}_{T,p}\right) \equiv \left\|\vec{R}_p\right\| = \left\{\sum_{i=1}^{3}\left[\nu_{T,p,i} + \nu'_{p,\theta'_p}\frac{\partial\Lambda'_{p,i}}{\partial\theta'_p} + \frac{\nu'_{p,\phi'_p}}{\sin\theta'_p}\frac{\partial\Lambda'_{p,i}}{\partial\phi'_p}\right]^2\right\}^{1/2}.$$

In terms of the spherical coordinates, $\vec{R}_p$ is expressed by

$$\vec{R}_p\left(\dot{\vec{\Lambda}}_p, \vec{\Lambda}'_p, \vec{R}_{T,p}\right) = \left\{\sum_{i=1}^{3}\left[\nu_{T,p,i} + \nu'_{p,\theta'_p}\frac{\partial\Lambda'_{p,i}}{\partial\theta'_p} + \frac{\nu'_{p,\phi'_p}}{\sin\theta'_p}\frac{\partial\Lambda'_{p,i}}{\partial\phi'_p}\right]^2\right\}^{1/2}\sum_{i=1}^{3}\dot{\Lambda}_{p,i}\hat{e}_i, \tag{C.30}$$

where

$$\dot{\Lambda}_{p,1}\left(\dot{\theta}_p, \dot{\phi}_p\right) = \sin\dot{\theta}_p\cos\dot{\phi}_p, \qquad \dot{\Lambda}_{p,2}\left(\dot{\theta}_p, \dot{\phi}_p\right) = \sin\dot{\theta}_p\sin\dot{\phi}_p, \qquad \dot{\Lambda}_{p,3}\left(\dot{\theta}_p\right) = \cos\dot{\theta}_p. \tag{C.31}$$

Here, the subscript p in $\vec{R}_p$ indicates that the vector $\vec{R}_p$ describe the points on the plate. If the plane's orientation constantly changes in time about its origin, then the same orientation change observed relative to the system origin is given by the velocity $d\vec{R}_p/dt$,

$$\begin{aligned}\dot{\vec{R}}_p \equiv \frac{d\vec{R}_p}{dt} = &\left\{\sum_{i=1}^{3}\left[\nu_{T,p,i} + \nu'_{p,\theta'_p}\frac{\partial\Lambda'_{p,i}}{\partial\theta'_p} + \frac{\nu'_{p,\phi'_p}}{\sin\theta'_p}\frac{\partial\Lambda'_{p,i}}{\partial\phi'_p}\right]^2\right\}^{-1/2}\sum_{j=1}^{3}\sum_{k=1}^{3}\left(\left[\nu_{T,p,k} + \nu'_{p,\theta'_p}\frac{\partial\Lambda'_{p,k}}{\partial\theta'_p}\right.\right.\\
&\left.+\frac{\nu'_{p,\phi'_p}}{\sin\theta'_p}\frac{\partial\Lambda'_{p,k}}{\partial\phi'_p}\right]\left[\dot{\nu}_{T,p,k} + \left\{\nu'_{p,\theta'_p}\frac{\partial^2\Lambda'_{p,k}}{\partial\left[\theta'_p\right]^2} + \frac{\nu'_{p,\phi'_p}}{\sin\theta'_p}\left(\frac{\partial^2\Lambda'_{p,k}}{\partial\theta'_p\partial\phi'_p} - \cot\theta'_p\frac{\partial\Lambda'_{p,k}}{\partial\phi'_p}\right)\right\}\dot{\theta'}_p\right.\\
&+\left\{\nu'_{p,\theta'_p}\frac{\partial^2\Lambda'_{p,k}}{\partial\phi'_p\partial\theta'_p} + \frac{\nu'_{p,\phi'_p}}{\sin\theta'_p}\frac{\partial^2\Lambda'_{p,k}}{\partial\left[\phi'_p\right]^2}\right\}\dot{\phi'}_p + \dot{\nu'}_{p,\theta'_p}\frac{\partial\Lambda'_{p,k}}{\partial\theta'_p} + \frac{\dot{\nu'}_{p,\phi'_p}}{\sin\theta'_p}\frac{\partial\Lambda'_{p,k}}{\partial\phi'_p}\Bigg]\dot{\Lambda}_{p,j}\\
&\left.+\sum_{i=1}^{3}\left[\nu_{T,p,i} + \nu'_{p,\theta'_p}\frac{\partial\Lambda'_{p,i}}{\partial\theta'_p} + \frac{\nu'_{p,\phi'_p}}{\sin\theta'_p}\frac{\partial\Lambda'_{p,i}}{\partial\phi'_p}\right]^2\left[\frac{\partial\dot{\Lambda}_{p,j}}{\partial\dot{\theta}_p}\frac{\partial\dot{\theta}_p}{\partial\phi'_p}\dot{\theta}'_p + \frac{\partial\dot{\Lambda}_{p,j}}{\partial\dot{\phi}_p}\frac{\partial\dot{\phi}_p}{\partial\phi'_p}\dot{\phi}'_p\right]\right)\hat{e}_j,\end{aligned} \tag{C.32}$$

where it is understood that $\Lambda'_{p,3}$ and $\dot{\Lambda}_{p,3}$ are independent of ϕ'_p and $\dot{\phi}_p$, respectively; and as a consequence, their differentiation with respect to ϕ'_p and $\dot{\phi}_p$ vanishes. Here $\dot{\theta'}_p$, $\dot{\phi'}_p$ are angular frequencies and $\dot{\nu}_{T,p,i}$ is the translation speed of plate relative to system origin. Also, $\dot{\nu'}_{p,\theta'_p}$, $\dot{\nu'}_{p,\phi'_p}$ are lattice vibrations along directions $\hat{\theta'}_p$ and $\hat{\phi'}_p$, respectively. For a static plate in which there are no lattice vibrations, $\dot{\nu'}_{p,\theta'_p}$ and $\dot{\nu'}_{p,\phi'_p}$ vanishes.

A cross-sectional view of the plate-hemisphere system is shown in Figure 3.8. The initial wave vector $\vec{k'}_i$ traveling toward the hemisphere would go through reflections according to the law of reflection and finally exit. It then continues toward the plate and reflect from it. Depending on the orientation of plate at the time of impact, the wave would either escape to infinity or re-enter the hemisphere to repeat the process all over again.

The equation (C.25) defines points on a plate, the Figure 3.7, relative to the plate origin. If S_p is a set of points on a plate whose members are defined by $\vec{R'}_p$ of equation (C.25), the wave reflection dynamics off the plate involve only those points of S_p in the intersection between the plate and the plane of incidence whose unit normal is $\hat{n'}_{p,1}$ given in equation (A.17). In order to determine the intersection between the plate and the incidence plane, the plate is first represented by a scalar field. From equation (C.23), the unit plate normal is

$$\hat{n'}_p = \sum_{i=1}^{3}\Lambda'_{p,i}\hat{e}_i.$$

The scalar field corresponding to the unit normal $\hat{n'}_p$ satisfies the relation

$$\vec{\nabla}' f_p\left(\nu_1', \nu_2', \nu_3'\right) \equiv \sum_{i=1}^{3} \hat{e}_i \frac{\partial f_p}{\partial \nu_i'} = \sum_{i=1}^{3} \Lambda_{p,i}' \hat{e}_i \quad \rightarrow \quad \sum_{i=1}^{3} \left[\frac{\partial f_p}{\partial \nu_i'} - \Lambda_{p,i}'\right] \hat{e}_i = 0.$$

The individual component of the equation is given by

$$\frac{\partial f_p}{\partial \nu_i'} - \Lambda_{p,i}' = 0, \qquad i = 1, 2, 3.$$

Notice that $\Lambda_{p,i}'$ is independent of ν_i'. An integration with respect to ν_i' yields the result

$$f_p\left(\nu_1', \nu_2', \nu_3'\right) = \sum_{i=1}^{3} \Lambda_{p,i}' \nu_i', \tag{C.33}$$

where the integration constant is set to zero because the plate contains its local origin. The intersection between the plane of incidence and the plate shown in Figure 3.6 satisfies the relation

$$f_p\left(\nu_1', \nu_2', \nu_3'\right) - f_{p,1}\left(\nu_1', \nu_2', \nu_3'\right) = 0 \quad \rightarrow \quad \sum_{i=1}^{3} \left[\Lambda_{p,i}' + \left\|\vec{n'}_{p,1}\right\|^{-1} \epsilon_{ijk} k_{1,j}' r_{0,k}'\right] \nu_i' = 0, \tag{C.34}$$

where $f_{p,1}\left(\nu_1', \nu_2', \nu_3'\right)$ is given in equation (A.43), and ν_i' is a scalar corresponding to the basis $\hat{e_i}$, of course. We have, from equation (C.25),

$$\nu_i' = \nu_{p,\theta_p'}' \frac{\partial \Lambda_{p,i}'}{\partial \theta_p'} + \frac{\nu_{p,\phi_p'}'}{\sin\theta_p'} \frac{\partial \Lambda_{p,i}'}{\partial \phi_p'}, \qquad i = 1, 2, 3. \tag{C.35}$$

Substituting ν_i' into equation (C.34), $\nu_{p,\theta_p'}'$ is solved as

$$\nu_{p,\theta_p'}' = -\frac{\nu_{p,\phi_p'}'}{\sin\theta_p'} \frac{\sum_{i=1}^{3} \frac{\partial \Lambda_{p,i}'}{\partial \phi_p'} \left[\Lambda_{p,i}' + \left\|\vec{n'}_{p,1}\right\|^{-1} \epsilon_{ijk} k_{1,j}' r_{0,k}'\right]}{\sum_{l=1}^{3} \frac{\partial \Lambda_{p,l}'}{\partial \theta_p'} \left[\Lambda_{p,l}' + \left\|\vec{n'}_{p,1}\right\|^{-1} \epsilon_{lmn} k_{1,m}' r_{0,n}'\right]}, \tag{C.36}$$

where the summation over indices j, k, m and n is implicit, also the quotient $\nu_{p,\phi_p'}' / \sin\theta_p'$ has been moved out of the summation. The $\vec{R'}_p$ given in equation (C.25) is then rewritten as

$$\vec{R'}_p = \frac{\nu_{p,\phi_p'}'}{\sin\theta_p'} \sum_{i=1}^{3} \left\{ \frac{\partial \Lambda_{p,i}'}{\partial \phi_p'} - \frac{\sum_{i=1}^{3} \frac{\partial \Lambda_{p,i}'}{\partial \phi_p'} \left[\Lambda_{p,i}' + \left\|\vec{n'}_{p,1}\right\|^{-1} \epsilon_{ijk} k_{1,j}' r_{0,k}'\right]}{\sum_{l=1}^{3} \frac{\partial \Lambda_{p,l}'}{\partial \theta_p'} \left[\Lambda_{p,l}' + \left\|\vec{n'}_{p,1}\right\|^{-1} \epsilon_{lmn} k_{1,m}' r_{0,n}'\right]} \frac{\partial \Lambda_{p,i}'}{\partial \theta_p'} \right\} \hat{e}_i. \tag{C.37}$$

Similarly, $\vec{R}_p$ given in equation (C.30) is rewritten as

$$\vec{R}_p = \left\{ \sum_{i=1}^{3} \left[\nu_{T,p,i} + \frac{\nu_{p,\phi_p'}'}{\sin\theta_p'} \left(\frac{\partial \Lambda_{p,i}'}{\partial \phi_p'} - \frac{\sum_{i=1}^{3} \frac{\partial \Lambda_{p,i}'}{\partial \phi_p'} \left[\Lambda_{p,i}' + \left\|\vec{n'}_{p,1}\right\|^{-1} \epsilon_{ijk} k_{1,j}' r_{0,k}'\right]}{\sum_{l=1}^{3} \frac{\partial \Lambda_{p,l}'}{\partial \theta_p'} \left[\Lambda_{p,l}' + \left\|\vec{n'}_{p,1}\right\|^{-1} \epsilon_{lmn} k_{1,m}' r_{0,n}'\right]} \frac{\partial \Lambda_{p,i}'}{\partial \theta_p'} \right) \right]^2 \right\}^{1/2} \times \sum_{i=1}^{3} \grave{\Lambda}_{p,i} \hat{e_i}, \tag{C.38}$$

where $\grave{\Lambda}_{p,i}$ is given in equation (C.31). If $N_{h,max}$ is the maximum count of reflections within the hemisphere before the wave escapes, the direction of the escaping wave, measured with respect to the system origin $\vec{R} = 0$, is

$$\vec{k}_{N_{h,max}+1} = \vec{R}_{h,N_{h,max}+1} - \vec{R}_{h,N_{h,max}}, \tag{C.39}$$

where $\vec{k}_{N_{h,max}+1} = \xi_{N_{h,max}+1}\vec{k'}_{N_{h,max}+1}$. Similarly, by the correspondence $\vec{R}_{h,N_{h,max}+1} \rightarrow \vec{R}_{h,i+3}$ and $\vec{R}_{h,N_{h,max}} \rightarrow \vec{R}_{h,i+2}$ in Figure 3.8, the direction of the escaping wave vector $\vec{k}$ is equivalently described by the relation

$$\zeta\vec{k}_{N_{h,max}+1} = \vec{R}_p - \vec{R}_{h,N_{h,max}} \tag{C.40}$$

where ζ is an appropriate positive scale factor. Combining equations (C.39) and (C.40), $\vec{R}_p$ is solved as

$$\vec{R}_p = \zeta\vec{R}_{h,N_{h,max}+1} + [1-\zeta]\,\vec{R}_{h,N_{h,max}}. \tag{C.41}$$

Because both $\vec{R}_p$ and $\vec{k}_{N_{h,max}+1}$ belong to a spanning set for the plane of incidence whose unit normal is $\hat{n'}_{p,1}$ given in equation (A.17), we observe that the following relationship

$$\vec{R}_p \times \vec{k}_{N_{h,max}+1} = \left\{\zeta\vec{R}_{h,N_{h,max}+1} + [1-\zeta]\,\vec{R}_{h,N_{h,max}}\right\} \times \vec{k}_{N_{h,max}+1} = \gamma\hat{n'}_{p,1} \tag{C.42}$$

hold, where γ is a proportional constant. Substituting the explicit form for $\hat{n'}_{p,1}$ from equation (A.17) into equation (C.42), it simplifies into the following equation

$$\sum_{i=1}^{3}\left[\zeta\epsilon_{ijk}R_{h,N_{h,max}+1,j}k_{N_{h,max}+1,k} + [1-\zeta]\,\epsilon_{ijk}R_{h,N_{h,max},j}k_{N_{h,max}+1,k} + \gamma\left\|\vec{n'}_{p,1}\right\|^{-1}\epsilon_{ijk}k'_{1,j}r'_{0,k}\right]\hat{e}_i = 0,$$

and its component equations are given by

$$\zeta\epsilon_{ijk}R_{h,N_{h,max}+1,j}k_{N_{h,max}+1,k} + [1-\zeta]\,\epsilon_{ijk}R_{h,N_{h,max},j}k_{N_{h,max}+1,k} + \gamma\left\|\vec{n'}_{p,1}\right\|^{-1}\epsilon_{ijk}k'_{1,j}r'_{0,k} = 0,$$

where $k_{N_{h,max}+1,k} = R_{h,N_{h,max}+1,k} - R_{h,N_{h,max},k}$ as described in equation (C.39). Finally, the scale factor ζ is solved as

$$\begin{aligned}\zeta \equiv \zeta_i = &\left[\epsilon_{ijk}R_{h,N_{h,max},j}R_{h,N_{h,max}+1,k} - \epsilon_{ijk}R_{h,N_{h,max},j}R_{h,N_{h,max},k} + \gamma\left\|\vec{n'}_{p,1}\right\|^{-1}\epsilon_{ijk}k'_{1,j}r'_{0,k}\right]\\ &\times\left[\epsilon_{ijk}R_{h,N_{h,max},j}R_{h,N_{h,max}+1,k} - \epsilon_{ijk}R_{h,N_{h,max},j}R_{h,N_{h,max},k} - \epsilon_{ijk}R_{h,N_{h,max}+1,j}R_{h,N_{h,max}+1,k}\right.\\ &\left.+\epsilon_{ijk}R_{h,N_{h,max}+1,j}R_{h,N_{h,max},k}\right]^{-1},\end{aligned} \tag{C.43}$$

where $i = 1,2,3$; $j = 1,2,3$ and $k = 1,2,3$. Here, the notation ζ_i have been adopted in place of ζ. It should be understood that for irrotational **3D** vectors, $\zeta_1 = \zeta_2 = \zeta_3 = \zeta$. For vectors in **2D** and **1D** space, it is understood then ζ_3, ζ_2 are absent, respectively. In current form, equation (C.43) is incomplete because γ is still arbitrary. This happens because ν'_{p,θ'_p} and ν'_{p,ϕ'_p} of $\vec{R}_p$, equation (C.30), still needs to be related to the scale parameter ζ_i. Substituting ζ_i for ζ in equation (C.41), it is rewritten as

$$\vec{R}_p = \zeta_i\vec{R}_{h,N_{h,max}+1} + [1-\zeta_i]\,\vec{R}_{h,N_{h,max}}$$

or using equation (C.6) to explicitly substitute for $\vec{R}_{h,N_{h,max}+1}$ and $\vec{R}_{h,N_{h,max}}$ for $N = N_{h,max}+1$, $N = N_{h,max}$,

respectively; and, regrouping the terms

$$\vec{R}_p = \sum_{i=1}^{3}\left(\zeta_i\left\{\sum_{j=1}^{3}\left[\nu_{T,h,j}+r'_i\Lambda'_{h,N_{h,max}+1,j}\right]^2\right\}^{1/2}\grave{\Lambda}_{h,N_{h,max}+1,i}+[1-\zeta_i]\right.$$
$$\left.\times\left\{\sum_{j=1}^{3}\left[\nu_{T,h,j}+r'_i\Lambda'_{h,N_{h,max},j}\right]^2\right\}^{1/2}\grave{\Lambda}_{h,N_{h,max},i}\right)\hat{e_i}, \tag{C.44}$$

where $\zeta_1=\zeta_2=\zeta_3=\zeta$. The subscript i of r'_i is not a summation index. Equating the above result for $\vec{R}_p$ with that of equation (C.38), we arrive at

$$\sum_{i=1}^{3}\left(\left\{\sum_{j=1}^{3}\left[\nu_{T,p,j}+\frac{\nu'_{p,\phi'_p}}{\sin\theta'_p}\left(\frac{\partial\Lambda'_{p,j}}{\partial\phi'_p}-\frac{\sum_{x=1}^{3}\frac{\partial\Lambda'_{p,x}}{\partial\phi'_p}\left[\Lambda'_{p,x}+\left\|\vec{n'}_{p,1}\right\|^{-1}\epsilon_{xyz}k'_{1,y}r'_{0,z}\right]}{\sum_{l=1}^{3}\frac{\partial\Lambda'_{p,l}}{\partial\theta'_p}\left[\Lambda'_{p,l}+\left\|\vec{n'}_{p,1}\right\|^{-1}\epsilon_{lmn}k'_{1,m}r'_{0,n}\right]}\frac{\partial\Lambda'_{p,j}}{\partial\theta'_p}\right)\right]^2\right\}^{1/2}\right.$$
$$\times\grave{\Lambda}_{p,i}-\zeta_i\left\{\sum_{j=1}^{3}\left[\nu_{T,h,j}+r'_i\Lambda'_{h,N_{h,max}+1,j}\right]^2\right\}^{1/2}\grave{\Lambda}_{h,N_{h,max}+1,i}+[\zeta_i-1]\,\grave{\Lambda}_{h,N_{h,max},i}$$
$$\left.\times\left\{\sum_{j=1}^{3}\left[\nu_{T,h,j}+r'_i\Lambda'_{h,N_{h,max},j}\right]^2\right\}^{1/2}\right)\hat{e_i}=0,$$

and its component equations are

$$\left\{\sum_{j=1}^{3}\left[\nu_{T,p,j}+\frac{\nu'_{p,\phi'_p}}{\sin\theta'_p}\left(\frac{\partial\Lambda'_{p,j}}{\partial\phi'_p}-\frac{\sum_{x=1}^{3}\frac{\partial\Lambda'_{p,x}}{\partial\phi'_p}\left[\Lambda'_{p,x}+\left\|\vec{n'}_{p,1}\right\|^{-1}\epsilon_{xyz}k'_{1,y}r'_{0,z}\right]}{\sum_{l=1}^{3}\frac{\partial\Lambda'_{p,l}}{\partial\theta'_p}\left[\Lambda'_{p,l}+\left\|\vec{n'}_{p,1}\right\|^{-1}\epsilon_{lmn}k'_{1,m}r'_{0,n}\right]}\frac{\partial\Lambda'_{p,j}}{\partial\theta'_p}\right)\right]^2\right\}^{1/2}\right.$$
$$\times\grave{\Lambda}_{p,i}-\zeta_i\left\{\sum_{j=1}^{3}\left[\nu_{T,h,j}+r'_i\Lambda'_{h,N_{h,max}+1,j}\right]^2\right\}^{1/2}\grave{\Lambda}_{h,N_{h,max}+1,i}+[\zeta_i-1]\,\grave{\Lambda}_{h,N_{h,max},i}$$
$$\left.\times\left\{\sum_{j=1}^{3}\left[\nu_{T,h,j}+r'_i\Lambda'_{h,N_{h,max},j}\right]^2\right\}^{1/2}=0, \right. \tag{C.45}$$

where $i=1,2,3$. Introducing the following definitions for convenience,

$$\left\{\begin{array}{c} A_\zeta=\left\{\sum_{j=1}^{3}\left[\nu_{T,h,j}+r'_i\Lambda'_{h,N_{h,max}+1,j}\right]^2\right\}^{1/2},\qquad B_\zeta=\left\{\sum_{j=1}^{3}\left[\nu_{T,h,j}+r'_i\Lambda'_{h,N_{h,max},j}\right]^2\right\}^{1/2},\\ C_\zeta=-\left(\sum_{x=1}^{3}\frac{\partial\Lambda'_{p,x}}{\partial\phi'_p}\left[\Lambda'_{p,x}+\left\|\vec{n'}_{p,1}\right\|^{-1}\epsilon_{xyz}k'_{1,y}r'_{0,z}\right]\right)\\ \times\left(\sum_{l=1}^{3}\frac{\partial\Lambda'_{p,l}}{\partial\theta'_p}\left[\Lambda'_{p,l}+\left\|\vec{n'}_{p,1}\right\|^{-1}\epsilon_{lmn}k'_{1,m}r'_{0,n}\right]\right)^{-1}, \end{array}\right. \tag{C.46}$$

the relation shown in equation (C.45) is rewritten as

$$\left\{\sum_{j=1}^{3}\left[\nu_{T,p,j}+\frac{\nu'_{p,\phi'_p}}{\sin\theta'_p}\left(\frac{\partial\Lambda'_{p,j}}{\partial\phi'_p}-C_\zeta\frac{\partial\Lambda'_{p,j}}{\partial\theta'_p}\right)\right]^2\right\}^{1/2}\grave{\Lambda}_{p,i}-\zeta_i A_\zeta\grave{\Lambda}_{h,N_{h,max}+1,i}+\left[\zeta_i-1\right]B_\zeta\grave{\Lambda}_{h,N_{h,max},i}=0,$$

where $i=1,2,3$. There are three such relations, one for each value of i. It is convenient to combine additively all three relations to form

$$\left\{\sum_{j=1}^{3}\left[\nu_{T,p,j}+\frac{\nu'_{p,\phi'_p}}{\sin\theta'_p}\left(\frac{\partial\Lambda'_{p,j}}{\partial\phi'_p}-C_\zeta\frac{\partial\Lambda'_{p,j}}{\partial\theta'_p}\right)\right]^2\right\}^{1/2}\sum_{i=1}^{3}\grave{\Lambda}_{p,i}-\zeta_i A_\zeta\sum_{i=1}^{3}\grave{\Lambda}_{h,N_{h,max}+1,i}+\left[\zeta_i-1\right]B_\zeta\sum_{i=1}^{3}\grave{\Lambda}_{h,N_{h,max},i}=0.$$

After regrouping the terms and squaring both sides, it becomes

$$\underbrace{\sum_{j=1}^{3}\left[\nu_{T,p,j}+\frac{\nu'_{p,\phi'_p}}{\sin\theta'_p}\left(\frac{\partial\Lambda'_{p,j}}{\partial\phi'_p}-C_\zeta\frac{\partial\Lambda'_{p,j}}{\partial\theta'_p}\right)\right]^2}_{L_\sum}=\left[\frac{\zeta_i A_\zeta\sum_{i=1}^{3}\grave{\Lambda}_{h,N_{h,max}+1,i}-\left[\zeta_i-1\right]B_\zeta\sum_{i=1}^{3}\grave{\Lambda}_{h,N_{h,max},i}}{\sum_{l=1}^{3}\grave{\Lambda}_{p,l}}\right]^2.$$

The summation labeled $L_\sum$ is rewritten as

$$L_\sum=\left[\nu'_{p,\phi'_p}\right]^2\sum_{j=1}^{3}\frac{1}{\sin^2\theta'_p}\left[\frac{\partial\Lambda'_{p,j}}{\partial\phi'_p}-C_\zeta\frac{\partial\Lambda'_{p,j}}{\partial\theta'_p}\right]^2+\nu'_{p,\phi'_p}\sum_{j=1}^{3}\left[\frac{2\nu_{T,p,j}}{\sin\theta'_p}\left(\frac{\partial\Lambda'_{p,j}}{\partial\phi'_p}-C_\zeta\frac{\partial\Lambda'_{p,j}}{\partial\theta'_p}\right)+\nu^2_{T,p,j}\right].$$

The above equation is simplified into a quadratic equation of ν'_{p,ϕ'_p},

$$\left[\nu'_{p,\phi'_p}\right]^2\sum_{j=1}^{3}\frac{1}{\sin^2\theta'_p}\left[\frac{\partial\Lambda'_{p,j}}{\partial\phi'_p}-C_\zeta\frac{\partial\Lambda'_{p,j}}{\partial\theta'_p}\right]^2+\nu'_{p,\phi'_p}\sum_{j=1}^{3}\left[\frac{2\nu_{T,p,j}}{\sin\theta'_p}\left(\frac{\partial\Lambda'_{p,j}}{\partial\phi'_p}-C_\zeta\frac{\partial\Lambda'_{p,j}}{\partial\theta'_p}\right)+\nu^2_{T,p,j}\right]-\left[\frac{\zeta_i A_\zeta\sum_{i=1}^{3}\grave{\Lambda}_{h,N_{h,max}+1,i}-\left[\zeta_i-1\right]B_\zeta\sum_{i=1}^{3}\grave{\Lambda}_{h,N_{h,max},i}}{\sum_{l=1}^{3}\grave{\Lambda}_{p,l}}\right]^2=0.$$

The two roots ν'_{p,ϕ'_p} are given by

$$\begin{aligned}\nu'_{p,\phi'_p}=&\left(-\sum_{j=1}^{3}\left[\frac{\nu_{T,p,j}}{\sin\theta'_p}\left(\frac{\partial\Lambda'_{p,j}}{\partial\phi'_p}-C_\zeta\frac{\partial\Lambda'_{p,j}}{\partial\theta'_p}\right)+\frac{1}{2}\nu^2_{T,p,j}\right]\pm\left\{\frac{1}{4}\left(\sum_{j=1}^{3}\left[\frac{2\nu_{T,p,j}}{\sin\theta'_p}\left(\frac{\partial\Lambda'_{p,j}}{\partial\phi'_p}-C_\zeta\frac{\partial\Lambda'_{p,j}}{\partial\theta'_p}\right)+\nu^2_{T,p,j}\right]\right)^2\right.\\&\left.+\sum_{j=1}^{3}\frac{1}{\sin^2\theta'_p}\left[\frac{\partial\Lambda'_{p,j}}{\partial\phi'_p}-C_\zeta\frac{\partial\Lambda'_{p,j}}{\partial\theta'_p}\right]^2\left[\frac{\zeta_i A_\zeta\sum_{i=1}^{3}\grave{\Lambda}_{h,N_{h,max}+1,i}-\left[\zeta_i-1\right]B_\zeta\sum_{i=1}^{3}\grave{\Lambda}_{h,N_{h,max},i}}{\sum_{l=1}^{3}\grave{\Lambda}_{p,l}}\right]^2\right\}^{1/2}\Bigg)\\&\times\left(\sum_{j=1}^{3}\frac{1}{\sin^2\theta'_p}\left[\frac{\partial\Lambda'_{p,j}}{\partial\phi'_p}-C_\zeta\frac{\partial\Lambda'_{p,j}}{\partial\theta'_p}\right]^2\right)^{-1},\end{aligned}\tag{C.47}$$

where A_ζ, B_ζ and C_ζ are defined in equation (C.46). It is understood that one does not mix summation indices of A_ζ, B_ζ and C_ζ with those already present above. The result for ν'_{p,ϕ'_p} is still incomplete because the factor γ in ζ_i needs

to be fixed by normalization. Unfortunately, the translation property of the plate, $\nu_{T,p,j}$, makes it difficult to extract ζ_i out of the radical. Besides the stated difficulty regarding ζ_i, ν'_{p,ϕ'_p} is still ambiguous in deciding which of the two roots correspond to the actual reflection point on the plate. Fortunately, for the plate-hemisphere system of Figure 3.7, the choice of system origin is arbitrary. One can always choose the plate origin to be the system origin and the translation of the plate can be equivalently simulated by a translation of the hemisphere origin in the opposite direction. Then, in the rest frame of the plate, the translational motion of the plate is zero, i.e., $\nu_{T,p,j} = 0$. In this frame, ν'_{p,ϕ'_p} takes on much simplified form

$$\nu'_{p,\phi'_p} = \pm \sin\theta'_p \frac{\zeta_i A_\zeta \sum_{i=1}^{3} \grave{\Lambda}_{h,N_{h,max}+1,i} - [\zeta_i - 1]\, B_\zeta \sum_{i=1}^{3} \grave{\Lambda}_{h,N_{h,max},i}}{\left\{\sum_{j=1}^{3}\left[\frac{\partial\Lambda'_{p,j}}{\partial\phi'_p} - C_\zeta \frac{\partial\Lambda'_{p,j}}{\partial\theta'_p}\right]^2\right\}^{1/2} \sum_{l=1}^{3} \grave{\Lambda}_{p,l}}.$$

For the sign ambiguity in ν'_{p,ϕ'_p}, it can be quickly fixed by noting that for $\nu_{T,p,j} = 0$, equation (C.45) yields

$$\nu'_{p,\phi'_p} = \frac{\zeta_i \sum_{i=1}^{3}\left[A_\zeta \grave{\Lambda}_{h,N_{h,max}+1,i} - B_\zeta \grave{\Lambda}_{h,N_{h,max},i}\right] + B_\zeta \sum_{i=1}^{3} \grave{\Lambda}_{h,N_{h,max},i}}{\left[\sin\theta'_p\right]^{-1}\left\{\sum_{j=1}^{3}\left[\frac{\partial\Lambda'_{p,j}}{\partial\phi'_p} - C_\zeta \frac{\partial\Lambda'_{p,j}}{\partial\theta'_p}\right]^2\right\}^{1/2} \sum_{l=1}^{3} \grave{\Lambda}_{p,l}}, \qquad \nu_{T,p,j} = 0, \tag{C.48}$$

where A_ζ, B_ζ and C_ζ are defined in equation (C.46) with $\nu_{T,p,j} = 0$. It is to be noticed that for a situation where $\nu_{T,p,j} = 0$, $\grave{\Lambda}$ becomes identical to Λ' in form. One can obtain $\grave{\Lambda}$ simply by replacing the primed variables with the unprimed ones in Λ'. For convenience, ζ_i of equation (C.43) is rewritten as

$$\zeta_i = C_\gamma^{-1} A_\gamma + \gamma C_\gamma^{-1} B_\gamma,$$

where

$$\begin{cases} A_\gamma = \epsilon_{ijk} R_{h,N_{h,max},j}\left[R_{h,N_{h,max}+1,k} - R_{h,N_{h,max},k}\right], \qquad B_\gamma = \left\|\vec{n'}_{p,1}\right\|^{-1} \epsilon_{ijk} k'_{1,j} r'_{0,k}, \\ C_\gamma = \epsilon_{ijk}\left[R_{h,N_{h,max},j} - R_{h,N_{h,max}+1,j}\right]\left[R_{h,N_{h,max}+1,k} - R_{h,N_{h,max},k}\right]. \end{cases} \tag{C.49}$$

Furthermore introducing the definitions,

$$\begin{cases} A_\beta = \sum_{i=1}^{3}\left[A_\zeta \grave{\Lambda}_{h,N_{h,max}+1,i} - B_\zeta \grave{\Lambda}_{h,N_{h,max},i}\right], \qquad B_\beta = \sum_{i=1}^{3} \grave{\Lambda}_{h,N_{h,max},i}, \\ C_\beta = \left\{\sum_{j=1}^{3}\left[\frac{\partial\Lambda'_{p,j}}{\partial\phi'_p} - C_\zeta \frac{\partial\Lambda'_{p,j}}{\partial\theta'_p}\right]^2\right\}^{1/2} \sum_{l=1}^{3} \grave{\Lambda}_{p,l}, \end{cases} \tag{C.50}$$

the ν'_{p,ϕ'_p} of equation (C.48) is rewritten as

$$\nu'_{p,\phi'_p} = \left[C_\beta^{-1} C_\gamma^{-1} A_\gamma A_\beta + \gamma C_\beta^{-1} C_\gamma^{-1} B_\gamma A_\beta + C_\beta^{-1} B_\zeta B_\beta\right] \sin\theta'_p, \qquad \nu_{T,p,j} = 0.$$

Substituting the last expression for ν'_{p,ϕ'_p} into equation (C.38), we arrive at

$$\vec{R}_p = \left[C_\beta^{-1} C_\gamma^{-1} A_\gamma A_\beta + \gamma C_\beta^{-1} C_\gamma^{-1} B_\gamma A_\beta + C_\beta^{-1} B_\zeta B_\beta\right]\left\{\sum_{i=1}^{3}\left[\frac{\partial\Lambda'_{p,i}}{\partial\phi'_p} - C_\zeta \frac{\partial\Lambda'_{p,i}}{\partial\theta'_p}\right]^2\right\}^{1/2} \sum_{i=1}^{3} \grave{\Lambda}_{p,i} \hat{e}_i, \tag{C.51}$$

where $\nu_{T,p,i} = 0$. The vector cross product $\vec{R}_p \times \vec{k}_{N_{h,max}+1}$ is given by

$$\vec{R}_p \times \vec{k}_{N_{h,max}+1} = \sum_{i=1}^{3} \epsilon_{ijk} R_{p,j} k_{N_{h,max}+1,k} \hat{e}_i$$

or

$$\vec{R}_p \times \vec{k}_{N_{h,max}+1} = \left[C_\beta^{-1}C_\gamma^{-1}A_\gamma A_\beta + \gamma C_\beta^{-1}C_\gamma^{-1}B_\gamma A_\beta + C_\beta^{-1}B_\zeta B_\beta\right]\left\{\sum_{j=1}^{3}\left[\frac{\partial\Lambda'_{p,j}}{\partial\phi'_p} - C_\zeta\frac{\partial\Lambda'_{p,j}}{\partial\theta'_p}\right]^2\right\}^{1/2} \times \sum_{i=1}^{3}\epsilon_{ijk}\grave{\Lambda}_{p,j}k_{N_{h,max}+1,k}\hat{e_i}.$$

Finally, substituting above vector cross product $\vec{R}_p \times \vec{k}_{N_{h,max}+1}$ into equation (C.42) and regrouping the terms, it becomes

$$\sum_{i=1}^{3}\left(\left[C_\beta^{-1}C_\gamma^{-1}A_\gamma A_\beta + \gamma C_\beta^{-1}C_\gamma^{-1}B_\gamma A_\beta + C_\beta^{-1}B_\zeta B_\beta\right]\left\{\sum_{j=1}^{3}\left[\frac{\partial\Lambda'_{p,j}}{\partial\phi'_p} - C_\zeta\frac{\partial\Lambda'_{p,j}}{\partial\theta'_p}\right]^2\right\}^{1/2} \times\epsilon_{ijk}\grave{\Lambda}_{p,j}k_{N_{h,max}+1,k} - \gamma\left\|\vec{n'}_{p,1}\right\|^{-1}\epsilon_{ijk}k'_{1,j}r'_{0,k}\right)\hat{e_i} = 0,$$

where $\hat{n'}_{p,1} = \left\|\vec{n'}_{p,1}\right\|^{-1}\sum_{i=1}^{3}\epsilon_{ijk}k'_{1,j}r'_{0,k}\hat{e_i}$ have been used. And for the component equations

$$\left[C_\beta^{-1}C_\gamma^{-1}A_\gamma A_\beta + \gamma C_\beta^{-1}C_\gamma^{-1}B_\gamma A_\beta + C_\beta^{-1}B_\zeta B_\beta\right]\left\{\sum_{j=1}^{3}\left[\frac{\partial\Lambda'_{p,j}}{\partial\phi'_p} - C_\zeta\frac{\partial\Lambda'_{p,j}}{\partial\theta'_p}\right]^2\right\}^{1/2} \times\epsilon_{ijk}\grave{\Lambda}_{p,j}k_{N_{h,max}+1,k} - \gamma\left\|\vec{n'}_{p,1}\right\|^{-1}\epsilon_{ijk}k'_{1,j}r'_{0,k} = 0,$$

where $i = 1, 2, 3$. There are three such relations and they are additively combined to yield

$$\left[C_\beta^{-1}C_\gamma^{-1}A_\gamma A_\beta + \gamma C_\beta^{-1}C_\gamma^{-1}B_\gamma A_\beta + C_\beta^{-1}B_\zeta B_\beta\right]\left\{\sum_{j=1}^{3}\left[\frac{\partial\Lambda'_{p,j}}{\partial\phi'_p} - C_\zeta\frac{\partial\Lambda'_{p,j}}{\partial\theta'_p}\right]^2\right\}^{1/2} \times\sum_{i=1}^{3}\epsilon_{ijk}\grave{\Lambda}_{p,j}k_{N_{h,max}+1,k} - \gamma\left\|\vec{n'}_{p,1}\right\|^{-1}\sum_{i=1}^{3}\epsilon_{ijk}k'_{1,j}r'_{0,k} = 0.$$

Finally, γ is solved to give the result

$$\gamma \equiv \gamma_o = \left(\left\|\vec{n'}_{p,1}\right\|^{-1}\sum_{i=1}^{3}\epsilon_{ijk}k'_{1,j}r'_{0,k} - C_\beta^{-1}C_\gamma^{-1}B_\gamma A_\beta\left\{\sum_{j=1}^{3}\left[\frac{\partial\Lambda'_{p,j}}{\partial\phi'_p} - C_\zeta\frac{\partial\Lambda'_{p,j}}{\partial\theta'_p}\right]^2\right\}^{1/2} \times\sum_{i=1}^{3}\epsilon_{ijk}\grave{\Lambda}_{p,j}k_{N_{h,max}+1,k}\right)^{-1}\left(\left[C_\beta^{-1}C_\gamma^{-1}A_\gamma A_\beta + C_\beta^{-1}B_\zeta B_\beta\right] \times\left\{\sum_{j=1}^{3}\left[\frac{\partial\Lambda'_{p,j}}{\partial\phi'_p} - C_\zeta\frac{\partial\Lambda'_{p,j}}{\partial\theta'_p}\right]^2\right\}^{1/2}\sum_{i=1}^{3}\epsilon_{ijk}\grave{\Lambda}_{p,j}k_{N_{h,max}+1,k}\right). \tag{C.52}$$

The parameter ν'_{p,ϕ'_p} is now completely defined,

$$\nu'_{p,\phi'_p} = \left[C_\beta^{-1}C_\gamma^{-1}A_\gamma A_\beta + \gamma_o C_\beta^{-1}C_\gamma^{-1}B_\gamma A_\beta + C_\beta^{-1}B_\zeta B_\beta\right]\sin\theta'_p, \qquad \nu_{T,p,j} = 0, \tag{C.53}$$

where $(A_\zeta, B_\zeta, C_\zeta)$, $(A_\gamma, B_\gamma, C_\gamma)$, $(A_\beta, B_\beta, C_\beta)$ and γ_o are given by equations (C.46), (C.49), (C.50) and (C.52),

respectively. With ν'_{p,ϕ'_p} defined in equation (C.53), the reflection point on the plate is obtained from equation (C.38),

$$\vec{R}_p = \left\{ \sum_{s=1}^{3} \left[\frac{\partial \Lambda'_{p,s}}{\partial \phi'_p} - \frac{\sum_{i=1}^{3} \frac{\partial \Lambda'_{p,i}}{\partial \phi'_p} \left[\Lambda'_{p,i} + \left\| \vec{n'}_{p,1} \right\|^{-1} \epsilon_{ijk} k'_{1,j} r'_{0,k} \right]}{\sum_{l=1}^{3} \frac{\partial \Lambda'_{p,l}}{\partial \theta'_p} \left[\Lambda'_{p,l} + \left\| \vec{n'}_{p,1} \right\|^{-1} \epsilon_{lmn} k'_{1,m} r'_{0,n} \right]} \frac{\partial \Lambda'_{p,s}}{\partial \theta'_p} \right]^2 \right\}^{1/2}$$
$$\times \left[C_\beta^{-1} C_\gamma^{-1} A_\gamma A_\beta + \gamma_o C_\beta^{-1} C_\gamma^{-1} B_\gamma A_\beta + C_\beta^{-1} B_\zeta B_\beta \right] \sum_{i=1}^{3} \grave{\Lambda}_{p,i} \hat{e}_i, \tag{C.54}$$

where $\nu_{T,p,j} = 0$. It should be noticed that for a situation where $\nu_{T,p,j} = 0$, $\grave{\Lambda}$ becomes identical to Λ' in form, and $\grave{\Lambda}$ can be obtained simply by replacing the primed variables with the unprimed ones.

To see if the wave reflected from the plate at location $\vec{R}_p$ re-enters the hemisphere cavity or escape to infinity, we consider the reflected wave $\vec{k}_{r,N_{h,max}+1}$,

$$\vec{k}_{r,N_{h,max}+1} = \alpha_{r,\perp} \left[\hat{n'}_p \times \vec{k}_{N_{h,max}+1} \right] \times \hat{n'}_p - \alpha_{r,\parallel} \hat{n'}_p \bullet \vec{k}_{N_{h,max}+1} \hat{n'}_p, \tag{C.55}$$

where the relation found in equation (A.14) have been used. As always, it is convenient to express vectors in component forms. Making the changes in variables $(l,m,n) \rightarrow (i,j,k)$, $(m,q,r) \rightarrow (j,l,m)$, $\hat{n'} \rightarrow \hat{n'}_p$ and $\vec{k'}_i \rightarrow \vec{k}_{N_{h,max}+1}$, the component result of equation (A.16) is used to get

$$\vec{k}_{r,N_{h,max}+1} = \sum_{i=1}^{3} \sum_{k=1}^{3} \left\{ \alpha_{r,\perp} \left[k_{N_{h,max}+1,i} n'_{p,k} n'_{p,k} - n'_{p,i} k_{N_{h,max}+1,k} n'_{p,k} \right] \right.$$
$$\left. - \alpha_{r,\parallel} n'_{p,k} k_{N_{h,max}+1,k} n'_{p,i} \right\} \hat{e}_i, \tag{C.56}$$

where $n'_{p,i}$ and $n'_{p,k}$ are coefficients of the normalized $\hat{n'}_p$. All wave vectors entering the hemisphere cavity satisfy the relation

$$\vec{R}_p + \sum_{i=1}^{3} \left[\vec{\xi}_\kappa \bullet \hat{e}_i \right] \left[\vec{k}_{r,N_{h,max}+1} \bullet \hat{e}_i \right] \hat{e}_i - \vec{R}_0 = 0, \qquad \vec{R}_0 = \sum_{i=1}^{3} \left[\nu_{T,h,i} + r'_{0,i} \right] \hat{e}_i, \tag{C.57}$$

where $\vec{\xi}_\kappa$ is a real-valued positive scale vector and $\vec{R}_0$ is the points on the opening face of hemisphere. The scale vector $\vec{\xi}_\kappa$ has the form

$$\vec{\xi}_\kappa = \sum_{i=1}^{3} \xi_{\kappa,i} \hat{e}_i.$$

With the scale vector $\vec{\xi}_\kappa$ defined above; and, $\vec{R}_p$ and $\vec{k}_{r,N_{h,max}+1}$ defined in equations (C.54) and (C.56), respectively, equation (C.57) is rewritten in component form

$$\sum_{i=1}^{3} \left(\left\{ \sum_{s=1}^{3} \left[\frac{\partial \Lambda'_{p,s}}{\partial \phi'_p} - \frac{\sum_{i=1}^{3} \frac{\partial \Lambda'_{p,i}}{\partial \phi'_p} \left[\Lambda'_{p,i} + \left\| \vec{n'}_{p,1} \right\|^{-1} \epsilon_{ijk} k'_{1,j} r'_{0,k} \right]}{\sum_{l=1}^{3} \frac{\partial \Lambda'_{p,l}}{\partial \theta'_p} \left[\Lambda'_{p,l} + \left\| \vec{n'}_{p,1} \right\|^{-1} \epsilon_{lmn} k'_{1,m} r'_{0,n} \right]} \frac{\partial \Lambda'_{p,s}}{\partial \theta'_p} \right]^2 \right\}^{1/2} \right.$$
$$\times \left[C_\beta^{-1} C_\gamma^{-1} A_\gamma A_\beta + \gamma_o C_\beta^{-1} C_\gamma^{-1} B_\gamma A_\beta + C_\beta^{-1} B_\zeta B_\beta \right] \grave{\Lambda}_{p,i} + \xi_{\kappa,i} \sum_{k=1}^{3} \left\{ \alpha_{r,\perp} \left[k_{N_{h,max}+1,i} \right. \right.$$
$$\left. \left. \times n'_{p,k} n'_{p,k} - n'_{p,i} k_{N_{h,max}+1,k} n'_{p,k} \right] - \alpha_{r,\parallel} n'_{p,k} k_{N_{h,max}+1,k} n'_{p,i} \right\} - \nu_{T,h,i} - r'_{0,i} \Big) \hat{e}_i = 0,$$

which yields the component equations,

$$\left\{\sum_{s=1}^{3}\left[\frac{\partial\Lambda'_{p,s}}{\partial\phi'_p}-\frac{\sum_{i=1}^{3}\frac{\partial\Lambda'_{p,i}}{\partial\phi'_p}\left[\Lambda'_{p,i}+\left\|\vec{n'}_{p,1}\right\|^{-1}\epsilon_{ijk}k'_{1,j}r'_{0,k}\right]}{\sum_{l=1}^{3}\frac{\partial\Lambda'_{p,l}}{\partial\theta'_p}\left[\Lambda'_{p,l}+\left\|\vec{n'}_{p,1}\right\|^{-1}\epsilon_{lmn}k'_{1,m}r'_{0,n}\right]}\frac{\partial\Lambda'_{p,s}}{\partial\theta'_p}\right]^2\right\}^{1/2}\left[C_\beta^{-1}C_\gamma^{-1}A_\gamma A_\beta\right.$$
$$\left.+\gamma_o C_\beta^{-1}C_\gamma^{-1}B_\gamma A_\beta+C_\beta^{-1}B_\zeta B_\beta\right]\grave{\Lambda}_{p,i}+\xi_{\kappa,i}\sum_{k=1}^{3}\left\{\alpha_{r,\perp}\left[k_{N_{h,max}+1,i}n'_{p,k}n'_{p,k}\right.\right.$$
$$\left.\left.-n'_{p,i}k_{N_{h,max}+1,k}n'_{p,k}\right]-\alpha_{r,\parallel}n'_{p,k}k_{N_{h,max}+1,k}n'_{p,i}\right\}-\nu_{T,h,i}-r'_{0,i}=0,$$

where $i=1,2,3$. Finally, $\xi_{\kappa,i}$ is solved as

$$\xi_{\kappa,i}=\left(\nu_{T,h,i}+r'_{0,i}-\left\{\sum_{s=1}^{3}\left[\frac{\partial\Lambda'_{p,s}}{\partial\phi'_p}-\frac{\sum_{i=1}^{3}\frac{\partial\Lambda'_{p,i}}{\partial\phi'_p}\left[\Lambda'_{p,i}+\left\|\vec{n'}_{p,1}\right\|^{-1}\epsilon_{ijk}k'_{1,j}r'_{0,k}\right]}{\sum_{l=1}^{3}\frac{\partial\Lambda'_{p,l}}{\partial\theta'_p}\left[\Lambda'_{p,l}+\left\|\vec{n'}_{p,1}\right\|^{-1}\epsilon_{lmn}k'_{1,m}r'_{0,n}\right]}\frac{\partial\Lambda'_{p,s}}{\partial\theta'_p}\right]^2\right\}^{1/2}\right)$$
$$\times\left[C_\beta^{-1}C_\gamma^{-1}A_\gamma A_\beta+\gamma_o C_\beta^{-1}C_\gamma^{-1}B_\gamma A_\beta+C_\beta^{-1}B_\zeta B_\beta\right]\grave{\Lambda}_{p,i}\Bigg)\Bigg(\sum_{k=1}^{3}\left\{\alpha_{r,\perp}\left[k_{N_{h,max}+1,i}n'_{p,k}n'_{p,k}\right.\right.$$
$$\left.\left.-n'_{p,i}k_{N_{h,max}+1,k}n'_{p,k}\right]-\alpha_{r,\parallel}n'_{p,k}k_{N_{h,max}+1,k}n'_{p,i}\right\}\Bigg)^{-1},\tag{C.58}$$

where $i=1,2,3$.

The above result can be applied in setting the re-entry criteria. Notice that $\vec{R}_0\leq r'_i$, which implies $r'_{0,i}\leq r'_i$, where r'_i is the radius of the hemisphere. It can be concluded then that all waves re-entering hemisphere cavity would satisfy the condition $\xi_{\kappa,1}=\xi_{\kappa,2}=\xi_{\kappa,3}$. On the other hand, those waves that escapes to infinity cannot have all three $\xi_{\kappa,i}$ equaling to a same constant. The re-entry condition $\xi_{\kappa,1}=\xi_{\kappa,2}=\xi_{\kappa,3}$ is just another way of stating the existence of parametric line along the vector $\vec{k}_{r,N_{h,max}+1}$ that happens to pierce through a hemisphere opening. When such a line does not exist, the initial wave vector direction has to be rotated accordingly to a new direction, such that in its rotated direction there is a parametric line that pierces through the hemisphere opening; it leads to the condition that all three $\xi_{\kappa,i}$ cannot equal to a same constant. The re-entry criteria are now summarized for bookkeeping purpose,

$$\begin{cases}\xi_{\kappa,1}=\xi_{\kappa,2}=\xi_{\kappa,3}\rightarrow Wave-ReEnters-Hemisphere,\\ ELSE\rightarrow Wave-Escapes-to-Infinity,\end{cases}\tag{C.59}$$

where $ELSE$ is the case where $\xi_{\kappa,1}=\xi_{\kappa,2}=\xi_{\kappa,3}$ cannot be satisfied.

D. Dynamical Casimir Force

The original derivations and developments of this thesis pertaining to the dynamical Casimir force are included in this appendix. It is referenced by the text of the thesis to supply all the fine details.

D.1. Formalism of Zero-Point Energy and its Force

For massless fields, the energy-momentum relation is given by

$$\mathcal{H}'_{n_s} \equiv E_{Total} = pc, \tag{D.1}$$

where p is the momentum and c the speed of light. The field propagating in an arbitrary direction has a momentum $\vec{p'} = \sum_{i=1}^{3} p'_i \hat{e}_i$. The associated field energy-momentum relation is hence

$$\mathcal{H}'_{n_s} - c\left\{\sum_{i=1}^{3}\left[p'_i\right]^2\right\}^{1/2} = 0.$$

The differentiation of the above equation gives

$$d\left[\mathcal{H}'_{n_s} - c\left\{\sum_{i=1}^{3}\left[p'_i\right]^2\right\}^{1/2}\right] \equiv d\mathcal{H}'_{n_s} - cd\left\{\sum_{i=1}^{3}\left[p'_i\right]^2\right\}^{1/2} = 0. \tag{D.2}$$

The total differential energy $d\mathcal{H}'_{n_s}$ is

$$d\mathcal{H}'_{n_s} = \sum_{i=1}^{3}\frac{\partial\mathcal{H}'_{n_s}}{\partial k'_i}\frac{\partial k'_i}{\partial p'_i}dp'_i = \sum_{i=1}^{3}\left(\left[n_s+\frac{1}{2}\right]\hbar\right)^{-1}\frac{\partial\mathcal{H}'_{n_s}}{\partial k'_i}dp'_i, \tag{D.3}$$

where the relation $p'_i = \left[n_s + \frac{1}{2}\right]\hbar k'_i$ has been used. The total differential momentum is

$$d\left\{\sum_{i=1}^{3}\left[p'_i\right]^2\right\}^{1/2} = \left\{\sum_{i=1}^{3}\left[p'_i\right]^2\right\}^{-1/2}\sum_{i=1}^{3}p'_i dp'_i.$$

The combined result is

$$\sum_{i=1}^{3}\left[\left(\left[n_s+\frac{1}{2}\right]\hbar\right)^{-1}\frac{\partial\mathcal{H}'_{n_s}}{\partial k'_i} - \left\{\sum_{i=1}^{3}\left[p'_i\right]^2\right\}^{-1/2}cp'_i\right]dp'_i = 0. \tag{D.4}$$

Because all the momentum differentials are linearly independent, their coefficients are zero,

$$\left(\left[n_s+\frac{1}{2}\right]\hbar\right)^{-1}\frac{\partial\mathcal{H}'_{n_s}}{\partial k'_i} - \left\{\sum_{i=1}^{3}\left[p'_i\right]^2\right\}^{-1/2}cp'_i = 0, \qquad i = 1,2,3.$$

There are three such equations. Then, additively combining the three relations, and rearranging the terms, we have

$$\left\{\sum_{i=1}^{3}\left[p_i'\right]^2\right\}^{1/2}\sum_{i=1}^{3}\left(\left[n_s+\frac{1}{2}\right]\hbar\right)^{-1}\frac{\partial\mathcal{H}'_{n_s}}{\partial k_i'}=\sum_{i=1}^{3}cp_i'.$$

Squaring both sides to get rid of the radical leads to

$$\left[\sum_{i=1}^{3}\left(\left[n_s+\frac{1}{2}\right]\hbar\right)^{-1}\frac{\partial\mathcal{H}'_{n_s}}{\partial k_i'}\right]^2\sum_{i=1}^{3}\left[p_i'\right]^2=c^2\left[\sum_{i=1}^{3}p_i'\right]^2. \tag{D.5}$$

The summations $\sum_{i=1}^{3}\left[p_i'\right]^2$ and $\left[\sum_{i=1}^{3}p_i'\right]^2$ are rewritten as

$$\sum_{i=1}^{3}\left[p_i'\right]^2=\left[p_\alpha'\right]^2+\sum_{i=1}^{3}\left(1-\delta_{i\alpha}\right)\left[p_i'\right]^2=\left[p_\alpha'\right]^2+\sum_{i=1}^{3}\left(1-\delta_{i\alpha}\right)\left(\left[n_s+\frac{1}{2}\right]\hbar\right)^2\left[k_i'\right]^2,$$

$$\begin{aligned}\left[\sum_{i=1}^{3}p_i'\right]^2&=\left[p_\alpha'+\sum_{i=1}^{3}\left(1-\delta_{i\alpha}\right)p_i'\right]^2=\left[p_\alpha'\right]^2+2\sum_{i=1}^{3}\left(1-\delta_{i\alpha}\right)p_i'p_\alpha'+\left[\sum_{i=1}^{3}\left(1-\delta_{i\alpha}\right)p_i'\right]^2\\&=\left[p_\alpha'\right]^2+2\sum_{i=1}^{3}\left(1-\delta_{i\alpha}\right)\left[n_s+\frac{1}{2}\right]\hbar k_i'p_\alpha'+\left(\left[n_s+\frac{1}{2}\right]\hbar\right)^2\left[\sum_{i=1}^{3}\left(1-\delta_{i\alpha}\right)k_i'\right]^2,\end{aligned}$$

where p_i' has been replaced by $\left[n_s+\frac{1}{2}\right]\hbar k_i'$. Substituting the result into equation (D.5) and rearranging the terms in powers of p_α', we have

$$\begin{aligned}&\left(\left[\sum_{i=1}^{3}\frac{\partial\mathcal{H}'_{n_s}}{\partial k_i'}\right]^2-\left(\left[n_s+\frac{1}{2}\right]\hbar c\right)^2\right)\left[p_\alpha'\right]^2-2\left[n_s+\frac{1}{2}\right]\hbar\sum_{i=1}^{3}\left(1-\delta_{i\alpha}\right)\left(\left[n_s+\frac{1}{2}\right]\hbar c\right)^2k_i'p_\alpha'\\&\quad-\left[\sum_{i=1}^{3}\left(1-\delta_{i\alpha}\right)\left(\left[n_s+\frac{1}{2}\right]\hbar c\right)^2k_i'\right]^2+\left[\sum_{i=1}^{3}\frac{\partial\mathcal{H}'_{n_s}}{\partial k_i'}\right]^2\sum_{i=1}^{3}\left(1-\delta_{i\alpha}\right)\left(\left[n_s+\frac{1}{2}\right]\hbar\right)^2\left[k_i'\right]^2=0.\end{aligned}$$

Defining the following quantities,

$$\begin{cases}C_{\alpha,1}=\sum_{i=1}^{3}\frac{\partial\mathcal{H}'_{n_s}}{\partial k_i'}, & C_{\alpha,2}=\sum_{i=1}^{3}\left(1-\delta_{i\alpha}\right)\left(\left[n_s+\frac{1}{2}\right]\hbar c\right)^2k_i',\\ C_{\alpha,3}=\sum_{i=1}^{3}\left(1-\delta_{i\alpha}\right)\left(\left[n_s+\frac{1}{2}\right]\hbar\right)^2\left[k_i'\right]^2,\end{cases} \tag{D.6}$$

the above quadratic equation is rewritten as

$$\left[C_{\alpha,1}^2-\left(\left[n_s+\frac{1}{2}\right]\hbar c\right)^2\right]\left[p_\alpha'\right]^2-2\left[n_s+\frac{1}{2}\right]\hbar C_{\alpha,2}p_\alpha'-C_{\alpha,2}^2+C_{\alpha,1}^2C_{\alpha,3}=0.$$

Finally, the root p_α' is found to be

$$p_\alpha'=\frac{\left[n_s+\frac{1}{2}\right]\hbar C_{\alpha,2}}{C_{\alpha,1}^2-\left(\left[n_s+\frac{1}{2}\right]\hbar c\right)^2}+\left\{\frac{\left[n_s+\frac{1}{2}\right]^2\hbar^2C_{\alpha,2}^2}{\left[C_{\alpha,1}^2-\left(\left[n_s+\frac{1}{2}\right]\hbar c\right)^2\right]^2}+\frac{C_{\alpha,2}^2-C_{\alpha,1}^2C_{\alpha,3}}{C_{\alpha,1}^2-\left(\left[n_s+\frac{1}{2}\right]\hbar c\right)^2}\right\}^{1/2}, \tag{D.7}$$

where the positive root have been chosen since p_α' is an α component magnitude of the total field momentum $\vec{p'}$, therefore it is a positive scalar, $p_\alpha'\geq 0$.

D. Dynamical Casimir Force

By definition, force is equal to the change in momentum per unit time,

$$\vec{\mathcal{F}'} = \frac{d}{dt}\vec{p'} = \frac{d}{dt}\sum_{\alpha=1}^{3} p'_\alpha \hat{e_\alpha} = \sum_{\alpha=1}^{3}\left[\frac{dp'_\alpha}{dt}\hat{e_\alpha} + p'_\alpha\frac{d\hat{e_\alpha}}{dt}\right] = \sum_{\alpha=1}^{3}\frac{dp'_\alpha}{dt}\hat{e_\alpha} = \sum_{\alpha=1}^{3}\vec{\mathcal{F}'}_\alpha.$$

The explicit expression for $\vec{\mathcal{F}'}_\alpha$ is found to be

$$\begin{aligned}\vec{\mathcal{F}'}_\alpha = \Bigg\{ &\left(\frac{C_{\alpha,1}C_{\alpha,4}\left[C_{\alpha,1}^2C_{\alpha,3}-C_{\alpha,2}^2\right]}{\left[C_{\alpha,1}^2-\left(\left[n_s+\frac{1}{2}\right]\hbar c\right)^2\right]^2} - \frac{2\left[n_s+\frac{1}{2}\right]^2\hbar^2 C_{\alpha,1}C_{\alpha,2}^2C_{\alpha,4}}{\left[C_{\alpha,1}^2-\left(\left[n_s+\frac{1}{2}\right]\hbar c\right)^2\right]^3} - \frac{C_{\alpha,1}C_{\alpha,3}C_{\alpha,4}}{C_{\alpha,1}^2-\left(\left[n_s+\frac{1}{2}\right]\hbar c\right)^2}\right.\\ &\left.-\frac{2\left[n_s+\frac{1}{2}\right]\hbar C_{\alpha,1}C_{\alpha,2}}{\left[C_{\alpha,1}^2-\left(\left[n_s+\frac{1}{2}\right]\hbar c\right)^2\right]^2}\right)\frac{dC_{\alpha,1}}{dt} + \left(\frac{\left[n_s+\frac{1}{2}\right]^2\hbar^2C_{\alpha,2}C_{\alpha,4}}{\left[C_{\alpha,1}^2-\left(\left[n_s+\frac{1}{2}\right]\hbar c\right)^2\right]^2} + \frac{C_{\alpha,2}C_{\alpha,4}}{C_{\alpha,1}^2-\left(\left[n_s+\frac{1}{2}\right]\hbar c\right)^2}\right.\\ &\left.+\frac{\left[n_s+\frac{1}{2}\right]\hbar}{C_{\alpha,1}^2-\left(\left[n_s+\frac{1}{2}\right]\hbar c\right)^2}\right)\frac{dC_{\alpha,2}}{dt} - \frac{\frac{1}{2}C_{\alpha,1}^2C_{\alpha,4}}{C_{\alpha,1}^2-\left(\left[n_s+\frac{1}{2}\right]\hbar c\right)^2}\frac{dC_{\alpha,3}}{dt}\Bigg\}\hat{e_\alpha},\end{aligned} \tag{D.8}$$

where

$$C_{\alpha,4} = \left(\frac{\left[n_s+\frac{1}{2}\right]^2\hbar^2C_{\alpha,2}^2}{\left[C_{\alpha,1}^2-\left(\left[n_s+\frac{1}{2}\right]\hbar c\right)^2\right]^2} + \frac{C_{\alpha,2}^2-C_{\alpha,1}^2C_{\alpha,3}}{C_{\alpha,1}^2-\left(\left[n_s+\frac{1}{2}\right]\hbar c\right)^2}\right)^{-1/2}. \tag{D.9}$$

Before computing the three time derivatives $dC_{\alpha,1}/dt$, $dC_{\alpha,2}/dt$ and $dC_{\alpha,3}/dt$, we should notice that $k'_i(n_i) = n_i f_i(L_i)$. Hence, the derivative dk'_i/dt can be written as

$$\frac{dk'_i}{dt} = \frac{\partial k'_i}{\partial n_i}\frac{dn_i}{dt}f_i(L_i) + n_i\frac{\partial f_i}{\partial L_i}\frac{dL_i}{dt} = f_i(L_i)\frac{\partial k'_i}{\partial n_i}\dot{n}_i + n_i\frac{\partial f_i}{\partial L_i}\dot{L}_i. \tag{D.10}$$

The three derivatives $dC_{\alpha,1}/dt$, $dC_{\alpha,2}/dt$ and $dC_{\alpha,3}/dt$ are given by

$$\begin{aligned}\frac{dC_{\alpha,1}}{dt} &= \sum_{i=1}^{3}\sum_{j=1}^{3}\frac{\partial^2\mathcal{H}'_{n_s}}{\partial k'_j\partial k'_i}\frac{dk'_j}{dt} = \sum_{i=1}^{3}\sum_{j=1}^{3}\frac{\partial^2\mathcal{H}'_{n_s}}{\partial k'_j\partial k'_i}\left[f_j(L_j)\frac{\partial k'_j}{\partial n_j}\dot{n}_j + n_j\frac{\partial f_j}{\partial L_j}\dot{L}_j\right]\\ &= \sum_{i=1}^{3}\frac{\partial^2\mathcal{H}'_{n_s}}{\partial\left[k'_i\right]^2}\left[f_i(L_i)\frac{\partial k'_i}{\partial n_i}\dot{n}_i + n_i\frac{\partial f_i}{\partial L_i}\dot{L}_i\right] + \sum_{i=1}^{3}\sum_{j=1}^{3}\left\{(1-\delta_{ij})\frac{\partial^2\mathcal{H}'_{n_s}}{\partial k'_j\partial k'_i}\right.\\ &\left.\times\left[f_j(L_j)\frac{\partial k'_j}{\partial n_j}\dot{n}_j + n_j\frac{\partial f_j}{\partial L_j}\dot{L}_j\right]\right\},\end{aligned} \tag{D.11}$$

$$\frac{dC_{\alpha,2}}{dt} = \sum_{i=1}^{3}(1-\delta_{i\alpha})\left[n_s+\frac{1}{2}\right]\left[f_i(L_i)\frac{\partial k'_i}{\partial n_i}\dot{n}_i + n_i\frac{\partial f_i}{\partial L_i}\dot{L}_i\right], \tag{D.12}$$

$$\frac{dC_{\alpha,3}}{dt} = 2\sum_{i=1}^{3}(1-\delta_{i\alpha})\left[n_s+\frac{1}{2}\right]^2 k'_i\left[f_i(L_i)\frac{\partial k'_i}{\partial n_i}\dot{n}_i + n_i\frac{\partial f_i}{\partial L_i}\dot{L}_i\right], \tag{D.13}$$

where $C_{\alpha,1}$, $C_{\alpha,2}$ and $C_{\alpha,3}$ are defined in equation (D.6). It is noted that the derivative dk'_i/dt, and also each of $dC_{\alpha,1}/dt$, $dC_{\alpha,2}/dt$ and $dC_{\alpha,3}/dt$, consists of two contributing parts, one is proportional to $\dot{n}_i$ and the other involves $\dot{L}_i$. The force expression in equation (D.8) has then two contributing parts. The force contribution involving $\dot{n}_i$ has a physical meaning that the boundaries are being driven to generate the extra wave modes that would otherwise be

missing when such drivers were not present. The force contribution involving $\dot{L}_i$ is the effect of feedbacks from the moving boundaries. This feedback effect due to the moving boundaries tends to either cool or heat the conducting boundaries. For an isolated, non-driven conducting boundaries, the force contribution proportional to $\dot{n}_i$ vanishes. For what is concerned with in this thesis, only isolated systems are studied; and, therefore, $\dot{n}_i = 0$. The expression of force is then rewritten as

$$\begin{aligned}
\vec{\mathcal{F}'}_\alpha = &\left\{ \left(\frac{C_{\alpha,1}C_{\alpha,4}\left[C_{\alpha,1}^2 C_{\alpha,3} - C_{\alpha,2}^2\right]}{\left[C_{\alpha,1}^2 - \left(\left[n_s+\frac{1}{2}\right]\hbar c\right)^2\right]^2} - \frac{2\left[n_s+\frac{1}{2}\right]^2 \hbar^2 C_{\alpha,1}C_{\alpha,2}^2 C_{\alpha,4}}{\left[C_{\alpha,1}^2 - \left(\left[n_s+\frac{1}{2}\right]\hbar c\right)^2\right]^3} - \frac{C_{\alpha,1}C_{\alpha,3}C_{\alpha,4}}{C_{\alpha,1}^2 - \left(\left[n_s+\frac{1}{2}\right]\hbar c\right)^2} \right.\right. \\
&\left.\left. - \frac{2\left[n_s+\frac{1}{2}\right]\hbar C_{\alpha,1}C_{\alpha,2}}{\left[C_{\alpha,1}^2 - \left(\left[n_s+\frac{1}{2}\right]\hbar c\right)^2\right]^2} \right) \left(\sum_{i=1}^{3} \frac{\partial^2 \mathcal{H}'_{n_s}}{\partial\left[k'_i\right]^2} n_i \frac{\partial f_i}{\partial L_i}\dot{L}_i + \sum_{i=1}^{3}\sum_{j=1}^{3}(1-\delta_{ij})\frac{\partial^2 \mathcal{H}'_{n_s}}{\partial k'_j \partial k'_i} n_j \frac{\partial f_j}{\partial L_j}\dot{L}_j \right) \right. \\
&+ \left(\frac{\left[n_s+\frac{1}{2}\right]^2 \hbar^2 C_{\alpha,2}C_{\alpha,4}}{\left[C_{\alpha,1}^2 - \left(\left[n_s+\frac{1}{2}\right]\hbar c\right)^2\right]^2} + \frac{C_{\alpha,2}C_{\alpha,4}}{C_{\alpha,1}^2 - \left(\left[n_s+\frac{1}{2}\right]\hbar c\right)^2} + \frac{\left[n_s+\frac{1}{2}\right]\hbar}{C_{\alpha,1}^2 - \left(\left[n_s+\frac{1}{2}\right]\hbar c\right)^2} \right) \sum_{i=1}^{3}(1-\delta_{i\alpha}) \\
&\left. \times \left[n_s+\frac{1}{2} \right] n_i \frac{\partial f_i}{\partial L_i}\dot{L}_i - \frac{\frac{1}{2}C_{\alpha,1}^2 C_{\alpha,4}}{C_{\alpha,1}^2 - \left(\left[n_s+\frac{1}{2}\right]\hbar c\right)^2} 2\sum_{i=1}^{3}(1-\delta_{i\alpha})\left[n_s+\frac{1}{2}\right]^2 k'_i n_i \frac{\partial f_i}{\partial L_i}\dot{L}_i \right\} \hat{e_\alpha}.
\end{aligned}$$

It can be simplified with the following definitions,

$$\begin{aligned}
C_{\alpha,5} = &\frac{C_{\alpha,1}C_{\alpha,4}\left[C_{\alpha,1}^2 C_{\alpha,3} - C_{\alpha,2}^2\right]}{\left[C_{\alpha,1}^2 - \left(\left[n_s+\frac{1}{2}\right]\hbar c\right)^2\right]^2} - \frac{2\left[n_s+\frac{1}{2}\right]^2 \hbar^2 C_{\alpha,1}C_{\alpha,2}^2 C_{\alpha,4}}{\left[C_{\alpha,1}^2 - \left(\left[n_s+\frac{1}{2}\right]\hbar c\right)^2\right]^3} \\
&- \frac{C_{\alpha,1}C_{\alpha,3}C_{\alpha,4}}{C_{\alpha,1}^2 - \left(\left[n_s+\frac{1}{2}\right]\hbar c\right)^2} - \frac{2\left[n_s+\frac{1}{2}\right]\hbar C_{\alpha,1}C_{\alpha,2}}{\left[C_{\alpha,1}^2 - \left(\left[n_s+\frac{1}{2}\right]\hbar c\right)^2\right]^2},
\end{aligned} \tag{D.14}$$

$$C_{\alpha,6} = \frac{\left[n_s+\frac{1}{2}\right]^2 \hbar^2 C_{\alpha,2}C_{\alpha,4}}{\left[C_{\alpha,1}^2 - \left(\left[n_s+\frac{1}{2}\right]\hbar c\right)^2\right]^2} + \frac{C_{\alpha,2}C_{\alpha,4}}{C_{\alpha,1}^2 - \left(\left[n_s+\frac{1}{2}\right]\hbar c\right)^2} + \frac{\left[n_s+\frac{1}{2}\right]\hbar}{C_{\alpha,1}^2 - \left(\left[n_s+\frac{1}{2}\right]\hbar c\right)^2}, \tag{D.15}$$

$$C_{\alpha,7} = \frac{C_{\alpha,1}^2 C_{\alpha,4}}{C_{\alpha,1}^2 - \left(\left[n_s+\frac{1}{2}\right]\hbar c\right)^2}. \tag{D.16}$$

The dynamical force can then be rewritten as

$$\begin{aligned}
\vec{\mathcal{F}'}_\alpha = \sum_{i=1}^{3} &\left\{ n_i \frac{\partial f_i}{\partial L_i} \left[C_{\alpha,5}\frac{\partial^2 \mathcal{H}'_{n_s}}{\partial\left[k'_i\right]^2} + (1-\delta_{i\alpha})\left(C_{\alpha,6} - C_{\alpha,7}\left[n_s+\frac{1}{2}\right]k'_i \right)\left[n_s+\frac{1}{2}\right] \right] \dot{L}_i \right. \\
&\left. + \sum_{j=1}^{3}(1-\delta_{ij})\, C_{\alpha,5} n_j \frac{\partial f_j}{\partial L_j}\frac{\partial^2 \mathcal{H}'_{n_s}}{\partial k'_j \partial k'_i}\dot{L}_j \right\} \hat{e_\alpha},
\end{aligned} \tag{D.17}$$

where $C_{\alpha,5}$, $C_{\alpha,6}$ and $C_{\alpha,7}$ are defined in equations (D.14), (D.15) and (D.16). The force equation (D.17) vanishes for the **1D** case, which is an expected result. The reason is explained as follow: Recall that equation (D.4) reads

$$\sum_{i=1}^{3}\left[\left(\left[n_s+\frac{1}{2}\right]\hbar \right)^{-1} \frac{\partial \mathcal{H}'_{n_s}}{\partial k'_i} - \left\{ \sum_{i=1}^{3}\left[p'_i\right]^2 \right\}^{-1/2} cp'_i \right] dp'_i = 0.$$

For the **1D** case, the summation runs only once and the above expression simplifies to

$$\left[\left(\left[n_s+\frac{1}{2}\right]\hbar\right)^{-1}\frac{\partial\mathcal{H}'_{n_s}}{\partial k'_i}-c\right]dp'_i=0 \quad\rightarrow\quad \left(\left[n_s+\frac{1}{2}\right]\hbar\right)^{-1}\frac{\partial\mathcal{H}'_{n_s}}{\partial k'_i}-c=0.$$

This is a classic situation where the problem has been over specified. For the **3D** case, equation (D.4) is really a combination of two constraints, $\sum_{i=1}^{3}\left[p'_i\right]^2$ and $\mathcal{H}'_{n_s}$. For the **1D** case, there is only one constraint, $\mathcal{H}'_{n_s}$. Hence, equation (D.4) becomes an over specification. In order to avoid the problem caused by over specifications in this formulation, the one dimensional force expression can be obtained directly by differentiating equation (D.1) instead of using the above formulation for the three dimensional case. We have then for the force expression in **1D** case:

$$p'=\frac{1}{c}\mathcal{H}'_{n_s} \quad\rightarrow\quad \frac{dp'}{dt}=\frac{1}{c}\frac{\partial\mathcal{H}'_{n_s}}{\partial k'}\frac{dk'}{dt}=\frac{1}{c}\frac{\partial\mathcal{H}'_{n_s}}{\partial k'}\left[f\left(L\right)\frac{\partial k'}{\partial n}\dot{n}+n\frac{\partial f}{\partial L}\dot{L}\right].$$

For an isolated, non-driven systems,

$$\vec{\mathcal{F}}'=\frac{n}{c}\frac{\partial f}{\partial L}\frac{\partial\mathcal{H}'_{n_s}}{\partial k'}\dot{L}\hat{e}, \tag{D.18}$$

where $\vec{\mathcal{F}}'$ is the force expression in **1D** space. Here the subscript α of $\vec{\mathcal{F}}'_{\alpha}$ have been dropped for simplicity, since it is a one dimensional force.

D.2. Equations of Motion for the Driven Parallel Plates

Consider the one dimensional system of two parallel plates shown in Figure 3.10. Defining the boundary length $L_{i,\Re}$ as the magnitude of a vector $\hat{e_i}\left[\vec{L}_{\Re}\bullet\hat{e_i}\right]$, where $\Re$ denotes the region, the following relation is found from Figure 3.10,

$$\vec{L}_{\Re}=\vec{R}_{rp,\Re}-\vec{R}_{lp,\Re}=\sum_{i=1}^{3}\left[\vec{R}_{rp,\Re}\bullet\hat{e_i}-\vec{R}_{lp,\Re}\bullet\hat{e_i}\right]\hat{e_i}. \tag{D.19}$$

Hence, the velocity $d\vec{L}_{\Re}/dt$ is

$$\frac{d\vec{L}_{\Re}}{dt}=\frac{d\vec{R}_{rp,\Re}}{dt}-\frac{d\vec{R}_{lp,\Re}}{dt}=\sum_{i=1}^{3}\left[\frac{d\vec{R}_{rp,\Re}}{dt}\bullet\hat{e_i}-\frac{d\vec{R}_{lp,\Re}}{dt}\bullet\hat{e_i}\right]\hat{e_i} \tag{D.20}$$

and the corresponding component magnitude is given by

$$\dot{L}_{i,\Re}\equiv\frac{d\vec{L}_{\Re}}{dt}\bullet\hat{e_i}=\frac{d\vec{R}_{rp,\Re}}{dt}\bullet\hat{e_i}-\frac{d\vec{R}_{lp,\Re}}{dt}\bullet\hat{e_i}. \tag{D.21}$$

Substituting the result $\dot{L}_{i,\Re}$ of equation (D.21) for $\dot{L}_{\alpha}$ in the one dimensional dynamical force expression of equation (D.18),

$$\vec{\mathcal{F}}'_{\alpha,\Re}=\frac{n_{\alpha,\Re}}{c}\frac{\partial f_{\alpha,\Re}}{\partial L_{\alpha,\Re}}\frac{\partial\mathcal{H}'_{n_s,\Re}}{\partial k'_{\alpha,\Re}}\left[\frac{d\vec{R}_{rp,\Re}}{dt}\bullet\hat{e_\alpha}-\frac{d\vec{R}_{lp,\Re}}{dt}\bullet\hat{e_\alpha}\right]\hat{e_\alpha}, \tag{D.22}$$

where $\dot{L}_{i,\Re}\equiv\dot{L}_{\alpha}$ and $i\equiv\alpha$. The subscript $\Re$ denotes the corresponding quantities associated with the region $\Re=1,2,3$, e.g., $\mathcal{H}'_{n_s,\Re}$ denotes the field energy in region $\Re$. For simplicity, the following notational convention is adopted

$$\dot{R}_{a,b}=\frac{d\vec{R}_a}{dt}\bullet\hat{e}_b, \qquad \ddot{R}_{a,b}=\frac{d^2\vec{R}_a}{dt^2}\bullet\hat{e}_b,$$

$$g_{\alpha,\Re} = \frac{n_{\alpha,\Re}}{c}\left(\frac{\partial f_{\alpha,\Re}}{\partial L_{\alpha,\Re}}\right)\left(\frac{\partial \mathcal{H}'_{n_s,\Re}}{\partial k'_{\alpha,\Re}}\right). \tag{D.23}$$

The force expression of equation (D.22) is then rewritten as

$$\vec{\mathcal{F}'}_{\alpha,\Re} = g_{\alpha,\Re}\left[\dot{R}_{rp,\Re,\alpha} - \dot{R}_{lp,\Re,\alpha}\right]\hat{e_\alpha}, \tag{D.24}$$

Before writing down equations of motion for each plates illustrated in Figure 3.10, the associated center of mass point relative the the surface point vectors $\vec{R}_{rp,\Re,\alpha}$ for each plates needs to be determined. The center of mass point $\vec{R}_{rp,cm}$for plate labeled "right plate" in Figure 3.10 is related to the surface point vector $\vec{R}_{rp,\Re}$ through a relation

$$\vec{R}_{rp,cm}(t) = \vec{R}_{rp,\Re=2}(t) + \vec{R}_{rp,cm-\Re}(t),$$

where $\vec{R}_{rp,cm-\Re}(t) \equiv \vec{R}_{rp,cm-2}(t)$ is a displacement between surface and the center of mass point. The α component of the center of mass point $\vec{R}_{rp,cm}$ is then

$$R_{rp,cm,\alpha}(t) \equiv \hat{e_\alpha} \bullet \vec{R}_{rp,cm}(t) = \hat{e_\alpha} \bullet \vec{R}_{rp,2}(t) + \hat{e_\alpha} \bullet \vec{R}_{rp,cm-2}(t) = R_{rp,2,\alpha}(t) + R_{rp,cm-2,\alpha}(t). \tag{D.25}$$

The component of the center of mass point speed is given by

$$\dot{R}_{rp,cm,\alpha}(t) = \dot{R}_{rp,2,\alpha}(t) + \dot{R}_{rp,cm-2,\alpha}(t). \tag{D.26}$$

Similarly, for the plate labeled "left plate," the center of mass point is related to the surface vector point $\vec{R}_{lp,\Re=2}(t)$ by

$$\vec{R}_{lp,cm}(t) = \vec{R}_{lp,\Re=2}(t) - \vec{R}_{lp,cm-\Re}(t),$$

and the component along the direction $\hat{e_\alpha}$ is

$$R_{lp,cm,\alpha}(t) = R_{lp,2,\alpha}(t) - R_{lp,cm-2,\alpha}(t), \qquad \dot{R}_{lp,cm,\alpha}(t) = \dot{R}_{lp,2,\alpha}(t) - \dot{R}_{lp,cm-2,\alpha}(t). \tag{D.27}$$

Using the above center of mass relations, equations (D.25), (D.26) and (D.27), along with the force equation (D.24), the net force acting on a plate labeled "right plate" along the direction of $\hat{e_\alpha}$ in the configuration shown in Figure 3.10 is

$$m_{rp}\ddot{R}_{rp,cm,\alpha} = \left[\vec{\mathcal{F}'}_{\alpha,\Re=2} + \vec{\mathcal{F}'}_{\alpha,\Re=3}\right] \bullet \hat{e_\alpha}$$

or

$$\begin{aligned} m_{rp}\ddot{R}_{rp,cm,\alpha} = {} & g_{\alpha,2}\left[\dot{R}_{rp,cm,\alpha} - \dot{R}_{lp,cm,\alpha} - \dot{R}_{rp,cm-2,\alpha} - \dot{R}_{lp,cm-2,\alpha}\right] \\ & + g_{\alpha,3}\left[\dot{R}_{dpr,cm,\alpha} - \dot{R}_{rp,cm,\alpha} - \dot{R}_{dpr,cm-2,\alpha} - \dot{R}_{rp,cm-2,\alpha}\right] \end{aligned} \tag{D.28}$$

where m_{rp} is the mass of the "right plate." If the plate surface is not vibrating longitudinally along the direction of $\hat{e_\alpha}$, the displacements $R_{rp,cm-2,\alpha}$ and $R_{dpr,cm-2,\alpha}$ are constants; hence, $\dot{R}_{rp,cm-2,\alpha} = \dot{R}_{dpr,cm-2,\alpha} = 0$. For static surfaces, the above net force relation simplifies to

$$m_{rp}\ddot{R}_{rp,cm,\alpha} = s_{rp,2}g_{\alpha,2}\left[\dot{R}_{rp,cm,\alpha} - \dot{R}_{lp,cm,\alpha}\right] + s_{rp,3}g_{\alpha,3}\left[\dot{R}_{dpr,cm,\alpha} - \dot{R}_{rp,cm,\alpha}\right], \tag{D.29}$$

where $s_{rp,2}$ and $s_{rp,3}$ have been inserted for convenience due to the force sign convention to be set later. Similarly, for the plate labeled "left plate" in Figure 3.10, the net force relation along the direction of $\hat{e_\alpha}$ is

$$m_{lp}\ddot{R}_{lp,cm,\alpha}(t) = \left[\vec{\mathcal{F}'}_{\alpha,\beta,\Re=1} + \vec{\mathcal{F}'}_{\alpha,\beta,\Re=2}\right] \bullet \hat{e_\alpha}$$

or, for the case where plate surfaces do not have longitudinal vibrations,

$$m_{lp}\ddot{R}_{lp,cm,\alpha} = s_{lp,1}g_{\alpha,1}\left[\dot{R}_{lp,cm,\alpha} - \dot{R}_{dpl,cm,\alpha}\right] + s_{lp,2}g_{\alpha,2}\left[\dot{R}_{rp,cm,\alpha} - \dot{R}_{lp,cm,\alpha}\right], \tag{D.30}$$

where m_{lp} is a mass of "left plate" and the terms $s_{lp,1}$ and $s_{lp,2}$ have been inserted for convenience due to the force sign convention to be set later. We have now the two coupled differential equations,

$$m_{rp}\ddot{R}_{rp,cm,\alpha} + s_{rp,3}g_{\alpha,3}\dot{R}_{rp,cm,\alpha} - s_{rp,2}g_{\alpha,2}\dot{R}_{rp,cm,\alpha} + s_{rp,2}g_{\alpha,2}\dot{R}_{lp,cm,\alpha} = s_{rp,3}g_{\alpha,3}\dot{R}_{dpr,cm,\alpha},$$

$$m_{lp}\ddot{R}_{lp,cm,\alpha} + s_{lp,2}g_{\alpha,2}\dot{R}_{lp,cm,\alpha} - s_{lp,1}g_{\alpha,1}\dot{R}_{lp,cm,\alpha} - s_{lp,2}g_{\alpha,2}\dot{R}_{rp,cm,\alpha} = -s_{lp,1}g_{\alpha,1}\dot{R}_{dpl,cm,\alpha}.$$

Introducing the following definitions,

$$\begin{cases} \eta_1 = m_{rp}^{-1}\left[s_{rp,2}g_{\alpha,2} - s_{rp,3}g_{\alpha,3}\right], & \eta_2 = -s_{rp,2}g_{\alpha,2}m_{rp}^{-1} \\ \eta_3 = m_{lp}^{-1}\left[s_{lp,1}g_{\alpha,1} - s_{lp,2}g_{\alpha,2}\right], & \eta_4 = s_{lp,2}g_{\alpha,2}m_{lp}^{-1}, \\ \xi_{rp} = s_{rp,3}g_{\alpha,3}m_{rp}^{-1}\dot{R}_{dpr,cm,\alpha}, & \xi_{lp} = -s_{lp,1}g_{\alpha,1}m_{lp}^{-1}, \\ R_1 = R_{rp,cm,\alpha}, & R_2 = R_{lp,cm,\alpha}, \end{cases} \tag{D.31}$$

the coupled differential equations are rewritten as

$$\ddot{R}_1 - \eta_1\dot{R}_1 - \eta_2\dot{R}_2 = \xi_{rp}, \qquad \ddot{R}_2 - \eta_3\dot{R}_2 - \eta_4\dot{R}_1 = \xi_{lp}. \tag{D.32}$$

The equations of motion shown in equation (D.32) are a system of two linear second-order inhomogeneous differential equations. In order to rewrite the coupled linear inhomogeneous differential equation (D.32) into a set of first-order linear inhomogeneous equation, a set of new variables are defined first,

$$\begin{cases} \dot{R}_1 = R_3, \qquad \dot{R}_2 = R_4, \\ \dot{R}_3 = \ddot{R}_1 = \xi_{rp} + \eta_1\dot{R}_1 + \eta_2\dot{R}_2 = \xi_{rp} + \eta_1 R_3 + \eta_2 R_4, \\ \dot{R}_4 = \ddot{R}_2 = \xi_{lp} + \eta_3\dot{R}_2 + \eta_4\dot{R}_1 = \xi_{lp} + \eta_3 R_4 + \eta_4 R_3. \end{cases} \tag{D.33}$$

Using these new variables defined in equation (D.33), equation (D.32) can be cast into first-order inhomogeneous equation in matrix form,

$$\dot{\vec{R}} = \widetilde{M}\cdot\vec{R} + \vec{\xi} \quad \rightarrow \quad \begin{bmatrix} \dot{R}_1 \\ \dot{R}_2 \\ \dot{R}_3 \\ \dot{R}_4 \end{bmatrix} = \begin{bmatrix} 0 & 0 & 1 & 0 \\ 0 & 0 & 0 & 1 \\ 0 & 0 & \eta_1 & \eta_2 \\ 0 & 0 & \eta_4 & \eta_3 \end{bmatrix} \cdot \begin{bmatrix} R_1 \\ R_2 \\ R_3 \\ R_4 \end{bmatrix} + \begin{bmatrix} 0 \\ 0 \\ \xi_{rp} \\ \xi_{lp} \end{bmatrix}.$$

The above first-order inhomogeneous equation is equivalent to

$$R_1 = \int_{t_0}^{t} R_3 dt', \qquad R_2 = \int_{t_0}^{t} R_4 dt', \tag{D.34}$$

and

$$\underbrace{\begin{bmatrix} \dot{R}_3 \\ \dot{R}_4 \end{bmatrix}}_{\dot{\vec{R}}_\eta} = \underbrace{\begin{bmatrix} \eta_1 & \eta_2 \\ \eta_4 & \eta_3 \end{bmatrix}}_{\widetilde{M}_\eta} \cdot \underbrace{\begin{bmatrix} R_3 \\ R_4 \end{bmatrix}}_{\vec{R}_\eta} + \underbrace{\begin{bmatrix} \xi_{rp} \\ \xi_{lp} \end{bmatrix}}_{\vec{\xi}}. \tag{D.35}$$

For the homogeneous system

$$\underbrace{\begin{bmatrix} \dot{R}_3 \\ \dot{R}_4 \end{bmatrix}}_{\dot{\vec{R}}_\eta} = \underbrace{\begin{bmatrix} \eta_1 & \eta_2 \\ \eta_4 & \eta_3 \end{bmatrix}}_{\widetilde{M}_\eta} \cdot \underbrace{\begin{bmatrix} R_3 \\ R_4 \end{bmatrix}}_{\vec{R}_\eta}, \tag{D.36}$$

the eigenvalues are found from the root of the characteristic equation

$$\det\left(\lambda\widetilde{I} - \widetilde{M}_\eta\right) \equiv \lambda^2 - \left[\eta_1 + \eta_3\right]\lambda + \eta_1\eta_3 - \eta_2\eta_4 = 0.$$

The two eigenvalues are

$$\lambda_3 = \frac{\eta_1+\eta_3}{2} + \left\{\frac{1}{4}\left[\eta_1-\eta_3\right]^2 + \eta_2\eta_4\right\}^{1/2}, \qquad \lambda_4 = \frac{\eta_1+\eta_3}{2} - \left\{\frac{1}{4}\left[\eta_1-\eta_3\right]^2 + \eta_2\eta_4\right\}^{1/2}. \tag{D.37}$$

And, the two corresponding eigenvectors are found to be

$$\vec{R}_{\lambda_3} = \grave{R}_4 \begin{bmatrix} \frac{\eta_2}{\lambda_3-\eta_1} \\ 1 \end{bmatrix}, \qquad \grave{R}_4 = \left\{\left[\frac{\eta_2}{\lambda_3-\eta_1}\right]^2 + 1\right\}^{-1/2}, \tag{D.38}$$

and

$$\vec{R}_{\lambda_4} = \grave{R}_3 \begin{bmatrix} 1 \\ \frac{\lambda_4-\eta_1}{\eta_2} \end{bmatrix}, \qquad \grave{R}_3 = \left\{1 + \left[\frac{\lambda_4-\eta_1}{\eta_2}\right]^2\right\}^{-1/2}, \tag{D.39}$$

where $\grave{R}_3$ and $\grave{R}_4$ are the normalization constants. The solutions for the matrix equation (D.36) are then

$$\vec{\phi}_{\lambda_3} = \vec{R}_{\lambda_3}\exp\left(\lambda_3 t\right) = \grave{R}_4 \begin{bmatrix} \frac{\eta_2}{\lambda_3-\eta_1}\exp\left(\lambda_3 t\right) \\ \exp\left(\lambda_3 t\right) \end{bmatrix}, \qquad \vec{\phi}_{\lambda_4} = \vec{R}_{\lambda_4}\exp\left(\lambda_4 t\right) = \grave{R}_3 \begin{bmatrix} \exp\left(\lambda_4 t\right) \\ \frac{\lambda_4-\eta_1}{\eta_2}\exp\left(\lambda_4 t\right) \end{bmatrix}.$$

The fundamental matrix solution $\widetilde{\Phi}\left(t\right) = \left[\vec{\phi}_{\lambda_3}\left(t\right), \vec{\phi}_{\lambda_4}\left(t\right)\right]$ is given by

$$\widetilde{\Phi}\left(t\right) = \begin{bmatrix} \frac{\eta_2}{\lambda_3-\eta_1}\grave{R}_4\exp\left(\lambda_3 t\right) & \grave{R}_3\exp\left(\lambda_4 t\right) \\ \grave{R}_4\exp\left(\lambda_3 t\right) & \frac{\lambda_4-\eta_1}{\eta_2}\grave{R}_3\exp\left(\lambda_4 t\right) \end{bmatrix}. \tag{D.40}$$

The fundamental matrix solution $\widetilde{\Phi}\left(t\right)$ has an inverse

$$\widetilde{\Phi}^{-1}\left(t\right) = \frac{1}{\det\left(\widetilde{\Phi}\left(t\right)\right)} \begin{bmatrix} \frac{\lambda_4-\eta_1}{\eta_2}\grave{R}_3\exp\left(\lambda_4 t\right) & -\grave{R}_3\exp\left(\lambda_4 t\right) \\ -\grave{R}_4\exp\left(\lambda_3 t\right) & \frac{\eta_2}{\lambda_3-\eta_1}\grave{R}_4\exp\left(\lambda_3 t\right) \end{bmatrix},$$

where

$$\det\left(\widetilde{\Phi}\left(t\right)\right) = \left[\frac{\lambda_4-\eta_1}{\lambda_3-\eta_1} - 1\right]\grave{R}_3\grave{R}_4\exp\left(\left[\lambda_3+\lambda_4\right]t\right). \tag{D.41}$$

The principal matrix solution $\widetilde{\Psi}\left(t,t_0\right) = \widetilde{\Phi}\left(t\right)\cdot\widetilde{\Phi}^{-1}\left(t_0\right)$ of equation (D.35) becomes then

$$\widetilde{\Psi}\left(t,t_0\right) = \frac{1}{\det\left(\widetilde{\Phi}\left(t_0\right)\right)} \begin{bmatrix} \psi_{11}\left(t,t_0\right) & \psi_{12}\left(t,t_0\right) \\ \psi_{21}\left(t,t_0\right) & \psi_{22}\left(t,t_0\right) \end{bmatrix}, \tag{D.42}$$

where

$$\psi_{11}(t,t_0) = \grave{R}_3\grave{R}_4\left[\frac{\lambda_4-\eta_1}{\lambda_3-\eta_1}\exp(\lambda_3 t+\lambda_4 t_0)-\exp(\lambda_4 t+\lambda_3 t_0)\right], \tag{D.43}$$

$$\psi_{12}(t,t_0) = \grave{R}_3\grave{R}_4\left[\frac{\eta_2}{\lambda_3-\eta_1}\exp(\lambda_4 t+\lambda_3 t_0)-\frac{\eta_2}{\lambda_3-\eta_1}\exp(\lambda_3 t+\lambda_4 t_0)\right], \tag{D.44}$$

$$\psi_{21}(t,t_0) = \grave{R}_3\grave{R}_4\left[\frac{\lambda_4-\eta_1}{\eta_2}\exp(\lambda_3 t+\lambda_4 t_0)-\frac{\lambda_4-\eta_1}{\eta_2}\exp(\lambda_4 t+\lambda_3 t_0)\right], \tag{D.45}$$

$$\psi_{22}(t,t_0) = \grave{R}_3\grave{R}_4\left[\frac{\lambda_4-\eta_1}{\lambda_3-\eta_1}\exp(\lambda_4 t+\lambda_3 t_0)-\exp(\lambda_3 t+\lambda_4 t_0)\right]. \tag{D.46}$$

The inverse of principal matrix solution $\widetilde{\Psi}(t,t_0)$ is

$$\widetilde{\Psi}^{-1}(t,t_0) = \frac{1}{\det\left(\widetilde{\Psi}(t,t_0)\right)\det\left(\widetilde{\Phi}(t_0)\right)}\begin{bmatrix}\psi_{22}(t,t_0) & -\psi_{12}(t,t_0)\\ -\psi_{21}(t,t_0) & \psi_{11}(t,t_0)\end{bmatrix}, \tag{D.47}$$

where

$$\det\left(\widetilde{\Psi}(t,t_0)\right) = \left[\det\left(\widetilde{\Phi}(t_0)\right)\right]^{-2}\left[\psi_{11}(t,t_0)\,\psi_{22}(t,t_0)-\psi_{12}(t,t_0)\,\psi_{21}(t,t_0)\right]. \tag{D.48}$$

Using a variation-of-parameters technique, the solution to the inhomogeneous first-order differential equation (D.35) is

$$\vec{R}_\eta(t) = \widetilde{\Psi}(t,t_0)\cdot\vec{R}_\eta(t_0)+\widetilde{\Psi}(t,t_0)\cdot\int_{t_0}^{t}\widetilde{\Psi}^{-1}(t',t_0)\cdot\vec{\xi}(t')\,dt',$$

where it is understood the multiplications are that of the matrix operations. Substituting into this integral equation the results for $\vec{R}_\eta(t)$, $\vec{\xi}(t')$, $\widetilde{\Psi}(t)$ and $\widetilde{\Psi}^{-1}(t')$ given by equations (D.35), (D.42) and (D.47),

$$\begin{bmatrix}R_3(t)\\ R_4(t)\end{bmatrix} = \frac{1}{\det\left(\widetilde{\Phi}(t_0)\right)}\left(\begin{bmatrix}\psi_{11}(t,t_0) & \psi_{12}(t,t_0)\\ \psi_{21}(t,t_0) & \psi_{22}(t,t_0)\end{bmatrix}\cdot\begin{bmatrix}R_3(t_0)\\ R_4(t_0)\end{bmatrix}+\begin{bmatrix}\psi_{11}(t,t_0) & \psi_{12}(t,t_0)\\ \psi_{21}(t,t_0) & \psi_{22}(t,t_0)\end{bmatrix}\right.$$
$$\left.\cdot\int_{t_0}^{t}\left\{\frac{1}{\det\left(\widetilde{\Psi}(t',t_0)\right)}\begin{bmatrix}\psi_{22}(t',t_0) & -\psi_{12}(t',t_0)\\ -\psi_{21}(t',t_0) & \psi_{11}(t',t_0)\end{bmatrix}\cdot\begin{bmatrix}\xi_{rp}(t')\\ \xi_{lp}(t')\end{bmatrix}\right\}dt'\right)$$

or

$$\begin{aligned}R_3(t) = \frac{1}{\det\left(\widetilde{\Phi}(t_0)\right)}&\left\{\psi_{11}(t,t_0)\,R_3(t_0)+\psi_{12}(t,t_0)\,R_4(t_0)+\frac{\psi_{11}(t,t_0)}{\det\left(\widetilde{\Phi}(t_0)\right)}\right.\\ &\times\left[\int_{t_0}^{t}\frac{\psi_{22}(t',t_0)\,\xi_{rp}(t')}{\det\left(\widetilde{\Psi}(t',t_0)\right)}dt'-\int_{t_0}^{t}\frac{\psi_{12}(t',t_0)\,\xi_{lp}(t')}{\det\left(\widetilde{\Psi}(t',t_0)\right)}dt'\right]+\frac{\psi_{12}(t,t_0)}{\det\left(\widetilde{\Phi}(t_0)\right)}\\ &\left.\times\left[\int_{t_0}^{t}\frac{\psi_{11}(t',t_0)\,\xi_{lp}(t')}{\det\left(\widetilde{\Psi}(t',t_0)\right)}dt'-\int_{t_0}^{t}\frac{\psi_{21}(t',t_0)\,\xi_{rp}(t')}{\det\left(\widetilde{\Psi}(t',t_0)\right)}dt'\right]\right\},\end{aligned} \tag{D.49}$$

$$R_4(t) = \frac{1}{\det\left(\widetilde{\Phi}(t_0)\right)}\left\{\psi_{21}(t,t_0)\,R_3(t_0) + \psi_{22}(t,t_0)\,R_4(t_0) + \frac{\psi_{21}(t,t_0)}{\det\left(\widetilde{\Phi}(t_0)\right)}\right.$$
$$\times\left[\int_{t_0}^{t}\frac{\psi_{22}(t',t_0)\,\xi_{rp}(t')}{\det\left(\widetilde{\Psi}(t',t_0)\right)}dt' - \int_{t_0}^{t}\frac{\psi_{12}(t',t_0)\,\xi_{lp}(t')}{\det\left(\widetilde{\Psi}(t',t_0)\right)}dt'\right] + \frac{\psi_{22}(t,t_0)}{\det\left(\widetilde{\Phi}(t_0)\right)}$$
$$\left.\times\left[\int_{t_0}^{t}\frac{\psi_{11}(t',t_0)\,\xi_{lp}(t')}{\det\left(\widetilde{\Psi}(t',t_0)\right)}dt' - \int_{t_0}^{t}\frac{\psi_{21}(t',t_0)\,\xi_{rp}(t')}{\det\left(\widetilde{\Psi}(t',t_0)\right)}dt'\right]\right\}. \tag{D.50}$$

It is noted from equation (D.34), $R_3(t_0)$ and $R_4(t_0)$ are initial speeds,

$$\dot{R}_{rp,cm,\alpha}(t_0) \equiv \dot{R}_1(t_0) = R_3(t_0), \qquad \dot{R}_{lp,cm,\alpha}(t_0) \equiv \dot{R}_2(t_0) = R_4(t_0).$$

Hence,

$$\dot{R}_{rp,cm,\alpha}(t) = \left[\frac{\lambda_4(;t_0)-\eta_1(;t_0)}{\lambda_3(;t_0)-\eta_1(;t_0)} - 1\right]^{-1}\frac{\psi_{11}(t,t_0)\,\dot{R}_{rp,cm,\alpha}(t_0) + \psi_{12}(t,t_0)\,\dot{R}_{lp,cm,\alpha}(t_0)}{\exp\left(\left[\lambda_3(;t_0)+\lambda_4(;t_0)\right]t_0\right)}$$
$$+\psi_{11}(t,t_0)\int_{t_0}^{t}\frac{\psi_{22}(t',t_0)\,\xi_{rp}(t') - \psi_{12}(t',t_0)\,\xi_{lp}(t')}{\psi_{11}(t',t_0)\,\psi_{22}(t',t_0) - \psi_{12}(t',t_0)\,\psi_{21}(t',t_0)}dt' + \psi_{12}(t,t_0)$$
$$\times\int_{t_0}^{t}\frac{\psi_{11}(t',t_0)\,\xi_{lp}(t') - \psi_{21}(t',t_0)\,\xi_{rp}(t')}{\psi_{11}(t',t_0)\,\psi_{22}(t',t_0) - \psi_{12}(t',t_0)\,\psi_{21}(t',t_0)}dt', \tag{D.51}$$

$$\dot{R}_{lp,cm,\alpha}(t) = \left[\frac{\lambda_4(;t_0)-\eta_1(;t_0)}{\lambda_3(;t_0)-\eta_1(;t_0)} - 1\right]^{-1}\frac{\psi_{21}(t,t_0)\,\dot{R}_{rp,cm,\alpha} + \psi_{22}(t,t_0)\,\dot{R}_{lp,cm,\alpha}(t_0)}{\exp\left(\left[\lambda_3(;t_0)+\lambda_4(;t_0)\right]t_0\right)}$$
$$+\psi_{21}(t,t_0)\int_{t_0}^{t}\frac{\psi_{22}(t',t_0)\,\xi_{rp}(t') - \psi_{12}(t',t_0)\,\xi_{lp}(t')}{\psi_{11}(t',t_0)\,\psi_{22}(t',t_0) - \psi_{12}(t',t_0)\,\psi_{21}(t',t_0)}dt' + \psi_{22}(t,t_0)$$
$$\times\int_{t_0}^{t}\frac{\psi_{11}(t',t_0)\,\xi_{lp}(t') - \psi_{21}(t',t_0)\,\xi_{rp}(t')}{\psi_{11}(t',t_0)\,\psi_{22}(t',t_0) - \psi_{12}(t',t_0)\,\psi_{21}(t',t_0)}dt', \tag{D.52}$$

where substitutions have been made for the determinants $\det\left(\widetilde{\Phi}(t_0)\right)$ and $\det\left(\widetilde{\Psi}(t',t_0)\right)$ from equations (D.41) and (D.48). It is to be understood that the notation $(;t_0)$ on η_1, λ_3 and λ_4 implies implicit time dependence for these terms. Finally, integration of both sides of equations (D.51) and (D.52) with respect to time gives the results

$$R_{rp,cm,\alpha}(t) = \left[\frac{\lambda_4(;t_0)-\eta_1(;t_0)}{\lambda_3(;t_0)-\eta_1(;t_0)} - 1\right]^{-1}\int_{t_0}^{t}\left[\frac{\psi_{11}(\tau,t_0)\,\dot{R}_{rp,cm,\alpha}(t_0) + \psi_{12}(\tau,t_0)\,\dot{R}_{lp,cm,\alpha}(t_0)}{\exp\left(\left[\lambda_3(;t_0)+\lambda_4(;t_0)\right]t_0\right)}\right.$$
$$+\psi_{11}(\tau,t_0)\int_{t_0}^{\tau}\frac{\psi_{22}(t',t_0)\,\xi_{rp}(t') - \psi_{12}(t',t_0)\,\xi_{lp}(t')}{\psi_{11}(t',t_0)\,\psi_{22}(t',t_0) - \psi_{12}(t',t_0)\,\psi_{21}(t',t_0)}dt' + \psi_{12}(\tau,t_0)$$
$$\left.\times\int_{t_0}^{\tau}\frac{\psi_{11}(t',t_0)\,\xi_{lp}(t') - \psi_{21}(t',t_0)\,\xi_{rp}(t')}{\psi_{11}(t',t_0)\,\psi_{22}(t',t_0) - \psi_{12}(t',t_0)\,\psi_{21}(t',t_0)}dt'\right]d\tau + R_{rp,cm,\alpha}(t_0), \tag{D.53}$$

$$R_{lp,cm,\alpha}(t) = \left[\frac{\lambda_4(;t_0)-\eta_1(;t_0)}{\lambda_3(;t_0)-\eta_1(;t_0)} - 1\right]^{-1}\int_{t_0}^{t}\left[\frac{\psi_{21}(\tau,t_0)\,\dot{R}_{rp,cm,\alpha}(t_0) + \psi_{22}(\tau,t_0)\,\dot{R}_{lp,cm,\alpha}(t_0)}{\exp\left(\left[\lambda_3(;t_0)+\lambda_4(;t_0)\right]t_0\right)}\right.$$
$$+\psi_{21}(\tau,t_0)\int_{t_0}^{\tau}\frac{\psi_{22}(t',t_0)\,\xi_{rp}(t') - \psi_{12}(t',t_0)\,\xi_{lp}(t')}{\psi_{11}(t',t_0)\,\psi_{22}(t',t_0) - \psi_{12}(t',t_0)\,\psi_{21}(t',t_0)}dt' + \psi_{22}(\tau,t_0)$$
$$\left.\times\int_{t_0}^{\tau}\frac{\psi_{11}(t',t_0)\,\xi_{lp}(t') - \psi_{21}(t',t_0)\,\xi_{rp}(t')}{\psi_{11}(t',t_0)\,\psi_{22}(t',t_0) - \psi_{12}(t',t_0)\,\psi_{21}(t',t_0)}dt'\right]d\tau + R_{lp,cm,\alpha}(t_0), \tag{D.54}$$

where the terms ψ_{11}, ψ_{12}, ψ_{21} and ψ_{22} are defined in equations (D.43), (D.44), (D.45) and (D.46). The remaining integrations are straightforward; hence, their explicit forms are not shown.

As a closing remark of this section, one may argue that for the static case, $\dot{R}_{rp,cm,\alpha}(t_0)$ and $\dot{R}_{lp,cm,\alpha}(t_0)$ must be zero because the conductors seem to be fixed in position. This argument is flawed for any wall totally fixed in position upon impact would require an infinite amount of energy. One has to consider the conservation of momentum simultaneously. The wall has to have moved by the amount $\triangle R_{wall} = \dot{R}_{wall}\triangle t$, where $\triangle t$ is the total duration of impact, and $\dot{R}_{wall}$ is calculated from the momentum conservation and it is non-zero. The same argument can be applied to the apparatus shown in Figure 3.10. For that system

$$\|\vec{p}_{virtual-photon}\| = \frac{1}{c}\mathcal{H}'_{n_s,\Re}(t_0), \qquad \begin{cases} \dot{R}_{rp,cm,\alpha}(t_0) = \left\|\dot{\vec{R}}_{lp,3}(t_0) + \dot{\vec{R}}_{rp,2}(t_0)\right\|, \\ \dot{R}_{lp,cm,\alpha}(t_0) = \left\|\dot{\vec{R}}_{rp,1}(t_0) + \dot{\vec{R}}_{lp,2}(t_0)\right\| \end{cases}$$

or, for simplicity, assuming impact without any angle,

$$\dot{R}_{rp,cm,\alpha}(t_0) = \frac{2}{m_{rp}c}\left\|\mathcal{H}'_{n_s,3}(t_0) - \mathcal{H}'_{n_s,2}(t_0)\right\|, \qquad \dot{R}_{lp,cm,\alpha}(t_0) = \frac{2}{m_{lp}c}\left\|\mathcal{H}'_{n_s,1}(t_0) - \mathcal{H}'_{n_s,2}(t_0)\right\|,$$

where the difference under the magnitude symbol implies that the energies from different regions act to counteract each other.

E. Extended List of References

These are the additional references pertaining to the Casimir effect which have not been explicitly used in this thesis. Nonetheless, these references were listed here to provide further information to those with possible research interest in the field of physics concerning the Casimir phenomenon.

Larry Spruch, “Long-Range Casimir Interactions,” Science 272, 1452-1455 (1996).

Peter W. Milonni and Mei-Li Shih, “Casimir Forces,” Contemporary Physics 33, No. 5, 313-322 (1992).

I. J. R. Aitchison, “Nothing’s plenty: The Vacuum in Modern Quantum Field Theory,” Contemporary Physics 26, No. 4, 333-391 (1985).

M. H. Wallis, “Essay Review: Field Theorists Strike Back—Stochastic Electrodynamics,” Contemporary Physics 39, 483-486 (1998).

R. Weigand and J. M. Guerra, “The Vacuum Field Energy in a Constant Volume Cavity,” European J. Phys. 18, 40-42 (1997).

E. Elizalde and A. Romeo, “Essentials of the Casimir Effect and its Computation,” Am. J. Phys. 59, No. 8, 711-719 (1991).

V. M. Mostepanenko and N. N. Trunov, “The Casimir Effect and its Applications,” Oxford (1997).

G. Barton, “New Aspects of the Casimir Effect: Fluctuations and Radiative Reaction,” Advances in Atomic and Molecular Physics, Suppl. 2, P. R. Berman, ed., Academic Press, 425-458, New York (1994).

Marc-Thierry Jaekel and Serge Reynaud, “Movement and Fluctuations of the Vacuum,” Rep. Prog. Physics 60, 863-887 (1997).

I. E. Dzyaloshinskii, E. M. Lifshitz, and L. P. Pitaevskii, “The General Theory of van der Waals Forces,” Advances in Physics 10, 165-209 (1961).

G. Bressi, G. Garugno, R. Onofrio, and G. Ruoso, “Measurement of the Casimir Force Between Parallel Metallic Surfaces,” Phys. Rev. Lett. 88, 041804 (2002).

T. Ederth, “Template-stripped Gold Surfaces with 0.4-nm RMS Roughness Suitable for Force Measurements: Application to the Casimir Force in the 20-100-nm Range,” Phys. Rev. A 62, 062104 (2000).

M. Bordag, B. Geyer, G. L. Klimchitskaya and V. M. Mostepanenko, “Stronger Constraints for Nanometer Scale Yukawa-type Hypothetical Interactions the new Measurement of the Casimir Force,” Phys. Rev. D 60, 055004 (1999).

V. B. Svetovoy and M. V. Lokhanin, “Precise Calculation of the Casimir Force Between Gold Surfaces,” Mod. Phys. Lett. A 15, 1437-1444 (2000).

F. Chen, U. Mohideen, G. L. Klimchitskaya and V. M. Mostepanenko, “Demonstration of the Lateral Casimir Force,” Phys. Rev. Lett. 88, 101801 (2002).

M. Bordag, B. Geyer, G. L. Klimchitskaya and V. M. Mostepanenko, "Constraints for Hypothetical Interactions from a Recent Demonstration of the Casimir Force and Some Possible Improvements," Phys. Rev. D 58 (1998).

G. L. Klimchitskaya, Anushree Roy, U. Mohideen, and V. M. Mostepanenko, "Complete Roughness and Conductivity Corrections for Casimir Force Measurements," Phys. Rev. A 60, 3487-3495 (1999).

V. B. Bezerra, G. L. Klimchitskaya, and V. M. Mostepanenko, "Higher-order Conductivity Corrections to the Casimir Force," Phys. Rev. A 62, 014012 (2000).

T. Emig, A. Hanke, R. Golestanian, and M. Kardar, "Probing the Strong Boundary Shape Dependence of the Casimir Force," Phys. Rev. Lett. 87, 260402 (2001).

R. Balian and B. Duplantier, "Electromagnetic Waves Near Perfect Conductors. I. Multiple Scattering Expansions. Distribution of Modes," Annals of Physics 104, 300-335, New York (1977).

R. Balian and B. Duplantier, "Electromagnetic Waves Near Perfect Conductors. II. Casimir Effect," Annals of Physics 112, 165-208, New York (1978).

M. Bordag and J. Lindig, "Radiative Corrections to the Casimir Force on a Sphere," Phys. Rev. D 58, 1-16 (1998).

V. Hushwater, "Repulsive Casimir Force as a Result of Vacuum Radiation Pressure," American Journal of Physics 65, 381-384 (1997).

Martin Schaden, Larry Spruch, and Fei Zhou, "Unified Treatment of Some Casimir Energies and Lamb Shifts: A Dielectric Between Two Ideal Conductors," Phys. Rev. A 57, 1108-1120 (1998).

Martin Schaden and Larry Spruch, "Infinity-free Semiclassical Evaluation of Casimir Effects," Phys. Rev. A 58, 935-953 (1998).

A. Bulgac and A. Wirzba, "Casimir Interaction Among Objects Immersed in a Fermionic Environment," Phys. Rev. Lett. 87 (2001).

V. B. Bezerra, G. L. Klimchitskaya, and C. Romero, "Casimir Force Between a Flat Plate and a Spherical Lens: Application to the Result of a New Experiment," Mod. Phys. Lett. A 12, 2613-2622 (1997).

V. B. Bezerra, G. L. Klimchitskaya, and C. Romero, "Surface Roughness Contribution to the Casimir Interaction Between an Isolated Atom and a Cavity Wall," Phys. Rev. A 61 (2000).

C. Genet, A. Lambrecht, and S. Reynaud, "Correlation Between Plasma and Temperature Corrections to the Casimir Force," Int. J. Mod. Phys. A 17, 761-766 (2002).

J. Feinberg, A. Mann, M. Revzen, "Casimir Effect: The Classical Limit," Annals of Physics 288, 103, New York (2001).

L. Spruch, "Classical Casimir Interactions of Some Simple Systems at Very High Temperature," Phys. Rev. A 66, 022103 (2002).

M. Schaden and L. Spruch, "Classical Casimir Effect: The Interaction of Ideal Parallel Walls at a Finite Temperature," Phys. Rev. A 65, 034101 (2002).

M. Schaden and L. Spruch, "Semiclassical Casimir Energies at Finite Temperature," Phys. Rev. A 65, 022108 (2002).

M. Bostrom, J. J. Longdell, and B. W. Ninham, "Atom-atom Interactions at and Between Metal Surfaces at Nonzero Temperature," Phys. Rev. A 64, 062702 (2001).

G. Barton, "Perturbative Casimir Shifts of Nondispersive Spheres at Finite Temperature," Phys. Rev. A 64, 032103 (2001).

G. Barton, "Long-Range Casimir-Polder-Feinberg-Sucher Intermolecular Potential at Nonzero Temperature," Phys. Rev. A 64, 032102 (2001).

G. L. Klimchitskaya and V. M. Mostepanenko, "Investigation of the Temperature Dependence of the Casimir Force Between Real Metals," Phys. Rev. A 63, 062108 (2001).

M. Bordag, B. Geyer, G. L. Klimchitskaya, and V. M. Mostepanenko, "Casimir Force at Both Nonzero Temperature and Finite Conductivity," Phys. Rev. Lett. 85, 503-506 (2000).

V. B. Svetovoy and M. V. Lokhanin, "Linear Temperature Correction to the Casimir Force," Phys. Lett. A 280, 177-181 (2001).

H. Wennerstrom, J. Daicic, and B. W. Ninham, "Temperature Dependence of Atom-Atom Interactions," Phys. Rev. A 60, 2581-2584 (1999).

C. Genet, A. Lambrecht, and S. Reynaud, "Temperature Dependence of the Casimir Effect Between Metallic Mirrors," Phys. Rev. A 62, 012110 (2000).

G. H. Goedecke and R. C. Wood, "Casimir-Polder Interaction at Finite Temperature," Phys. Rev. A 60, 2577-2580 (1999).

B. W. Ninham and J. Daicic, "Lifshitz Theory of Casimir Forces at Finite Temperature," Phys. Rev. A 57, 1870-1880 (1998).

Ramin Golestanian and Mehran Kardar, "Path-Integral Approach to the Dynamical Casimir Effect with Fluctuating Boundaries," Phys. Rev. A 58, 1713-1722 (1998).

Diego A. R. Dalvit and Francisco D. Mazzitelli, "Renormalization-Group Approach to the Dynamical Casimir Effect," Phys. Rev. A 57, 2113-2119 (1998).

Diego A. R. Dalvit and P. A. Maia Neto, "Decoherence via the Dynamical Casimir Effect," Phys. Rev. Lett. 84, 798-801 (2000).

P. A. Maia Neto and D. A. R. Dalvit, "Radiation Pressure as a Source of Decoherence," Phys. Rev. A 62, 042103 (2000).

S. Liberati, F. Belgiorno, M. Visser, D. W. Sciama, "Sonoluminescense as a QED Vacuum Effect: Probing Schwinger's Proposal," arxiv.org, quant-ph/9805031.

G. Plunien, R. Schutzhold, and G. Soff, "Dynamical Casimir Effect at Finite Temperature," Phys. Rev. Lett. 84, 798-801882-1885 (2000).

R. Matloob, "Casimir effect between two dielectric slabs," Phys. Rev. A 60, 3421-3428 (1999).

R. Matloob, A. Keshavarz, and D. Sedighi, "Casimir effect for two lossy dispersive dielectric slabs," Phys. Rev. A 60, 3410-3420 (1999).

K. D. Olum, "Superluminal travel requires negative energies," Phys. Rev. Lett. 81, 3567-3570 (1998).

C. L. Adler and N. M. Lawandy, "Retarded dispersion forces in periodic dielectric media," Phys. Rev. Lett. 66, 2617-2620 (1991).

L. H. Ford, "Casimir force between a dielectric sphere and a wall: A model for amplification of vacuum fluctuations," Phys. Rev. A 58, 4279-4286 (1998).

I. Brevik, M. Lygren, and V. N. Marachevsky, "Casimir-Polder effect for a perfectly conducting wedge," Annals of Physics 267, 134-42 (1998).

S. Leseduarte and August Romeo, "Complete zeta-function approach to the electromagnetic Casimir effect for sphere and circles," Annals of Physics 250, 448-484 (1996).

R. Blanco, K. Dechoum, H. M. Franca, and E. Santos, "Casimir interaction between a microscopic dipole oscillator and a macroscopic solenoid," Phys. Rev. A 57, 724-730 (1998).

Jens O. Andersen, "Energy level shift in two-dimensional hydrogen atoms near a metallic rod," Phys. Rev. Lett. A 180, 203-207 (1993).

M. J. Jamieson, G. W. F. Drake, and A. Dalgarno, "Retarded dipole-dipole dispersion interaction potential for helium," Phys. Rev. A 51, 3358-3361 (1995).

Fei Luo, Geunsik Kim, George C. McBane, Clayton F. Giese, and W. Ronald Gentry, "Influence of retardation on the vibrational wave function and binding energy of the helium dimer," Journal of Chemical Physics 98, 9687 (1993).

P. Kharchenko, J. F. Babb, and A. Dalgarno, "Long-range interaction of sodium atoms," Phys. Rev. A 55, 3566-3572 (1997).

S. Al-Awfi and M. Babiker, "Atom dynamics between conducting plates," Phys. Rev. A 58, 2274-2281 (1998).

U. Ritschel, and M. Gerwinski, "Casimir forces at tricritical points: theory and possible experiments," Physica A 243, 362-7 (1997).

C. H. Story, N. E. Rothery, and E. A. Hessels, "Precision Separated-Oscillatory-Field Measurement of the $n = 10^+ F_{3^-}^+ G_4$ Interval in Helium: A Precision Test of Long-Range Relativistic, Radiative, and Retardation Effects," Phys. Rev. Lett. 75, 3249-3252 (1995).

Nelson E. Claytor, E. A. Hessels, and S. R. Lundeen, "Fast-beam measurements of the 10D-10F fine-structure intervals in helium," Phys. Rev. A 52, 165-177 (1995).

Bibliography

[1] J. D. Jackson, "Classical Electrodynamics, Third Edition," John Wiley & Sons, Inc., U.S.A. (1999).

[2] H. B. G. Casimir and D. Polder, "The Influence of Retardation on the London-van der Waals Forces," Phys. Rev. 73, 360-372 (1948).

[3] H. B. G. Casimir, "On the Attraction Between Two Perfectly Conducting Plates," Proc. Kon. Ned. Akad. Wetenschap 51, 793 (1948).

[4] Timothy H. Boyer, "Quantum Electromagnetic Zero-Point Energy of a Conducting Spherical Shell and the Casimir Model for a Charged Particle*," Phys. Rev. 174, 1764 (1968).

[5] G. Jordan Maclay, "Analysis of zero-point electromagnetic energy and Casimir forces in conducting rectangular cavities," Phys. Rev. A 61, 052110-1 (2000).

[6] O. Kenneth, I. Klich, A. Mann and M. Revzen, "Repulsive Casimir Forces," Phys. Rev. Lett. 89, 033001-1 (2002).

[7] S. K. Lamoreaux, "Demonstration of the Casimir Force in the 0.6 to 6 μm Range," Phys. Rev. Lett. 78, 5 (1997).

[8] U. Mohideen and Anushree Roy, "Precision Measurement of the Casimir Force from 0.1 to 0.9 μm," Phys. Rev. Lett. 78, 5 (1998).

[9] E. Buks and M. L. Roukes, "Stiction, adhesion energy, and the Casimir effect in micromechanical systems," Phys. Rev. B 63, 033402 (2001).

[10] H. B. Chan, V. A. Aksyuk, R. N. Kleiman, D. J. Bishop, and F. Capasso, "Nonlinear Micromechanical Casimir Oscillator," Phys. Rev. Lett. 87, 211801-1 (2001).

[11] J. H. Gundlach and S. M. Merkowitz, "Precise Calibration of the Intrinsic strength of Gravity and Measuring the Mass of the Earth."

[12] A. Feigel, "Quantum Vacuum Contribution to the Momentum of Dielectric Media," Phys. Rev. Lett. 92, 2 (2004).

[13] Emre S. Tasci and Sakir Erkoc, "Simulation of the Casimir-Polder effect for various Geometries," International Journal of Modern Physics C, Vol. 13, No. 7, 979-985 (2002).

[14] Kimball A. Milton, "The Casimir Effect, Physical Manifestations of Zero-Point Energy," World Scientific Publishing Co. Pte. Ltd., Singapore (2001).

[15] J. Schwinger, L. L. DeRaad, Jr., and K. A. Milton, "Casimir Effect in Dielectrics," Ann. Phys. (New York) 115, 1 (1978).

[16] J. Schwinger, "Casimir Light: The Source," Proceedings of the National Academy of Science, U.S.A., Vol. 90, March, 1993, pg 2105-2106.

[17] Peter W. Milonni, "The Quantum Vacuum, An Introduction to Quantum Electrodynamics," Academic Press, Inc., U.S.A. (1994).

[18] O. Kenneth and S. Nussinov, "Small object limit of the Casimir effect and the sign of the Casimir force," Phys. Rev. D 65, 085014-1 (2002).

[19] C. I. Sukenik, M. G. Boshier, D. Cho, V. Sandoghdar, and E. A. Hinds, “Measurement of the Casimir-Polder Force,” Phys. Rev. Lett. 70, 560-563 (1993).

[20] J. H. de Boer, Trans. Faraday Soc. 32, 10 (1936); H. C. Hamaker, Physica 4, 1058 (1937).

[21] L. D. Landau and E. M. Lifshitz, “Electrodynamics of Continuous Media,” Pergamon Press, Section 90, Oxford (1966).

[22] E. M. Lifshitz, “The Theory of Molecular Attractive Forces Between Solids,” Sov. Phys. JETP 2, 73 (1956).

[23] M. Abramowitz and I. A. Stegun, “Handbook of Mathematical Functions,” (Formula 3.6.28) Dover Books, New York (1971).

[24] E. T. Whittaker and G. N. Watson, “A Course of Modern Analysis (4th Edition),” (Page 127) Cambridge University Press, New York (1969).

[25] P. W. Milonni, R. J. Cook and M. E. Goggin, “Radiation pressure from the vacuum: Physical interpretation of the Casimir force,” Phys. Rev. A 38, 1621 (1988).

[26] P. C. W. Davies, “Scalar Particle Production in Schwarzschild and Rindler Metrics,” J. Phys. A 8, 609 (1975).

[27] W. G. Unruh, “Notes on Black-Hole Evaporation,” Phys. Rev. D 14, 870 (1976).

[28] D. F. Gaitan, L. A. Crum, C. C. Church, and R. A. Roy, “Sonoluminescense and bubble dynamics for a single, stable, cavitation bubble,” J. Acoust. Soc. Am., Vol. 91, 3166 (1992).

[29] C. Eberlein, “Theory of quantum radiation observed as sonoluminescense,” Phys. Rev. A, 2772 (1996).

[30] B. Gompf, R. Gunther, G. Nick, R. Pecha, and W. Eisenmenger, “ Resolving Sonoluminescense Pulse Width with Time-Correlated Single Photon Counting,” Phys. Rev. Lett. 79, 1405 (1997).

[31] R. A. Hiller, S. J. Putterman, and K. R. Weninger, “Time-Resolved Spectra of Sonoluminescense,” Phys. Rev. Lett. 80, 1090 (1998).

[32] M. J. Moran and D. Sweider, “Measurement of Sonoluminescense Temporal Pulse Shape,” Phys. Rev. Lett. 80, 4987 (1998).

[33] A. Prosperetti, “A new mechanism for sonoluminescense,” Journal of the Acoustical Society of America, April 1997 (Vol. 101, Issue 4, Pages 2003-07).